Early post-restoration recovery of tidal wetland structure and function at the Southern Flow Corridor project, Tillamook Bay, Oregon

---

Christopher Janousek[1], Scott Bailey[2,6], Stan van de Wetering[3], Laura Brophy[4], Scott Bridgham[5], Matthew Schultz[5,7], Maxwell Tice-Lewis[3]

[1]Department of Fisheries and Wildlife, Oregon State University, Corvallis, OR
[2]Tillamook Estuaries Partnership, Garibaldi, OR
[3]Confederated Tribes of Siletz Indians, Siletz, OR
[4]Institute for Applied Ecology, Corvallis, OR
[5]University of Oregon, Eugene, OR
[6]Current affiliation: Chelan County Natural Resources Department, Wenatchee, WA
[7]Current affiliation: Oregon Health & Science University, Portland, OR

A report submitted to the National Oceanic and Atmospheric Administration and Tillamook County, Oregon, March 2021.

Cover image:
Post-restoration view of the Southern Flow Corridor restoration site, August 2020. Image by C. Janousek.

Recommended citation:
Janousek C, Bailey S, van de Wetering S, Brophy L, Bridgham S, Schultz M, Tice-Lewis M. 2021. Early post-restoration recovery of tidal wetland structure and function at the Southern Flow Corridor project, Tillamook Bay, Oregon. Oregon State University, Tillamook Estuaries Partnership, Confederated Tribes of Siletz Indians, Institute for Applied Ecology, and University of Oregon.

Contents

Acknowledgements

We thank the many individuals and institutions that contributed to the implementation of the Southern Flow Corridor (SFC) project and restoration effectiveness monitoring over the course of this research. Laura Brown, Michael Ewald, Dillon Blacketer, Issac Kentta, Erin Peck and Rob Wheatcroft were instrumental in collection and analysis of pre-restoration and early post-restoration monitoring data; they were assisted in the field by Danielle Aguilar, Guy Banner, Julie Brown, Peter Idema, Chris Knutsen, Patrick Hayden, Ron Rehn, Susanna Perlstein, and Jake Turner. For field and lab assistance from 2017-2019, we thank Craig Cornu, Anne Matthews, Philip Matthews, Ian Rodger, Rob Russell, Shawn Beeler, Ryan Montgomery, Emil Sadofsky, Cory LeeWays, and Laura McCullough. We additionally thank Chad Allen, Greg Hublou, John Thorne, Tillamook County, and the Tillamook County Pioneer Museum who kindly allowed access to their properties for our pre- and post-restoration monitoring.

Pre- and post-restoration monitoring was supported by grants from the National Oceanic and Atmospheric Administration (cooperative agreement NA16NMF4630215), the US Fish and Wildlife Service (cooperative agreement F14AC00452), and the Oregon Watershed Enhancement Board (grant 214-1043-11003). We express thanks to the Tillamook Estuaries Partnership, the US Environmental Protection Agency, Green Point Consulting, and Oregon State University which provided additional in-kind support including equipment loans.

This report was prepared by the authors using federal funds under award NA16NMF4630215 from NOAA's Community-based Restoration Program, U.S. Department of Commerce. The statements, fundings, conclusions, and recommendations are those of the authors and do not necessarily reflect the view of NOAA or the U.S. Department of Commerce.

Executive summary

A substantial fraction of estuarine tidal wetlands have been lost to development or other human uses in the Pacific Northwest since the 1800s. Wetland restoration, typically through tidal re-connection, can restore normal tidal hydrology to these areas and improve estuarine capacity to support ecosystem functions and services. Restoration may initiate a cascade of ecosystem-level impacts to channel and groundwater hydrology, soils, vegetation and fauna, and carbon cycling. Construction of the large Southern Flow Corridor (SFC) restoration project (179 ha) was implemented in southern Tillamook Bay in 2016 to reduce urban flooding and to enhance other wetland ecosystem services such as fisheries production and carbon sequestration. The project occurred on former tidal wetlands (originally emergent tidal marshes and forested tidal swamp) that had been diked for over 60 years prior to restoration. During the diked period, the site was used for crop agriculture, cattle grazing, and non-tidal freshwater marsh mitigation. Much of the site had been abandoned from active agricultural use for several years prior to restoration.

We conducted pre-restoration (2013-2015) and early post-restoration (2017-2020) measurements of a wide range of hydrologic, soil, and biological parameters at SFC and least-disturbed reference tidal wetlands to assess early post-restoration change in ecosystem structure. Within the SFC site, we evaluated how pre-restoration differences in elevation and land-use/land-cover zones influenced early restoration trajectories. We compared conditions at SFC with two types of reference wetlands in Tillamook Bay: low and high reference marshes. Before restoration, SFC wetlands were more comparable to low reference marsh than high marsh in elevation and had fresh and slightly acidic soils with relatively low dry season-groundwater levels. SFC tidal channels were also fresh with maximum water levels much lower than fully-tidal reference channels. SFC vegetation was a mix of freshwater-adapted native and non-native species including reed canarygrass. Pre-restoration conditions differed to some extent by land-cover/land-use zone, with the northern zone being higher in elevation while the cropped zone at the southern part of the site was relatively low in elevation.

Within two years of dike removal, hydrology, soils, and vegetation changed markedly at SFC, moving towards reference wetland conditions. Soil pH, salinity, and dry-season groundwater level tended to increase and existing vegetation began to die back, creating bare ground. Reed canarygrass in particular declined considerably in the middle and cropped zones in the site. Within 2-4 years of dike removal, many brackish-tolerant estuarine species began to colonize and spread across the southern and middle regions of SFC. Early soil accretion rates at SFC were high, especially in the cropped zone which was low in elevation both before and after restoration. Changes in channel morphology were observed in some locations, including channel widening and bottom scour.

Restoration at SFC also led to changes in fish and benthic invertebrate communities in tidal channels. Juvenile chinook and chum salmon increased in abundance at SFC following restoration. Other finfish species such as juvenile coho salmon, staghorn sculpin, three-spined stickleback, and juvenile surfperch were found utilizing channels within the restored site, although not necessarily increasing substantially in abundance due to the restoration. Benthic invertebrate communities shifted to include more amphipods and less insects after restoration activities. Larval and adult mosquitos were captured at sites inside and near the SFC project both before and after restoration, but mosquito numbers were very low.

In one of the first studies of greenhouse gas emissions from tidal wetlands in the Pacific Northwest, we found that fluxes of methane and carbon dioxide were driven by complex interactions of groundwater table, salinity, and temperature at SFC and in reference and disturbed (diked former) tidal wetlands. Methane emissions were highly variable in reference wetlands and at SFC, but high when

groundwater levels were high and salinity was low. Nitrous oxide emissions were generally very low across all the wetland types measured. Monitoring and developing mitigation strategies for methane in tidal wetland restoration projects may be desirable for restoration practitioners since it is a powerful greenhouse gas.

Our data provide an early snapshot of ecosystem change across an array of physical and biological parameters at the SFC site shortly after restoration of tidal flows at the site. Our findings suggest that several parameters, processes and functions at the SFC site are well on their way towards becoming similar to reference tidal wetland conditions. Processes and parameters that were already similar to (or exceeded) reference conditions two years after restoration included groundwater level, channel maximum water level, soil salinity and pH, soil accretion rate, and abundance of some finfish species. Other parameters and processes may take more time to become similar to reference marshes. In terms of support for native plant, invertebrate, and finfish species, our monitoring data suggest the project is enhancing tidal wetland functions in Tillamook Bay. The heterogenous nature of SFC prior to restoration allowed us to examine the role of land use/land cover in post-restoration change. We found that early rates of recovery in soils and vegetation at SFC were linked to pre-restoration gradients of elevation and land-use/land-cover differences.

As development of the site proceeds, we anticipate on-going changes such as widening of channels, sediment accretion that raises wetland elevations, succession of plant composition, and potentially establishment (or persistence) of tidal forested or scrub-shrub wetlands in portions of the SFC site that have sufficiently high elevation and low salinities. To further characterize rates of change, and to collect data necessary for possible adaptive management in the future, we recommend continued periodic measurement of key ecosystem parameters at the SFC site and in reference wetlands in the coming decades. We suggest that additional data on wetland processes (such as carbon dynamics, soil accretion, fish use, and food web structure) would be a powerful complement to the parameters that have ben monitored to date. Finally, in terms of monitoring design we note that this project highlighted the value of including a variety of reference wetlands (at both low and high elevation), since their inclusion allows a more robust picture of restoration site development in comparison to the diversity of least-disturbed wetlands within an estuary.

Data availability

In addition to the data presented in this report, major datasets for this project are publically available. Data release 1 and data release 2 at the Knowledge Network for Biocomplexity contain datasets for wetland elevation, soil parameters, accretion rates, channel and groundwater hydrology, and vegetation plots. Carbon sequestration rate data are reported in Brophy et al. (2018) and Peck et al. (2020). Greenhouse gas emissions data will be forthcoming at the Coastal Carbon Research Coordination Network. Vegetation mapping shape files are available by contacting Laura Brophy at laura@appliedeco.org. Channel morphology, fish, and invertebrate data are available from Stan van de Wetering at Biological Programs Director, CTSI, P.O. Box 549, Siletz, OR 97380. For other correspondence, please contact the first author at janousec@oregonstate.edu.

Abbreviations and key definitions

BACI – before-after-control-impact
GHG – greenhouse gas(es)
Mesohaline – salinities between 5 and 18 ppt
MHHW – mean higher high water
MTL – mean tide level
NAVD88 – North American Vertical Datum of 1988
NGS – National Geodetic Survey
NOAA – National Oceanic and Atmospheric Administration
Oligohaline – salinities between 0.5 and 5 ppt
Polyhaline – salinities between 18 and 30 ppt
RTK-GPS – Real-time kinematic global positioning system
SET – Surface elevation table
SFC – Southern Flow Corridor project in Tillamook Bay
SLR – sea-level rise
USFWS – United States Fish and Wildlife Service
UTM – Universal Transverse Mercator coordinate system

Chapter 1: SFC project background and monitoring objectives

Christopher Janousek, Laura Brophy, and Scott Bailey

Introduction

Tidal wetlands, including saltwater to freshwater emergent marshes, tidal scrub-shrub wetlands, and tidal forested wetlands were historically common in bays, estuaries, and river deltas throughout the Pacific Northwest (PNW) region of the United States (Marcoe and Pilson 2017, Brophy 2019). These vegetated wetlands occupy the upper half of the intertidal zone (a vertical range of about 1.5 - 2.0 m) in soft-sediment areas of coastal bays and along tidal reaches of coastal rivers. Along with estuarine tideflats and seagrass meadows, which typically occur at lower elevations in the intertidal zone, tidal marshes and tidal swamps are important components of estuarine habitat diversity and sustain numerous important estuarine functions. Emergent herbaceous plants such as grasses and sedges as well as woody species like *Picea sitchensis* (Sitka spruce) are the "foundation species" (Dayton 1972) in these ecosystems, forming three-dimensional habitat structure and affecting the flow of energy, carbon, and nutrients through the coastal zone.

West coast estuaries, and the types of tidal wetlands they support, are diverse. In the PNW, estuaries range from the large fjord of the Salish Sea and its river deltas to the large Columbia River Estuary to smaller bays, lagoons, and estuaries on the outer coast of Washington, Oregon, and northern California (Lee and Brown 2009, Emmett et al. 2000). Oregon's outer coast estuaries, including Tillamook Bay, are fed by streams and rivers that originate in the cool, temperate rain forests of the coast range. Geomorphically, drowned-river mouth estuaries are the most common type along the west coast of the US; these formed as sea-levels rose following the last ice age and filled river mouths (Emmett et al. 2000). Tillamook Bay is principally classified as a drowned-river mouth estuary with five rivers (the Miami, Kilchis, Trask, Wilson, and Tillamook) that supply freshwater to the estuary from coastal watersheds, though it also is bounded on the west by an ocean-built sand bar (Emmett et al. 2000).

Tidal wetland functions and services. Estuarine wetlands such as brackish tidal marshes sustain many important functions and services in the coastal zone, including support of fish and wildlife populations and other processes of direct and indirect benefit to human communities (Adamus 2006). Tidal wetlands are highly productive ecosystems, contributing to estuarine food webs via plant detritus consumed by benthic and pelagic animals (Bottom et al. 2005, Nordström et al. 2014). Phytoplankton, benthic micro- and macro-algae, seagrasses, and emergent vascular plants all contribute to coastal productivity and carbon cycles. Coastal wetlands also efficiently remove nitrogen from local waters (Zhao et al. 2019).

Across the North Pacific, estuarine wetlands are particularly valued for their role in the life cycles of salmonids, anadromous fish that migrate through estuaries in their transit from rivers and streams to the open ocean. Vegetated tidal wetlands and their associated tidal channels help sustain salmonids through provision of food-rich habitat, especially during juvenile phases of the life cycle, and through the cooling effect of vegetation (Sather et al. 2016, Davis et al. 2019, Woo et al. 2019). Tidal wetlands also potentially provide juvenile salmonids with refuge from predation (Bottom et al. 2005). Some PNW salmonid species spend considerable time in estuarine environments. For example, juvenile Chinook (*Oncorhynchus tshawytscha*) reside in estuaries as juveniles before they migrate out to the ocean (Bottom et al. 2005), and some juvenile Coho salmon (*O. kisutch*) feed in estuaries before

returning upstream for a period prior to eventual migration out to sea (Koski 2009). Habitat diversity within estuaries may promote prey diversity, which in turn sustains salmonid life history diversity that helps keep fish populations resilient (Koski 2009, Woo et al. 2019). Restoration of vegetated tidal wetlands in the brackish zone of estuaries may provide additional habitat and increase the food availability for salmonid species that are more likely to use estuarine environments during their life cycles (Koski 2009).

Tidal wetlands such as emergent marshes are also recognized for their important role in carbon sequestration, termed "blue carbon." While most organic carbon fixed by wetland plants and algae is re-mineralized through decomposition, consumed in wetland food chains, or exported, the rest is stored long-term in soils or in plant biomass (Rosentreter et al. 2018). Preservation potential varies as microbial communities, environmental conditions, and plant-microbe interactions affect rates of decomposition (Spivak et al. 2019). Tidal wetlands thus hold substantial stocks of organic carbon in soils that have accumulated over centuries (Hinson et al. 2017, Kauffman et al. 2020). These ecosystems also continue to sequester new carbon at high rates from both on-site productivity and from capture of organic matter produced elsewhere in the watershed (Chmura et al. 2003, Macreadie et al. 2017, Drexler et al. 2020). There is currently strong interest in the blue carbon function of coastal wetlands because this is one of several potential natural methods of compensating for global carbon emissions due to human activities (Irving et al. 2011). Although tidal wetlands only account for a relatively small percentage of terrestrial habitat area, their relatively high carbon stocks and sequestration rates per unit area make them important conservation and restoration targets from a carbon mitigation perspective (Mcleod et al. 2011, Chmura et al. 2003). In the PNW, recent research confirms that the region's tidal marshes and forested tidal swamps (temperate analogues of tropical mangrove ecosystems) hold substantial organic soil carbon stocks (Kauffman et al. 2020, Peck et al. 2020).

Tidal wetlands also benefit coastal areas through protection from waves and storms (Shepard et al. 2011, Barbier et al. 2013, Reed et al. 2018). The gradual elevation slope and often-dense vegetation of intertidal wetlands slows water velocities and reduces storm-generated waves during high tide flooding events. This protective service may reduce the economic cost of storm damage (Barbier et al. 2013) and may become increasingly important for communities located next to estuaries as sea levels rise and storm-surge heights increase (Barnard et al. 2019). As sea level rises, these benefits may be threatened if land development limits the landward migration of tidal wetlands (Enwright et al. 2016), so forward-thinking conservation of existing and potential future tidal wetlands is increasingly important.

Farther up estuaries where open water is less extensive, tidal wetlands may also protect upland areas from flooding by storing floodwaters from storm surges originating in the ocean or from high river flows off coastal watersheds (Smolders et al. 2015). For example, Stark et al. (2017) modeled the hydrologic effects of tidal wetland restoration in the Scheldt Estuary in northern Europe. They found that greater tidal wetland area within the estuary increased the tidal prism and lowered tidal amplitude in other areas of the estuary. Freshwater non-tidal wetlands in flood plains also similarly tend to reduce flooding impacts (Bullock and Acreman 2003).

The varied ecosystem services provided by estuarine wetlands, including those described above as well as others listed in Adamus (2006), contribute economic value to coastal communities (Barbier et al. 2011). In the Pacific Northwest, economic sectors such as commercial and recreational fishing are dependent on healthy, functioning estuaries (PSMFC, undated), and many residents in the region perceive declines in fish habitat as an important environmental threat (Huppert et al. 2003). Additionally, some of the aesthetic, cultural, and spiritual values of natural coastal habitats cannot be quantified monetarily, but they add to the overall well-being of coastal communities, including indigenous populations that have lived along PNW coastlines for millenia.

Tidal wetland loss. While the ecological and economic benefits of estuarine wetlands are increasingly documented, a large percentage of tidal wetlands across the PNW have been lost since the beginning of European settlement (Brophy 2019, Brophy et al. 2019). The proximity of tidal wetlands to navigable estuarine waterways and their relatively flat topography along the otherwise mountainous areas of the PNW coastal region make them attractive locations for land development or diking for agricultural use. In areas such as the Lower Columbia River Estuary, estimated loss of tidal wetland habitats are as high as 50-80% (Marcoe and Pilson 2017; Brophy et al. 2019). An estimated 70% of the area of emergent marsh and 92% of the area of forested tidal wetlands formerly occurring in the Tillamook Bay Estuary have been lost (Brophy 2019).

To convert tidal areas to agricultural use, tidal wetlands are typically cut off hydrologically from the rest of the estuary (a land use change also known as "reclamation") by construction of dikes that reduce or eliminate incoming tidal flows. Dikes are often fitted with tide gates that allow freshwater flows (e.g., accumulated rainfall) out of the wetland at low tide but close at high tide to prevent incoming tidal flooding. The loss (or reduction) in tidal flow in a diked former tidal wetland leads to a variety of changes to the site's physical characteristics (e.g., salinity, inundation, groundwater, elevation, soil properties) and biological characteristics (e.g., vegetation, fish, and wildlife use) (Roman et al. 1984, Portnoy and Giblin 1997, Spencer et al. 2017). Such dikes are common throughout Oregon estuaries.

Restoration to enhance services. Restoration is an important management tool for enhancing tidal wetland functions and services when they have been lost or diminished because of habitat loss, fragmentation, or disturbance (Crooks et al. 2014, Greiner et al. 2013). Restoration can be active or passive, but it generally involves the resumption of tidal exchange in former tidal wetlands by breaching portions of dikes surrounding wetlands or by complete dike removal (Hood 2014). The restoration of tidal hydrology to a former tidal wetland is a key catalyst that affects subsequent vegetation and soil development and fish access to wetland resources.

Restoring tidal exchange to tidal wetlands can reestablish or enhance ecosystem functions and services that were diminished while the wetland was surrounded by dikes. For instance, restoration can enhance estuarine uptake and storage of organic carbon where that historic capacity was lost (Andrews et al. 2008, Crooks et al. 2014) and it can reduce rates of methane production, a powerful greenhouse gas, by increasing soil salinity (Kroeger et al. 2017). Additionally, tidal wetland restoration may benefit fish and other wildlife species by increasing habitat area and prey availability (Roegner et al. 2010, Woo et al. 2018, Davis et al. 2019). Finally, wetland restoration can enhance the climate change resilience of estuaries and nearby built communities by expanding coastal areas that can mitigate storm surges, provide flood water storage, and allow migration of wetlands land-ward with sea-level rise.

Tidal wetland restoration projects are increasingly common on the outer Oregon coast and Lower Columbia River estuaries (e.g., Frenkel and Morlan 1991, Cornu and Sadro 2002, Brophy 2009, Brown et al. 2016a, Bailey 2017, Diefenderfer et al. 2013). The projects range considerably in size and the engineering approaches used, but collectively they help reverse the trend of wetland loss in the PNW that threatens to diminish the benefits of these key coastal habitats.

Although restoration of tidal hydrology is a critical first step for enhancing tidal wetland functions and services, ecosystem recovery towards reference conditions may take decades. Each major structural and functional attributes – surface water hydrology, groundwater hydrology, soil characteristics, vegetation attributes, faunal community structure, productivity, nutrient cycling, bird and fish use – may change at different rates as the restored site develops (Craft et al. 1999, Zedler 2000, Kidd 2017). Some structural or functional attributes such as soil properties may take many years to reach approximate equivalency with reference conditions, and it is also possible that some features of a restored wetland will never reach equivalence with reference conditions (Simenstad and Thom 1996, Craft et al. 1999), particularly if rapid climate change and sea-level rise reduce the time available for

ecosystems to approach least-disturbed conditions. Successful projects may also require adaptive management as on-going monitoring data provide additional guidance for specific interventions.

The Southern Flow Corridor Project

The Southern Flow Corridor project (hereafter SFC) in Tillamook County is one of Oregon's largest tidal wetland restoration projects implemented to date (Fig 1.1), with tidal flows restored to 179 ha and an overall project size of 280 ha (Tillamook County 2018). Located at the confluence of three of the five major rivers that feed into Tillamook Bay, the project was developed as a cooperative effort of local landowners, government, non-profit organizations and other regional stakeholders. The main impetus for restoring SFC to tidal wetland habitat was the need to alleviate periodic flooding in and near the town of Tillamook, OR, which lies just east of the project site. For instance, the 1996 flood caused $53 million in damages to Tillamook County (Levesque 2013). By removing dikes and restoring tidal wetland, the implementation of the SFC project was expected to reduce flooding in nearby areas (Northwest Hydraulic Consultants 2011). A 2018 report showed that a reduction in flood height was achieved after SFC project implementation (Northwest Hydraulic Consultants 2018).

While flood mitigation was a primary goal of the project, the restoration of such a large area of former tidal wetlands in Tillamook Bay was also anticipated to provide additional ecological benefits, including salmonid production (Brophy and van de Wetering 2014). Native salmonid species that utilize Tillamook Bay's watersheds include coho and chinook salmon and steelhead. These species play an important role in the economic and cultural life of PNW coastal communities. Abundances of salmonids across the PNW have been declining, and while mechanisms are not well understood (David et al. 2016), loss of suitable wetland habitat within estuaries and fishing pressure may be contributing factors (Magnusson and Hilborn 2003, Bottom et al. 2005, Price et al. 2019). Increases in fish abundance from restoration actions would benefit recreational fisheries and presumably also increase population resilience into the future as climate continues to change.

Diked areas within the SFC project area were also identified as high to moderately-high restoration opportunities in a recent restoration prioritization conducted for all of Tillamook Bay (Ewald and Brophy 2012). The site scored high in assessments of wetland connectivity, salmonid diversity, and vegetation diversity (Ewald and Brophy 2012). Historically, most of the site was emergent marsh, but included some forested tidal swamp (Ewald and Brophy 2012). The latter wetland type has been particularly impacted in Oregon, with an estimated loss of 96% of historical coverage (Brophy 2019).

The SFC project is the culmination of decades of community involvement and study, which advanced with more urgency following the winter floods of 2005-2006 and the procurement of an Oregon Solutions status for the project (Levesque 2013). The preliminary engineering design for SFC was completed in 2011 (NHC 2011). The final as-built project included five major components: levee and tide gate removal at the outer perimeter of the site, construction of a new setback levee at the eastern end of the site to protect property outside of the project area, removal of internal roads and four structures, fill of agricultural ditches, and excavation of historical tidal channels across the wetland (Tillamook County 2018; Figure 1.2, 1.3).

During summer 2016, a total of 8.4 km of levees were lowered and 15 tide gates were removed from the perimeter of the site (Tillamook County 2018) which allowed tidal flow into the major remnant tidal channels (Nolan Slough and Blind Slough). Small sections of levee were retained in a few locations where large trees had been growing above tidal influence. To increase hydrologic connectivity at the project site, 16.9 km of tidal channels were excavated at the site between 2016-2017 (Figure 1.2). Channels were generally excavated where historical channels were observed in 1939 aerial photographs. Many excavated tidal channels about 1 m in width (Figure 1.3). Project crews also filled 7.2 km of linear agricultural ditches that were dug following diking (Tillamook County 2018). Although stabilizing

vegetation was planted in construction areas, vegetation was not planted on the general wetland surface at SFC; instead, native plants were expected to re-establish through natural dispersal from nearby least-disturbed tidal wetlands. There were no major modifications to wetland surface elevation aside from the activities mentioned above.

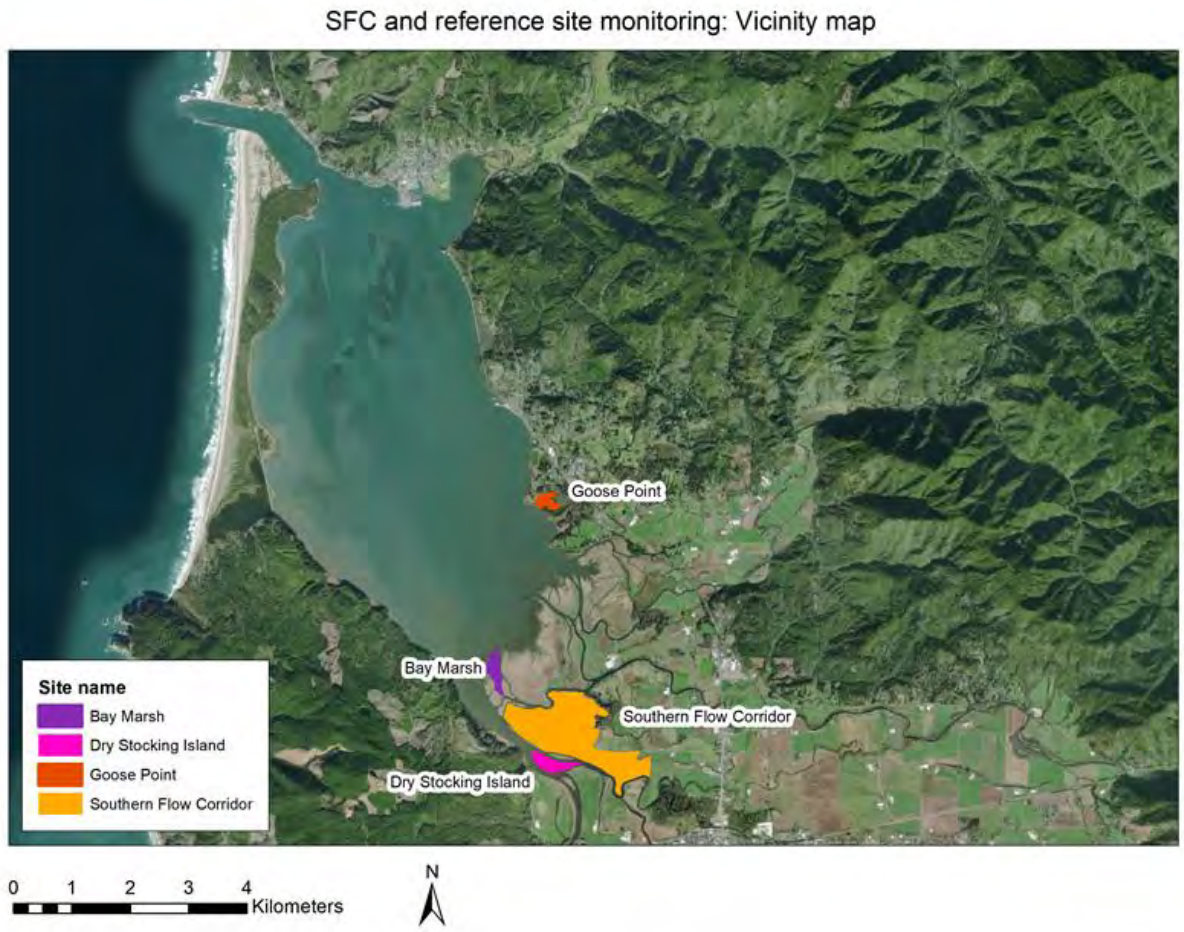

Figure 1.1. Location of the Southern Flow Corridor (SFC) project and reference tidal wetlands in the Tillamook Estuary.

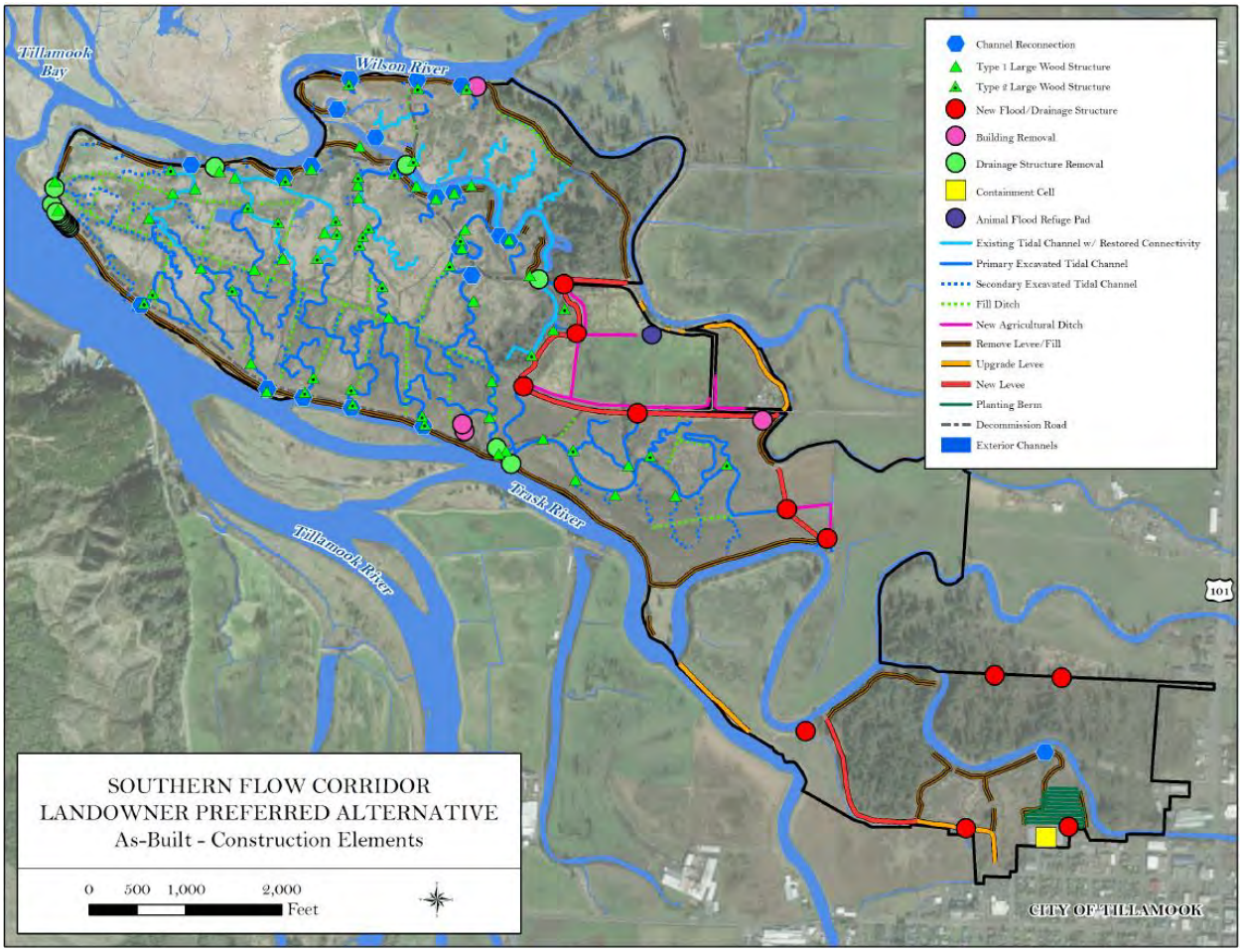

Figure 1.2. Map of restoration activities at the SFC site including levee and tide gate removal, set-back levee construction, and new tidal channel excavation. Map from Tillamook County (2018) and reproduced with permission.

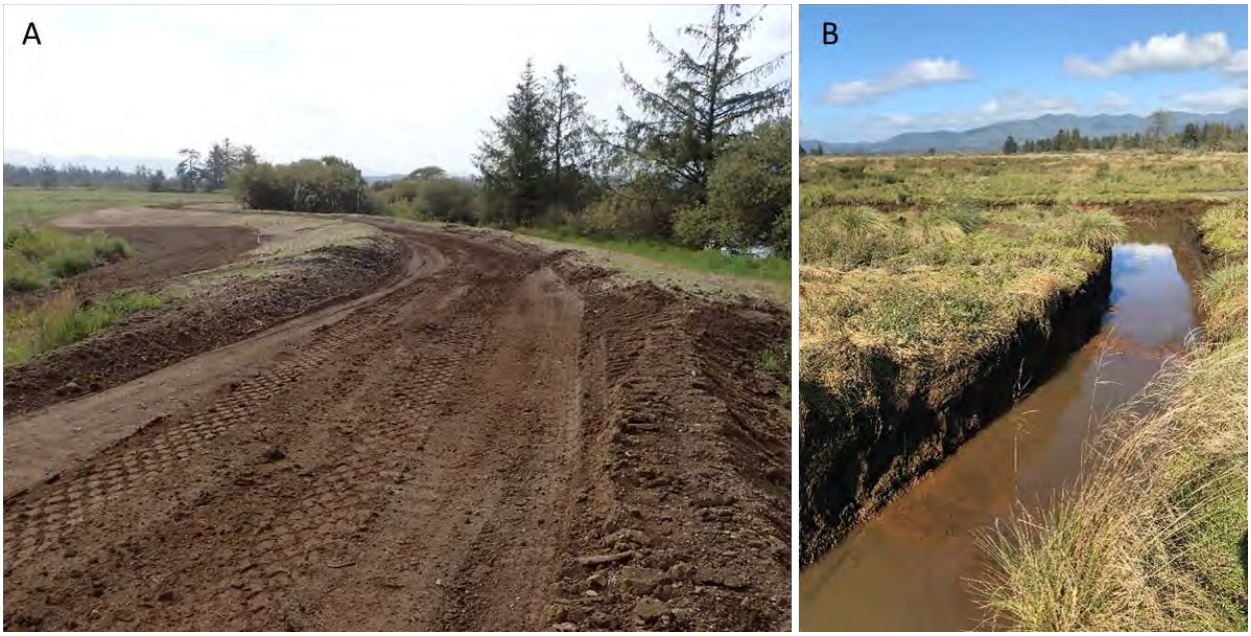

Figure 1.3. Site engineering at SFC during 2016-2017 to implement restoration. (A) Setback levee constructed at the eastern end of the site (photo by C. Janousek, Aug 2017). (B) Example excavated tidal channel toward the southern end of SFC (photo by C. Janousek, Sept 2019).

Monitoring objectives

As with other wetland restoration projects in the Pacific Northwest (e.g., Borde et al. 2012, Brown et al. 2016a), our team conducted pre- and post-restoration sampling across a range of ecosystem parameters to assess the impacts of tidal restoration on wetland physical characteristics, processes, and biological assemblages. As articulated in the SFC monitoring plan (Brophy and van de Wetering 2014), monitoring included the goals of determining wetland restoration effectiveness, identifying potential adaptive management needs, and generating data to communicate project results to stakeholders and the public and to guide future restoration work in the region.

In Chapters 2-8 of this report, we focus on monitoring to determine wetland restoration effectiveness and ecosystem recovery. We had the following major objectives: (1) assess change in wetland elevation and soil accretion, soil characteristics, channel and groundwater hydrology, vegetation cover and composition, benthic invertebrate assemblages, and fish abundance and behavior following restoration at SFC and compare change with reference marshes; (2) evaluate how change in ecosystem parameters varied among distinct land-cover/land-use zones and with elevation within the SFC site; and (3) assess general trends in mosquito presence at SFC before and after project implementation. In Chapter 9, we report on post-restoration greenhouse gas emissions measurements at SFC, reference wetlands, and diked former tidal wetlands. In Chapter 10, we summarize lessons learned from the project both in terms of restoration implementation and effectiveness monitoring and make recommendations for future tidal wetland restoration work in the PNW. This report focuses on the ecosystem aspects of SFC restoration, whereas a report by NHC (2018) describes measurements and modeling pertinent to the flood reduction goals of the project. A subset of parameters described in this report are included in a recent peer-reviewed publication (Janousek et al. 2021).

Sampling design

In 2014 and 2015, our team conducted pre-restoration monitoring of a range of physical and biological parameters within SFC and in several nearby least-disturbed reference wetlands in Tillamook Bay (Brown et al. 2016b). For most parameters described in this report, we used a before-after control-impact (BACI) study design (Stewart-Oaten et al. 1986), but with the following modifications: (i) we only monitored some parameters such as vegetation and soils once before and after project implementation, (ii) we used two different types of reference wetlands, each occurring at two different sites, for comparison with the restored area (Underwood 1994), and (iii) we stratified sampling and analyses based on land-use/land-cover zones within SFC because the site was large and had heterogeneous vegetation types and management activities in the decades prior to restoration. We measured the following parameters at SFC and reference sites prior to project implementation in 2013-2015: groundwater level and temperature; tidal channel water level, temperature, and salinity; wetland surface elevation; soil pH, conductivity, and organic matter content; channel morphology; emergent vegetation cover, composition, and richness; benthic macroinvertebrate communities; fish abundance and migration behavior; and mosquito presence. From 2017-2018 following restoration, we monitored all pre-restoration parameters listed above as well as several additional parameters including groundwater salinity and greenhouse gas fluxes. From 2013-2020 we measured rates of soil accretion.

Reference wetlands. Reference sites included two low marsh sites at the western end of Dry Stocking Island and at Bay Marsh, and two high marsh sites at the eastern and northern end of Dry Stocking Island and Goose Point marsh (Figures 1.1, 1.4, 1.5, 1.6). Low and high emergent brackish marsh represent two common types of tidal wetlands that occur across Oregon's estuaries and represent likely near-term (low marsh) and longer-term (high marsh) successional states as SFC develops following restoration (Jefferson 1975, Brophy and van de Wetering 2014). Bay Marsh is likely the youngest of the three reference sites, having developed into emergent wetland since European settlement, while Dry Stocking Island also expanded in area during this time (Brophy and van de Wetering 2014).

Land-use/land-cover zones at SFC. For many of the analyses presented in this report (wetland elevation, soils, and vegetation), we divided the SFC site into five distinct land-use/land-cover zones based on their geographic location, vegetation composition, and pre-restoration land use history (Fig. 1.7). The north zone (also denoted "N" in figures and tables in this report) consisted of a 16.6 ha area between the Wilson River to the north and Blind Slough to the south, which was diked in the 1960's, later than other areas at SFC (Brophy and van de Wetering 2014). Prior to restoration, this zone consisted of a mixture of non-tidal emergent freshwater marsh, willow-dominated wetlands, and forested wetlands (Sitka spruce, red elderberry, salmonberry), and was probably grazed at some point in the past (Brophy and van de Wetering 2014). Before this zone was diked, it was historically likely emergent marsh towards the west and forested tidal swamp to the east (Ewald and Brophy 2012).

The middle zone ("M") was located to the south of the north zone below Blind Slough, stretching from the western end of the project site to the setback levee in the east (65.6 ha). Like the north zone, this area was not intensively managed before restoration, although it was managed for waterfowl and had been used for agriculture in the more distant past (Brophy and van de Wetering 2014). The middle zone consisted primarily of emergent marsh with some shrubs and trees (e.g., elderberry), but woody cover was lower than in the north zone.

The south zone ("S") was a small parcel (5.5 ha) of mixed emergent marsh/forested land that was a freshwater wetland mitigation site before the restoration of tidal influence. This area has been actively planted with native freshwater plants, including some woody species.

Two additional areas of SFC near the south zone were more intensively managed prior to tidal restoration. The cropped zone ("CR") extended along the southern boundary of the site and consisted of

a series of fields that were actively managed for grass hay production (42.8 ha). This area was drained by a linear agricultural ditch on its northern boundary with the middle zone, and a series of parallel south-to-north oriented agricultural ditches. These ditches were filled as part of the tidal restoration in 2016. Finally, the grazed zone ("GR") was located in the vicinity of Nolan Slough, to the east of the cropped zone and north of the Trask River and was seasonally grazed by cattle prior to project implementation (8.6 ha).

To monitor channel morphology, channel hydrology, and fish and invertebrate assemblages, we focused measurements on several sections of rivers and tidal channels within and near SFC and reference marshes (Brophy and van de Wetering 2014). For channel hydrology, reference stations were located next to Dry Stocking Island between the Trask and Tillamook rivers, a major channel through Bay Marsh, the mouth of Blind Slough, and a major channel in Goose Pt. marsh. Within SFC, we monitored stations along Blind Slough and its tributaries, and Nolan Slough. Similarly, we conducted fish and invertebrate monitoring within SFC in Nolan Slough, Blind Slough and its tributary, and channels connecting to the Wilson River; and in reaches along the Wilson and Trask Rivers as reference sites. Detailed methods, results and discussion for each parameter follow in Chapters 2-9.

Figure 1.4. Bay marsh, one of the two reference sites with low emergent marsh, located to the northwest of SFC (photo by C. Janousek, Sept 2019).

Figure 1.5. Goose Point marsh, one of the two reference sites with high emergent marsh, located north of SFC near the town of Bay City, OR (photo by C. Janousek, Sept 2017).

Figure 1.6. Dry Stocking Island, the third reference site sampled, including both low marsh (foreground) and high marsh (background). The Island is located just south of SFC between the Trask and Tillamook Rivers (photo by C. Janousek, July 2018).

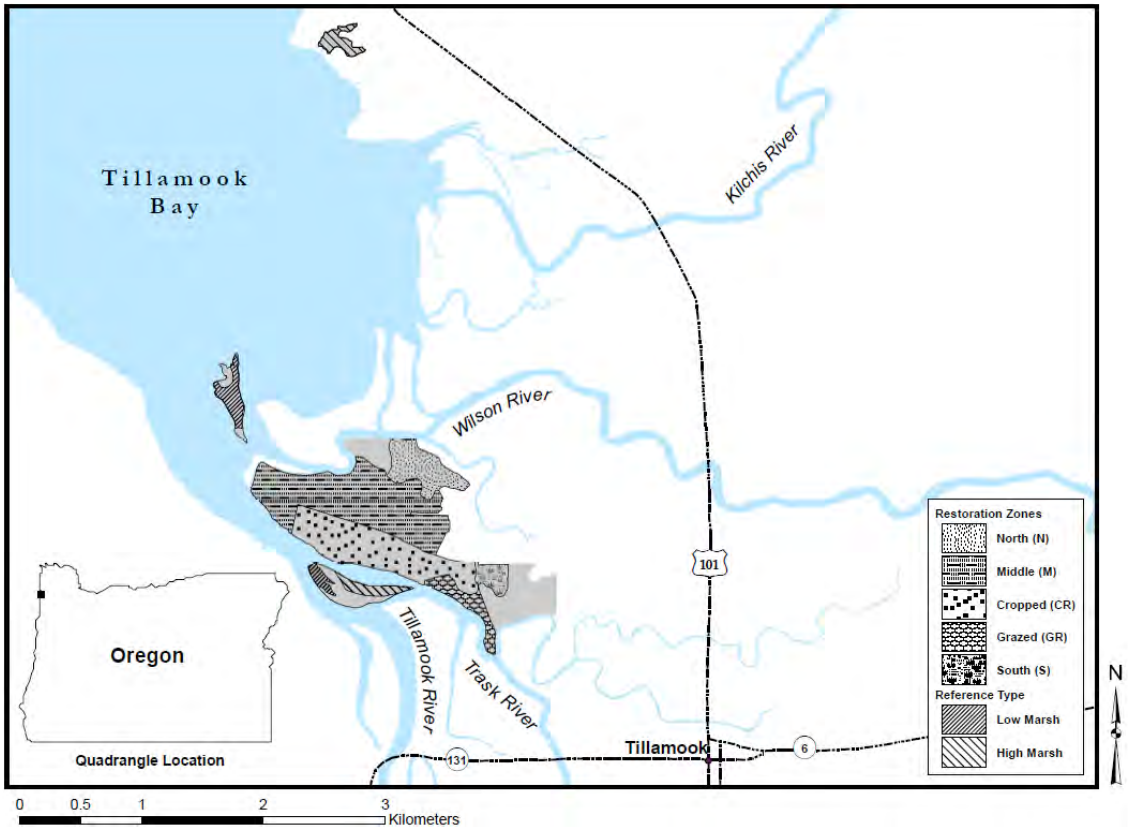

Figure 1.7. Land use zones within the SFC project site.

Citations

Adamus PR. 2006. Hydrogeomorphic (HGM) Assessment Guidebook for Tidal Wetlands of the Oregon Coast, Part 1: Rapid Assessment Method. Produced for the Coos Watershed Association, Oregon Department of State Lands, and U.S.E.P.A.-Region 10. Coos Watershed Association, Charleston, OR. Accessed 9/5/20.

Andrews JE, Samways G, Shimmield GB. 2008. Historical storage budgets of organic carbon, nutrient and contaminant elements in saltmarsh sediments: Biogeochemical context for managed realignment, Humber Estuary, UK. Science of the Total Environment 405:1-13.

Bailey SJ. 2017. Miami wetlands enhancement project: Six-year post-implementation monitoring report. Tillamook Estuaries Partnership, Garibaldi, OR.

Barbier EB, Georgiou IY, Enchelmeyer B, Reed DJ. 2013. The value of wetlands in protecting southeast Louisiana from hurricane storm surges. PloS ONE 8:e58715

Barbier EB, Hacker SD, Kennedy C, Koch EW, Stier AC, Silliman BR. 2011. The value of estuarine and coastal ecosystem services. Ecological Monographs 81:169-193.

Barnard PL, Erikson LH, Foxgrover AC, Finzi Hart JA, Limber P, O'Neill AC, van Ormondt M, Vitousek S, Wood N, Hayden MK, Jones JM. 2019. Dynamic flood modeling essential to assess the coastal impacts of climate change. Scientific Reports 9:4309.

Borde AB, Cullinan VI, Diefenderfer HL, Thom RM, Kaufmann RM, Zimmerman SA, Sagar J, eBuenau KE, Crobett C. 2012. Lower Columbia River and Estuary Ecosystem Restoration Program Reference Site Study: 2011 Restoration Analysis - FINAL REPORT. PNNL-21433. Pacific Northwest National Laboratory, Richland, WA.

Bottom DL, Simenstad CA, Burke J, Baptista AM, Jay DA, Jones KK, Casillas E, Schiewe MH. 2005. Salmon at river's end: the role of the estuary in the decline and recovery of Columbia River salmon. U.S. Dept. Commerce, NOAA Technical Memo. NMFS-NWFSC-68.

Brophy LS. 2009. Effectiveness monitoring at tidal wetland restoration and reference sites in the Siuslaw River Estuary: A tidal swamp focus. Green Point Consulting, Corvallis, OR.

Brophy LS. 2019. Comparing historical losses of forested, scrub-shrub, and emergent tidal wetlands on the Oregon coast, USA: A paradigm shift for estuarine restoration and conservation. Institute for Applied Ecology, Corvallis, OR. Prepared for Pacific States Marine Fisheries Commission and the Pacific Marine and Estuarine Fish Habitat Partnership.

Brophy LS, Peck EK, Bailey SJ, Cornu CE, Wheatcroft RA, Brown LA. 2018. Southern Flow Corridor effectiveness monitoring, 2015-2017: blue carbon and sediment accretion. Prepared for Tillamook County and the Tillamook Estuaries Partnership, Tillamook, Oregon, USA. Institute for Applied Ecology, Corvallis, OR.

Brophy LS, Greene CM, Hare V, Holycross B, Lanier A, Heady W, O'Connor K, Imaki H, Haddad T, Dana R. 2019. Insights into estuary habitat loss in the western United States using a new method for mapping maximum extent of tidal wetlands. PLoS ONE 14:e0218558.

Brophy LS, van de Wetering S. 2014. Southern Flow Corridor project effectiveness monitoring plan. Institute for Applied Ecology and the Confederated Tribes of Siletz Indians. Corvallis, OR.

Brown LA, Ewald MJ, Brophy LS. 2016a. Ni-les'tun tidal wetland restoration effectiveness monitoring: Year 4 post-restoration (2015). Estuary Technical Group, Institute for Applied Ecology, Corvallis, OR.

Brown LA, Ewald MJ, Brophy LS, van de Wetering S. 2016b. Southern Flow Corridor baseline effectiveness monitoring: 2014. Corvallis, Oregon: Estuary Technical Group, Institute for Applied Ecology. Prepared for Tillamook County, OR.

Bullock A, Acreman M. 2003. The role of wetlands in the hydrological cycle. Hydrology and Earth System Sciences 7:358-389.

Chmura GL, Anisfeld SC, Cahoon DR, Lynch JC. 2003. Global carbon sequestration in tidal, saline wetland soils. Global Biogeochemical Cycles 17:1111.

Cornu CE, Sadro S. 2002. Physical and functional responses to experimental marsh surface elevation manipulation in Coos Bay's South Slough. Restoration Ecology 10:474-486.

Craft C, Reader J, Sacco JN, Broome SW. 1999. Twenty-five years of ecosystem development of constructed *Spartina alterniflora* (Loisel) marshes. Ecological Applications 9:1405-1419.

Crooks S, Rybczyk J, O'Connell K, Devier DL, Poppe K, Emmett-Mattox S. 2014. Coastal blue carbon opportunity assessment for the Snohomish Estuary: the climate benefits of estuary restoration. Environmental Science Associates, Western Washington University, EarthCorps, and Restore America's Estuaries.

David AT, Simenstad CA, Cordell JR, Toft JD, Ellings CS, Gray A, Berge HB. 2016. Wetland loss, juvenile salmon foraging performance, and density dependence in Pacific Northwest estuaries. Estuaries and Coasts 39:767-780.

Davis MJ, Woo I, Ellings CS, Hodgson S, Beauchamp DA, Nakai G, de La Cruz SEW. 2019. Freshwater tidal forests and estuarine wetlands may confer early life growth advantages for Delta-reared chinook salmon. Transactions of the American Fisheries Society 148:289–307.

Dayton PK. 1972. Toward an understanding of community resilience and the potential effects of enrichments to the benthos at McMurdo Sound, Antarctica. In: Proceedings of the Colloquium on Conservation Problems in Antarctica, BC Parker (ed), Allen Press, Lawrence, KS, p.81-95.

Diefenderfer HL, Johnson GE, Thom RM, Borde AB, Woodley CM, Weitkamp LA, Buenau KE, et al. 2013. An evidence-based evaluation of the cumulative effects of tidal freshwater and estuarine ecosystem restoration on endangered juvenile salmon in the Columbia River: Final report. PNNL-23037. Pacific Northwest National Laboratory, Richland, WA.

Drexler JZ, Davis MJ, Woo I, de la Cruz S. 2020. Carbon sources in the sediments of a restoring vs. historically unaltered salt marsh. Estuaries and Coasts 43:1345-1360.

Emmett R, Llansó R, Newton J, Thom R, Hornberger M, Morgan C, Levings C, Copping A, Fishman P. 2000. Geographic signatures of North American west coast estuaries. Estuaries 6:765-792.

Enwright NM, Griffith KT, Osland MJ. 2016. Barriers to and opportunities for landward migration of coastal wetlands with sea-level rise. Frontiers in Ecology and the Environment 14:307-316.

Ewald MJ, Brophy LS. 2012. Tidal wetland prioritization for the Tillamook Bay Estuary. Prepared for the Tillamook Estuaries Partnership, Garibaldi, OR. Green Point Consulting, Corvallis, OR.

Frenkel RE, Morlan JC. 1991. Can we restore our salt marshes? Lessons from the Salmon River, Oregon. The Northwest Environmental Journal 7:119-135.

Greiner JT, McGlathery KJ, Gunnell J, McKee BA. 2013. Seagrass restoration enhances “blue carbon” sequestration in coastal waters. PLoS ONE 8:e72469.

Hinson AL, Feagin RA, Eriksson M, Najjar RG, Herrmann M, Bianchi TS, Kemp M, Hutchings JA, Crooks S, Boutton T. 2017. The spatial distribution of soil organic carbon in tidal wetland soils of the continental United States. Global Change Biology 12:5468-5480.

Huppert DD, Johnson RL, Leahy J, Bell K. 2003. Interactions between human communities and estuaries in the Pacific Northwest: trends and implications for management. Estuaries 26:994-1009.

Hood WG. 2014. Differences in tidal channel network geometry between reference marshes and marshes restored by historical dike breaching. Ecological Engineering 71:563-573.

Irving AD, Connell SD, Russell BD. 2011. Restoring coastal plants to improve global carbon storage. PloS ONE 6:e18311

Janousek CN, Bailey SJ, Brophy LS. 2021. Early ecosystem development varies with elevation and pre-restoration land use/land cover in a Pacific Northwest tidal wetland restoration project. Estuaries and Coasts 44:13-29.

Jefferson CA. 1975. Plant communities and succession in Oregon coastal salt marshes. PhD dissertation, Oregon State University, Corvallis, OR.

Kauffman JB, Giovanonni L, Kelly J, Dunstan N, Borde A, Diefenderfer H, Cornu C, Janousek C, Apple J, Brophy L. 2020. Total ecosystem carbon stocks at the marine-terrestrial interface: Blue carbon of the Pacific Northwest Coast, United States. Global Change Biology 26:5679-5692.

Kidd SA. 2017. Ecosystem recovery in estuarine wetlands of the Columbia River estuary. Portland State University Dissertations and Theses, Paper 3637.

Koski KV. 2009. The fate of Coho salmon nomads: the story of an estuarine-rearing strategy promoting resilience. Ecology and Society 14:4

Kroeger KD, Crooks S, Moseman-Valtierra S, Tang J. 2017. Restoring tides to reduce methane emissions in impounded wetlands: a new and potent blue carbon climate change intervention. Scientific Reports 7:11914.

Lee II H, Brown CA. (eds). 2009. Classification of regional patterns of environmental drivers and benthic habitats in Pacific Northwest Estuaries. U.S. EPA, Office of Research and Development, National Health and Environmental Effects Research Laboratory, Western Ecology Division. EPA/600/R-09/140, Corvallis, OR.

Levesque P. 2013. A history of the Oregon Solutions Southern Flow Corridor Project – Landowner Preferred Alternative, a review of the alternatives and a summary of public involvement. Tillamook County, OR. Accessed 9/8/20.

Macreadie PI, Ollivier QR, Kelleway JJ, Serrano O, Carnell PE, Ewers Lewis CJ, Atwood TB, Sanderman J, Baldock J, Connolly RM, Duarte CM, Lavery PS, Steven A, Lovelock CE. 2017. Carbon sequestration by Australian tidal marshes. Scientific Reports 7:44071.

Magnusson A, Hilborn R. 2003. Estuarine influence on survival rates of Coho (*Oncorhynchus kisutch*) and Chinook salmon (*Oncorhynchus tshawytscha*) released from hatcheries on the U.S. Pacific coast. Estuaries 26:1094-1103.

Marcoe K, Pilson S. 2017. Habitat change in the lower Columbia River estuary, 1870-2009. Journal of Coastal Conservation 21:505-525.

Mcleod E, Chmura, GL, Bouillon, Salm R, Björk M, Duarte CM, Lovelock CE, Schlesinger WH, Silliman BR. 2011. A blueprint for blue carbon: toward an improved understanding of the role of vegetated coastal habitats in sequestering CO_2. Frontiers in Ecology and the Environment 9:552-560.

Nordström MC, Currin CA, Talley TS, Whitcraft CR, Levin LA. 2014. Benthic food-web succession in a developing salt marsh. Marine Ecology Progress Series 500:43-55.

Northwest Hydraulic Consultants (NHC). 2011. Southern Flow Corridor Landowner Preferred Alternative Preliminary Design Report. Prepared for Oregon Solutions Design Team under contract to Tillamook County. Prepared by Northwest Hydraulic Consultants, Seattle, WA. Accessed 9/8/20.

Northwest Hydraulic Consultants (NHC) 2018. Southern flow corridor: As-built project validation of peak water level reduction during the October 2017 flood. Final report for Port of Tillamook Bay and Tillamook County, Seattle, WA. Accessed 9/8/2020.

Peck EK, Wheatcroft RA, Brophy LS. 2020. Controls on sediment accretion and blue carbon burial in tidal saline wetlands: Insights from the Oregon coast, U.S.A. JGR: Biogeosciences 125:e2019JG005464.

Portnoy JW, Giblin AE. 1997. Effects of historic tidal restrictions on salt marsh sediment chemistry. Biogeochemistry 36:275-303.

Price MHH, Connors BM, Candy JR, McIntosh B, Beacham TD, Moore JW, Reynolds JD. 2019. Genetics of century-old fish scales reveal population patterns of decline. Conservation Letters e12669.

PSMFC (Pacific States Marine Fisheries Commission). Undated. Estuarine and wetland dependent fish of the Pacific Northwest. F.I.S.H. Habitat Education Program.

Reed D, van Wesenbeeck B, Herman PML, Meselhe E. 2018. Tidal flat-wetland systems as flood defenses: understanding biogeomorphic controls. Estuarine, Coastal and Shelf Science 213:269-282.

Roegner GC, Dawley EW, Russel M, Whiting A, Teel DJ. 2010. Juvenile salmonid use of reconnected tidal freshwater wetlands in Grays River, Lower Columbia River Basin. Transactions of the American Fisheries Society 139:1211-1232.

Roman CT, Niering WA, Warren RS. 1984. Salt marsh vegetation change in response to tidal restriction. Environmental Management 8:141-150.

Rosentreter JA, Maher DT, Erler DV, Murray RH, Eyre BD. 2018. Methane emissions partially offset "blue carbon" burial in mangroves. Science Advances 4:eaao4985

Shepard CC, Crain CM, Beck MW. 2011. The protective role of coastal marshes: a systematic review and meta-analysis. PloS ONE 6:e27374.

Simenstad CA, Thom RM. 1996. Functional equivalency trajectories of the restored Gog-Le-Hi-Te estuarine wetland. Ecological Applications 6:38-56.

Smolders S, Plancke Y, Ides S, Meire P, Temmerman S. 2015. Role of intertidal wetlands for tidal and storm tide attenuation along a confined estuary: a model study. Natural Hazards Earth System Science 15:1659-1675.

Spencer KL, Carr SJ, Diggens LM, Tempest JA, Morris MA, Harvey GL. 2017. The impact of pre-restoration land-use and disturbance on sediment structure, hydrology and the sediment geochemical environment in restored saltmarshes. Science of the Total Environment 587-588: 47-58.

Spivak AC, Sanderman J, Bowen JL, Canuel EA, Hopkinson CS. 2019. Global-change controls on soil-carbon accumulation and loss in coastal vegetated ecosystems. Nature Geoscience 12:685-692.

Stark J, Smolder S, Meire P, Temmerman S. 2017. Impact of intertidal area characteristics on estuarine tidal hydrodynamics: A modelling study for the Scheldt Estuary. Estuarine, Coastal and Shelf Science 198:138-155.

Stewart A, Murdoch WW, Parker KR. 1986. Environmental impact assessment: "pseudoreplication" in time? Ecology 67:929-940.

Tillamook County. 2018. Performance progress report for Grant NA13NMF4630133: Reporting period ending 12/31/2017. Prepared for NOAA Restoration Center, Office of Habitat Conservation. Tillamook County, Tillamook, OR.

Underwood AJ. 1994. On beyond BACI: sampling designs that might reliably detect environmental disturbances. Ecological Applications 4:3-15.

Woo I, Davis MJ, Ellings CS, Nakai G, Takekawa JY, de la Cruz S. 2018. Enhanced invertebrate prey production following estuarine restoration supports foraging for multiple species of juvenile salmonids (*Oncorhynchus* spp.). Restoration Ecology 26:964-975.

Woo I, Davis MJ, Ellings CS, Hodgson S, Takekawa JY, Nakai G, de la Cruz SEW. 2019. A mosaic of estuarine habitat types with prey resources from multiple environmental strata supports a diversified foraging portfolio for juvenile Chinook salmon. Estuaries and Coasts 42:1938-1954.

Zedler JB. 2000. Progress in wetland restoration ecology. Trends in Ecology and Evolution 15:402-407.

Zhao C, Liu S, Jiang Z, Wu Y, Cui L, Huang X, Macreadie PI. 2019. Nitrogen purification potential limited by nitrite reduction process in coastal eutrophic wetlands. Science of the Total Environment 694:133702

Chapter 2: Wetland elevation, soil accretion, and soil composition

Christopher Janousek, Scott Bailey, and Laura Brophy

Key findings

- Pre-restoration elevations at SFC varied by land-use/land-cover zone, but were generally more similar to reference low marsh than reference high marsh.
- Soil accretion rates were generally higher at SFC than in reference high marsh, and tended to be greater in lower elevation areas.
- Soil carbon content was similar between SFC and reference wetlands and changed little following restoration.
- Before restoration, SFC soils were fresher and more acidic than reference wetlands, but salinity and to some extent, pH, increased after restoration of tidal flows.
- Pre- to post-restoration change in salinity and pH was strongly linked to wetland elevation at SFC, with lower, more inundated areas increasing most in salinity and pH.

Introduction

The diking of tidal wetlands for conversion to non-tidal land uses can result in significant impacts to their geomorphic structure. One of the most commonly documented impacts of diking is a decline in wetland surface elevation relative to wetlands that are still tidally-influenced (Frenkel and Morlan 1981, Brand et al. 2012, Clifton et al. 2018). Elevation loss at a diked site may occur because of several soil-related processes including compaction, drainage and aeration, and oxidation of organic matter (Belperio 1993, Portnoy and Gilbin 1997, Miller et al. 2008, Drexler et al. 2009).

In the Pacific Northwest, elevation loss of up to 1 m in diked former tidal wetlands has been estimated by comparing the surface elevation of these sites with nearby least-disturbed tidal wetlands (Frenkel and Morlan 1991, Brophy 2009, Cornu & Janousek, unpublished). In some cases, such as the freshwater tidal wetlands of the Sacramento-San Joaquin Delta in Northern California, elevation loss due to oxidation of peat soils can be so substantial (on the order of several meters), that future restoration of such sites to intertidal wetlands may not be possible (Drexler et al. 2009). The degree to which a former tidal wetland faces an elevation deficit may be related to several factors including the length of time it was diked, the presence or absence of land-use activities that worsen soil compaction (e.g., intensive agricultural uses), and the degree of soil dewatering and organic matter loss during the period the site was non-tidal.

Because surface elevation in tidal wetlands is closely linked to many aspects of ecosystem structure and function such as hydrology, vegetation, and soil conditions (Janousek and Folger 2014, Alvarez et al. 2015, Diefenderfer et al. 2018, Chapter 5 of this report), elevation loss due to diking is an important consideration in assessing how a site may recover after restoration of tidal influence. For successful restoration of a former tidal wetland to vegetated tidal marsh or forested tidal swamp, the site's elevation must be in the range that supports establishment and growth of vascular plants, or it must be able to gain new elevation by vertical accretion. Emergent tidal marshes in the PNW typically occur in the upper half of the intertidal zone, from just above local mean tide level (MTL), up to the

elevation of annual high tides, which is above local mean higher high water (MHHW) (Jefferson 1975, Brophy et al. 2019, Janousek et al. 2019; Figure 2.1). Tidal swamps, which include forested and scrub-shrub wetlands, also occur in the high intertidal zone in the PNW, generally in estuarine areas that are lower in salinity (Brophy 2009, Brophy et al. 2011). At elevations below MTL, emergent vegetation is likely to be absent in PNW estuaries, but mudflats or eelgrass (*Zostera marina*) beds may be found.

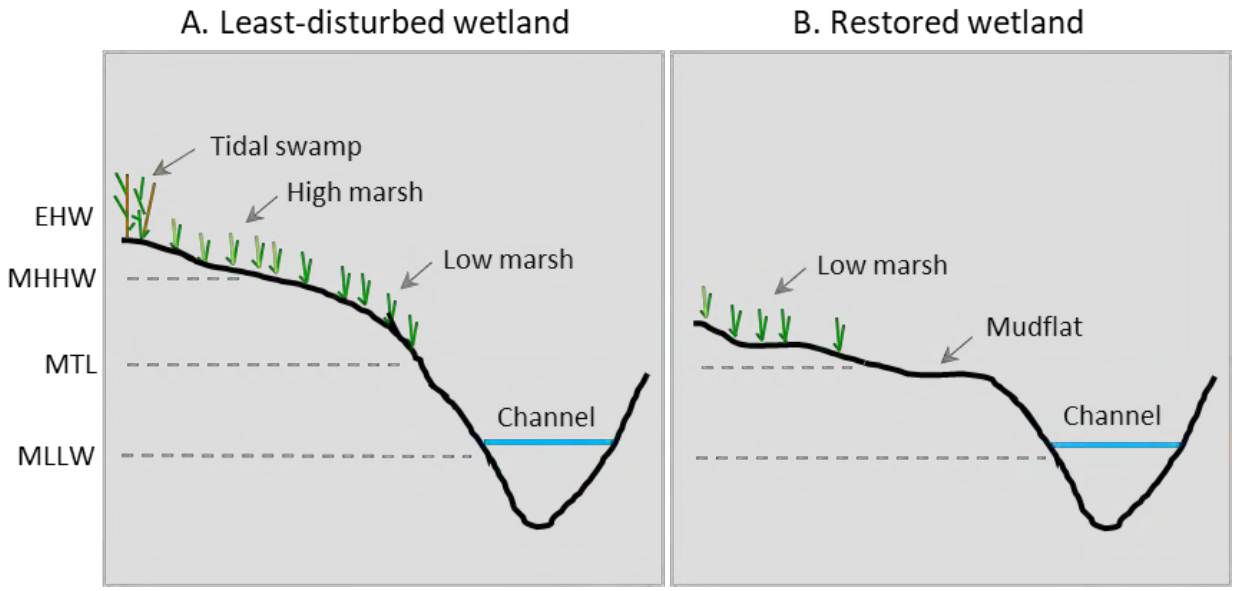

Figure 2.1. Typical elevation profiles of tidal wetlands in the Pacific Northwest with respect to tidal datums. (A) A hypothetical least-disturbed tidal wetland with a gradient of vegetated habitats from low and high emergent marsh to tidal swamp. (B) A hypothetical profile of a newly restored tidal wetland that is only high enough to support low emergent marsh. EHW = extreme high water, MHHW = mean higher high water, MTL = mean tide level, MLLW = mean lower low water.

To better understand wetland development following dike removal or breaching, and to develop realistic management goals for a given restoration project, it is important to assess the elevation profile of a potential restoration site. For instance, a restored site that has subsided may initially support algae, plants, and invertebrates that are characteristic of low marsh, or it may even be too low for successful vascular plant colonization without first gaining elevation by accretion. In contrast, a site that is relatively high in the tidal frame may be infrequently inundated by tides after restoration and be more likely to retain freshwater species established during the pre-diking period, including invasive species. Although least-disturbed tidal wetlands are generally quite flat due to the depositional processes that form them, wetland elevation may vary within a restoration site due to factors like land use history and construction activities, resulting in a range of vegetation types and/or unvegetated areas (Brand et al. 2012).

Tidal wetlands are geomorphically dynamic ecosystems, with changing elevation in response to variability in local sea levels (Saintilan et al. 2020). Wetlands typically gain elevation by accretion of both mineral and organic matter. Suspended sediment is delivered to the wetland surface by periodic inundation during high tides and by river flow, which then settles on the wetland surface when water velocities slow due to vegetation cover (Davis et al. 2017). Plants also help prevent soil erosion (Taylor et al. 2019). Additionally, plant productivity contributes organic matter, and thus volume, to the soil

column (Callaway et al. 1997, Nyman et al. 2006). Over centuries, many tidal wetlands are believed to have accreted vertically at rates that match long-term rates of sea-level rise (Kirwan et al. 2016a), although more recently an increasing number of wetlands may be losing elevation relative to sea-level due to climate change and other anthropogenic impacts (Blum and Roberts 2009, Cahoon 2015).

Documenting rates of soil accretion and absolute rates of vertical change, especially following the restoration of tidal influence, is important in restoration monitoring to help assess whether a new site is changing at a pace comparable to local rates of sea-level rise. Accretion rate data informs an understanding of overall site development, including the types of plant species anticipated to colonize the site. Additionally, soil accretion is an important determinant of the amount of carbon sequestered by a wetland site, an important function of tidal wetlands (Brophy et al. 2018, McTigue et al. 2019, Peck et al. 2020).

In addition to their elevation relative to local tides, the composition of tidal wetland soils is important for their effect on estuarine biogeochemical processes, and their influence on wetland vegetation and faunal communities. Tidal wetland soils are often highly saturated and low in oxygen. Soil salinities can range from fresh to hypersaline depending on proximity to the ocean, the degree of freshwater inputs from rivers and groundwater flow, and rates of evapotranspiration. Waterlogged saline to brackish soils can create a relatively physiologically stressful environment for vascular plants, but a favorable environment for the long-term storage of high densities of carbon (Mcleod et al. 2011, Kauffman et al. 2020, Peck et al. 2020).

Like tidal wetland elevation and accretion rates, soil properties may be dramatically altered after diking. Some commonly observed impacts include dewatering and compaction of soils and oxidation of organic matter that has accumulated over centuries to millennia (Frenkel and Morlan 1991). The loss of soil organic matter can also affect many other soil physical characteristics such as bulk density, porosity, hydraulic conductivity, and water-holding capacity. These changes can in turn alter soil processes such as nutrient cycling, biological productivity, and carbon dynamics, for example causing the former wetland to become a net producer of greenhouse gases as centuries of stored carbon are released into the atmosphere (Drexler et al. 2009).

Other changes to the soil environment upon conversion of a tidal wetland to non-tidal land uses include biogeochemical changes such as drainage and increased oxygen availability that leads to changes in soil reduction-oxidation potential (redox). With the loss of regular tidal inundation salts may be leached from soil pore water, which may result in methane release from soils that still remain saturated (Poffenbarger et al. 2011). Typically, tidal wetland diking also leads to a decline in pH as regular inundation by more saline water is lost (Portnoy and Giblin 1997).

Restoration of tidal inundation has the potential to reverse the many biogeochemical changes and loss of elevation that often occur with wetland diking and drainage. Elevation can be restored by accretion of mineral sediment and plant root growth which adds to soil volume (Nyman et al. 2006, Cherry et al. 2009). Other soil characteristics such as pH, redox potential, pore water salinity, groundwater dynamics, bulk density, and nutrient and organic matter content may move towards reference conditions once a diked wetland is restored to regular tidal inundation and greater connectivity to the estuarine landscape (Portnoy and Giblin 1997).

Monitoring objectives. Since elevation and soil composition are key drivers of wetland structure and processes, we assessed baseline (2014) and post-restoration (2018) status of wetland surface elevation and soil properties at the SFC project site. We compared these attributes between SFC zones with different land-use/land-cover histories and compared SFC zones with low and high marsh reference sites in Tillamook Bay. We also measured the degree of elevation change between pre-and post-restoration sampling at SFC, and quantified rates of soil accretion twice over a seven year period within SFC and reference sites. In addition to examining differences between land-use/land-cover zones at the

restored site, we also determined how elevation was linked to vertical accretion and changes in soil properties.

Materials and methods

Wetland elevation. We determined wetland surface elevation at SFC and in reference marshes with real-time kinematic global positioning system (RTK-GPS) surveys by measuring the ground surface at replicate plots where we also assessed vegetation composition (n = 173; see Chapter 5 for vegetation results). We used Trimble R8 and Spectra Physics GPS rovers connected to the Oregon Real Time GPS Network (ORGN) which provided real-time position correctors. Elevation data were measured in the North American Vertical Datum of 1988 (NAVD88) with the geoid12A model. We generally occupied each measurement location for 10 seconds. Vegetation plots were distributed randomly within land-use/land-cover zones throughout SFC and therefore provide a good representation of the overall wetland surface elevation of each zone.

We re-measured wetland elevation during the post-restoration monitoring period in 2018 at most of the original vegetation plots (n = 166). We navigated to the approximate location of each plot using a hand-held Garmin GPS (original plot locations were not physically marked in the field in 2014). We resurveyed wetland elevation, and then compared horizontal positions in 2018 with values in 2014. This post hoc comparison showed that the majority of plots (n = 100) were resampled to within 3 m of the location measured in 2014. We computed the elevation change between 2018 and 2014 at these 100 plots and assessed the degree of elevation change between SFC zones and low and high reference marsh. Other techniques such as surface elevation tables (Cahoon et al. 2012), or repeated laser leveling from a stable benchmark (Hensel and Cain 2018) are typically better suited to more precisely measure elevation change in tidal wetlands at the mm-scale, but the large sample size in our RTK data set allowed us to tentatively assess elevation change broadly at SFC.

To convert NAVD88 values measured by RTK-GPS into a vertical datum more relevant to tidal inundation, we used a scaled elevation metric, $z^* = (z - MTL)/(MHHW - MTL)$, where z was the measured NAVD88 elevation at a given point, MTL was local mean tide level, and MHHW was local mean higher high water (all in meters relative to NAVD88; Swanson et al. 2014). We obtained NAVD88 values for MTL and MHHW from data published for a temporary NOAA tide gauge station located at Dick Point in southern Tillamook Bay and for tidal benchmark 943 7381 A associated with the gauge (BBDB44 in the OPUS database of the National Geodetic Survey(NGS)).

We validated RTK-GPS rover performance in the field by conducting additional measurements on stable benchmarks in the Tillamook Bay area, particularly benchmark 943 7831 A. These measurements confirmed that the rovers and real-time connection to ORGN were providing accurate and precise data (Table 2.1).

We compared differences in wetland surface elevation between the five land-use/land-cover zones at SFC and two types of reference marshes for both the pre-and post-restoration sampling periods with Kruskal-Wallis tests (one-factor non-parametric ANOVA; datasets had highly unequal variances so we used a non-parametric test). We conducted Dunn's test of pair-wise means comparisons using package "FSA" in R v3.5.0. We computed the magnitude of elevation change between sampling periods by subtracting 2014 values from 2018 data and then calculating the mean and 95% confidence intervals of elevation change for each land-use/land-cover zone. Values with confidence intervals that did not include zero were interpreted as significant change.

Table 2.1. Summary of RTK GPS elevation measurements (in meters relative to NAVD88) at three stable benchmarks in Tillamook Bay. Replicate measurements to determine means and standard deviation (SD) were usually conducted hours or days apart to account for changes in satellite geometry. Published elevation data for Dick Pt. was from the NGS OPUS database, and for Boquist Rd. from an NGS datasheet.

			Elevation measurements (m, NAVD88)				
Benchmark	RTK rovers	Years measured	RTK mean	RTK SD	Range	n	Published elevation
7540A (Garibaldi)	Trimble R8, Spectra Physics	2017-2018	4.456	0.009	0.031	9	NA
943 7381 A (Dick Pt.)	Trimble R8	2018	4.015	0.012	0.043	11	4.027
E48 (RD0994; Boquist Rd.)	Trimble R8	2018	5.183	0.005	0.009	3	5.175

Soil accretion. We used the feldspar marker horizon technique (Cahoon and Turner 1989) to quantify annual rates of soil accretion at SFC and reference marshes. Using GIS, we randomly determined replicate plot locations in four of the five land-use/land-cover zones at SFC (we did not establish plots in the grazed zone due to potential for disturbance by roaming cattle before restoration) and in both low and high-elevation reference marshes (Table 2.2; Figure 2.2). These plots were co-located with other monitoring activities, as described in the SFC monitoring plan (Brophy and van de Wetering 2014). During fall 2013, prior to restoration activities at SFC, we established an accretion plot at each selected location by marking the four corners of a 1.0 m^2 plot with 0.5 inch diameter PVC pipe inserted into the soil ("a" plots). At each plot we deposited approximately 2.7 kg of white feldspar material on the soil surface to form a marker horizon layer approximately 0.5-1.5 cm thick in the center 0.25 m^2 area inside the larger 1.0 m^2 plot (Brophy et al. 2017; Figure 2.3). The field team minimized disturbance to existing vegetation while adding the feldspar, and marked a wide perimeter around the 1.0 m^2 plots with tall PVC poles (and in some cases, temporary plastic fencing) to prevent disturbance by machinery during restoration activities. Using RTK-GPS, we determined the ground surface elevation at the edge of each 1.0 m^2 plot.

During early October 2018, 4.9 years after plot establishment, we sampled soils in the accretion plots by removing 1-3 soil wedges from the central 0.25 m^2 area with a knife (Figure 2.3). These same plots were also sampled in 2014 (see Brown et al. 2016) and in 2017 (see Brophy et al. 2018) yielding estimates of accretion over shorter time spans. In 2017, comparison of the knife method with the cryocoring method of sampling soils suggested that both yielded comparable data (Brophy et al. 2018). On each soil wedge we measured the distance between the top of the wedge and the top of the feldspar layer on all sides that showed distinct layers (up to four sides per wedge), averaged those measurements, and then averaged values from all wedges sampled from each plot. We divided the average deposition by the time elapsed since plot establishment (4.9 yr) to determine an annual average accretion rate.

At the time of the 2018 sampling, we also established a second set of accretion plots ("b" plots), each typically located about 2 m away from the original plots established in 2013. The addition of these plots was prompted by the 2017 sampling which suggested that feldspar layers at some of the original "a" plots, especially at SFC, were not adequately established. As with "a" plots, we staked out a 1.0 m^2 plot with PVC and deposited a feldspar layer in the center 0.25 m^2 of the plots. However, in contrast to the establishment of "a" plots, we more thoroughly removed dead plant matter, and sometimes fibrous root mats, present on the soil surface in order to ensure that a better layer was established. Using RTK-

GPS, we measured the elevation of the wetland surface at the edge of both the original “a” and new “b” accretion plots in fall 2018.

In summer 2020, we sampled most of the “b” accretion plots established in 2018. As before, we used a knife to cut a small wedge from one or more positions within the 0.25 m^2 central portion of the plot and measured the vertical length of accreted soil above the feldspar layer on up to four sides of the wedge. Although covering a shorter periods than data from the “a” plots, the 2020 sampling at “b” plots provided data on accretion rates during just the post-restoration period.

We compared annual vertical accretion rates between SFC zones and reference marshes with one-factor ANOVA for both the 2018 and 2020 sampling after checking for heterogeneity of variances with Levene’s test. Due to a smaller sample size from some SFC zones for the “a” plot sampling in 2018, we combined data from the north, middle, and south zones into one group of samples (labeled “NMS” herein) and compared those rates with the cropped zone at SFC and with low and high reference marshes (all of which had higher sample sizes). For the 2020 sampling, we had higher sample sizes and compared rates among low reference marsh, high reference marsh, and four SFC zones. No data were available for the grazed zone since accretion plots were not established there in 2013 or in 2018. We tested for pair-wise differences among mean soil accretion among zones with Tukey’s HSD test at $\alpha = 0.05$ using package “lsmeans”. For both time periods over which annual accretion rates were determined, we used linear regression to test whether accretion rates varied with wetland surface elevation (z*). We conducted separate analyses for plots from SFC and reference marshes due to their different histories. We conducted all accretion rate analyses with R v3.5.0-3.6.2.

Table 2.2 Number of soil accretion plots established in 2013 (“a” plots) and in 2018 (“b” plots) and successfully sampled in 2018 (“a” plots) and in 2020 (“b” plots) at SFC and in reference wetlands.

Wetland site and zone	"a" plots established in 2013	"a" plots sampled in 2018	"b" plots established in 2018	"b" plots sampled in 2020	Example dominant vegetation at time of "a" plot establishment
Reference low marsh (LM)	5	5	5	4	*Carex lyngbyei*
Reference high marsh (HM)	6	5	6	6	*Deschampsia cespitosa* , *Potentilla anserina* , *Phalaris arundinacea*
SFC, north zone (N)	5	4	5	4	*P. arundinacea* , *Impatiens capensis* , *Oenanthe sarmentosa*
SFC, middle zone (M)	10	1	10	5	*P. arundinacea* , *Carex obnupta*
SFC, south zone (S)	2	1	2	2	*Lotus corniculatus* , *C. obnupta* , *Epilobium ciliatum* , *P. arundinacea*
SFC, cropped zone (CR)	10	6	9	5	*P. arundinacea* , *Schedonorus arundinaceus* , *Holcus lanatus* , *Agrostis stolonifera*
SFC, grazed zone (GR)	0	0	0	0	NA

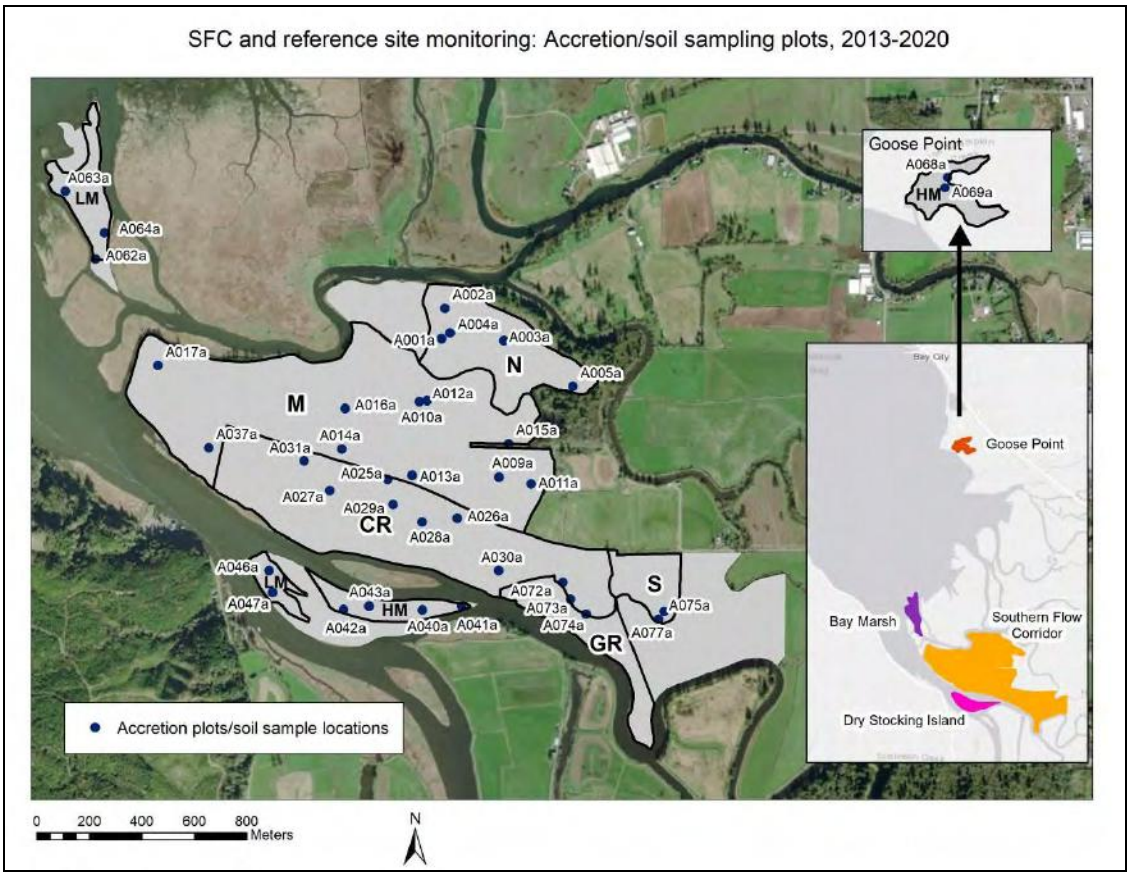

Figure 2.2. Locations for soil accretion plots and soil sampling for 2013-2020 at SFC and reference sites. Not all plots were monitored in each sample year; see report for details. Land use zones are shown (N, M, CR, S, GR, LM, HM). Background: ESRI World Imagery.

Figure 2.3. (A) Establishment of a feldspar marker horizon layer inside a 1.0 m^2 plot in 2013, and (B) example of a sediment wedge collected in 2018 to measure accretion 4.9 years after plot establishment. Photos by C. Janousek.

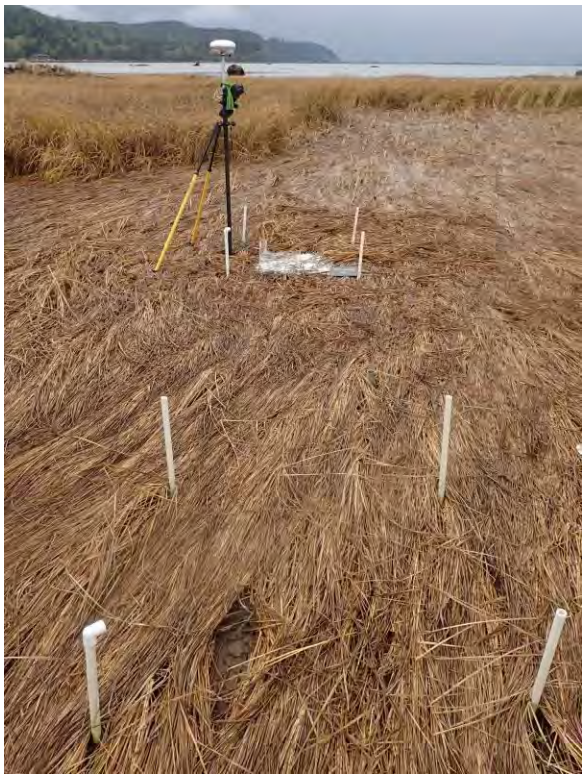

Figure 2.4. Establishment of a feldspar marker horizon layer in a "b" plot in 2018 (background) at one of the low marsh reference sites a few meters away from the older "a" plot established in 2013 (foreground). An RTK rover was used to measure wetland surface elevation at the edge of the plot. Photo by C. Janousek.

Soil characteristics. To quantify soil characteristics at SFC and reference marshes, we sampled surface soils (to about 15-20 cm depth) in the vicinity of each soil accretion plot. We sampled soils during summer of 2014 and summer of 2018 at the time of vegetation surveys (Chapter 5). Near each accretion plot, we used a soil auger or hand spade to collect and pool sub-samples from 3-8 haphazardly-chosen locations dispersed around the accretion plot. We sent samples to analytical labs for analysis of organic matter content, pH, and conductivity (AgSource laboratory for 2014 samples; Oregon State University's College of Agricultural Sciences analytical laboratory for 2018 samples). Organic matter content (%OM) was determined by loss-on-ignition (360°C for 2 hr in 2014; 385°C for 18 hr in 2018) by the labs, and we then converted these values to estimates of percent carbon by using the following equation from Peck (2017): $\%C_{org} = 0.29*\%OM + 0.0021*\%OM^2$. In 2014, soil electrical conductivity was measured with a 1:2 soil:water preparation. In 2018 soil pH and conductivity was measured with a Hanna benchtop meter on a 1:1 soil:water preparation. We converted conductivity to salinity using the equation in Fofonoff and Millard (1983).

We used one factor ANOVA (or non-parametric Kruskal-Wallis tests for data sets with unequal variances) to analyze differences in soil characteristics between SFC zones and low and high reference marsh during both the pre-restoration and post-restoration periods. Following each main test, we also conducted pair-wise tests of differences between land-cover/land-use zones (Tukey's HSD test for parametric analyses; Dunn's test for non-parametric analyses) for both the pre- and post-restoration

sampling periods. To assess temporal change in each soil parameter over time, we calculated the difference between 2018 and 2014 values at each accretion plot and computed the mean difference (and 95% confidence intervals) for each wetland zone. For positive differences with confidence intervals that did not cross zero, we concluded there was a significant increase in that parameter following restoration. We also tested whether the degree of change between pre- and post-restoration sampling periods was correlated with wetland elevation by regressing the magnitude of change on pre-restoration elevation measured at the accretion plots. We conducted soil composition analyses in R 3.5.0.

Results and discussion

Wetland elevation. Wetland elevation varied during the pre-restoration sampling period between reference low and high marsh and different land-use/land-cover zones at SFC (Figure 2.5A; Appendix Table A2.1; Kruskal-Wallis test, $\chi^2 = 88.7$, df = 6, $P < 0.0001$). At SFC, the median elevation of all five land-cover/land-use zones during the pre-restoration monitoring period was below local MHHW. However, elevation varied; the north and grazed zones tended to have the highest elevation and the cropped zone had the lowest median elevation, similar to reference low marsh. Consistent with the intended sampling design for reference sites, reference low marsh occurred below local MHHW ($z^* < 1$) while high marsh occurred above MHHW.

During the post-restoration sampling period in 2018, overall differences in wetland surface elevation between zones persisted (Figure 2.5B; Appendix Table A2.1; Kruskal-Wallis test, $\chi^2 = 89.5$, df = 6, $P < 0.0001$). Low and high reference marsh were below and above MHHW respectively, while all SFC zones still had a median elevation below local MHHW indicating that they began development as restored tidal wetland sites at elevations similar to reference low marsh. In the early post-restoration monitoring period, the north and grazed zones were again highest in elevation, and the cropped zone was lowest in elevation within SFC.

We used 100 elevation measurements across SFC and reference wetlands to examine the degree of elevation change between the pre- and post-restoration monitoring periods (data from plots sampled within 3 m of the same location in both years were included). Most land-use/land-cover zones when considered individually did not show significant change in elevation between sampling periods as indicated by confidence intervals that overlapped zero (Figure 2.6). However, when pooling all data from reference marsh (n = 28) and SFC (n = 72) there was a median increase in elevation at SFC of 3.2 cm, and a median decrease in elevation in reference marshes of 2.8 cm, which was a small, but statistically significant difference between wetland types (Kruskal-Wallis test, $\chi^2 = 23.0$, df = 1, $P < 0.0001$).

We also tested whether the degree of elevation change observed between 2014 and 2018 as measured by RTK-GPS was correlated with pre-restoration elevation relative to the tide frame. In reference marshes, elevation change was more negative at higher elevations ($R^2_{adj} = 0.21$, $P = 0.008$), suggesting slight elevation loss, but at SFC where our sample size was larger, there was no relationship between elevation change and pre-restoration elevation ($R^2_{adj} = -0.01$, $P = 0.84$; Figure 2.6).

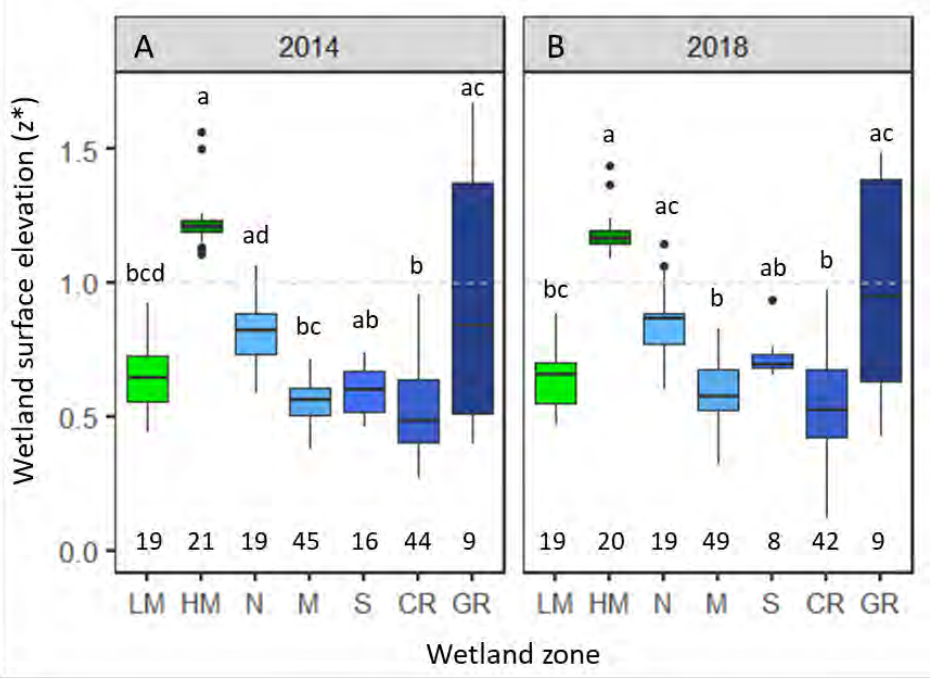

Figure 2.5. Differences in wetland surface elevation by land-use/land-cover zone at SFC and reference marshes in the pre-restoration sampling period in 2014 (A), and the post-restoration sampling period in 2018 (B). Numbers at the bottom of the panels show sample sizes. In this and subsequent boxplot figures in this chapter, the horizontal line represents the sample median, the upper and lower extent of the boxes are the 25% and 75% quartiles of the distribution, whiskers represent 1.5 times the interquartile range, and points represent outliers. Box plots sharing the same letter within each panel are not statistically different from each other.

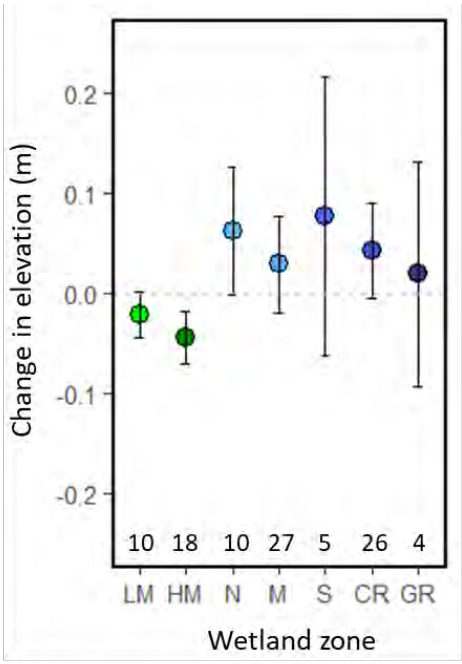

Figure 2.6. Change in wetland surface elevation (means ± 95% confidence intervals) between pre- and post-restoration sampling periods by wetland land-use/land-cover zone. Numbers at the bottom of the figure show sample sizes for each land-use/land-cover zone. Zones with error bars that do not cross zero show significant change between sampling periods.

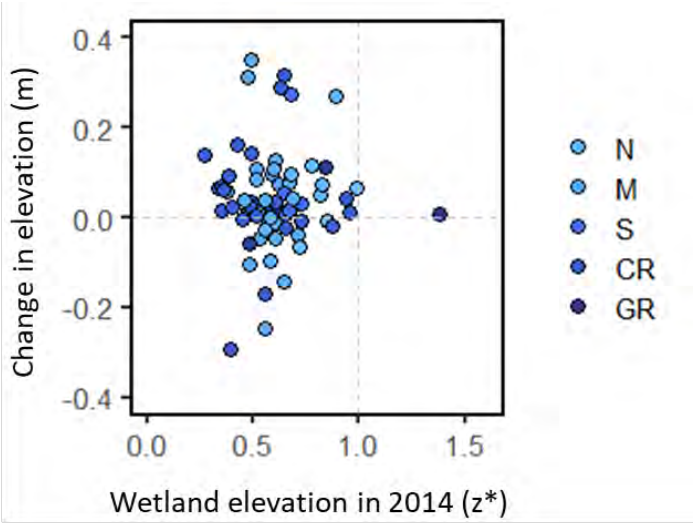

Figure 2.7. Estimated change in wetland surface elevation (in meters) in five land-use/land-cover zones at SFC as a by pre-restoration wetland elevation (z*).

Our RTK measurements tentatively suggest some elevation gain at SFC (and elevation loss within reference marshes) between 2014 and 2018, but we caution that our method was not ideal for this analysis. For instance, we were not able to re-sample the exact locations measured in 2014, and RTK-GPS methods typically can have up to several cm of vertical error for individual measurements. Other methods such as surface elevation tables or laser leveling are more precise approaches for detecting elevation change at the sub-cm level (Cahoon et al. 2002; Cain & Hensel 2018) and would be advisable for long-term detection of elevation change. However, RTK-GPS may successfully detect elevation gain or loss that exceeds typical RTK error (~5 cm), such as observed in San Pablo marsh in northern San Francisco Bay (Thorne et al. 2013).

Comparison of pre-restoration elevation data at SFC with high marsh led Brown et al. (2016) to conclude that the various areas of SFC may have lost between 30 and 78 cm of elevation between diking and restoration (assuming SFC previously had an elevation similar to recent high marsh elevations). This large disparity between reference high marsh and SFC was confirmed in our elevation sampling in 2018. This range of estimated elevation loss at SFC is consistent with other estimates for the Oregon coast (Table 2.3).

Vertical soil accretion. From 2013 to 2018, a period spanning both pre-and post-restoration periods at SFC, there were differences in annual vertical soil accretion rates among reference wetlands and SFC zones ($F_{3,18} = 11.8$, $P = 0.0002$; Figure 2.8A; Appendix Table A2.2). Accretion rates were highest in the cropped zone at SFC (mean = 12.2 mm yr^{-1}) and lowest in reference high marsh (mean = 2.8 mm yr^{-1}). Reference low marsh and the other measured zones at SFC (north, middle, and south zones combined) had intermediate rates of soil accretion (6.3 mm yr^{-1} and 8.0 mm yr^{-1} respectively).

From 2018 to 2020, during the post-restoration period, accretion rates at SFC tended to be somewhat lower than values calculated during the 2013-2018 period (Appendix Table A2.3). However, rates still varied by wetland zone during this period, much as they did between 2013 and 2018 ($F_{5,20} = 17.4$, $P = 0.0004$; Figure 2.8B). Rates were higher in the north and middle zones (and marginally, but not significantly, higher in reference low marsh and the cropped zone) than in reference high marsh. The greatest difference in accretion rates between the 2013 to 2018 and 2018 to 2020 periods was in the cropped zone where rates declined from a mean of 12.2 mm yr^{-1} to 4.2 mm yr^{-1}.

Table 2.3. Estimates of elevation loss from other former tidal wetlands in Oregon that have been restored.

Estuary, state	Restored site	Diked period	Pre-diking wetland type	Intervening land use	Restoring wetland type	Elevation change (cm)	Reference
Coquille, OR	Ni-les'tun	<1939 - 2011	Emergent marsh	Ag use	Emergent marsh	-30 to -60	Brophy et al. 2014
Coos Bay, OR	Kunz marsh	early 1900s-1996	High marsh	Ag use with ditches	Emergent marsh	up to -80	Cornu & Sadro 2002
Yaquina, OR	Y27 (phase 1)	<1939 - 2002	Tidal swamp	Ag then muted tidal marsh	Emergent marsh	-30 to -91	Brophy 2004
Salmon River, OR	Various	1961 - 1978	Emergent marsh	Ag then muted tidal marsh	Emergent marsh	-30	Frenkel & Morlan 1991
Siuslaw River, OR	S59	<1939 - 1996	Tidal swamp	Ag then muted tidal marsh	Emergent marsh	-61 to -91	Brophy 2009
Siuslaw River, OR	S65	<1939 - 2007	Tidal swamp	Pasture	Tidal swamp	~0	Brophy 2009

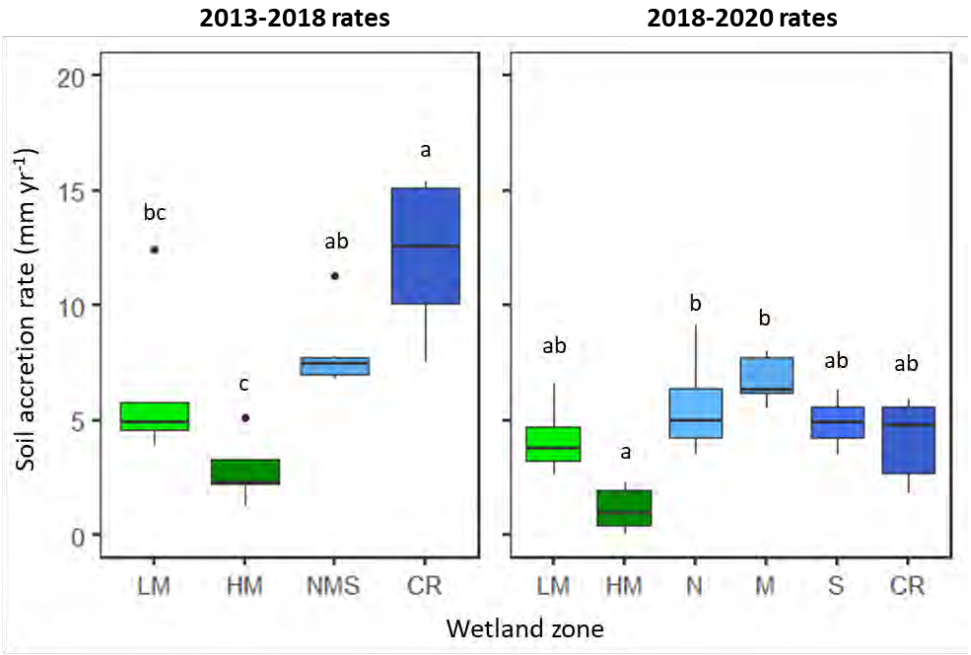

Figure 2.8. Boxplots of differences in annual sediment accretion rates by wetland zone estimated with feldspar marker horizon plots during the (A) 2013-2018, and (B) 2018-2020 periods. LM = reference low marsh, HM = reference high marsh, CR = cropped zone at SFC, N = north zone at SFC, M = middle zone at SFC, S = south zone at SFC, and NMS = combined samples from the north, middle, and south zones at SFC.

In general, soil accretion rates were lower in higher-elevation areas of both SFC and reference wetlands. During the 2013-2018 sampling period, there was a trend towards a negative relationship between elevation and accretion rate in reference marshes (R^2_{adj} = 0.17, P = 0.13, n = 10; Figure 2.9A) and a statistically significant negative relationship at SFC (R^2_{adj} = 0.49, P = 0.007, n = 12; Figure 2.9B), indicating that lower areas were accreting more rapidly. During the 2018-2020 sampling period, there was similarly a negative elevation-accretion relationship in reference marshes (R^2_{adj} = 0.63, P = 0.007, n = 9; Figure 2.10A), and a non-significant trend for a similar relationship at SFC (R^2_{adj} = 0.20, P = 0.09, n = 11; Figure 2.10B).

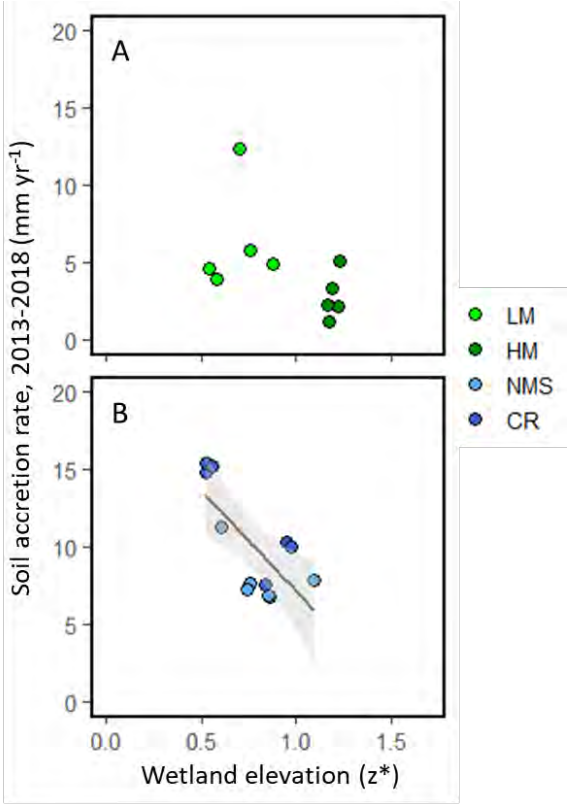

Figure 2.9. Differences in soil accretion rates during the 2013-2018 period as a function of wetland surface elevation (z* measured during the pre-restoration sampling period) in (A) reference marshes, and (B) SFC zones. "NMS" represents pooled samples from the north, middle, and south zones at SFC.

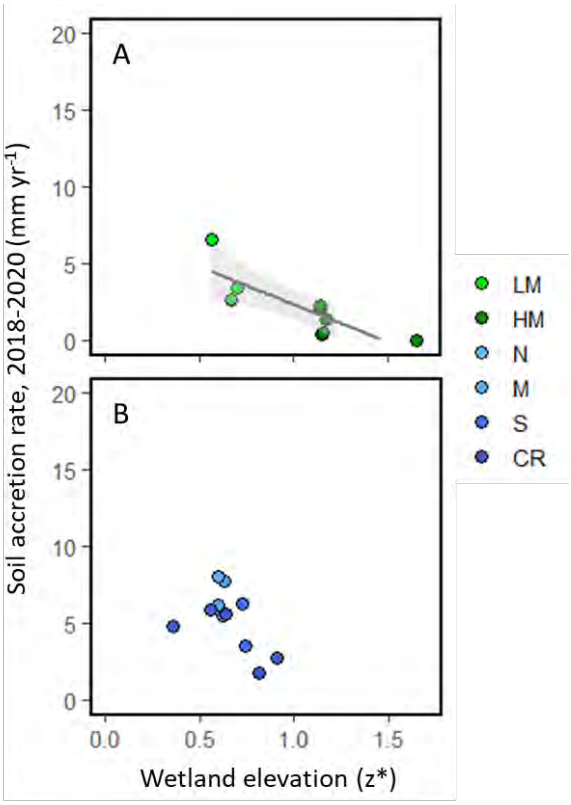

Figure 2.10. Differences in soil accretion rates during the 2018-2020 period as a function of wetland surface elevation (z* measured during the pre-restoration sampling period) in (A) reference marshes, and (B) SFC zones.

Soil accretion rates have been assessed in other restoring tidal wetlands along the west coast of the United States, which provide sources of comparison with early rates of change at SFC. At the Six Gill Slough restoration site in the Nisqually River Delta in Washington, Drexler et al. (2019) measured accretion rates of 7.9 mm yr^{-1}, about twice that of a higher elevation reference marsh. Farther north in the Salish Sea, Poppe and Rybczyk (2019) measured average net elevation change of +27.4 mm yr^{-1} using SETs at a restoration site in the Stillaguamish Estuary in northern Washington (restored site rates were nearly three times higher than their reference site). In a project in San Pablo Bay near San Francisco, California, Grismer et al. (2004) found rates of 7-8 mm yr^{-1} in a reference salt marsh dominated by *Salicornia pacifica*, while observing even higher rates in nearby restoring low elevation sites along the Napa River that were former salt ponds (24 mm yr^{-1}; Brand et al. 2012). Data from SFC and other west coast restoration projects show that restored sites typically have larger accretion rates than reference wetlands, findings that have implications for how much carbon restored sites may be able to sequester (Drexler et al. 2019) and whether their rate of vertical growth can keep pace with future sea-level rise. However, we note that the choice of reference wetland for comparison with a restored project is important for interpretation, since SFC rates roughly matched low reference marsh rates, but were much higher than high reference marsh rates. Monitoring both low and high marsh reference sites provided results useful for interpreting accretion rates in this study.

Greater vertical accretion rates in lower elevation tidal wetlands have been observed for both restored (Garbutt et al. 2006), and least-disturbed wetlands in other estuaries (Leonard 1997, Callaway et al. 1997), consistent with our results. Because lower elevation wetlands are inundated with water containing suspended sediments for longer, mineral soil deposition is expected to correlate with

elevation (Fagherazzi et al. 2012). At SFC, the cropped zone in particular was relatively low in the tidal frame (comparable to reference low marsh), and it showed high accretion rates, particularly during the 2013-2018 sampling period when post-restoration sediment movement may have been particularly pronounced.

Feldspar marker horizons are well suited to measure soil accretion rates over shorter time scales, but longer-term values are also insightful. Brophy et al. (2018) conducted decadal-scale estimates of soil accretion rates in Tillamook Bay reference wetlands and SFC by radio-isotope dating of downcore profiles of excess ^{210}Pb. While small in number, these cores were generally collected in the vicinity of several feldspar marker horizon plots, enabling a comparison of accretion rates by both methods (Table 2.4). A number of accretion values measured with ^{210}Pb were lower than values from monitoring of feldspar plots (consistent with the fact that there is more soil compaction measured on the longer time scales of radioisotope dating), but a few rates are higher. Both methods tend to confirm that there are higher accretion rates in low reference marsh than in high reference marsh. More broadly across Oregon tidal wetlands, recent decadal-scale measurements suggest that high marsh accretion rates are in the range of 0.8 to 4.1 mm yr^{-1} (Peck et al. 2020).

We were unfortunately unable to collect reliable data from a number of accretion plots established in 2013 at SFC ("a" plots), particularly those established in dense stands of reed canarygrass (*Phalaris arundinacea*), an invasive species. It is likely that the thick mats of fibrous roots in this species, which intergrade with surface soils, prevented establishment of a cohesive feldspar layer during the pre-restoration period. For example, in several samples taken from SFC plots in 2018, we observed flecks of feldspar in the cored samples, but not a discrete feldspar layer. To ensure adequate replication of feldspar marker horizon layers for future sampling at SFC, we established the set of "b" plots in 2018 (Figure 2.4). We were able to obtain reliable feldspar layers from the majority of "b" plots during 2020 sampling, although root growth or other factors may have prevented establishment or sampling of good feldspar layers in some cases.

Our elevation and accretion rate analyses suggest that SFC may be gaining elevation early in restoration. During the first several years of restoration we anticipated and observed substantial re-distribution of sediments, especially given major modifications and disturbance at the site including levee removal, channel excavation, and use of heavy machinery throughout the site to implement restoration actions.

We anticipate that the SFC site will continue to accrete and gain elevation over time, especially in lower elevation areas that are inundated more frequently. The growth of emergent vegetation (see Chapter 5), is likely to promote trapping of suspended sediment particles, and help facilitate vertical wetland growth. With sufficient sediment supply from the watershed (Tillamook, Trask and Wilson Rivers), SFC may reach mid- or high-elevation tidal marsh within several decades. However, lack of sediment supply as observed in other regions can lead to tidal wetland drowning (Blum and Roberts 2009). Restoration sites with lower accretion rates may take more than 50 years to gain elevation rendering them similar to reference wetlands (Diefenderfer et al. 2008). Further study is needed of the year-to-year variation in accretion rates (and how those relate to interannual variability in precipitation and storms), and whether spatial variation in accretion rates could be due to differences in plant composition or other factors (Leonard et al. 2002).

Table 2.4. Comparison of accretion rate estimates by feldspar marker horizons measured during two time periods, with decadal-scale ^{210}Pb radioisotope dating at nearby coring locations (from Brophy et al. 2018) at SFC and reference marshes. Feldspar plot standard deviations (SD) are based on two to three cores per 0.25 m^2 plot; ^{210}Pb standard errors (SE) are based on estimates of variance in the slope of excess ^{210}Pb concentration with depth.

Plot	Wetland zone	Feldspar accretion rate (mean ± SD), 2013-2018 (mm yr^{-1})	Feldspar accretion rate (mean ± SD), 2018-2020 (mm yr^{-1})	^{210}Pb accretion rate (mm yr^{-1})
A004	N	7.6	9.1	6.0 ± 0.7
A009	M	NA	6.2	1.2 ± 0.5
A043	HM	1.2 ± 0.1	1.4 ± 1.6	2.6 ± 0.4
A047	LM	3.9 ± 1.4	2.6 ± 1.0	>18
A063	LM	12.4 ± 0.4	3.4	10.0 ± 3.0
A064	LM	4.9 ± 0.9	NA	2.2 ± 0.2
A068	HM	3.3 ± 1.6	2.1 ± 1.7	2.2 ± 0.3

Soil composition. Carbon content in surface soils at SFC prior to restoration ranged from 5.8% in the south zone to 7.8% in the cropped zone (Figure 2.11A; Appendix Table A2.4). There was a similar range of carbon content in reference marsh soils at this time and no significant difference across SFC zones and reference wetlands (one factor ANOVA, $F_{5,32} = 1.5$, $P = 0.27$). During the post-restoration sampling period, soil carbon content remained at similar levels and did not differ among land-use/land-cover zones (Figure 2.11B; one factor ANOVA, $F_{5,28} = 0.7$, $P = 0.63$). Comparing carbon content between pre- and post-restoration sampling periods, there was not a significant change in any of the SFC zones or in reference wetlands (Figure 2.11C).

Although changes in land use activities following conversion of a tidal wetland can lead to loss of soil organic matter and carbon content (MacClellan 2011), we did not observe this specific impact of wetland conversion at SFC, at least for near-surface soils. One possible reason for this lack of carbon loss at SFC may be its relatively high plant cover and biomass (observed in pre-restoration sampling; see Chapter 5) that preserved organic matter content. Pre-restoration land use type and intensity varied across SFC before restoration, but even the more intensively managed cropped zone retained comparatively high organic matter content. Relatively high soil carbon content was also observed in two tidal wetland restoration sites in the Siuslaw Estuary in central Oregon (6.3-19.7%), generally overlapping the range of values measured at three reference wetlands (Brophy 2009).

Given that SFC soils had organic matter content similar to reference wetlands just prior to restoration, we don't anticipate major changes as restoration progresses. However, high soil accretion rates coupled with relatively high carbon content could enable the SFC site to sequester large quantities of new organic carbon (Brophy et al. 2018; also see Chapter 9). The carbon sequestration potential of other restored and created tidal wetlands has been quantified (Abbott et al. 2019), and high sequestration rates at SFC could be a valuable ecosystem service of the project over the coming decades in addition to its value for flood protection and fish production. Some degree of sea-level rise (as long as accretion rates are high enough), could even stimulate more organic carbon burial at the site (Rogers et al. 2019, Watanabe et al. 2019).

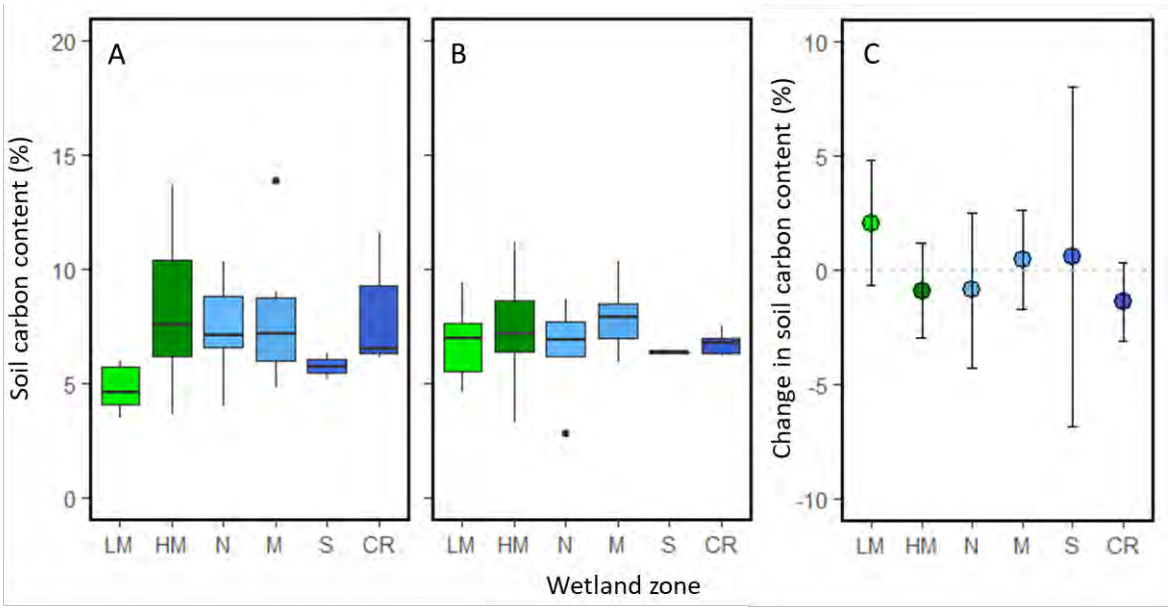

Figure 2.11. Differences in near-surface soil carbon content in low and high reference marshes and four SFC land-use/land-cover zones in 2014 (A) and 2018 (B). Change (mean ± 95% confidence intervals) between 2014 and 2018 in (C). Confidence intervals that cross zero suggest no significant change in soil carbon content between pre- and post-restoration sampling periods.

During the pre-restoration sampling period, near-surface soils in all four SFC zones we examined were fresh (<0.5 ppt; Figure 2.12A; Appendix Table A2.4). In contrast, reference low marsh soils (8.0 ± 0.9 ppt, mean ± SD) and high marsh soils (6.3 ± 1.5 ppt) tended to be in the low mesohaline range during the summer sampling period (Kruskal-Wallis test, $\chi^2 = 25.1$, df = 5, P = 0.0001). Following restoration, soils at SFC generally increased in salinity, becoming mesohaline, such that all SFC zones and reference wetlands had similar salinities by the summer of 2018 (Figure 2.12B; one factor ANOVA, $F_{5,24} = 1.2$, P = 0.32). The increase in salinity from the pre-restoration monitoring period was highest in the middle zone and also significant in the north and cropped zones (Figure 2.11C).

Large changes in soil pH also occurred at SFC following restoration. During the pre-restoration period, SFC soils were more acidic than reference wetlands (Figure 2.13A; Appendix Table A2.4; one-factor ANOVA, $F_{5,32} = 13.0$, P < 0.0001). Soil pH differed by wetland zone in the post-restoration sampling period (Figure 2.13B; one-factor ANOVA, $F_{5,28} = 3.7$, P = 0.02). The middle zone at SFC increased considerably in pH, while other zones at SFC and low reference marsh remained relatively unchanged (Figure 2.13C). Within SFC, increasing soil salinity was correlated with an increase in soil pH (r = 0.74, P = 0.0002; Figure 2.14A), but was not correlated with change in soil carbon content (r = 0.31, P = 0.19; Figure 2.14B).

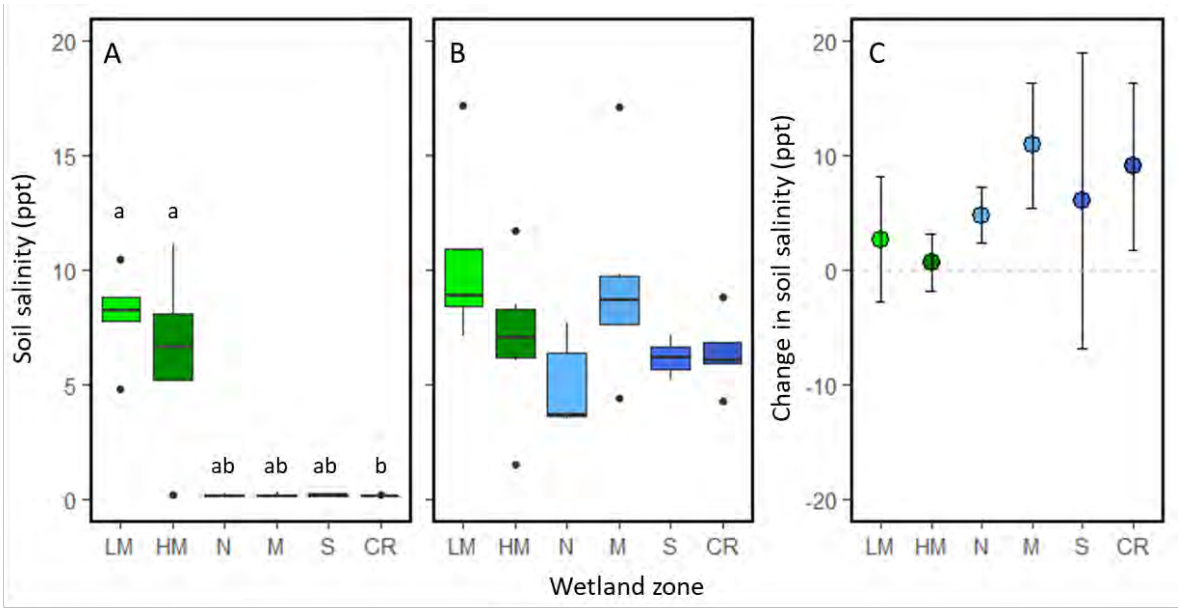

Figure 2.12. Differences in near-surface soil salinity in low and high reference marshes and four land-use/land-cover zones at SFC in 2014 (A) and 2018 (B). Zones sharing letters in A are not significantly different (Dunn's test); there were no significant differences among means in 2018 (Tukey's HSD test). Change (mean ± 95% confidence intervals) between 2014 and 2018 in (C). Confidence intervals that cross zero in C suggest no significant change in soil salinity between pre- and post-restoration sampling periods.

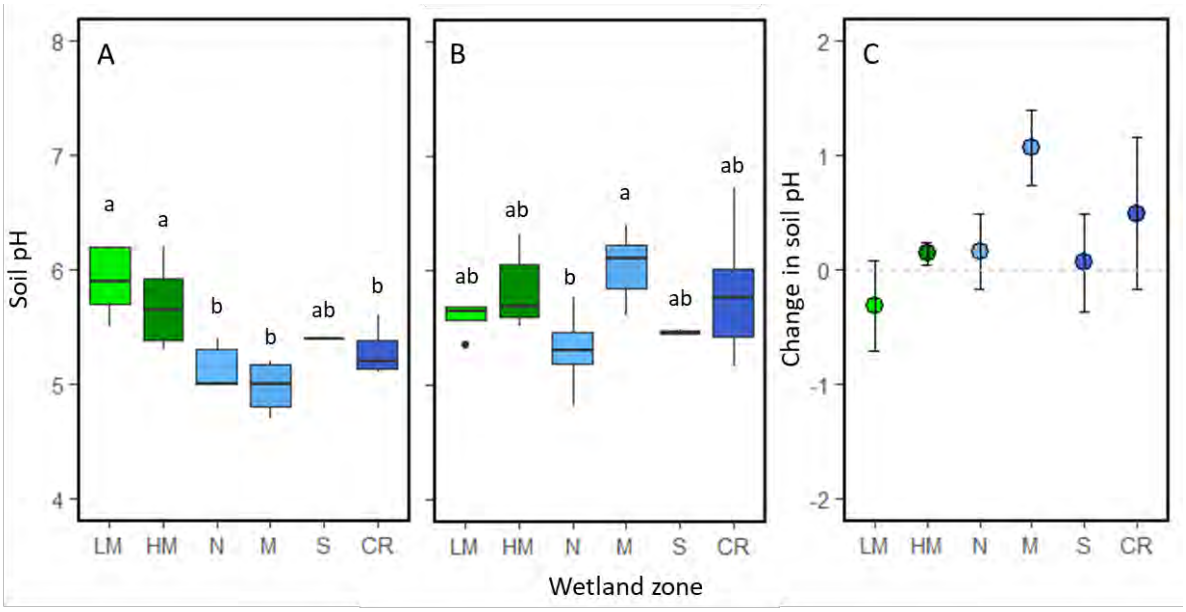

Figure 2.13. Differences in near-surface soil pH in low and high reference marshes and four land-cover/land-use zones at SFC in 2014 (A) and 2018 (B). Zones sharing letters in A and B are not significantly different (Tukey's HSD test). Change (mean ± 95% confidence intervals) between 2014 and 2018 in (C). Confidence intervals that cross zero suggest no significant change in soil pH between pre- and post-restoration sampling periods.

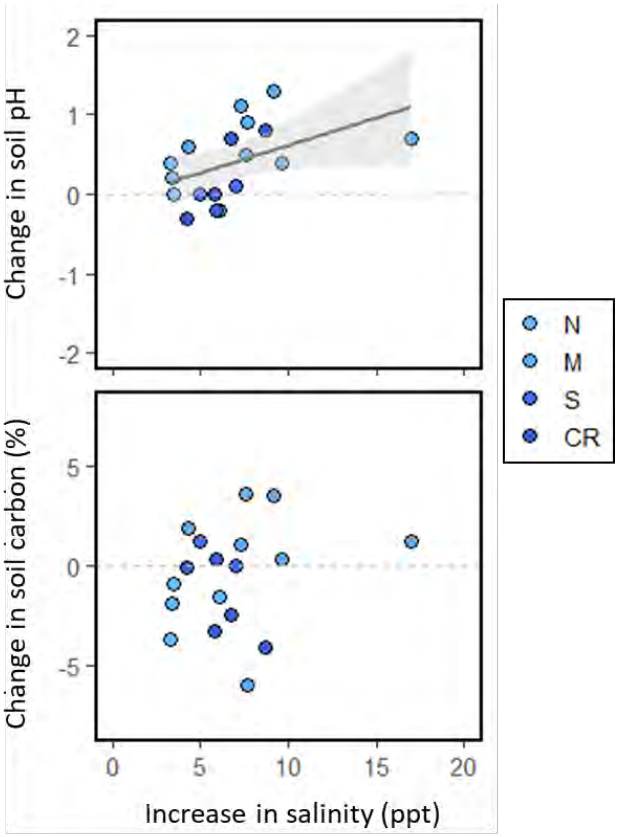

Figure 2.14. Correlations between pre-to-post restoration increases in soil salinity at SFC and change in (A) soil pH and (B) soil carbon content.

Within SFC, wetland elevation was correlated with changes in some soil properties. Pre-to-post-restoration change in soil pH was negatively associated with wetland elevation (R^2_{adj} = 0.59, P < 0.0001; Figure 2.15A), indicating that lower elevation areas had a greater increase in pH following restoration than higher elevation areas. Similarly, the increase in soil salinity following restoration was greatest in lower elevation areas at SFC (R^2_{adj} = 0.36, P = 0.004; Figure 2.15B). Since elevation is inversely related to inundation frequency and duration in tidal wetlands, regular tidal inundation and infiltration of seawater into sediment pore water in lower elevation areas of SFC is the probable cause of rapid change in soil salinity and pH. There was no relationship between elevation and change in soil carbon content (R^2_{adj} = -0.31, P = 0.41).

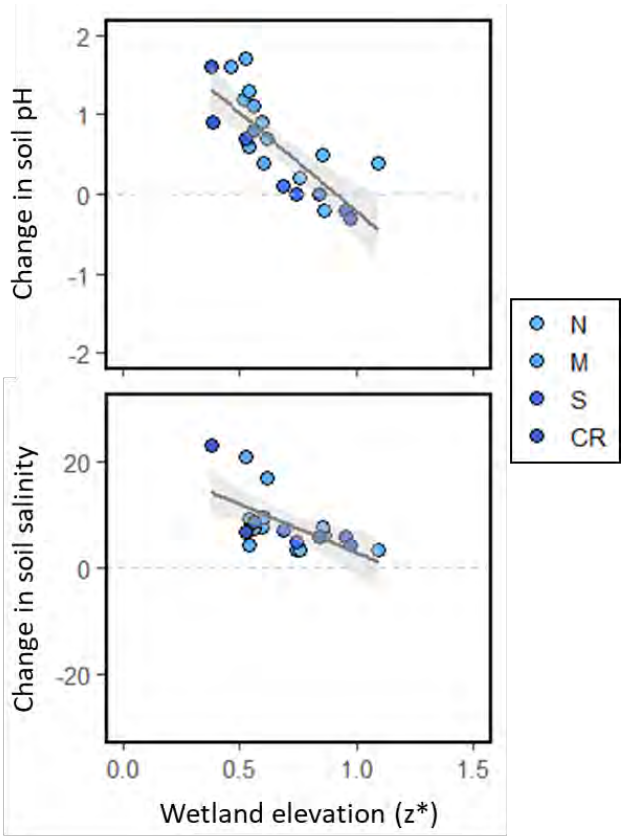

Figure 2.15. Change in pre-to-post restoration soil pH (A) and soil salinity (B) at SFC as a function of wetland elevation (z*). Elevation was measured during the pre-restoration monitoring period. Lines show linear regressions and 95% confidence intervals. Most monitored plots had both higher pH and salinity following restoration, but increases tended to be greater in lower elevation areas of the site.

Our data suggest rapid change in surface soils after dike removal at SFC, but since we did not collect data in the first few months following restoration, the exact pace of change is unknown. The relatively rapid change in soil biogeochemistry however, coincided with a substantial change in wetland vegetation, including marked die-off of reed canary grass (*Phalaris arundinacea*), an invasive plant that was abundant at SFC before restoration was implemented (vegetation change is detailed in Chapter 5). Notably, the degree of change in early site development did vary by land-use/land-cover zone and elevation. Changes in pH, for instance were greatest in the site's middle zone, and salinity increased the most in the middle and cropped zone regions of the site. These areas tended to also be lower in elevation (Figure 2.5), so they would be expected to experience greater inundation during high tides with more time for brackish water to mix into groundwater.

Restoration-associated increases in soil salinity and pH at SFC could affect important soil processes such as rates of organic matter decomposition that in turn affect nutrient re-mineralization, carbon cycling, and rates of carbon sequestration. Organic matter decomposition may be lower in more saline soils (Lane et al. 2016; Janousek et al. unpublished data from San Francisco Bay), but salinity effects may interact with other factors too (Stagg et al. 2018). Higher sediment pH with the resumption of tidal flows may also increase mobilization of cations such as ammonia that could provide a nutrient pulse (potentially transient) to growing plants and microbes (Helton et al. 2019). Finally, more saline soils are also expected to have lower redox potential (Stagg et al. 2018). While we did not document impacts of changes in soil biogeochemistry on nutrient and carbon cycling, restoration projects such as

SFC provide an excellent opportunity to test how evolving soil conditions affect these important wetland processes. Such data would improve our understanding of the net effects of tidal wetland restoration on estuary-wide carbon sequestration and nutrient dynamics.

The increase in salinity we generally observed in SFC soils following restoration is likely to impact an array of wetland organisms as the site develops. Salt-sensitive plants such as freshwater pasture grasses are expected to have reduced growth, or die, and be replaced by more salt-tolerant vegetation typical of Oregon's least-disturbed brackish tidal wetlands (Chapter 5). Similarly, assemblages of bacteria and benthic microalgae (not sampled in this study), and soil infauna (Chapter 7) may change from freshwater-adapted organisms to brackish assemblages.

The impacts of conversion of a tidal wetland to other land uses may persist for a long time, even after restoration. While we documented equivalency (soil carbon content) or rapid recovery (salinity, pH) of several soil parameters at SFC, development of soils characteristic of least-disturbed wetlands may take much longer in some projects. For example, Mossman et al. (2012) found that soil water, redox potential, and organic matter content in restored marshes of 1-17 years age tended to differ from reference conditions. Soil parameters in older "accidently" restored wetlands (unintended dike breaches) tended to be closer to reference sites. In two constructed coastal wetlands in North Carolina, Craft et al. (1999) found that soil carbon and nitrogen content tended to be lower than reference levels 25 years into wetland development. In the Columbia River Estuary, Kidd (2017) found that tidal wetland restoration sites developed similarity to reference sites after 3 to 6 years in characteristics such as species richness, soil organic matter, bulk density, pH, and salinity.

Climate change resilience of SFC. Further monitoring of soil accretion rates and overall net elevation change at SFC and reference wetlands in Tillamook Bay is needed to determine the longer-term capacity for resilience to sea-level rise. Both our feldspar results reported herein and radiometric dating by Brophy et al. (2018) and Peck et al. (2020) in Tillamook Bay suggest that accretion rates at SFC and reference wetlands are generally keeping pace with recent rates of SLR measured for northern and central Oregon (Table 2.5), and that for the time being, the estuary has an adequate sediment supply and a positive rate of vertical land motion. Overall, coastal wetlands in the PNW may be more resilient to SLR in the near term than other areas of the United States (e.g., Cahoon 2015, Thorne et al. 2018), but accelerating SLR or sudden coastal elevation loss associated with a major earthquake along the Cascadia subduction zone could shift wetlands in the region to an elevation deficit.

Long-term sustainability of tidal wetlands in the SFC project (and other tidal wetland sites in Tillamook Bay) is dependent on a number of interacting factors including regional vertical land motion, future rates of future SLR, the availability of accommodation space for landward migration of tidal wetlands, rates of lateral marsh erosion at the bay-ward edge, sediment availability, and sediment trapping efficiency by vegetation (Kirwan et al. 2016b, Sweet et al. 2017, Peck et al. 2020). Of these factors, ensuring that wetlands have room to migrate upslope with SLR and maintaining adequate sediment supply in estuarine watersheds are factors that can be affected by regional management decisions.

To improve the ability of researchers to assess wetland stability over the long-term in Tillamook Bay, we recommend expanding monitoring protocols in its tidal wetlands, so that data are available on the key processes that determine net elevation change. Specifically at SFC and reference sites, we recommend monitoring net elevation change over time (not just near-surface accretion, which does not account for elevation loss due compaction or decomposition deeper in the soil column, or potential tectonic and subsidence effects on elevation). Potential methods for monitoring elevation change include surface elevation tables (SETs; Lynch et al. 2015), or laser-level surveys from stable benchmarks conducted at sub-cm vertical resolution (e.g., Cain and Hensel 2018). During fall 2019, in fact, we established five deep rod benchmarks (Appendix Table A2.5) and potential laser-level survey transects at SFC and two reference sites, but additional funds will be needed to precisely survey mark locations

and begin longer-term elevation monitoring of the wetland surface. When more data are available on net rates of vertical elevation change in tidal wetlands and local rates of relative sea-level change for Tillamook Bay (provided currently at the Garibaldi tide station; tidesandcurrents.noaa.gov) the longer-term sustainability of the region's tidal wetlands can be assessed (Cahoon 2015).

Table 2.5. Historic rates of sea-level rise (SLR) and recent estimates of vertical land movement (VLM) at GPS stations near Tillamook Bay and nearby locations in northern Oregon. SLR data (means ± 95% confidence intervals) are from NOAA (tidesandcurrents.noaa.gov); VLM data (means ± SD) are from Montillet et al. (2018).

Estuary	VLM (mm yr^{-1})	VLM (GPS) station	SLR (mm yr^{-1})	SLR period	SLR station
Tillamook Bay	0.19 ± 0.38	CHZZ	2.58 ± 0.70	1970-2019	Garibaldi, NOAA stn 9437540
Yaquina Bay	-0.22 ± 0.34	P367	1.77 ± 0.66	1967-2019	South Beach NOAA stn 9435380
Lower Columbia	0.23 ± 0.16	TPW2	-0.15 ± 0.32	1925-2019	Astoria NOAA stn 9439040

Citations

Abbott KM, Elsey-Quirk T, DeLaune RD. 2019. Factors influencing blue carbon accumulation across a 32-year chronosequence of created coastal marshes. Ecosphere 10:e02828.

Alvarez MdP, Carol E, Hernández MA, Bouza PJ. 2015. Groundwater dynamic, temperature and salinity response to the tide in Patagonian marshes: Observations on a coastal wetland in San José Gulf, Argentina. Journal of South American Earth Sciences 62:1-11.

Belperio AP. 1993. Land subsidence and sea level rise in the Port Adelaide estuary: Implications for monitoring the greenhouse effects. Australian Journal of Earth Sciences 40:359-368.

Blum MD, Roberts HH. 2009. Drowning of the Mississippi Delta due to insufficient sediment supply and global sea-level rise. Nature Geoscience 2:488-491.

Brand LA, Smith LM, Takekawa JY, Athearn ND, Taylor K, Shellenbarger GG, Schoellhamer DH, Spenst R. 2012. Trajectory of early tidal marsh restoration: Elevation, sedimentation and colonization of breached salt ponds in the northern San Francisco Bay. Ecological Engineering 42:19-29.

Brophy LS. 2004. Yaquina estuarine restoration project: Final report. Report to MidCoast Watersheds Council, Newport, OR. Green Point Consulting, Corvallis, OR, 99 pp.

Brophy LS. 2009. Effectiveness monitoring at tidal wetland restoration and reference sites in the Siuslaw River Estuary: A tidal swamp focus. Report to Ecotrust, Portland, OR. Green Point Consulting, Corvallis, OR, 125 pp.

Brophy, LS, Cornu CE, Adamus PR, Christy JA, Gray A, MacClellan MA, Doumbia JA, and Tully RL. 2011. New tools for tidal wetland restoration: Development of a reference conditions database and a temperature sensor method for detecting tidal inundation in least-disturbed tidal wetlands of Oregon, USA. Report to the Cooperative Institute for Coastal and Estuarine Environmental Technology (CICEET), Durham, NH, 199 pp.

Brophy LS, van de Wetering S, Ewald MJ, Brown LA, Janousek CN. 2014. Ni-les'tun tidal wetland restoration effectiveness monitoring: Year 2 post-restoration (2013). Institute for Applied Ecology, Corvallis, OR, 166 pp.

Brophy LS, van de Wetering S. 2014. Southern Flow Corridor Project Effectiveness Monitoring Plan. Institute for Applied Ecology and Confederated Tribes of Siletz Indians, Corvallis, OR, 28 pp.

Brophy LS, Peck EK, Bailey SJ, Cornu CE, Wheatcroft RA, Brown LA, Ewald MJ. 2018. Southern Flow Corridor effectiveness monitoring, 2015-2017: Sediment accretion and blue carbon. Report prepared for Tillamook County and the Tillamook Estuaries Partnership, Tillamook, Oregon, USA. Institute for Applied Ecology, Corvallis, OR, 58 pp.

Brophy LS, Greene CM, Hare V, Holycross B, Lanier A, Heady W, O'Connor K, Imaki H, Haddad T, Dana R. 2019. Insights into estuary habitat loss in the western United States using a new method for mapping maximum extent of tidal wetlands. PLoS ONE 14:e0218558.

Brown LA, Ewald MJ, Brophy LS, van de Wetering S. 2016. Southern Flow Corridor baseline effectiveness monitoring: 2014. Estuary Technical Group, Institute for Applied Ecology, Corvallis, OR, 215 pp.

Buffington KJ, Janousek CN, Thorne KM, Dugger BD. 2020. Spatiotemporal patterns of mineral and organic matter deposition across two San Francisco Bay-Delta tidal marshes. Wetlands 40:1395-1407.

Cahoon DR. 2015. Estimating relative sea-level rise and submergence potential at a coastal wetland. Estuaries and Coasts 38:1077-1084.

Cahoon DR, Lynch JC, Perez BC, Segura B, Holland RD, Stelly C, Stephenson G, Hensel P. 2002. High-precision measurements of wetland sediment elevation: II. The rod surface elevation table. Journal of Sedimentary Research 72:734-739.

Cahoon DR, Turner RE. 1989. Accretion and canal impacts in a rapidly subsiding wetland II. Feldspar marker horizon technique. Estuaries 12:260-268.

Cain MR, Hensel PF. 2018. Wetland elevations at sub-centimeter precision: exploring the use of digital barcode leveling for elevation monitoring. Estuaries and Coasts 41:582-591.

Callaway JC, DeLaune RD, Patrick Jr WH. 1997. Sediment accretion rates from four coastal wetlands along the Gulf of Mexico. Journal of Coastal Research 13:181-191.

Cherry JA, McKee KL, Grace JB. 2009. Elevated CO2 enhances biological contributions to elevation change in coastal wetlands by offsetting stressors associated with sea-level rise. Journal of Ecology 97:67-77.

Clifton BC, Hood WG, Hinton SR. 2018. Floristic development in three oligohaline tidal wetlands after dike removal. Ecological Restoration 36:238-251.

Cornu CR, Sadro S. 2002. Physical and functional responses to experimental marsh surface elevation manipulation in Coos Bay's South Slough. Restoration Ecology 10:474-486.

Craft C, Reader J, Sacco JN, Broome SW. 1999. Twenty-five years of ecosystem development of constructed *Spartina alterniflora* (Loisel) marshes. Ecological Applications 9:1405-1419.

Davis J, Currin C, Morris JT. 2017. Impacts of fertilization and tidal inundation on elevation change in microtidal, low relief salt marshes. Estuaries and Coasts 40:1677-1687.

Diefenderfer HL, Coleman AM, Borde AM, Sinks IA. 2008. Hydraulic geometry and microtopography of tidal freshwater forested wetlands and implications for restoration, Columbia River, U.S.A. Ecohydrology and Hydrobiology 8:339-361.

Diefenderfer HL, Sinks IA, Zimmerman SA, Cullinan VI, Borde AB. 2018. Designing topographic heterogeneity for tidal wetland restoration. Ecological Engineering 123:212-225.

Drexler JZ, de Fontaine CS, Deveral SJ. 2009. The legacy of wetland drainage on the remaining peat in the Sacramento-San Joaquin Delta, California, USA. Wetlands 29:372-386.

Drexler JZ, Woo I, Fuller CC, Nakai G. 2019. Carbon accumulation and vertical accretion in a restored versus historic salt marsh in southern Puget Sound, Washington, United States. Restoration Ecology 27:1117-1127.

Fagherazzi S, Kirwan ML, Mudd SM, Guntenspergen GR, Temmerman S, D'Alpaos A, van de Koppel J, Rynczyk JM, Reyes R, Craft C, Clough J. 2012. Numerical models of salt marsh evolution: ecological, geomorphic, and climatic factors. Reviews of Geophysics 50:RG1002.

Fofonoff NP, Millard Jr. RC 1983. Algorithms for computation of fundamental properties of seawater. UNESCO Technical papers in marine science No. 44.

Frenkel RE, Morlan JC. 1991. Can we restore our salt marshes? Lessons from the Salmon River, Oregon. The Northwest Environmental Journal 7:119-135.

Garbutt RA, Reading CJ, Wolters M, Gray AJ, Rothery P. 2006. Monitoring the development of intertidal habitats on former agricultural land after the managed realignment of coastal defences at Tollesbury, Essex, UK. Marine Pollution Bulletin 53:155-164.

Grismer ME, Kollar J, Syder J. 2004. Assessment of hydraulic restoration of San Pablo marsh, California. Environmental Monitoring and Assessment 98:69-92.

Helton AM, Ardón M, Bernhardt ES. 2019. Hydrologic context alters greenhouse gas feedbacks of coastal wetland salinization. Ecosystems 22:1108-1125.

Janousek CN, Folger CL. 2014. Variation in tidal wetland plant diversity and composition within and among coastal estuaries: assessing the relative importance of environmental gradients. Journal of Vegetation Science 25:534-545.

Janousek CN, Thorne KM, Takekawa JY. 2019. Vertical zonation and niche breadth of tidal marsh plants along the northeast Pacific coast. Estuaries and Coasts 42:85-98.

Kidd SA. 2017. Ecosystem recovery in estuarine wetlands of the Columbia River estuary. PhD dissertation, Portland State University, Portland, OR.

Kirwan ML, Temmerman S, Skeehan EE, Guntenspergen GR, Fagherazzi S. 2016a. Overestimation of marsh vulnerability to sea level rise. Nature Climate Change 6:253-260.

Kirwan ML, Walters DC, Reay WG, Carr JA. 2016b. Sea level driven marsh expansion in a coupled model of marsh erosion and migration. Geophysical Research Letters 43:4366-4373.

Lane RR, Mack SK, Day JW, DeLaune RD, Madison MJ, Precht PR. 2016. Fate of soil organic carbon during wetland loss. Wetlands 36:1167-1181.

Lawrence PJ, Smith GR, Sullivan MJP, Mossman HL. 2018. Restored saltmarshes lack the topographic diversity found in natural habitat. Ecological Engineering 115:58-66.

Leonard LA. 1997. Controls of sediment transport and deposition in an incised mainland marsh basin, southeastern North Carolina. Wetlands 17:263-274.

Leonard LA, Wren PA, Beavers RL. 2002. Flow dynamics and sedimentation in *Spartina alterniflora* and *Phragmites australis* marshes of the Chesapeake Bay. Wetlands 22:415-424.

Lynch JC, Hensel P, Cahoon DR. 2015. The surface elevation table and marker horizon technique: A protocol for monitoring wetland elevation dynamics. Natural Resource Report NPS/NCBN/NRR-2015/1078. National Park Service, Fort Collins, CO, 62 pp.

MacClellan MA. 2011. Carbon content in Oregon tidal wetland soils. Appendix 8 in Brophy LS, Cornu CE, Adamus PR, Christy JA, Gray A, MacClellan MA, Doumbia JA, Tully RL. 2011. New tools for tidal wetland restoration: Development of a reference conditions database and a temperature sensor method for detecting tidal inundation in least-disturbed tidal wetlands of Oregon, USA. Prepared for the Cooperative Institute for Coastal and Estuarine Environmental Technology (CICEET), Durham NH.

McTigue N, Davis J, Rodriguez AB, McKee B, Atencio A, Currin C. 2019. Sea level rise explains changing carbon accumulation rates in a salt marsh over the past two millennia. JGR Biogeosciences 124:2945-2957.

Miller RL, Fram S, Fujii R, Wheeler G. 2008. Subsidence reversal in a re-established wetland in the Sacramento-San Joaquin Delta, California, USA. San Francisco Estuary Watershed Science 6:article 1.

Montillet J-P, Melbourne TI, Szeliga WM. 2018. GPS vertical land motion corrections to sea-level rise estimates in the Pacific Northwest. JGR Oceans 123:1196-1212.

Mossman HL, Davy AJ, Grant A. 2012. Does managed coastal realignment create saltmarshes with 'equivalent biological characteristics' to natural reference sites. Journal of Applied Ecology 49:1446-1456.

Nyman JA, Walters RJ, Delaune RD, Patrick Jr. WH. 2006. Marsh vertical accretion via vegetative growth. Estuarine, Coastal and Shelf Science 69:370-380.

Peck EK. 2017. Competing roles of sea level rise and sediment supply on sediment accretion and carbon burial in tidal wetlands; Northern Oregon, U.S.A. MS thesis, Oregon State University, Corvallis, OR.

Peck EK, Wheatcroft RA, Brophy LS. 2020. Controls on sediment accretion and blue carbon burial in tidal saline wetlands: insights from the Oregon Coast, USA. JGR Biogeosciences 125:e2019JG005464.

Poffenbarger HJ, Needelman BA, Megonigal JP. 2011. Salinity influence on methane emissions from tidal marshes. Wetlands 31:831-842.

Poppe K, Rybczyk J. 2019. A blue carbon assessment for the Stillaguamish River estuary: Quantifying the climate benefits of tidal marsh restoration. Summary report prepared by Western Washington University for Washington Sea Grant and the Nature Conservancy.

Portnoy JW, Giblin AE. 1997. Effects of historic tidal restrictions on salt marsh sediment chemistry. Biogeochemistry 36:275-303.

Reed DJ, Spencer T, Murray AL, French JR, Leonard L. 1999. Marsh surface sediment deposition and the role of tidal creeks: Implications for created and managed coastal marshes. Journal of Coastal Conservation 5:81-90.

Rogers K, Kelleway JJ, Saintilan N, Megonigal JP, Adams JB, Holmquist JR, Lu M, Schile-Beers L, Zawadski A, Mazumder D, Woodroffe CD. 2019. Wetland carbon storage controlled by millennial-scale variation in relative sea-level rise. Nature 567:91-96.

Saintilan N, Khan NS, Ashe E, Kelleway JJ, Rogers K, Woodroffe CD, Horton BP. 2020. Thresholds of mangrove survival under rapid sea level rise. Science 368:1118-1121.

Stagg CL, Baustian MM, Perry CL, Carruthers TJB, Hall CT. 2018. Direct and indirect controls on organic matter decomposition in four coastal wetland communities along a landscape salinity gradient. Journal of Ecology 106:655-670.

Sweet WV, Kopp RE, Weaver CP, Obeysekera J, Horton RM, Thieler ER, Zervas C. 2017. Global and regional sea level rise scenarios for the United States. NOAA Technical Report NOS CO-OPS 083, 55 pp + appendices.

Taylor BW, Paterson DM, Baxter JM. 2019. Sediment dynamics of natural and restored *Bolboschoenus maritimus* saltmarsh. Frontiers in Ecology and Evolution 7:237.

Thorne KM, Elliott-Fisk DL, Wylie GD, Perry WM, Takekawa JY. 2013. Importance of biogeomorphic and spatial properties in assessing a tidal salt marsh vulnerability to sea-level rise. Estuaries and Coasts 37:941-951.

Thorne K, MacDonald G, Guntenspergen G, Ambrose R, Buffington K, Dugger B, Freeman C , Janousek C, Brown L, Rosencranz J, Holmquist J, Smol J, Hargan K, Takekawa J. 2018. U.S. Pacific coast wetland resilience and vulnerability to sea-level rise. Science Advances 4:eaao3270

Watanabe K, Seike K, Kajihara R, Montani S, Kuwae T. 2019. Relative sea-level change regulates organic carbon accumulation in coastal habitats. Global Change Biology 25:1063-1077.

Chapter 3: Channel morphology

Stan van de Wetering and Maxwell Tice-Lewis

Key Findings

- Post-restoration monitoring of wetland tidal channel morphology suggests the process of channel network recovery has begun across SFC.
- As observed at other sites, channel morphology metrics at SFC were highly variable at year two in the recovery process.
- There was strong down-cutting at the mouths of large channels and a general trend towards deeper channels after restoration of tidal exchange at SFC, but the trend was not statistically significant at this stage of the restoration trajectory.
- Channel width did not change significantly between pre- and post-restoration sampling.

Introduction

Tidal channel order, density, and distribution are key features of least-disturbed and restored tidal wetlands (Zeff 1999, Hood 2002, D'Alpaos 2007, D' Alpaos 2010, So et al. 2015, Bridgeland et al. 2017). In-fill of tidal channels while diked may dramatically alter the surface topography of former tidal wetlands and their ability to deliver key wetland functions once restored. Natural channel networks contain sufficient channel densities for a range of channel sizes (stream order). Without the presence of a natural channel network, disturbed and restoring tidal wetlands are less able to maintain crucial ecosystem functions such as hydrologic connectivity between the deeper estuary and the vegetated wetland plain. This critical connection provides for an exchange of organisms and affects the transport of materials and energy through the ecosystem, including saline water, nutrients, organic carbon, and sediments (Reed et al. 1999, Buffington et al. 2020). Connectivity also determines the distribution of finfish food resources (e.g., invertebrate drift) and direct access by finfish to rearing habitats and benthic food resources.

Tidal wetland restoration sites in coastal Oregon typically have a recent (40-100 yr) history of agricultural use (Brophy et al. 2014, Brown et al. 2016). The soils have experienced compaction from agricultural activities and have thus become lower in surface elevation when compared to adjacent least-disturbed wetlands (Chapter 2). Historic agricultural uses typically involved filling of natural channels and the creation of a ditch network to transport water off the land surface. These patterns of filling and ditching along with highly variable spatial patterns of subsidence, can create complex wetland topography that affects tidal hydrology across a restoration site. It is the goal of most tidal restoration projects to obtain full tidal exchange across the site and reconstruct or mimic the historic channel network footprint (Coats et al. 1995, Hood 2002, Brophy et al. 2014, Hood 2015, Brown et al. 2016, Bridgeland et al. 2017).

Channel network design in restoration projects involves a number of challenges. First, detailed elevation data are needed to determine the boundaries of sub-basins (i.e., where the first and second order portions of a sub-basin channel network should occur). Second, implementation costs for digging adequately sized and placed first and second order channel networks may be prohibitive (Coats et al.

1995, van de Wetering et al. 2007, Bridgeland et al. 2017). For these reasons Oregon tidal wetland restoration projects have commonly involved only fourth and fifth order channel construction followed by a limited amount of third order construction (personal communication, Kelly Moroney, USFWS Oregon Coastal Refuges Complex). Finally, determining channel placement of any order within a historic wetland may be challenging, though the location of remnant historic channels, when present, may provide a guide.

Most practitioners choose to construct a channel network in order to restore intertidal wetland habitat and allow improved finfish access to some portion of the interior wetland (Coats et al. 1995, Hood 2002, Hood 2015, Hood 2018, Brown et al. 2016, Bridgeland et al. 2017). Our observations from the 500 acre Ni-les'tun restoration project in the Coquille River Estuary suggest that when first and second order channels are constructed they are highly variable in their ability to evolve into a functional network (van de Wetering et al., unpublished data 2020). Full channel network restoration is rarely achieved upon completion of the ground-based construction phase of tidal wetland restoration projects. For example, Lawrence et al. (2018) found that channel density in restored UK marshes was lower than that of reference wetlands. Similarly, in passively breached river deltas in the Salish Sea, restored sites had only 45% of the channel density observed in reference wetlands, although they did have greater channel surface area and longer channels (Hood 2014).

Restoration of the full channel network is often left to occur through the forces of tidal exchange over time. Even with relatively detailed elevation data, careful placement and distribution of channel order, and simplified approaches to modeling hydrodynamics across a site, channel development over time may still result in scour and fill of restored (excavated) channels across multiple channel orders (Gabeti 1998, D'Alpaos 2007, Bridgeland et al. 2017). When no smaller order channels are excavated, ponding of water on the wetland surface may occur between high tide periods (van de Wetering et al. 2007, Bridgeland et al. 2017). This can affect plant community composition (Grismer et al. 2004) as well as the rate of channel network development. When fewer lower order channels are excavated in a restoration project, overall development of the higher order channels requires more time because less tidal forcing occurs (Hood 2007, Brophy et al. 2014, Lanzoni and D'Alpaos 2015, Bridgeland et al. 2017). For finfish species, less tidal exchange across the whole wetland results in less transport of material and energy which is expected to reduce the ecological benefits of a project.

In this chapter we report on pre-and post-restoration measurements of tidal channel morphology at SFC and at two reference tidal wetland channels at Dry Stocking Island adjacent to SFC. Measurements of channel geometry have been used to describe channel hydraulics and sediment transport for several decades (Leopold et al. 1953, Harvey and Watson 1986, Olson-Rutz and Marlow 1992, Zeff 1999, Hood 2007, Lanzoni and D'Alpaos 2015, Hood 2020). Comparison of channel geometry is a useful method to evaluate change and rate of change in natural, least disturbed, and restored tidal channel networks. We compared channel bottom elevation (flow path) along with cross section depths, widths and width-to-depth ratios to track pre- to post-restoration changes in channel morphology and development. These simple metrics provide a useful tool to describe how hydraulic forces are affecting channel dimensions relative to tidal amplitude (flow volume), tidal velocity (volume over time), suspended sediment loading and aggradation, and bed roughness (bed grain size). We used a stratified approach to account for surface drainage area within each monitored sub-basin where the historic channels were present and providing degraded aquatic habitat prior to removal of the tide-gates and dikes. For this reason, our study sites encompass those areas likely to experience the greatest changes in depths (both scour and fill), widths, and channel migration during the initial years of post-restoration, but don't allow for an evaluation of the broader SFC site and the evolution of its lower order channel network. In addition, because several distributary channels were created during the restoration process, tidal flood and ebb patterns, specific to potential scour and fill, have become more complex and will likely result in additional variation in a given channel network's response to the restoration actions.

Materials and methods

We positioned our monitoring stations using a stratified approach to account for surface drainage area within each monitored sub-basin in a stepwise fashion. In addition, we attempted to monitor locations where anthropogenic disturbance had occurred recently (tide gate removal) or historically (dredging). We collected and analyzed field-based channel cross-section data at four SFC sub-basins and two reference sub-basins on Dry Stocking Island (DSI) in low and high marsh. We used the only two local least-disturbed channel networks adjacent to the SFC site as reference channels, which were located near the Wilson, Trask, and Tillamook rivers. Our reference channel drainage areas and associated channel dimensions were smaller than those monitored at the SFC site. In other Oregon coastal tidal wetlands, smaller order channels have a different geometry than larger order channels (So et al. 2009). Using a BACI approach allows us to measure change in the restoration channels relative to reference channels and therefore is not dependent upon using channel networks of similar size. We collected data during the fall and winter during pre-restoration (2014) and post-restoration (2018) sampling periods using high-precision RTK-GPS and laser-level methods. At SFC we evaluated 27 cross-sectional transects (called "transects" hereafter) (Figures 3.1-3.3). Nine transects were located in Blind Slough, with four of those transects downstream of the main tide gate and five upstream of the tide gate. Additionally, we measured six transects within SFC at Trib 1, Trib 2 and Nolan Slough (Figures 3.1-3.2). We measured nine transects in channels at the reference Dry Stocking Island site, with five in low tidal marsh and four in high tidal marsh (Figure 3.3). For simplicity, we refer to all monitored channels as sub-basins although both the channel order and sub-basin size varied. In addition, all SFC site sub-basins were influenced by the presence of distributary channels.

Within each channel, we placed transects from near the mouth of the channel (where channels were likely to be widest) to near their pre-restoration headwaters (Figure 3.1-3.3). To resample identical transects after restoration, we installed semi-permanent monuments at both ends of each transect. Monuments consisted of 1.2 m (4 ft) long, 0.63 cm (¼ in) rebar driven into the ground and encased with 1.5 m (5 ft) of 5 cm schedule 40 PVC pipe. We set back monuments from the bank edge to allow future measurements, even if channels migrated laterally. We measured the position and elevation of each monument with high-precision RTK GPS equipment with a 480 second occupation at 1 Hz; positions were referenced to UTM Zone 10N and NAVD88 using geoid model 12A. Vertical accuracy for these measurements was better than 5.5 cm at the 95% confidence level based on comparisons to nearby published survey control.

At each transect, we established a baseline using a CAM-Line thin-diameter graduated metal tape stretched between the transect end post monuments. We used a laser level to measure elevation at topographic breaks along the transect relative to a known elevation benchmark (usually a transect end post monument). The number of measurements per transect varied based on channel morphology; measurements were taken at breaks in the cross section's slope as interpreted in the field by the surveyor. When multiple elevation benchmarks were available for a given laser level setup, we performed a least-squares adjustment to assign the laser level elevation. For each elevation measurement along a transect, we recorded the distance along the transect and noted what feature was present at each measured point (e.g., left bank, flow-path, right bank). The elevation of each measurement represented the top of the visible sediment surface (including any soft fine sediment that was deposited). Prior to data analysis we generated elevation values at 10% intervals across the transect through interpolation of the break point values gathered in the field. We averaged the break point elevations immediately to the left and right of each interpolated interval, to provide the interpolated value.

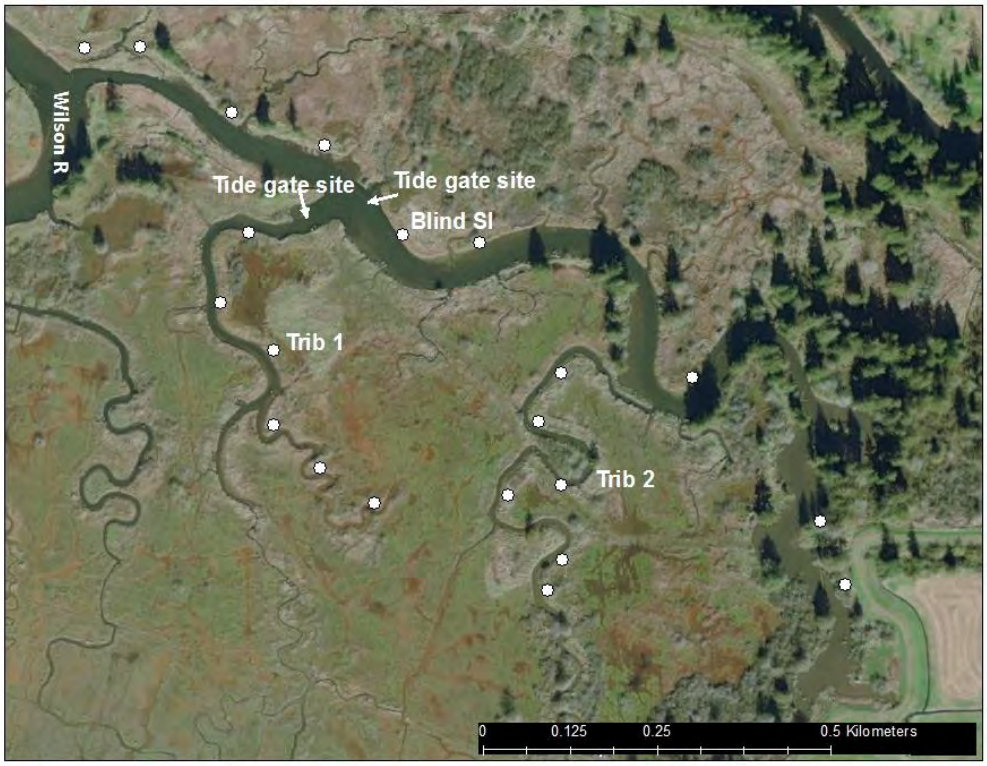

Figure 3.1. Blind Slough, Trib 1, and Trib 2 channel cross section locations within SFC.

Figure 3.2. Nolan Slough channel cross section locations within SFC.

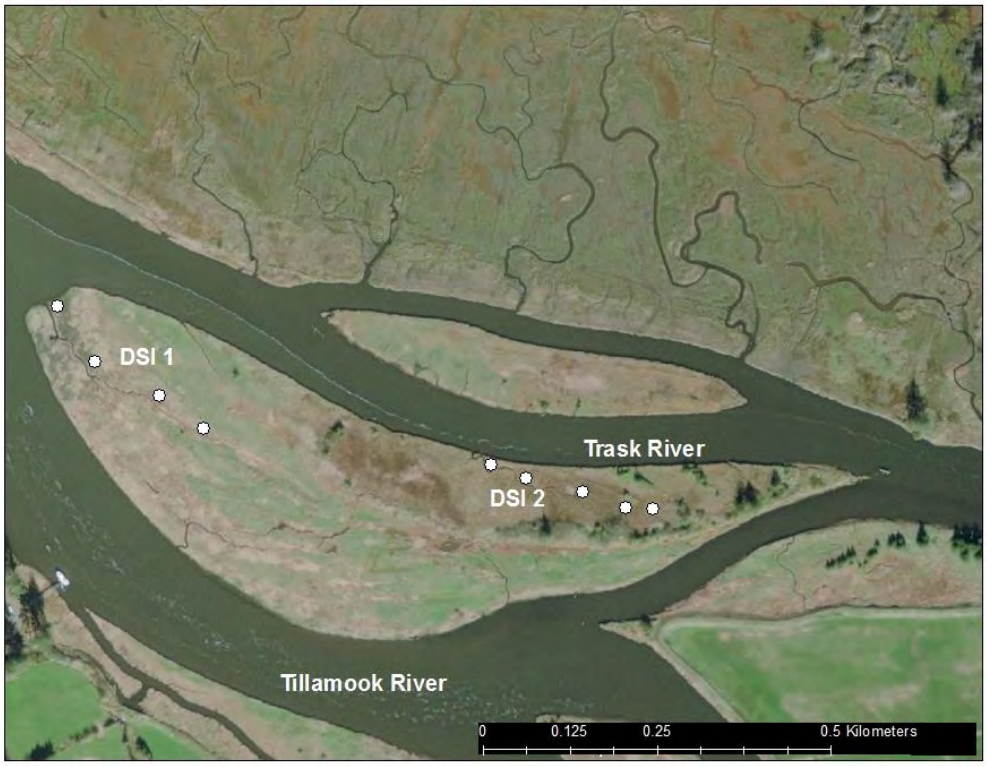

Figure 3.3. Channel cross section locations at Dry Stocking Island (DSI).

We characterized SFC sub-basin channel morphology using five metrics during the pre- and post-restoration monitoring periods: channel flow-path elevation (minimum elevation along an individual transect), channel bottom elevation (mean elevation), channel bankfull width (width measured across the top of the channel at the point where it intersects the marsh's surface on the right and left banks), and channel width-to-depth ratio (using flow path depth rather than mean depth). We evaluated differences between SFC and reference channels and differences between pre- and post-restoration sampling periods with two approaches. First, we combined all SFC data to evaluate the overall channel response to the restoration. Second, we evaluated each sub-basin separately. We considered data transformations for all metrics. We applied a natural log transformation to bankfull widths and bank width-to-depth ratios and analyzed all remaining metrics using untransformed data. Both analyses used a 2-way linear model and a type-III ANOVA for each of the five metrics of interest. In the first analysis we combined sub-basins to evaluate whether a significant interaction existed between site (SFC) and sampling period, which would suggest a change in channel morphology due to restoration implementation at SFC. In the second analysis we analyzed sub-basins separately using a Tukey HSD post-hoc test ($\alpha = 0.05$) to determine pairwise differences between treatment-period groups.

We also computed the change in channel metrics between 2014 and 2018 at individual measurement points and then computed the mean change and 95% confidence intervals (CI) for individual channel reaches (similar to the approach taken for individual marsh measurements in Chapters 2 and 5 of this report). We used the R package "lsmeans" to compute CI around estimates of mean change, which we note can provide different confidence intervals than direct computation of CI based on population standard error and t-statistics.

Results and discussion

Channel flow-path elevation. Changes in channel flow-path elevation provide insight into the extent of scour and head cutting that occurred due to the restoration of tidal influence. Restored channels had lower overall mean minimum elevations compared to the reference channels on Dry Stocking Island (Figure 3.4). Although we observed a drop in the pooled mean flow-path elevation (Figure 3.4), we found no significant change between sampling periods and no interaction between treatment and sampling period ($F = 1.52$, $df = 1$, $P = 0.22$) at this early point in the recovery process. Furthermore, no interaction was found between tributary and sampling period ($F = 1.07$, $df = 5$, $P = 0.39$) (Figure 3.5). The post-hoc pairwise comparisons for individual SFC sub-basins showed restoration sub-basin mean flow-path elevation began trending downward following restoration, but these decreases were not statistically significant due to the extent of variation in the data (Figure 3.5). Using the flow path elevations, we developed longitudinal channel profiles to describe the relative pattern of elevation change across each monitoring reach (Figure 3.6). Blind and Nolan Sloughs experienced deep head cuts at their downstream portions which prevented us from taking measurements during post-restoration because our elevation equipment would not record beyond a 3.0 m distance below mean high water. These two sloughs also experienced heavy scour at their mouths and deepening in some areas farther upstream.

In addition, cross section profiles for stations 2-5 for Blind Slough also show the dynamic nature of channels at SFC at year two post-restoration (Figure 3.7). For example, at station 2 there was not only a drop in flow path elevation (Figure 3.6) during post-restoration but the main channel itself shifted laterally and fill of the old channel occurred (Figure 3.7). Station 3 showed a limited drop in flow path elevation but a distinct lateral shift in the channel's flow path position with both fill and scour occurring. Limited shifts occurred for both the flow path elevation and position at station 4. Station 5 experienced a lateral shift and deepening of the flow path, as well as lateral fill.

It is important to note the extent of variation in the pre- and post-restoration data and what created that variation. Natural tidal channel networks by definition possess an elevation gradient across the network. These gradients can vary depending on drainage basin size as well as many other factors such as location within the tidal prism and sediment loading (Lanzoni and D'Alpoas 2015). The two DSI reference channels had steeper gradients than the four restoration channels (Figure 3.6), which aligns with our observations at other high marsh sites with small drainage areas (Brophy et al. 2014, Brophy et al. 2015). In addition, DSI upper was located at a higher base elevation when compared to DSI lower. Steeper gradients resulted in increased variation when considering within channel mean flow path values. The difference in base elevation of the two DSI reference channels also resulted in increased variation within the estimate for the pooled reference channel mean flow path. Although our choice of the two reference channel locations and the pooling of those data increased variability around the mean, we believe this variance will not reduce our ability to measure statistical significance as time passes. Based on observations from other Oregon tidal marshes (van de Wetering et al. 2007, Brophy et al. 2014) we predict that as time passes, scour and fill of the restoration channels will result in a more consistent gradient and lower mean flow path elevation, similar to that observed in least disturbed channels (Brophy et al. 2014). A more consistent gradient will result in less in-channel variation and will therefore improve the ability to detect change.

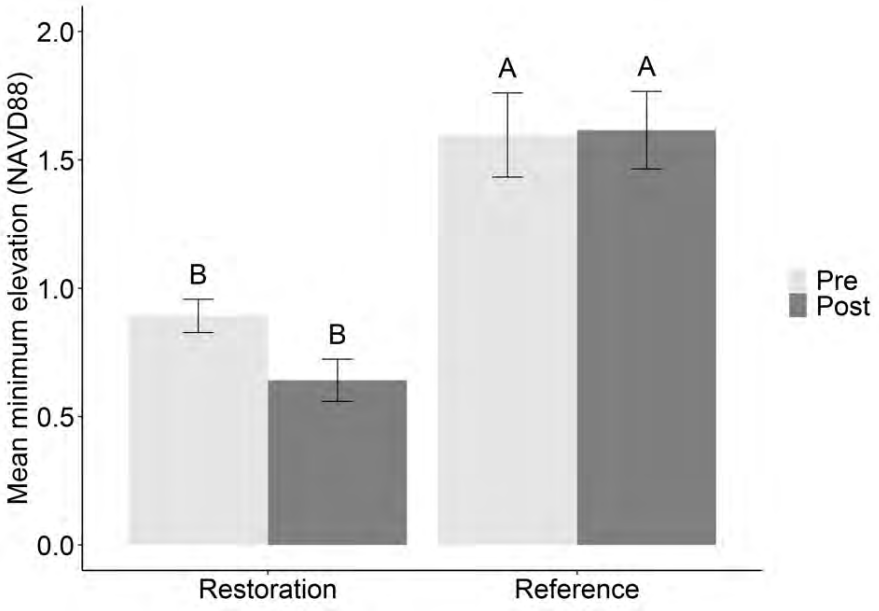

Figure 3.4. Mean channel flow-path elevation (minimum NAVD88) by treatment and sampling period (pre- and post-restoration). Error bars show one standard error; columns with no letters in common are significantly different (Tukey HSD, P < 0.05).

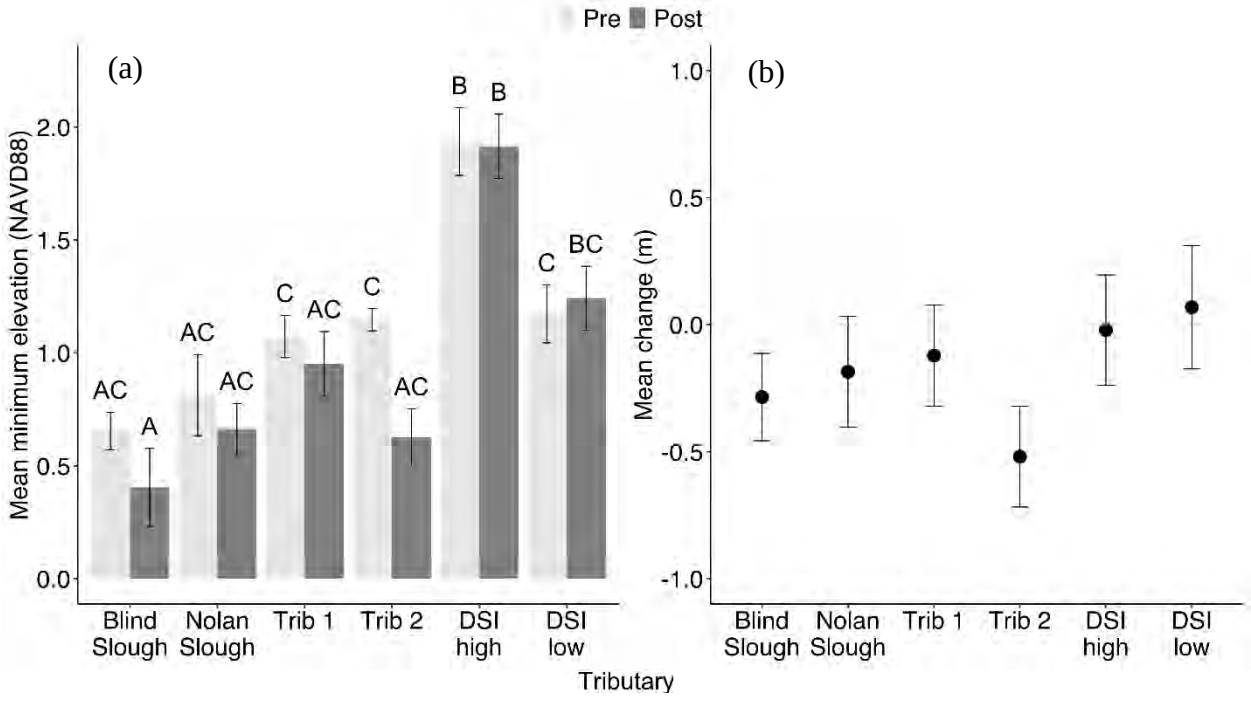

Figure 3.5. (a) Mean channel flow-path elevation (measured as minimum NAVD88) by individual sub-basin and sampling period. Error bars show one standard error; columns with no letters in common are significantly different (Tukey HSD, P < 0.05). (b) Mean change in flow path elevation and 95% confidence intervals.

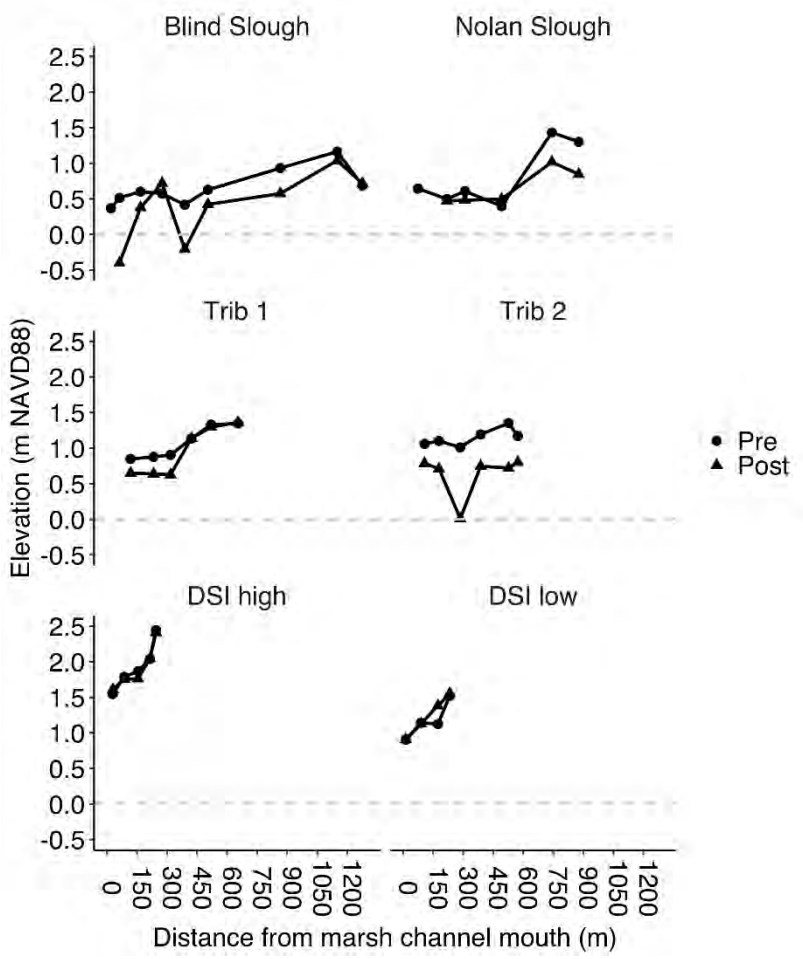

Figure 3.6. Longitudinal profile of flow-path elevation (measured as NAVD88 m) by SFC sub-basin.

Average channel bottom elevation. Mean channel bottom elevations were higher in reference wetlands than at SFC (Figure 3.8). As noted in the flow path results, this was due to the difference in the base elevation of the two channel networks – a product of factors such as drainage area, channel order, the tidal prism, and sediment loading. Although we observed a drop in the pooled mean channel bottom elevation at SFC (Figure 3.8), we found no significant change between sampling periods and no interaction between site and sampling period ($F = 0.49$, $df = 1$, $P = 0.49$) at this early point in the recovery process. Similarly, channel bottom elevation within sub-basins did not change significantly between sampling periods ($F = 1.93$, $df = 5$, $P = 0.10$) (Figure 3.9). Restored and reference sub-basins had similar within channel variance (Figure 3.9).

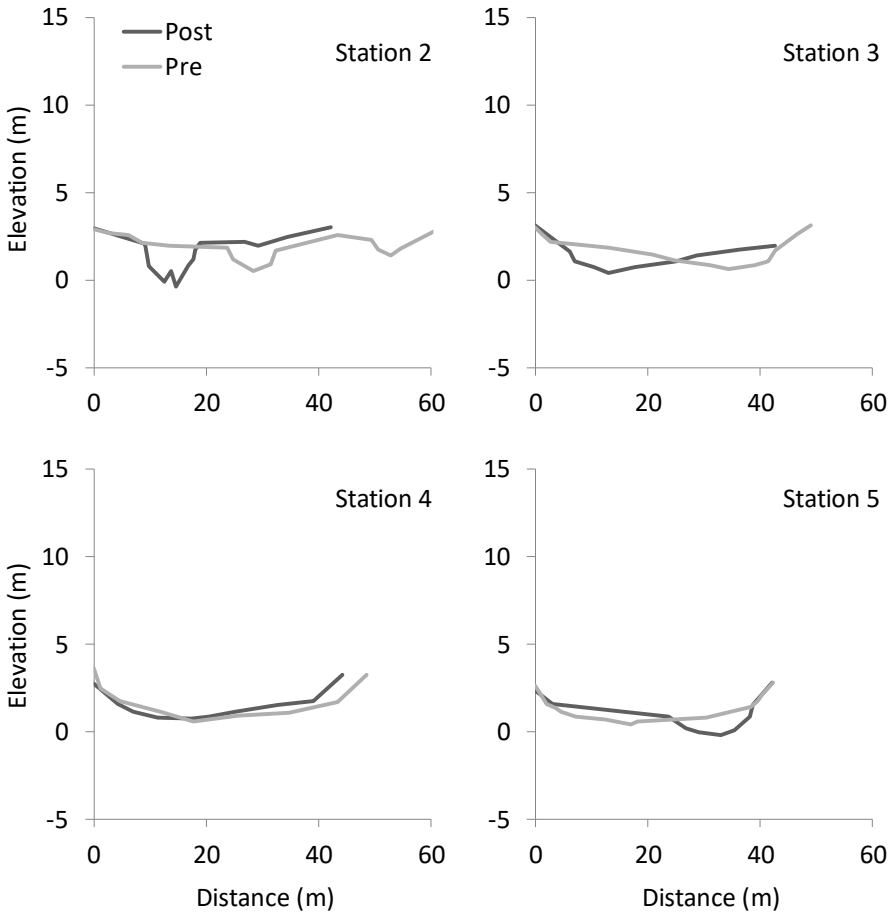

Figure 3.7. Cross section elevations (NAVD88 m) for Blind Slough stations 2-5 at SFC. Note the vertical scale has been adjusted (y-axis range reduced to 15m) to emphasize scour and fill pattern.

Channel bankfull width (BFW). For the pooled sub-basin assessment, channel bankfull width was several times greater in SFC channels than in reference channels due to the smaller size of the reference sub-basins and their smaller channel orders (see introduction and Figures 3.1-3.3). Although we observed a decrease in the pooled mean channel BFW (Figure 3.10), we found no significant change between sampling periods and no interaction between treatment and sampling period ($F = 0.40$, $df = 1$, $P = 0.53$) at this early point in the recovery process. Because the widths of the two reference channel networks were similar (Figure 3.11) the variation did not increase when those data were pooled. Conversely, when the SFC sub-basins were pooled the variation increased. This was due to the variation among sub-basins rather than within sub-basins (Figure 3.11). Furthermore, no significant interaction was found between tributary and sampling period ($F = 1.01$, $df = 5$, $P = 0.42$) (Figure 3.11). The post-hoc pairwise comparisons for individual sub-basins showed a trend of decreasing mean BFW with no statistical significance present for reference or restored sites following restoration (Figure 3.11). As described earlier, the site's agricultural history and consequent variable topography (due to factors such as subsidence, bank erosion, and fill) created challenges in evaluating BFW change at this early stage of recovery.

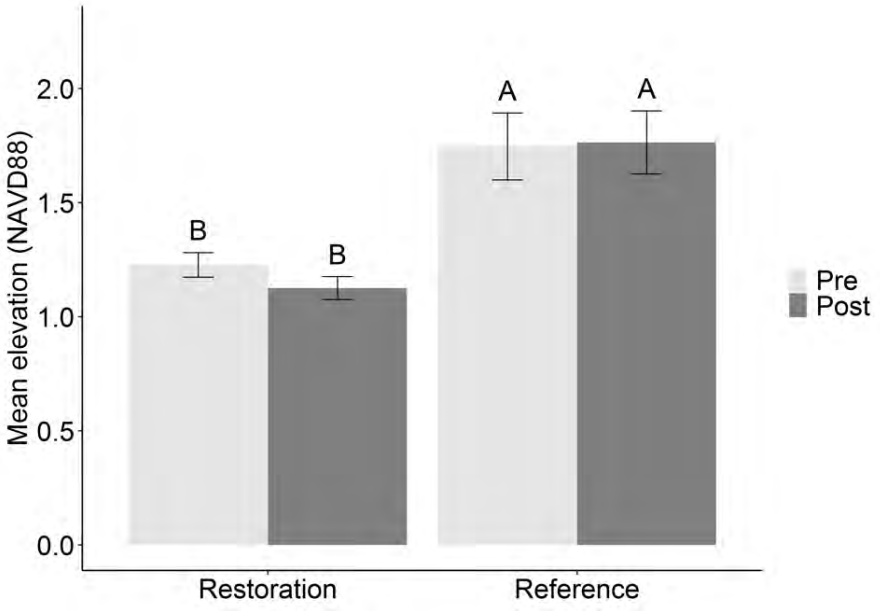

Figure 3.8. Mean channel bottom elevation (to top of fine sediment) by site and monitoring period. Error bars show one standard error; columns with no letters in common are significantly different (Tukey HSD, P < 0.05).

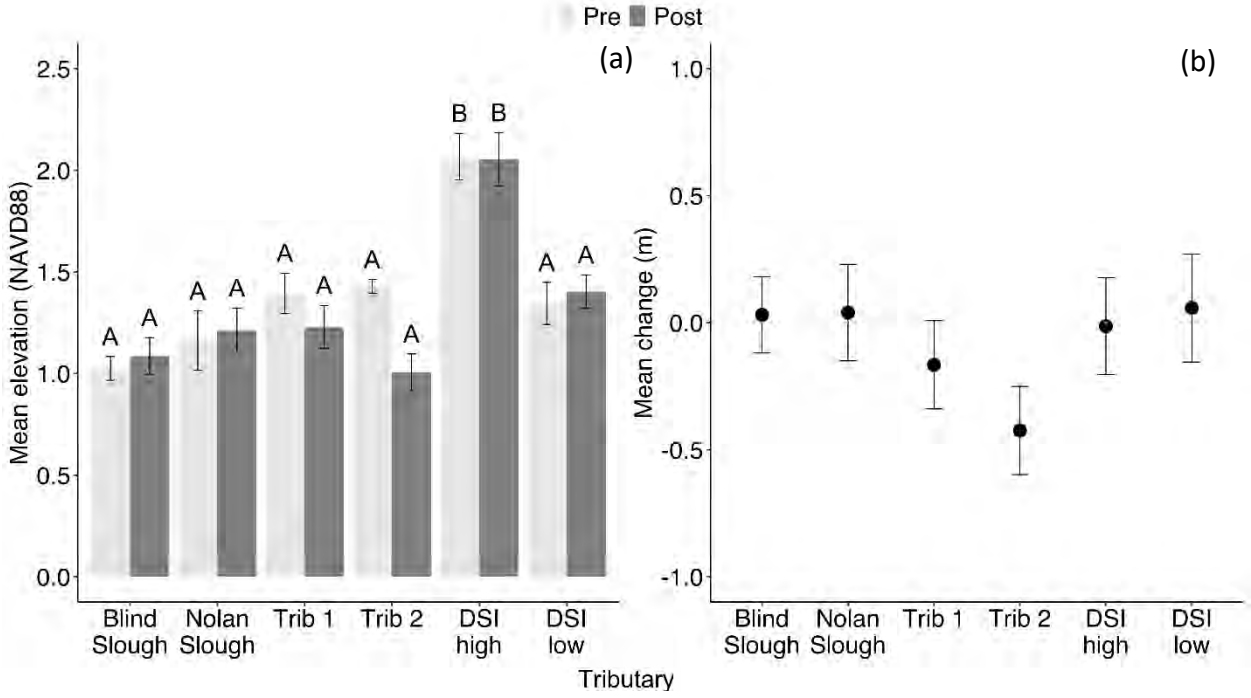

Figure 3.9. (a) Mean channel bottom elevation by individual sub-basin and monitoring period. Error bars show one standard error; columns with no letters in common are significantly different (Tukey HSD, P < 0.05). (b) Mean change and 95% confidence intervals for mean channel bottom elevation.

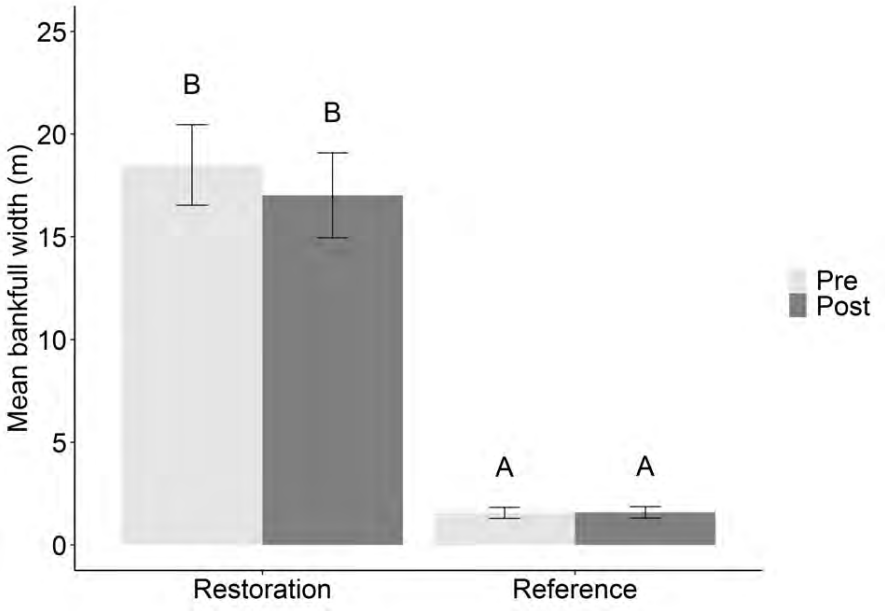

Figure 3.10. Mean bankfull width (BFW) by site and sampling period. Error bars show one standard error; columns with no letters in common are significantly different (Tukey HSD, P < 0.05).

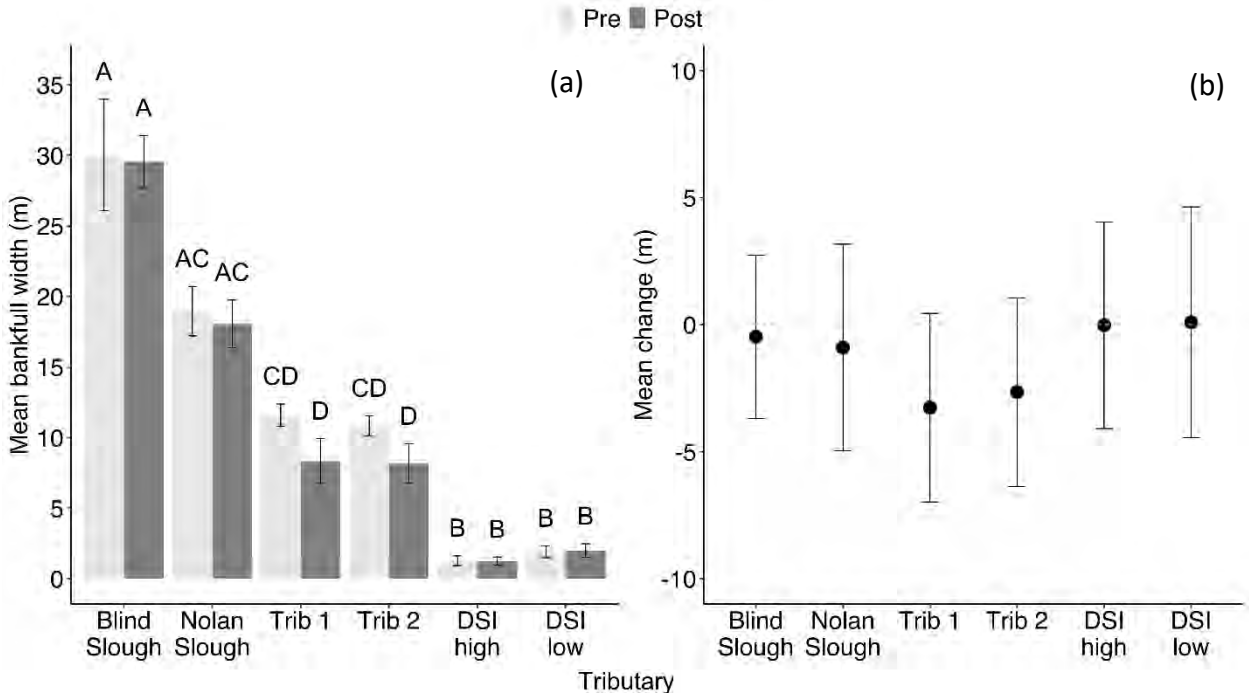

Figure 3.11. (a) Mean bankfull width (BFW) by sub-basin and sampling period. Error bars show one standard error; columns with no letters in common are significantly different (Tukey HSD, P < 0.05). (b) Mean change and 95% confidence intervals for bank full width.

Channel width-to-depth ratio. Mean channel width-to-depth ratio was much larger at SFC than in reference channels (Figure 3.12). As described previously this was a result of the reference channel networks having a smaller drainage surface area and therefore a smaller channel order and channel width, resulting in a smaller width-to-depth ratio. Although we observed a decrease in the pooled mean width-to-depth ratio for the SFC channels, we found no significant difference between sampling periods, nor a significant interaction between treatment and sampling period ($F = 2.71$, $df=1$, $P = 0.10$) at this early point in the recovery process. Furthermore, no significant interaction was found between tributary and sampling period ($F = 1.84$, $df = 5$, $P = 0.12$) (Figure 3.13). The post-hoc pairwise comparisons for individual sub-basins showed that channels in reference and restored sites had no significant increases or decreases in mean channel width-to-depth ratios following restoration. However, width-to-depth ratios for Blind Slough, Nolan Slough and Trib 2 decreased, as would be expected if channel scour (deepening) was occurring at a rate greater than channel widening (Figure 3.13).

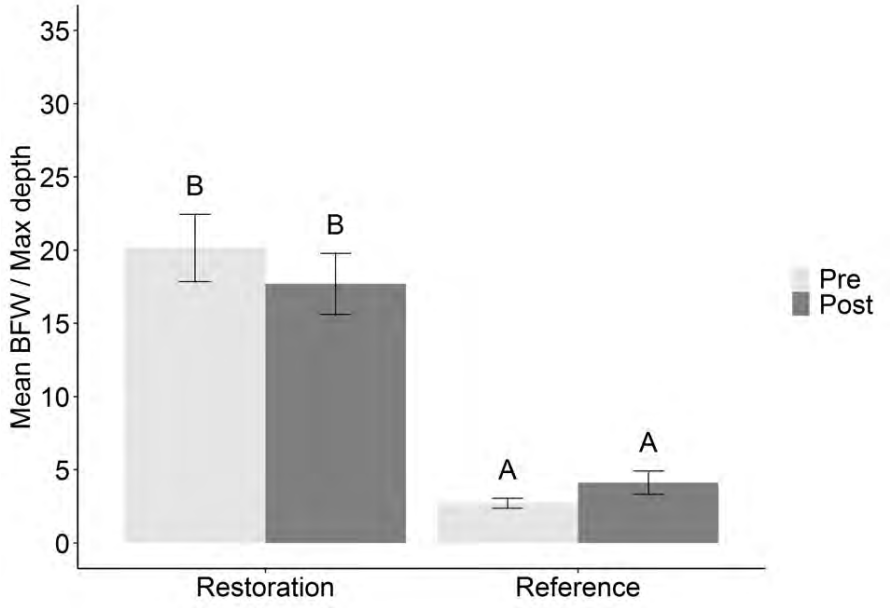

Figure 3.12. Mean channel width-to-depth ratio by site and sampling period with all monitored sub-basins lumped by site. Error bars show one standard error; columns with no letters in common are significantly different (Tukey HSD, $P < 0.05$).

The year two post-restoration monitoring suggests that the process of channel network recovery has begun at SFC. Generally, this recovery would be expected to include channel deepening, widening, or both, due to the increase in flow volumes after restoration of tidal exchange. As anticipated, restoring tidal exchange has led to down cutting of SFC channels, particularly near the mouths of channels, and a trend towards channel deepening. However due to variability, we did not observe a significant change in channel width at this stage of recovery. We have observed channel deepening (scour) and fill in the form of head cuts, scour pools, bank failures, and sediment deposits at other Oregon tidal wetland restoration sites during the recovery process (van de Wetering et al. 2007, Brophy et al. 2014). Because restoration of tidal exchange allows for increases in flow velocities and volumes, restored tidal channels are expected to initially produce down cutting into the channel sediments that accumulated during the diked period.

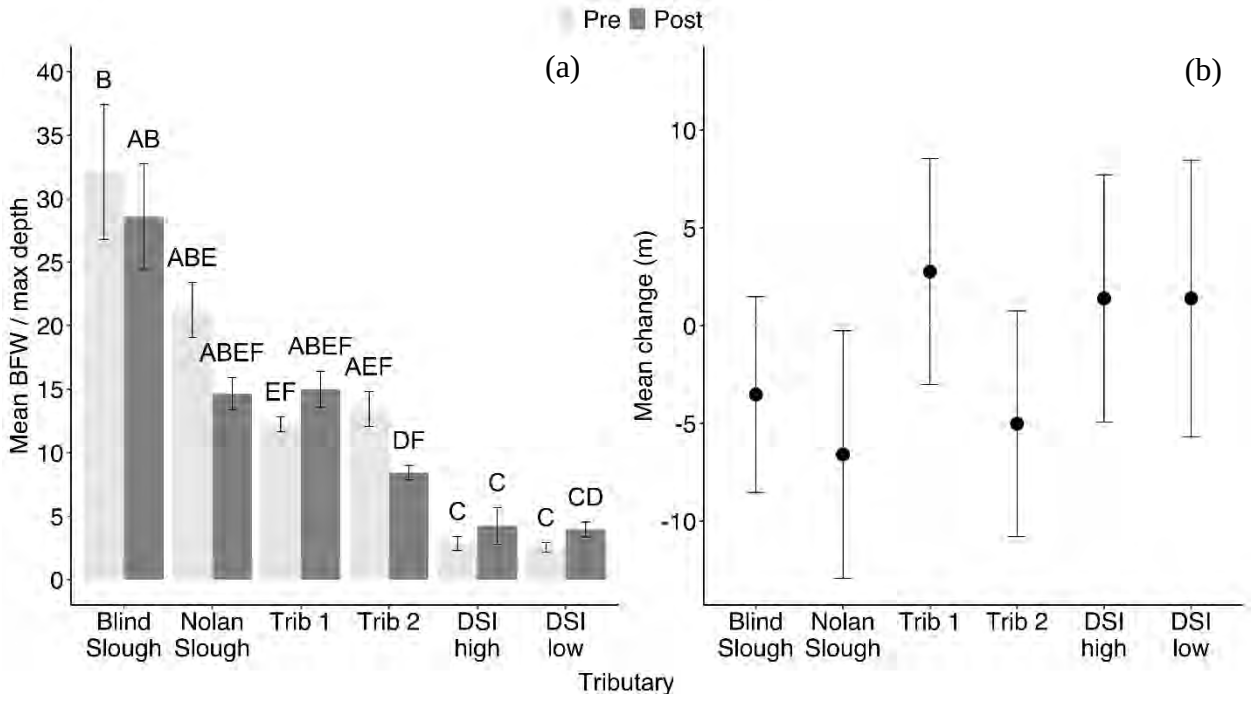

Figure 3.13. (a) Mean channel width-to-depth ratio by sub-basin and sampling period. Error bars show one standard error; columns with no letters in common are significantly different (Tukey HSD, $P < 0.05$). (b) Mean change and 95% confidence intervals for channel width to depth ratio.

Down cutting can result in associated bank toe erosion and bank failure and thus widening of the channel (Figure 3.14). If channel bed roughness is great enough to resist down cutting, channel widening will occur as a result of the channel's flow capacity moving toward equilibrium while accommodating increased hydraulic forces. In the Coquille River we observed a head cut and flow path scour response in the lowest portion of each of the three monitored tidal channel networks early in the recovery process (Brophy et al. 2014). This was immediately followed by channel migration and bar formation. As time passed this response moved further upstream in each respective study sub-basin network and the downstream portions of the channels began to move toward equilibrium (van de Wetering et al. unpublished 2020; Figure 3.15). We have observed this pattern occurring in other restoration channel networks (anecdotal observations from the Siuslaw, Alsea, Yaquina, Siletz, and Nestucca Estuaries 2001-2020). This temporal gradient of response can vary along the channel's long profile. As head cuts are added or removed along the channel's long profile, water velocities are expected to increase or decrease respectively. Longitudinal profiles at SFC suggest that the lower reaches of the four study channels are currently in the early phase of this process of bed scour and head cut migration.

Previous research has shown channel dimensions are correlated with drainage basin size when considering both non-tidal (Leopold 1953) and tidal basins (Hood 2002, Hood 2004, Hood 2007, So et al. 2009). Blind Slough is a large historic river channel that was cut off from its source channel at some point in the past. It is unclear whether it was historically part of the Trask River or Wilson River network, whether it was a distributary or main channel, and what process led to the current setting. There is now diked farmland that separates the upper Blind Slough channel from other channels found in this part of the Wilson-Trask-Tillamook delta area. Because of its historic association with a much larger freshwater watershed (much greater in size than the SFC site) the channel's width is much greater than other

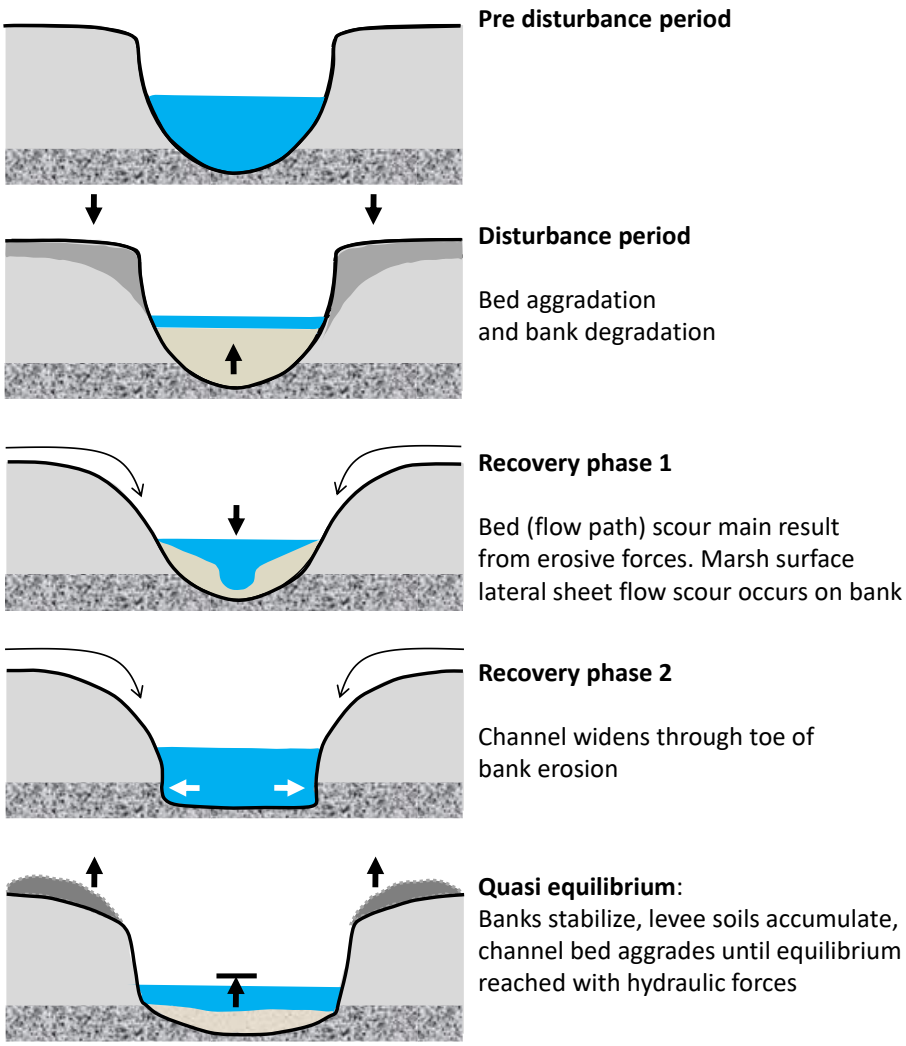

Figure 3.14. Schematic cross sectional view of the expected recovery process in a tidal channel restored to full tidal exchange.

SFC channels we sampled. The other three SFC monitoring basin channels are also positioned in the historically dynamic river delta area where the SFC tidal marsh is located. Using historical aerial imagery we estimate that before diking, Nolan Slough, Trib 1 and Trib 2 all fell within the range of observed ratios of drainage basin area to channel width and channel order for least disturbed channel networks described on the Oregon coast (So et al. 2009, Brown et al. 2016). Some of the variability we observed around our estimate of pooled means was associated with the size of the study sub-basin, and some could be attributed to the proportion of the sub-watershed sampled as we moved from the downstream to upstream portion of each SFC study channel reach. In the future, the factors driving this variation could be addressed by increasing sample size and testing for change within specific sub-watershed groupings based on channel volumes and sub-basin drainage area. Because the monitoring sub-basins are experiencing similar tidal amplitudes, suspended and bedload sediment patterns, and similar factors controlling channel mouth grade (elevation of Wilson and Trask River channel beds) we predict broad consistent patterns of change in SFC channel morphology will occur in the future as site recovery proceeds, and that consistency will translate to reduced variability in the data.

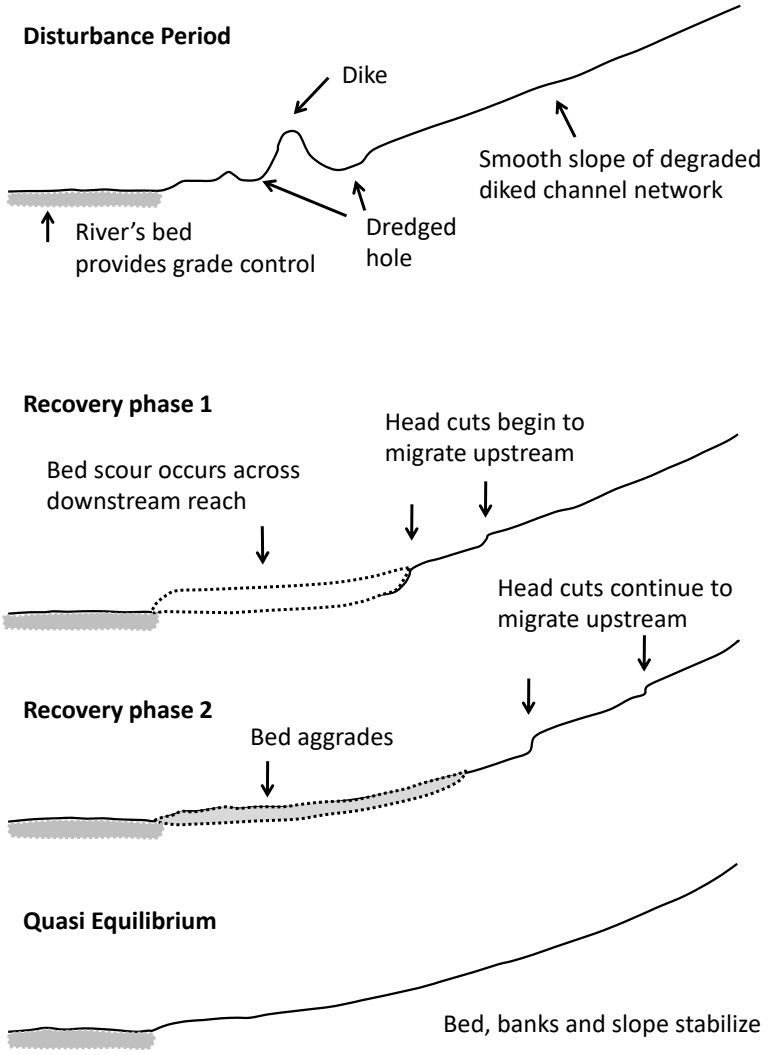

Figure 3.15. Schematic of longitudinal view of expected channel recovery process following hydrologic restoration.

Because hydraulic forces are continually moving channel morphology toward equilibrium, within SFC sub-basin variability will naturally be reduced over time, improving our ability to detect change in the future.

Based on our observations at other Oregon tidal wetland restoration projects (Brown et al. 2014, van de Wetering et al. 2007) we predict that the size and shape of SFC channels will become more similar to channels in least-disturbed tidal wetlands in Oregon such as the Coquille, Alsea, Siletz, and Siuslaw Estuaries (So et al. 2009). Changes in channel morphology at SFC are expected to lead to development of tidal pools and point bars, both features that will greatly improve the quality of the channels as juvenile finfish habitat. As the SFC channel network develops, we also predict sediment sorting and associated changes in particle size will occur that will provide new opportunities for benthic macroinvertebrate species (food resources for finfish) to inhabit the channels. Based on finfish use patterns we have observed at SFC and in other Oregon tidal wetlands (Siletz, Nestucca, Coquille) we predict these later morphological conditions will result in 10- to 100-fold increases in finfish use, but they may not begin to occur until a minimum of two decades post-restoration (van de Wetering et al. 2007, Brophy et al. 2014)

Citations

Bridgeland WT, Brophy LS, van de Wetering S, So KJ, van Hoy R, Lowe RW, Ledig BL 2017. Ni-les'tun Tidal Wetlands Restoration Project: Planning, Implementation, and Lessons Learned. Biological Technical Publication BTP-R1015-2017. U.S. Fish and Wildlife Service Oregon Coast National Wildlife Refuge Complex.

Brophy LS, van de Wetering S, Ewald MJ, Brown LA, Janousek CN. 2014. Ni-les'tun Tidal Wetland Restoration Effectiveness Monitoring: Year 2 Post-restoration (2013). Estuary Technical Group, Institute for Applied Ecology. Corvallis, OR.

Brophy, LS, Brown LA, Ewald MJ. 2015. Waite Ranch Baseline Effectiveness Monitoring: 2014. Prepared for the Siuslaw Watershed Council, Mapleton, Oregon. Estuary Technical Group, Institute for Applied Ecology, Corvallis, OR.

Brown LA, Ewald MJ, Brophy LS, van de Wetering S. 2016. Southern Flow Corridor Baseline Effectiveness Monitoring: 2014. Estuary Technical Group, Institute for Applied Ecology. Corvallis, OR.

Buffington KJ, Janousek CN, Thorne KM, Dugger BD. 2020. Spatiotemporal patterns of mineral and organic matter deposition across two San Francisco Bay-Delta tidal marshes. Wetlands 40:1395-1407.

Coats RN, Williams PB, Cuffe CK, Zedler JB, Reed D, Waltry SM, Noller JS. 1995. Design Guidelines for Tidal Channels in Coastal Wetlands, Rep. 934. U.S. Army Corps of Engineers Waterway Exp. Stn. Vicksburg, MS.

D'Alpaos AS, Lanzoni S, Marani M, Rinaldo A. 2007. Landscape evolution in tidal embayments: Modeling the interplay of erosion, sedimentation, and vegetation dynamics. Journal of Geophysical Research 112:1-17.

D'Alpaos AS, Marani M, Lanzoni S, Rinaldo A. 2010. On the tidal prism—channel area relations. Journal of Geophysical Research Atmospheres 115:1-13.

Gabeti EJ. 1998. Lateral migration and bank erosion in a saltmarsh tidal channel in San Francisco Bay, California. Estuaries 21:745-753.

Grismer ME, Kollar J, Snyder J. 2004. Assessment of hydraulic restoration of San Pablo Marsh, California. Environmental Monitoring and Assessment 98:69–92.

Harvey MD, Watson CC. 1986. Fluvial processes and morphological thresholds in incised channel restoration. Journal of the American Water Resources Association 22:359-368.

Hood WG. 2002. Application of landscape allometry to restoration of tidal channels. Restoration Ecology 10:213-222.

Hood WG. 2007. Scaling tidal channel geometry with marsh island area: A tool for habitat restoration, linked to channel formation process. Water Resources Research 43:1-15.

Hood WG. 2014. Differences in tidal channel network geometry between reference marshes and marshes restored by historical dike breaching. Ecological Engineering 71:563-573.

Hood WG. 2015. Predicting the number, orientation and spacing of dike breaches for tidal marsh restoration. Ecological Engineering 83:319–327.

Hood WG. 2018. Applying tidal landform scaling to habitat restoration planning, design, and monitoring. Estuarine Coastal and Shelf Science 244:1-10.

Horton RE. 1945. Erosional developments of streams and their drainage basins: Hydrophysical approach to quantitative morphology. Geological Society of America Bulletin 56:275-370.

Lanzoni S, D'Alpaos A. 2015. On funneling of tidal channels. Journal of Geophysical Research: Earth Surface 120:1-20.

Lawrence PJ, Smith GR, Sullivan MJP, Mossman HL. 2018. Restored saltmarshes lack the topographic diversity found in natural habitat. Ecological Engineering 115:58-66.

Olson-Rutz KM, Marlow CB. 1992. Analysis and interpretation of stream channel cross-sectional data. North American Journal of Fisheries Management 12:55-61.

Reed DJ, Spencer T, Murray AL, French JR, Leonard L. 1999. Marsh surface sediment deposition and the role of tidal creeks: Implications for created and managed coastal marshes. Journal of Coastal Conservation 5:81-90.

So, K, van de Wetering S, Van Hoy R, Mills J. 2009. An Analysis of Reference Tidal Channel Plan Form Characteristics for the Ni-les'tun Unit Restoration. U.S. Fish and Wildlife Service Pacific Northwest Regional Office.

van de Wetering S, French R, Hall A, Gray A, Smith B. 2007. Fisheries Restoration Efficacy Monitoring Report for the Little Nestucca USFWS Coastal Refuge Property. Confederated Tribes of Siletz Indians of Oregon.

Zeff MJ. 1999. Salt marsh tidal channel morphology: Applications for wetland creation and restoration. Restoration Ecology 7:205-211.

Chapter 4: Tidal channel and groundwater hydrology

Christopher Janousek, Scott Bailey, and Laura Brophy

Key findings

- Before restoration, remnant tidal channels at SFC had much lower daily maximum water levels than tidally influenced reference channels. After dike removal, channel water levels inside SFC were generally similar to the water levels at the nearby Dry Stocking Island reference channel showing full tidal restoration at the site.
- Channel water temperature varied seasonally at SFC but did not change markedly after restoration. Both before and after restoration, temperature was similar between SFC and the nearby Dry Stocking Island reference channel.
- Channel salinities were low within SFC before restoration, but increased after restoration with the resumption of tidal exchange. Winter salinities after restoration were fresh to oligohaline and summer salinities were mesohaline to polyhaline across the entire SFC site.
- Groundwater levels were lower at SFC than in reference high marshes before restoration, particularly during the dry season, but they increased markedly at SFC after restoration of tidal flows. After restoration, groundwater levels varied spatially within SFC, with the lower-elevation stations having near-constant saturation of surface soils.
- In reference wetlands and at SFC daily groundwater range (minimum to maximum water level) varied by season and by monthly tide stage (neap versus spring tide); at SFC range was also strongly affect by restoration.
- During the early post-restoration period, SFC groundwater varied seasonally and spatially in salinity. In the winter stations in the cropped and north zones were freshest (oligohaline), while groundwater in the middle zone was mesohaline. In the summer, groundwater all SFC zones tended to be mesohaline.

Introduction

Hydrology is one of the most important dynamic processes in tidal wetlands and is often viewed as a “master variable” that affects a range of structural and functional aspects of these ecosystems. Hydrologic variability affects the physicochemical environment of soils, fluxes of nutrients and gases, and organism abundance and behavior. Least-disturbed tidal wetlands typically have three major hydrologic drivers affecting surface and sub-surface movement of water: daily tidal fluctuations, river (fluvial) effects, and groundwater seepage from upland areas.

Daily tidal variability is the most obvious and regular component of tidal wetland hydrology. Along the Pacific Northwest coast, tidal cycles consist of two high and two low tides (mixed semi-diurnal) occurring over a period slightly greater than 24 hours. Tidal amplitude changes over the course of each month and includes two periods when tidal range is smaller (neap tides) and two periods when it is greater (spring tides). In Tillamook Bay, the typical daily tide range (difference between mean lower low water and mean higher high water) is about 2.1-2.5 m, depending on location in the estuary (tidesandcurrents.noaa.gov). Daily tidal variability drives, and interacts with, a range of important tidal

wetland processes including the daily filling and drainage of wetland channels, periodic inundation of the wetland plain, fluctuations in groundwater, and supply of sediments and nutrients to the ecosystem (Brophy et al. 2014).

Variability in river flows also affects water levels in tidal wetlands. Strong river flows can increase estuarine water levels, decrease salinity, and transport mineral sediment and dissolved organic matter from local watersheds to estuarine wetlands. The fluvial (riverine) component of tidal wetland hydrology has a distinct seasonal component in the PNW, where flows are minimal in the dry season (June-September) and substantially greater from fall through spring (October-May). Individual PNW estuaries differ considerably in their degree of riverine influence (Lee and Brown 2009). Tillamook Bay itself is a drowned river mouth estuary that has been classified as tide-dominated (Lee and Brown 2009). Five rivers are the major source of freshwater inputs into Tillamook Bay: Miami River, Kilchis River, Wilson River, Trask River, and Tillamook River.

The third major forcing factor affecting tidal wetland hydrology is sub-surface flows of water that mainly influence groundwater variability in tidal wetlands. Freshwater inflow from upland areas (Alvarez et al. 2015) may raise water tables in tidal wetlands (especially during low tide) and reduce groundwater salinity. Sub-surface vertical and horizontal flows of water are not nearly as well studied in tidal wetlands as surface flows (Alvarez et al. 2015; but see Brophy et al. 2014, 2017 for data from other Oregon tidal wetlands), even though groundwater variability is important to wetland plants and animals (Wilson et al. 2015). For example, soil saturation and salinity affect plant productivity (Schile et al. 2011), organic matter decomposition (Mueller et al. 2018), and greenhouse gas emissions (Chapter 9).

Former tidal wetlands that have been diked generally have dramatically different hydrology than least disturbed wetlands. Foremost, tidal inundation is lost (or reduced in the case of muted tidal wetlands), affecting groundwater hydrology, and transport of nutrients, salt, and sediments. Similarly, diked wetlands are cut off from river influence (except if levees are overtopped in rare cases of very high river flow), and may have other alterations that affect their connectivity to upland water tables as well. Least-disturbed and restoring tidal wetlands may have differences in hydrology due to a number of causes. Restoring wetlands that are lower in elevation than least-disturbed sites may have greater connectivity with the estuary via flows over the marsh edge than through channel networks (Temmerman et al. 2005). Restoring wetland channel networks may change rapidly (Chapter 3; Wallace et al. 2005).

Documenting hydrologic change upon dike removal and channel excavation at SFC was one of the key monitoring objectives of this project. In this chapter we report on changes to tidal channel and groundwater hydrology and water quality from the pre-restoration monitoring period to the post-restoration period at both SFC and in reference channels and marsh. For both sampling periods we examined variability in tidal channel water level, salinity, and temperature. For the post-restoration monitoring period we also examined groundwater salinity. Our analyses center on the simple hypothesis that dike removal at SFC led to rapid dramatic changes in both surface water and groundwater conditions inside the site. For groundwater dynamics, we also examined the effects of wetland restoration relative to other potential sources of variability including differences across seasons and spring-neap tidal cycles.

Materials and methods

Channel hydrology. To measure water level, temperature, and salinity in tidal channels, we deployed Hobo pressure sensors (Onset Corporation) and Odyssey conductivity and temperature loggers (Dataflow Systems Ltd, Christchurch, NZ) in channels associated with reference wetlands and in channels inside the historically diked area at SFC (Table 4.1, Figure 4.1). We deployed loggers inside 5-cm diameter PVC stilling wells, typically angled from the edge of the vegetated wetland bank into the

channel at approximately a 45-degree angle, with the loggers positioned at about mean tide level (MTL) at most stations (sensor elevation was lower at the Dry Stocking Island station which was installed in a stilling well on a vertical piling in the Trask River). Loggers recorded values every 15 minutes. During both the pre-and post-restoration monitoring periods, we measured the precise geodetic elevation of the sensors with RTK GPS using methods described in Chapter 2. We conducted up to three elevation measurements per station during the post-restoration monitoring period and averaged measurements (pre-restoration elevations from the DSI station were used as it was unchanged). To correct raw water level data due to variability in barometric pressure, we collected a time series of barometric pressure with an additional Hobo logger placed in vegetation about the highest tide level at the Goose Point reference site. We then used Onset Hoboware software to correct raw water level data.

Similarly, we made adjustments to the raw conductivity and temperature data collected with the Odyssey loggers as follows: (1) we converted raw specific conductance data to salinity using equations in Fofonoff and Millard (1983) or Wagner et al. (2006), and (2) we adjusted raw salinity and temperature data using logger-specific linear regression equations between raw logger output and temperature and salinity measured with YSI handheld meters (YSI Incorporated, Yellow Springs, OH) in a series of water baths. Using the water level time series from the same station, we filtered salinity and temperature time series to only include data when the Odyssey sensor was at least 2 cm underwater (moderate to high tide levels), thereby removing values representing air temperature or conductivity values ~0 when the logger was out of the water.

We obtained at least one year of data during each of the pre-restoration (2013-2014) and post-restoration (Sept 2017-Sept 2018) monitoring periods. For analyses here, we focus on two shorter segments of the time series (each 4 months) before and after restoration actions were implemented: the cool, wet season (Dec-Mar), and warm, dry season (June-Sept).

Channel hydrology analyses. For wet and dry season water level time series, we calculated the daily maximum water level at each station in the pre- and post-restoration monitoring periods. Because differences between sampling periods were so marked within SFC, we describe results qualitatively and graphically. For temperature and salinity data from channels, we determined the daily average water temperature and salinity during periods when the loggers were submerged. Similarly, we present data graphically by season for select stations inside and outside SFC.

Groundwater. Similar to tidal channel monitoring, we obtained time series of water levels in shallow groundwater wells at six locations within SFC and at two stations in high marsh reference wetlands (Figure 4.2, Table 4.2) during pre-restoration (May 2014 to May 2015), and post-restoration (Sept 2017-Sept 2018) periods. Wells consisted of capped 4 cm diameter PVC well screen inserted about 1.2 meters below the ground surface with an unperforated riser extending about 20-30 cm above ground. The wells were loosely capped with a 5 cm diameter PVC cap, though they let water into the wells through the top at high tide. Around the base of the well at the ground surface we placed a sodium bentonite seal (USACE 2000). Into each well we placed a Hobo U-20 logger (Onset Corporation) that recorded absolute pressure values every 15 minutes. We corrected raw pressure time series with barometric pressure as described above for channel loggers.

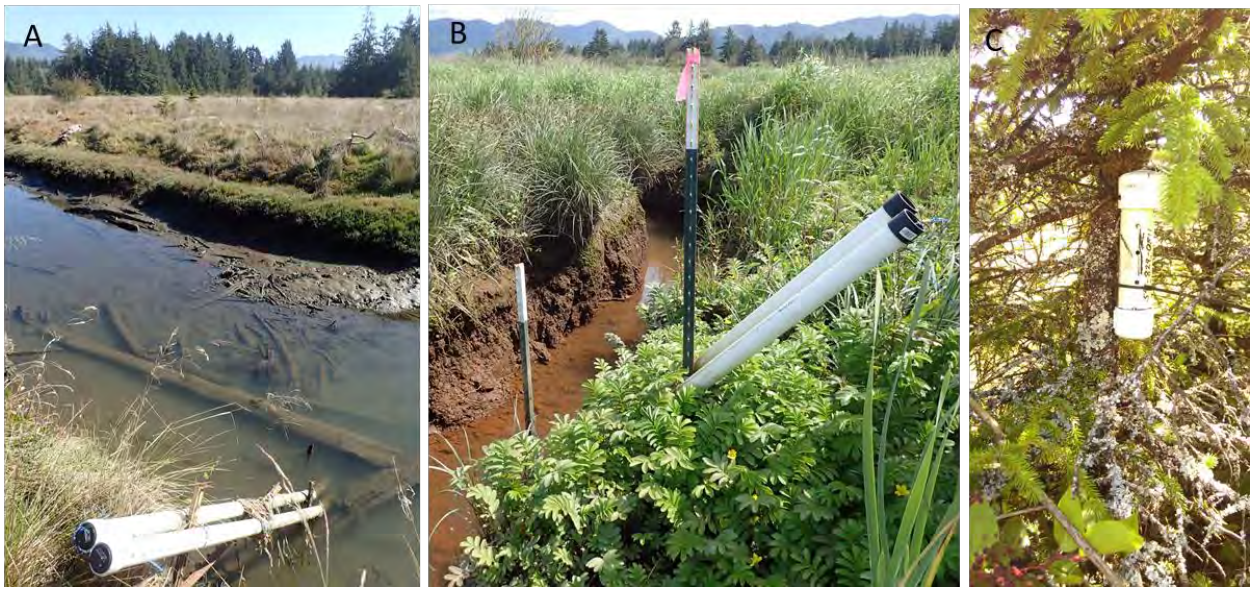

Figure 4.1. Representative water monitoring stations. A. Dual stilling wells with water level and salinity sensors in the main tidal channel at Goose Point reference marsh. B. Stilling wells in a constructed tidal channel at SFC. C. Barometric pressure monitoring station in a small Sitka Spruce tree at Goose Point marsh. Photos by C. Janousek.

Table 4.1. List of monitoring stations for tidal channel water level, temperature, and conductivity. Sensor elevations are relative to NAVD88 (with geoid12A). We present data for five of these stations in this report.

			Station location in 2018*		Sensor elevation (m)	
Station ID	Station ID	Channel type	Easting (m)	Northing (m)	Pressure sensor	Conductivity sensor
Wilson River adjacent to Dry Stocking Island	WR	Reference	431068	5035463	-0.34	1.27
Tidal channel near Bay Marsh	BM	Reference	430158	5036984	1.05	1.22
Main tidal channel at Goose Point marsh	GP-C	Reference	430796	5039842	1.32	1.27
Mouth of Blind Slough	BSmth	Reference	431167	5036464	1.21	1.23
Midpoint Blind Slough	BSmid	Restored	431525	5036276	1.20	1.20
Upper Blind Slough	BSupr	Restored	431857	5035983	1.10	1.11
Blind Slough Tributary	T1lwr	Restored	431290	5036183	1.15	1.16
E-W Drainage ditch/ upper Blind Slough Tributary	T1upr	Restored	431311	5035945	1.07	1.09
Nolan Slough	NS	Restored	431740	5035439	1.16	1.17

* Locations of several stations were slightly different in 2014.

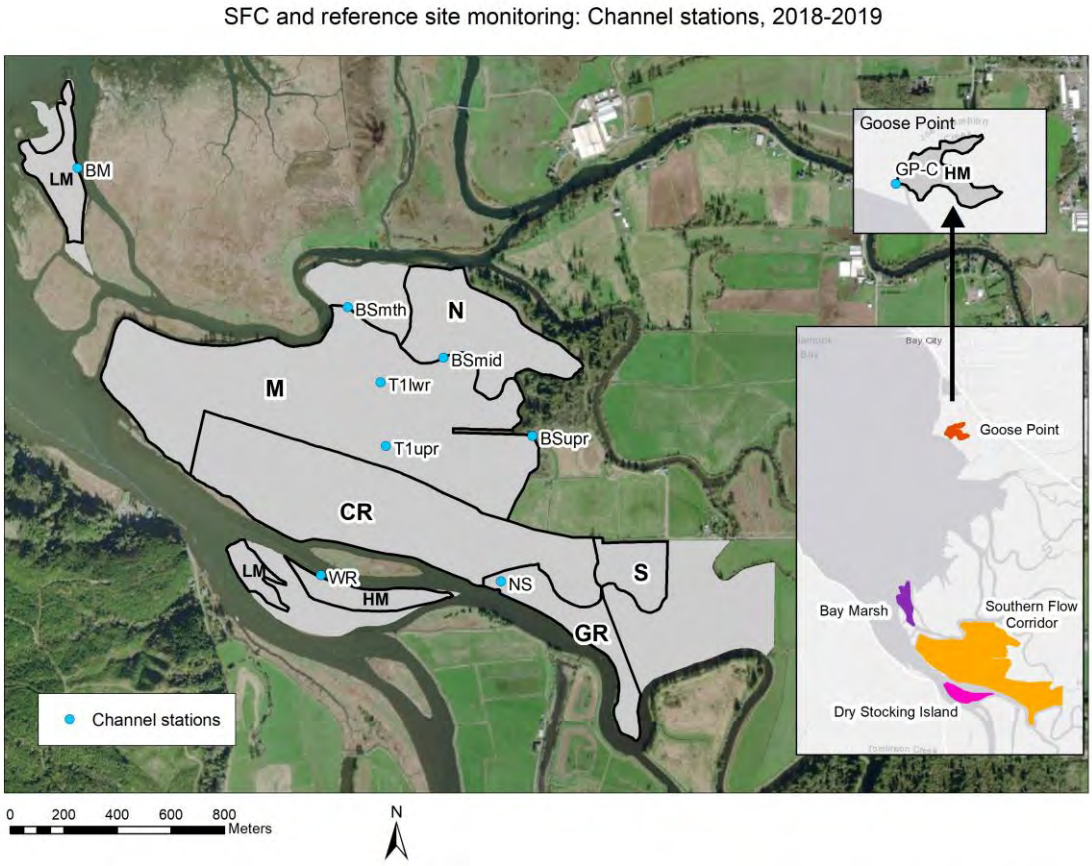

Figure 4.2. Map of channel monitoring stations at the SFC project and in reference wetlands.

During the post-restoration monitoring period, we added a second set of groundwater wells next to existing wells to measure groundwater salinity. These wells were shallower to sample conditions closer to the rhizosphere (they extended about 30 cm below the soil surface), slightly wider (5 cm diameter) to accommodate larger sensors, and had longer risers (approx. 60 cm) to prevent influx of freely-flowing water into the wells during high tides. We similarly used a sodium bentonite clay seal around the base of each well. At the bottom of each well we added an Odyssey conductivity logger, also programmed to obtain data every 15 min. Using the groundwater level time series, we subset the salinity and temperature data from the conductivity loggers so that we obtained a time series of values only when the loggers were submerged in groundwater, representing rhizosphere (rooting-zone) conditions.

Groundwater hydrology analyses. We determined differences in the distributions of groundwater levels in pre- versus post-restoration sampling periods with Kolmogorov-Smirnov tests using all of the 15 min water level values. We analyzed each station and season separately (we did not analyze Doty Creek data as there was no pre-restoration sampling, but show post-restoration values graphically). We used a bootstrapping method in the R package "Matching" to determine P-values in each test. Because very large sample sizes can lead to statistical significance for even small ecological differences, we also used the test statistic D (which ranges from 0 to 1) for each station and season as an effect size metric to quantify the relative change in water level distributions from pre- to post-restoration sampling periods. Values of D closer to 1 indicate greater differences in overall groundwater levels.

In addition to groundwater distributions relative to the soil surface, we analyzed how dynamic groundwater was at each station. We computed the daily range (max-min) of groundwater at each station for each season and sampling period. We also categorized each day by whether it fell on during a neap tide or spring tide period. Spring tide periods were defined as a 7-day window centered on each month's full and new moon (US Navy data). To determine how much variability in groundwater range was due to restoration (R), season (S), and monthly tide cycle (T) effects, we conducted 3-factor ANOVA at each station (2 factor for three stations where we did not have dry season data in the post-restoration period). We followed up on ANOVA analyses with hierarchical partitioning (Walsh and MacNally 2015) to quantify the relative importance of restoration, season, and tide cycle in each model.

Since we did not have pre-restoration groundwater salinity data, we present post-restoration salinity and temperature data graphically. Channel and groundwater analyses were conducted with R v.3.5.0, v.3.6.2 and v.4.0.3.

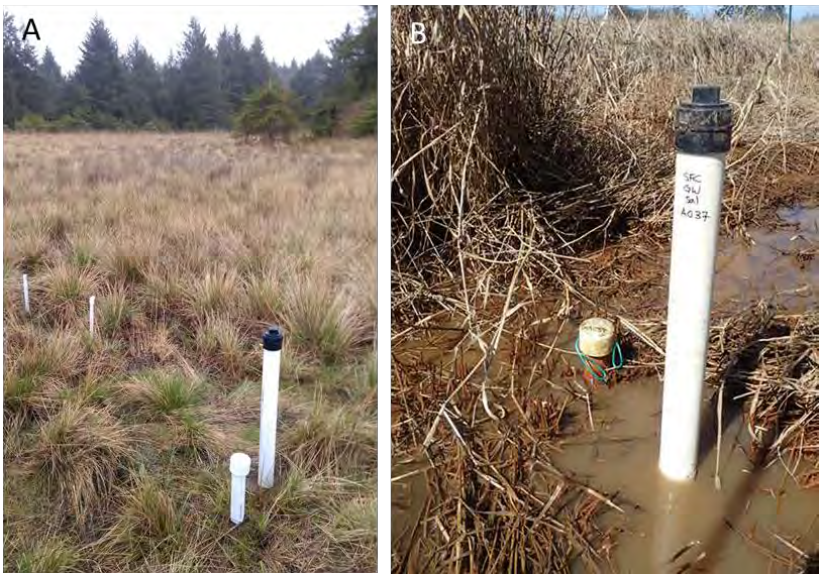

Figure 4.3. Pairs of groundwater wells at (A) Goose Point reference marsh, and (B) station A037 at SFC. Water level loggers in the shorter, deeper wells recorded time series of water level relative to the wetland surface during pre- and post-restoration monitoring periods. Conductivity loggers in the taller, and more shallow wells recorded groundwater salinity and temperature during the post-restoration monitoring period at about the bottom of the rooting zone. Photos by C. Janousek.

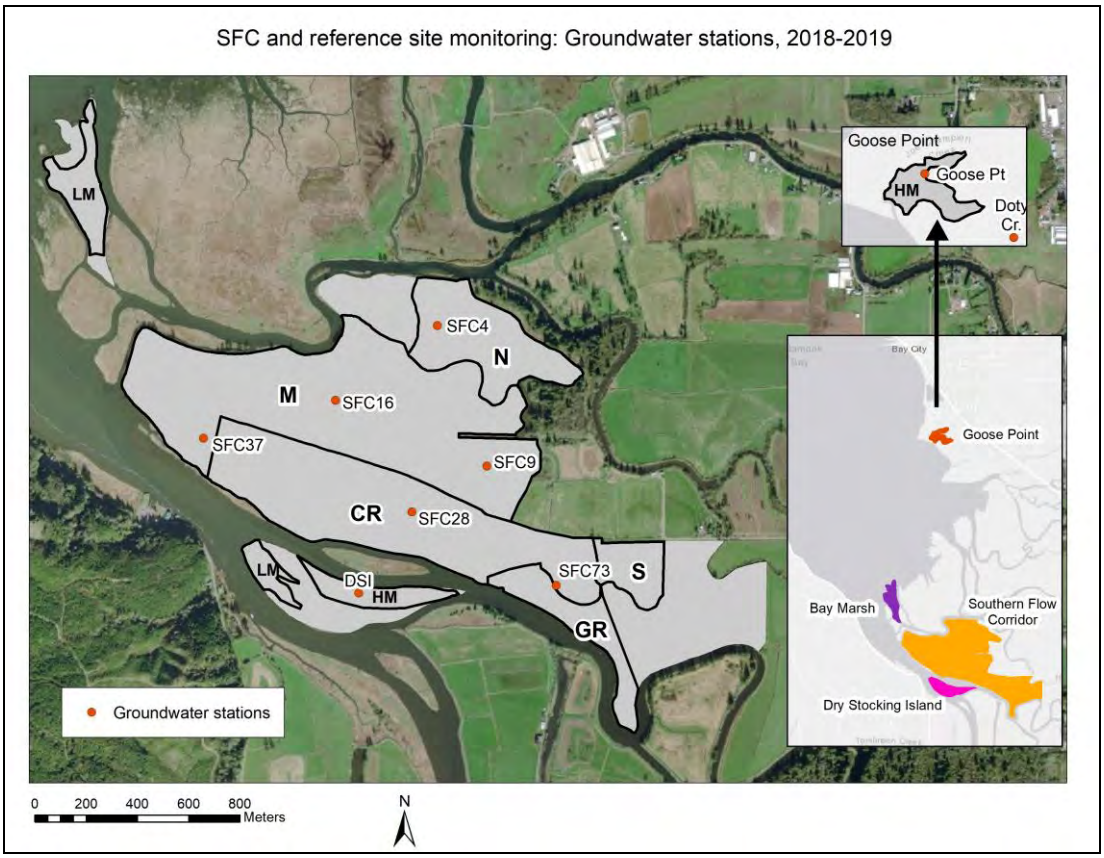

Figure 4.4. Map of groundwater monitoring stations for 2013-2014 and 2017-2018 at the SFC project and in reference wetlands. Land-use/land-cover zones are shown (N, M, CR, S, GR, LM, HM). Background: ESRI World Imagery.

Table 4.2. List of monitoring stations for groundwater water level, temperature, and conductivity. Easting and northing values are in UTM, 10N. Ground surface elevations are relative to NAVD88 (with geoid12A).

Station ID and location	Station code	Wetland type	Land-use/land-cover zone	Station location		Ground elevation (m)
				Easting (m)	Northing (m)	
A043, Dry Stocking Island	DSI	Reference	HM	431171	5035388	2.63
A068, Goose Pt marsh	GP	Reference	HM	430963	5039939	2.67
Doty Creek marsh	DC	Reference	HM	431310	5039691	2.46
A004, SFC	SFC4	Restored	N	431479	5036430	2.19
A009, SFC	SFC9	Restored	M	431672	5035883	1.86
A016, SFC	SFC16	Restored	M	431081	5036139	2.07
A028, SFC	SFC28	Restored	CR	431378	5035704	2.00
A037, SFC	SFC37	Restored	M	430566	5035991	1.98
A073, SFC	SFC73	Restored	CR	431941	5035419	2.43

Results and discussion

Channel water levels. Pre-restoration water levels inside SFC and in reference tidal channels are described in detail in Brown et al. (2016). In summary, pre-restoration maximum water levels internal to the SFC site were typically about 0.6-1.2 meters lower than in fully tidal channels during the dry season, and 0.7-1.0 meters lower during the wet season.

On the Wilson River (WR) near Dry Stocking Island (reference channel), maximum water levels were similar during pre-and post-restoration monitoring periods (Figure 4.5). They showed week-to-week variability in maximum water levels, associated with monthly spring and neap tide cycles. In SFC channels however, daily maximum water levels were markedly higher during the post-restoration monitoring period (2017-2018) than before dike removal, showing the expected large change in inundation regime as expected once tidal influence was restored. Representative maximum daily water level data for two stations internal to SFC are shown for the mouth of Nolan Slough, a station just inside the old levee protecting SFC (Figure 4.6), and for the lower Tributary 1 station which was well inside SFC in the M zone (Figure 4.7). Maximum daily water level data for additional stations inside SFC are provided in Appendix Figures A4.1-A4.2.

The pronounced increase in water levels inside SFC following restoration is expected to benefit anadromous fish which have declined markedly over the last century in the Pacific Northwest (PNW) (Price et al. 2019). Several salmonid species or stocks such as fall Chinook salmon (*Oncorhynchus tshawytscha*) are particularly dependent on estuaries for refuge and food as they complete migration cycles from spawning areas to the Pacific Ocean (Magnusson and Hilborn 2003, Bottom et al. 2005). Such species would have daily access to SFC tidal channels to forage and find refuge. Fish abundance and migration results are shown in detail in Chapter 6.

Restoration of tidal influence to SFC in 2016 also provided daily connectivity with the broader estuary enabling transport of water, nutrients, and sediments into and out of the interior of the site.

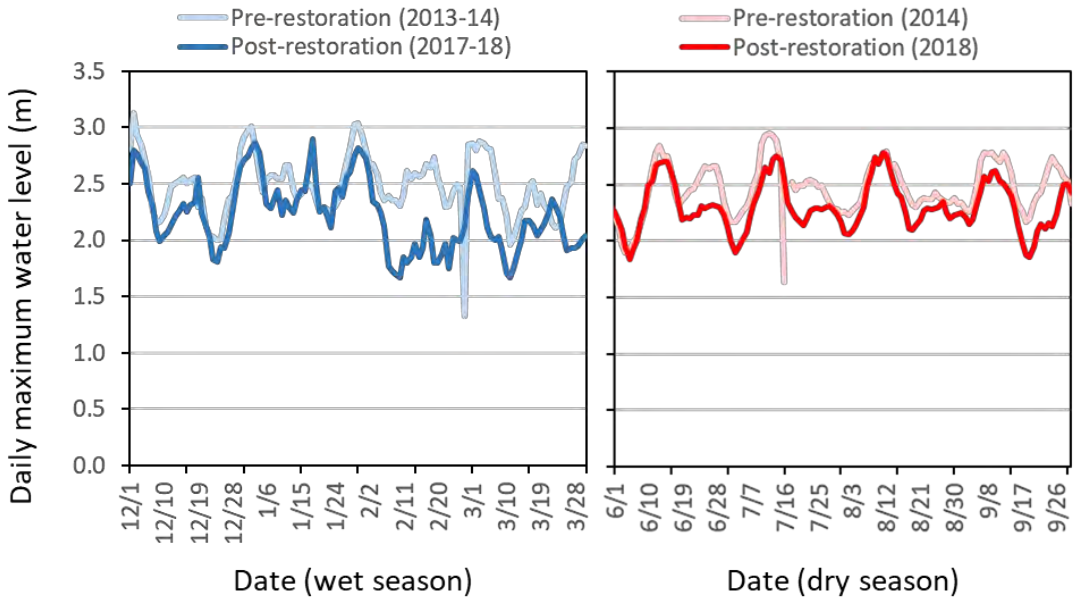

Figure 4.5. Time series of daily maximum water levels (in meters relative to NAVD88) at the Wilson River reference station near Dry Stocking Island for the annual wet (Dec-Mar) and dry (Jun-Sep) seasons during the pre- and post-restoration monitoring periods.

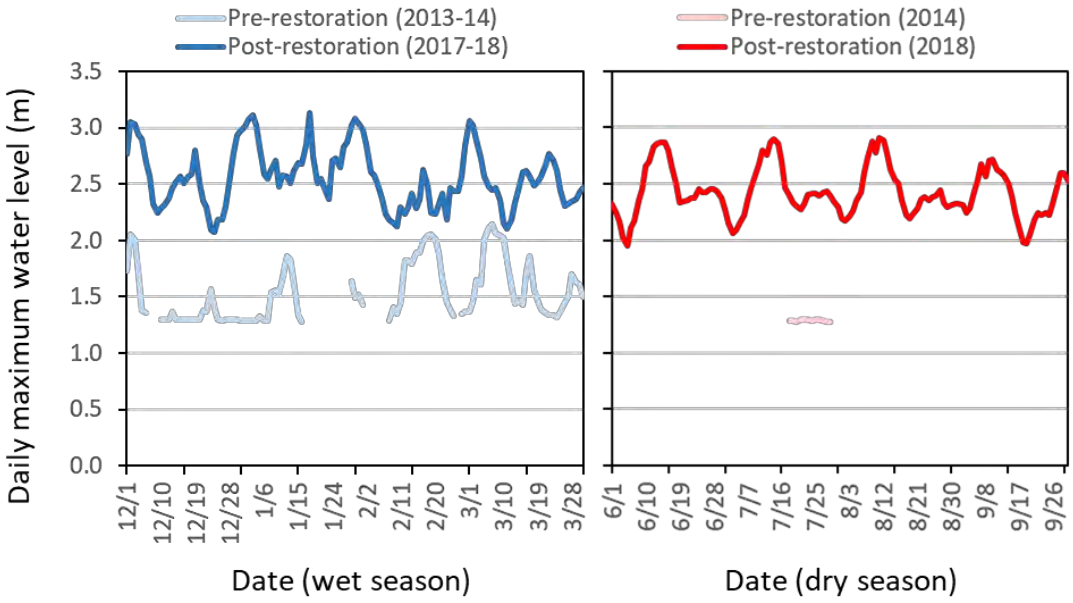

Figure 4.6. Time series of daily maximum water levels (in meters relative to NAVD88) near the mouth of Nolan Slough inside SFC for the annual wet (Dec-Mar) and dry (Jun-Sep) seasons during the pre- and post-restoration monitoring periods. Water level was only calculated when the sensor was submerged (it was seldom submerged during the dry season before restoration).

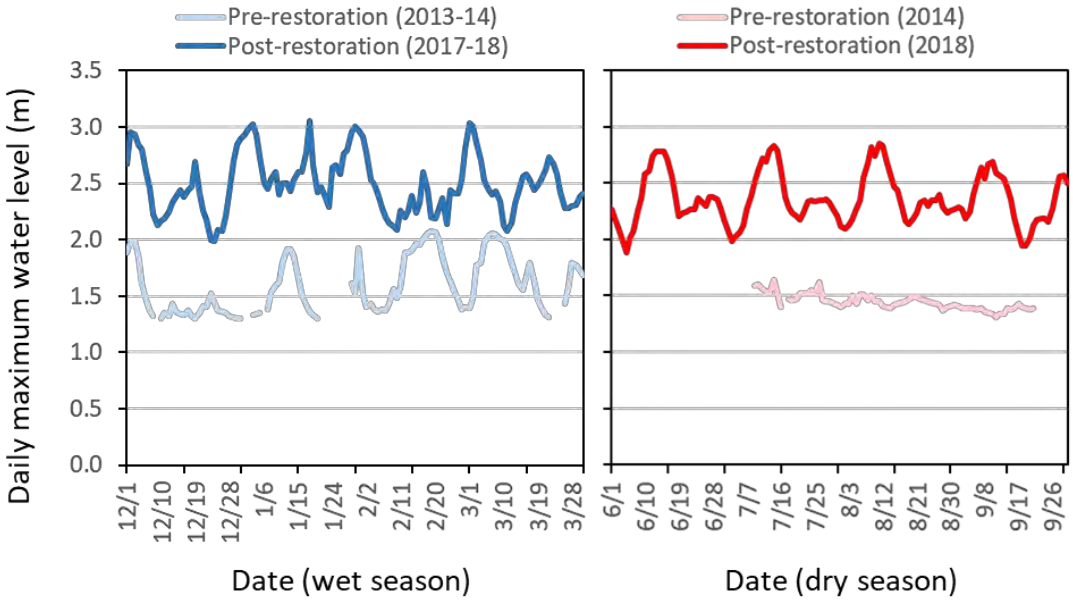

Figure 4.7. Time series of daily maximum water levels (in meters relative to NAVD88) at the lower Tributary 1 station inside SFC for the annual wet (Dec-Mar) and dry (Jun-Sep) seasons during the pre- and post-restoration monitoring periods. Water level was only calculated when the sensor was submerged.

Channel temperature and salinity. Both SFC channels and the nearby reference station on the Wilson River in southern Tillamook Bay showed a distinct seasonal signal in water temperatures, with wet season values tending to be below 10°C and dry season values often between 15-22°C (Figures 4.8-4.10). Channel water temperature did not differ markedly between sampling years (2014 versus 2018), although there were some periods of particularly low water temperatures (<5°C) in the winter months of 2014 at both reference and SFC stations. At Dry Stocking Island, seasonal temperatures were similar between 2014 and 2018. At SFC it was possible to compare pre- versus post-restoration channel temperatures for only some stations and some periods because conductivity loggers were often left exposed to air during low water levels in the pre-restoration monitoring period. When immersed, however, SFC stations tended to be cooler in the winter before restoration, but similar in temperature before and after restoration during the summer (Figure 4.10). Time series of additional SFC stations (BSupr, T1upr) are shown in Appendix Figures A4.3-A4.4.

Channel water monitoring stations also showed distinct seasonal differences in salinity between wet and dry seasons in both pre- and post-restoration monitoring periods inside and outside of SFC. Our reference station on the Wilson River near Dry Stocking Island was fresh to oligohaline during winter months and mesohaline to polyhaline during summer months during both water years monitored (Figure 4.11). Lower salinities at this station during spring and early summer 2014 could be due to higher precipitation and resulting greater river flow during the spring of 2014 versus 2018.

Within SFC, channel stations were fresh to oligohaline during winter months in both pre- and post-restoration periods at all stations (Figures 4.12-4.13; Appendix Figures A4.5-A4.6). During the summer, SFC stations were either not immersed (Figure 4.12, Appendix Figure A4.6), or showed some salinity intrusion into the site (Figure 4.13), despite the presence of levees and tide gates. Once tidal inundation was restored to SFC in 2016, channels became much saltier during the summer, reaching mesohaline to polyhaline conditions. Although we expected a salinity gradient at SFC once restored (saltier to the west and fresher to the east), in both the Blind Slough and Trib 1 channel systems we found relatively saline water at their upper stations in the summer (Figure A4.5, Appendix Figure A4.6). In fact, salinity at T1upr was very similar to the Wilson River station from mid to late summer in 2018.

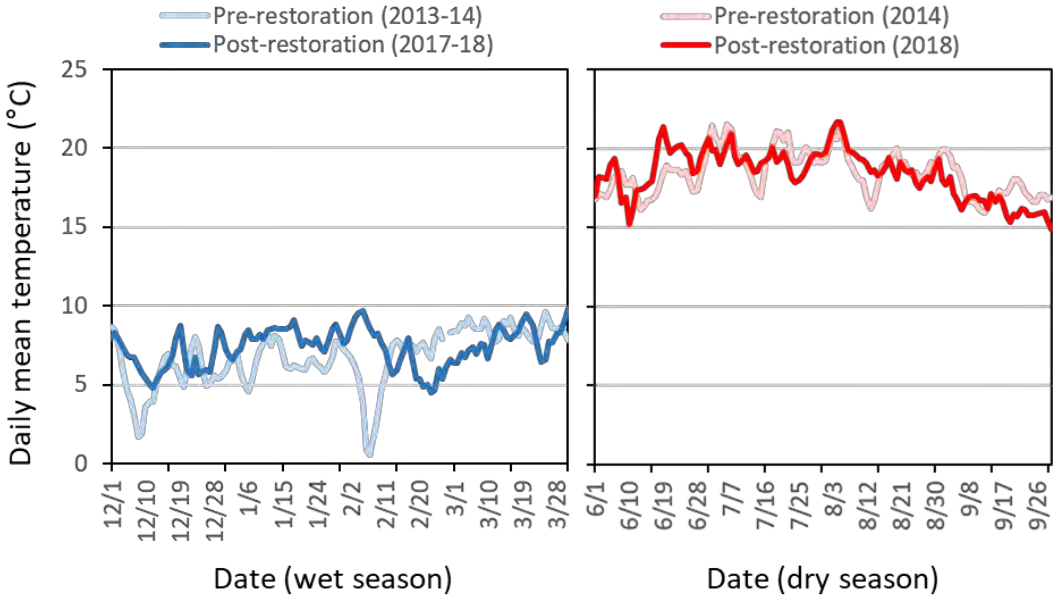

Figure 4.8. Time series of daily average temperature (°C) at the Dry Stocking Island reference station for the annual wet (Dec-Mar) and dry (Jun-Sep) seasons during the pre- and post-restoration monitoring periods. Temperature was only calculated when the sensor was submerged.

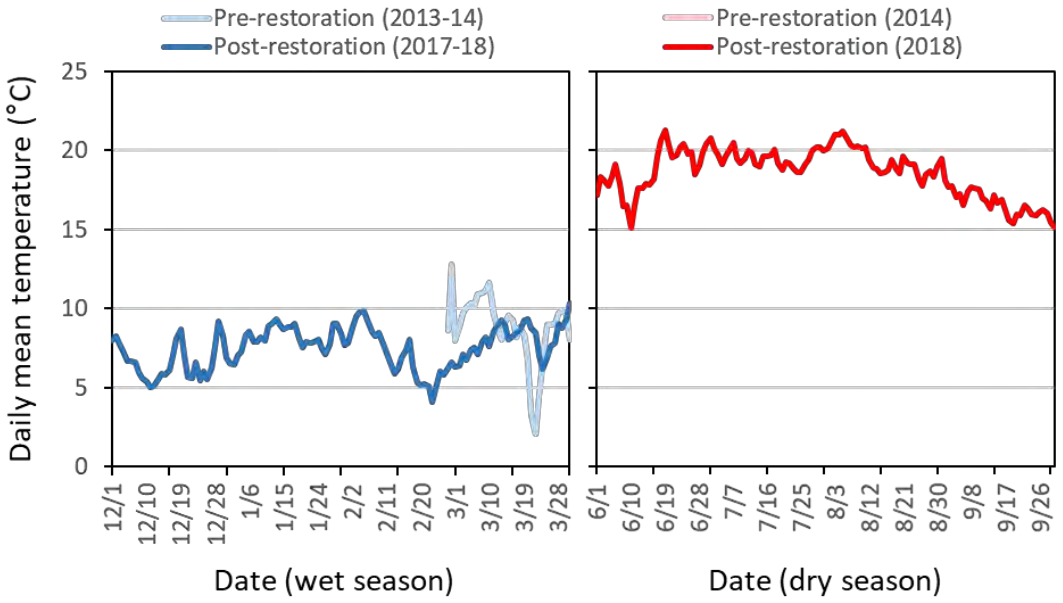

Figure 4.9. Time series of daily average temperature (°C) at the Nolan Slough station inside SFC for the annual wet (Dec-Mar) and dry (Jun-Sep) seasons during the pre- and post-restoration monitoring periods. Temperature was only calculated when the sensor was submerged (it was not submerged during the dry season before restoration or for part of the pre-restoration wet season).

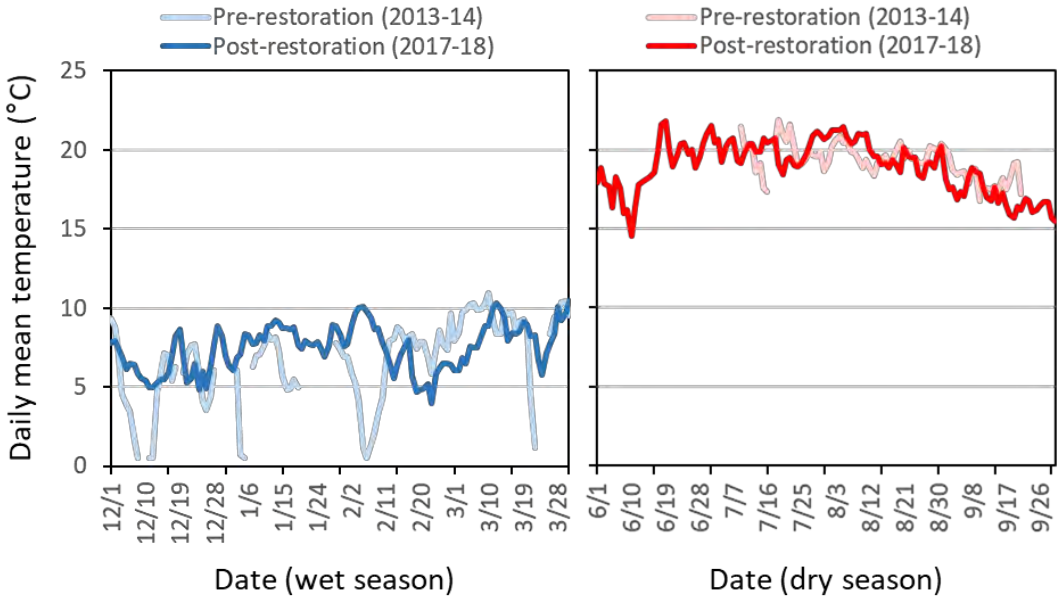

Figure 4.10. Time series of daily average temperature (°C) at the lower Tributary 1 station inside SFC for the annual wet (Dec-Mar) and dry (Jun-Sep) seasons during the pre- and post-restoration monitoring periods. Temperature was only calculated when the sensor was submerged.

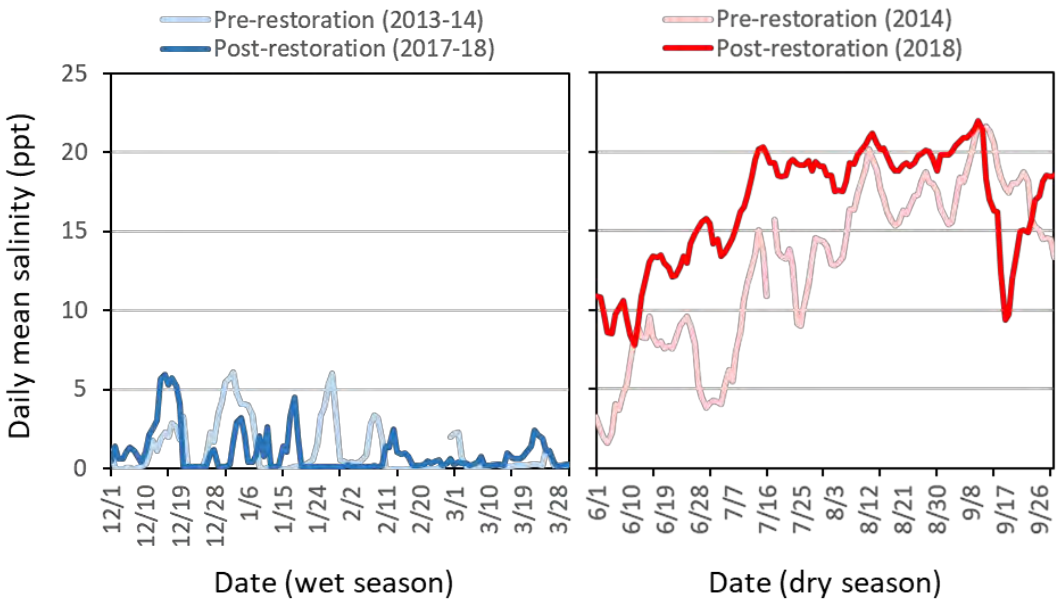

Figure 4.11. Time series of daily average salinity (ppt) at the Dry Stocking Island reference station for the annual wet (Dec-Mar) and dry (Jun-Sep) seasons during the pre- and post-restoration monitoring periods. Salinity was only calculated when the sensor was submerged.

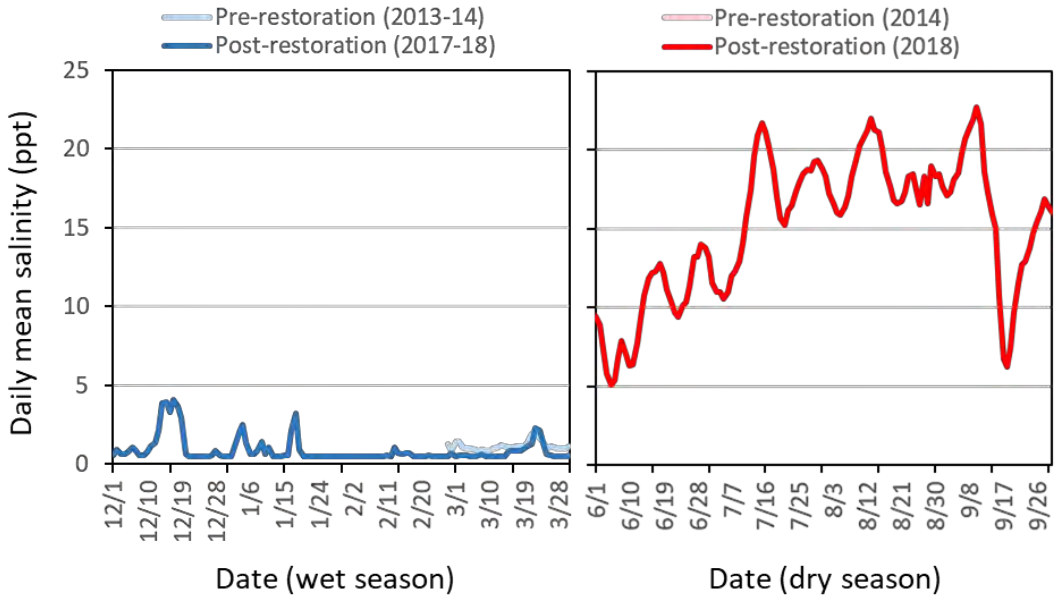

Figure 4.12. Time series of daily average salinity (ppt) at the Nolan Slough station inside SFC for the annual wet (Dec-Mar) and dry (Jun-Sep) seasons during the pre- and post-restoration monitoring periods. Salinity was only calculated when the sensor was submerged (it was not submerged during the dry season before restoration).

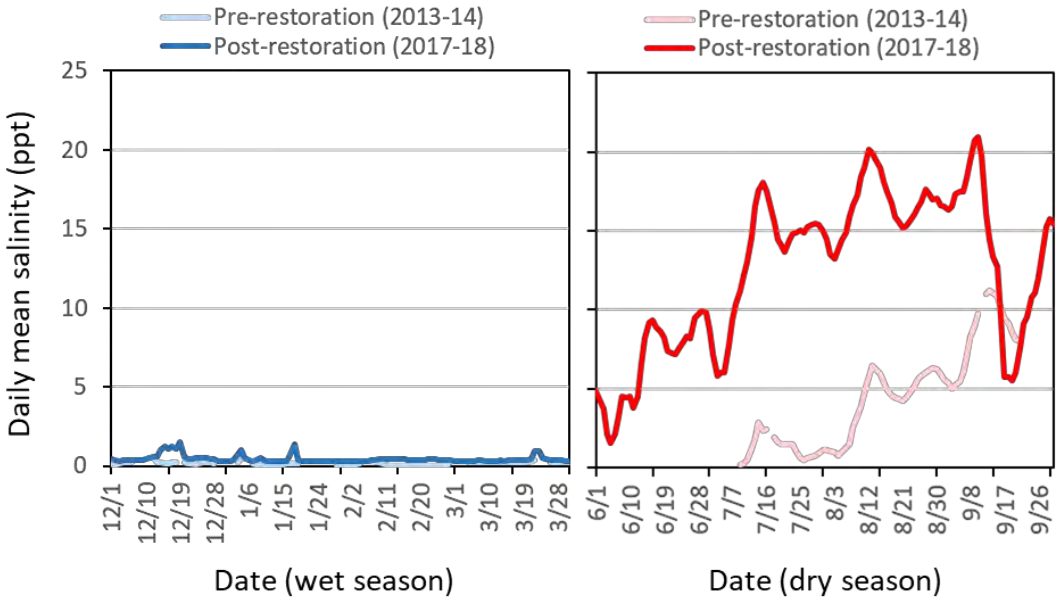

Figure 4.13. Time series of daily average salinity (ppt) at the lower Tributary 1 station inside SFC for the annual wet (Dec-Mar) and dry (Jun-Sep) seasons during the pre- and post-restoration monitoring periods. Salinity was only calculated when the sensor was submerged.

Groundwater levels. During the pre-restoration monitoring period there were major differences in groundwater dynamics between reference high marsh stations and stations located within SFC. Figures 4.14 and 4.15 show representative time series at the Dry Stocking Island reference station and the SFC A016 station during two-month periods in the summer and winter respectively. The Dry Stocking Island time series illustrates typical groundwater patterns in Oregon high marshes, where groundwater is "reset" to near the surface during the highest tides of the month and then gradually declines to deeper levels until the next monthly spring tides (Figure A4.14A; Brophy et al. 2014). The spring tide – associated rise in groundwater levels was also present at station A16 prior to restoration, but the magnitude of the effect was more muted (Figure A4.14B).

Restoration of tidal hydrology had a major effect on the height of groundwater levels at SFC stations, especially during the dry season (Figure 4.16; Table 4.3). While median wet season groundwater levels at SFC rose slightly following restoration, dry season groundwater levels increased substantially at all SFC stations. Restoration effects were statistically significant for all SFC stations at both seasons, but the magnitude of effect ("D" effect size value of Kolmogorov-Smirnov tests) was highest for dry season comparison (Table 4.3). Groundwater levels at three SFC stations (A004, A028, A073) were so low during the dry season prior to restoration that they were below the elevation of the water level sensor (located at 1.2-1.3 m below the surface). In reference wetlands there were statistically significant differences in groundwater levels between pre- and post-restoration monitoring periods (for both seasons), but this was due to very large sample sizes, not major ecological change in reference high marshes.

Groundwater stations in reference marshes and at SFC varied considerably in the percent time that the groundwater table reached the soil surface (or higher), and these patterns varied by season and monitoring period (Figure 4.17). For instance, at stations SFC9 and SFC37 both in the middle zone, water levels were at the soil surface or higher from about 75-100% of the time during the wet season before and after restoration and the dry season after restoration. Water levels reached the soil surface much

less frequently at stations SFC4 (north zone) and SFC73 (cropped zone). Similarly, groundwater infrequently reached the soil surface at the three reference high marsh stations regardless of season or monitoring period. These data support field observations of ponding at certain SFC stations (e.g., SFC9) following restoration. Ponding has been observed in other tidal wetland projects (Lawrence et al. 2018), including at the Ni-les'tun restoration project at Bandon National Wildlife Refuge in southern Oregon (Bridgeland et al. 2017). Post-restoration construction of additional drainage ditches in that project helped alleviate ponding that had contributed to high mosquito densities early in restoration (Bridgeland et al. 2017). Ponding could be due to small-scale soil compaction in some areas at or incomplete connections between excavated channels and all parts of the marsh plain. Ponding near station SFC9 is likely related to historical vegetation type (tidal forested wetland), the associated high soil organic content and consequent subsidence, as well as the low density of channels compared to least-disturbed reference sites (Brophy et al. 2015).

The combination of our channel and groundwater monitoring show the important role of tidal forcing on groundwater levels, as has been observed in other studies (Alvarez et al. 2015). Once tidal flows were restored to SFC channels, groundwater responded in turn. Post-restoration groundwater at SFC was closer to the wetland surface (especially in summer), creating greater saturation in the soil column, and it varied more across a day, responding to daily tidal forcing. Our groundwater level data also illustrate the effect of wetland elevation on overall groundwater levels in tidal wetlands. Groundwater stations at lower wetland elevations in SFC (e.g., stations SFC9, SFC 16, SFC37, and SFC 28) tended to have higher groundwater levels after restoration than stations at higher wetland elevations (e.g., station SFC73).

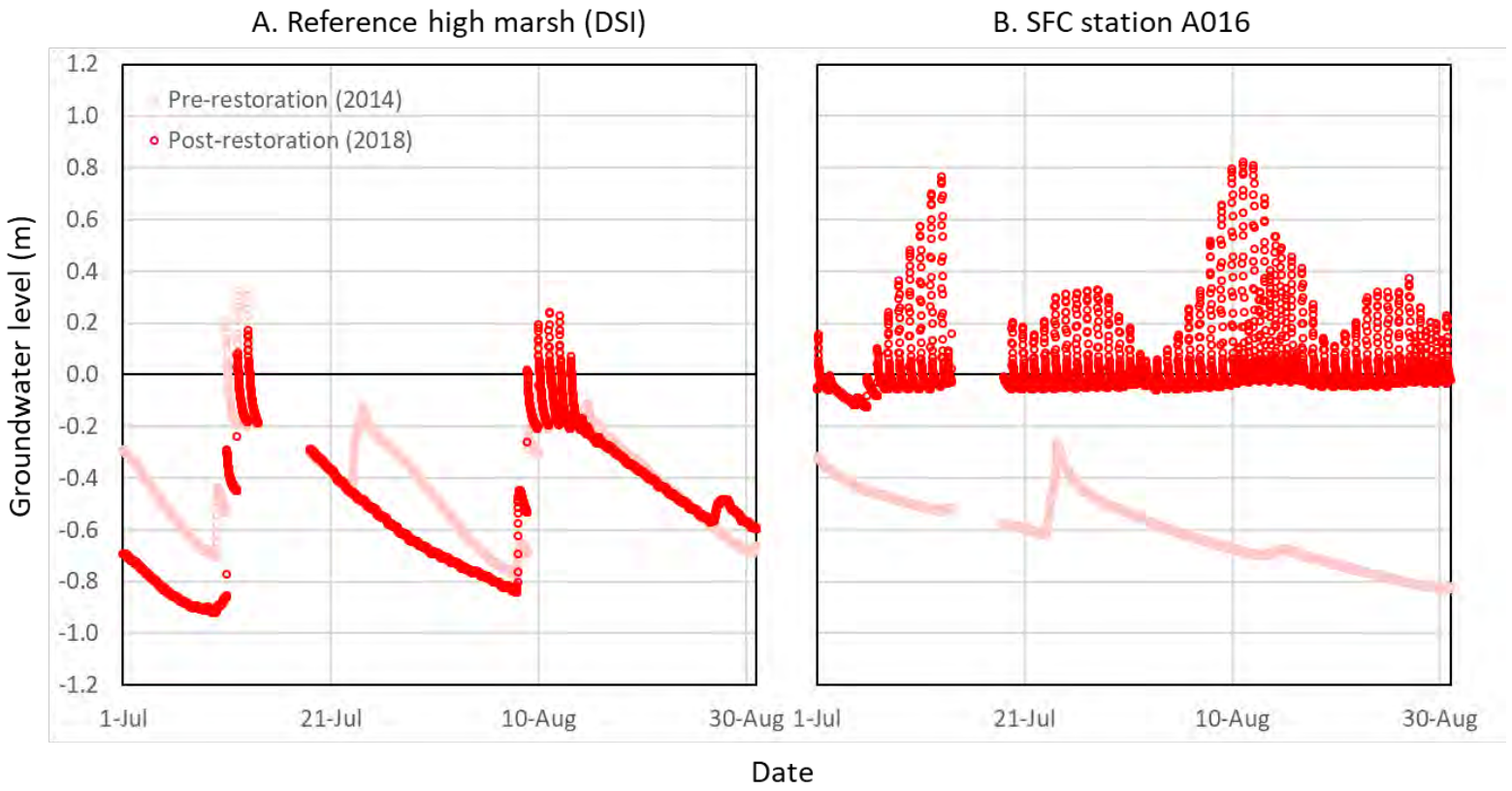

Figure 4.14. Representative time series of groundwater levels relative to the ground surface in (A) a reference high marsh at station DSI, and (B) SFC station A016 for a two month period during the annual dry season. Station A016 was at a relatively low elevation so groundwater was often at or near the sediment surface during the post-restoration period.

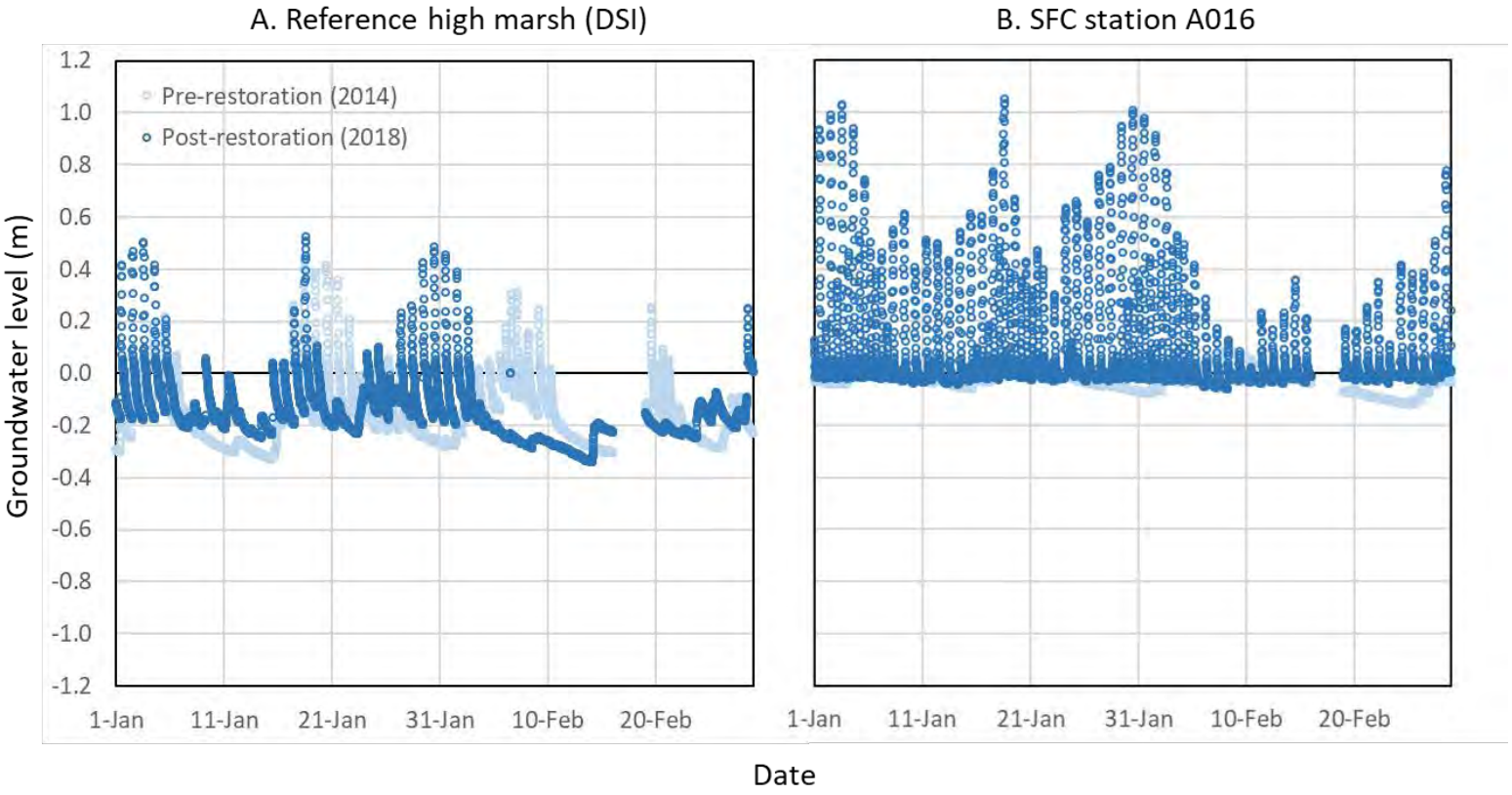

Figure 4.15. Representative time series of groundwater levels relative to the ground surface in (A) a reference high marsh at station DSI, and (B) SFC station A016 for a two-month period during the annual wet season.

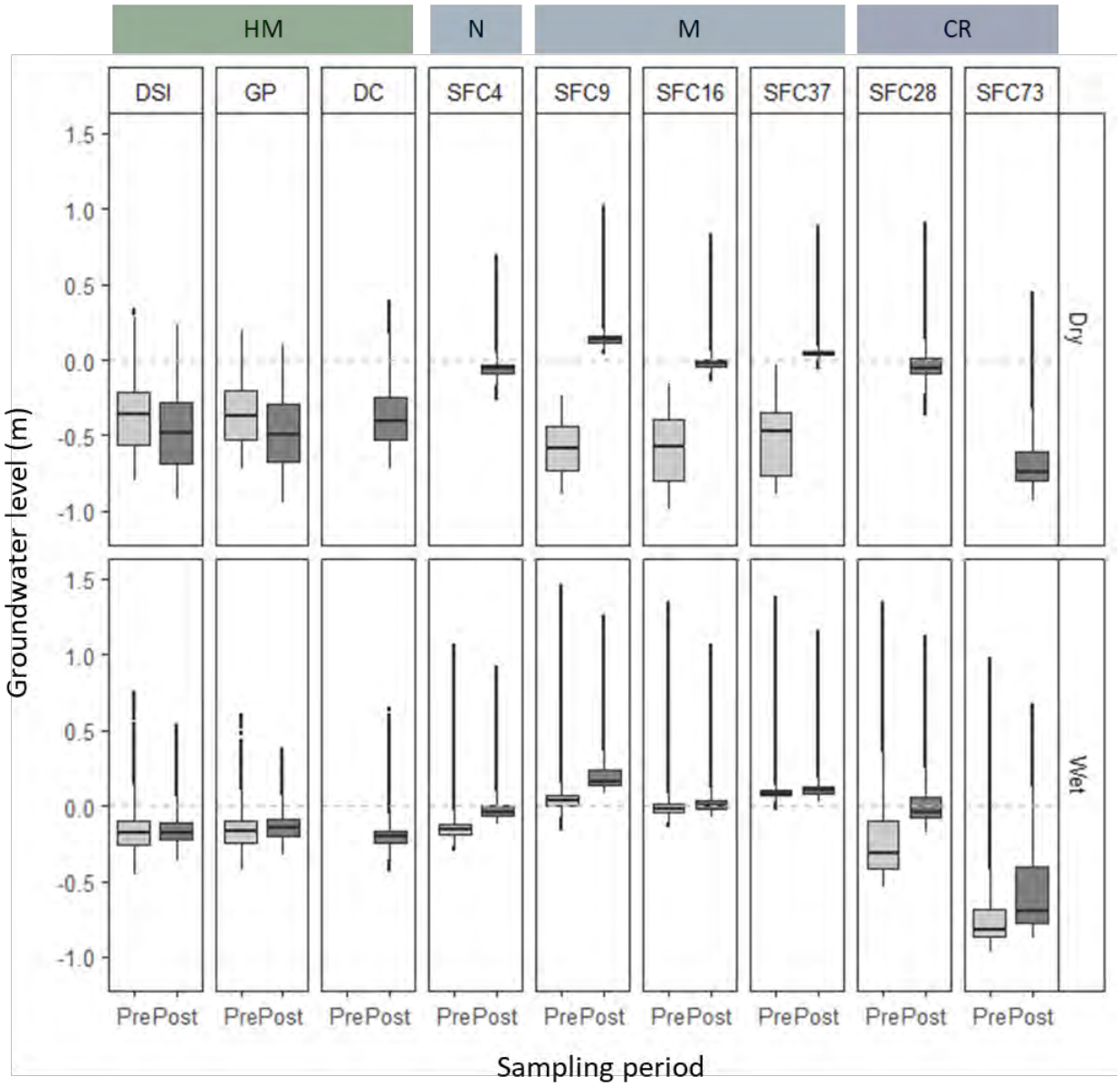

Figure 4.16. Boxplots showing the distribution of groundwater levels relative to the ground surface at three reference marsh stations (DSI, GP, DC) and six SFC stations during the pre-restoration (2014-2015) and post-restoration (2017-2018) monitoring periods. Values above zero indicate standing water on the wetland surface. Data are divided into dry season (top panels; June-Sept) and wet seasons (bottom panels; Nov-March) and are comprised of all 15 min values. HM = reference high marsh; N = SFC north zone; M = SFC middle zone; CR = SFC cropped zone. For statistical results of pre- versus post-restoration distributions, see Table 4.3. Horizontal bars represent median values; the top and bottom of the boxes show the 25% and 75% quantiles.

Table 4.3. Seasonal median and mean groundwater level (m relative to ground surface) by monitoring station and sampling period and differences in pre- versus post-restoration groundwater level distributions by station and season with Kolmogorov-Smirnov tests. Test statistics, D, range from 0 to 1 and illustrate the magnitude of differences between distributions, not just their statistical significance; values closer to 1 indicate larger differences in overall groundwater levels between pre- and post-restoration periods. Sample sizes for each median and mean range from n = 10843 to n = 11328. NA = no data; low = groundwater level consistently below the sensor depth, but quantifiable.

Station ID and location	Season	Pre-restoration		Post-restoration		K-S test	
		Median	Mean	Median	Mean	D	P-value
DSI, Dry Stocking Island	Dry	-0.36	-0.39	-0.48	-0.48	0.18	<0.001
	Wet	-0.18	-0.17	-0.18	-0.16	0.14	<0.001
GP, Goose Pt marsh	Dry	-0.37	-0.37	-0.49	-0.50	0.25	<0.001
	Wet	-0.17	-0.17	-0.14	-0.14	0.17	<0.001
DC, Doty Creek marsh	Dry	NA	NA	-0.40	-0.39	NA	NA
	Wet	NA	NA	-0.20	-0.20	NA	NA
SFC4	Dry	low	low	-0.06	-0.05	NA	NA
	Wet	-0.16	-0.14	-0.04	0.01	0.83	<0.001
SFC9	Dry	-0.58	-0.59	0.13	0.16	1.00	<0.001
	Wet	0.04	0.04	0.16	0.24	0.91	<0.001
SFC16	Dry	-0.58	-0.59	-0.02	0.01	1.00	<0.001
	Wet	-0.02	-0.01	0.00	0.06	0.32	<0.001
SFC28	Dry	low	low	-0.05	-0.02	NA	NA
	Wet	-0.32	-0.25	-0.05	0.04	0.68	<0.001
SFC37	Dry	-0.47	-0.53	0.04	0.08	1.00	<0.001
	Wet	0.08	0.09	0.10	0.16	0.35	<0.001
SFC73	Dry	low	low	-0.75	-0.66	NA	NA
	Wet	-0.82	-0.74	-0.70	-0.56	0.47	<0.001

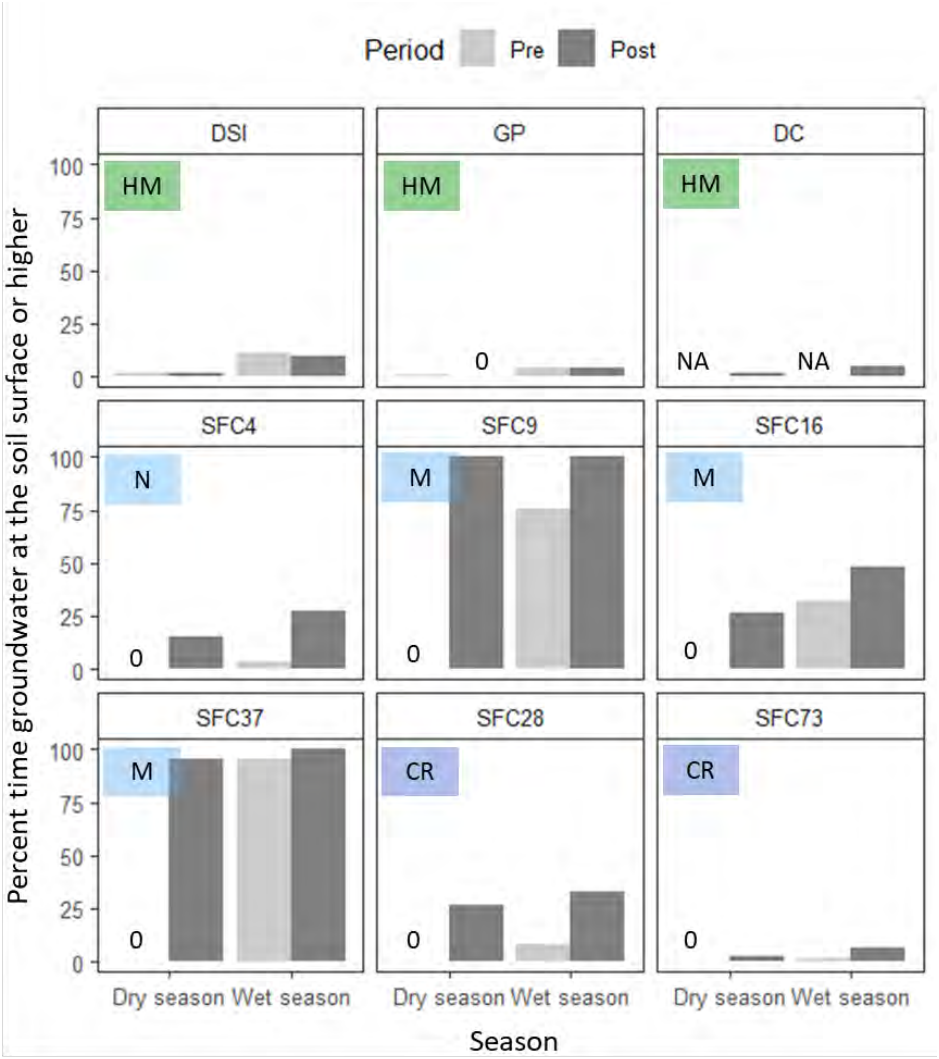

Figure 4.17. Percent of time that groundwater reached the soil surface (or higher) during the wet and dry seasons at nine groundwater stations in the pre- and post-restoration sampling periods. Stations DSI, GP and DC were in reference high marsh (HM); stations SFC4 was in the north zone (N); stations SFC9, SFC16, and SFC37 were in middle zone; and stations SFC28 and SFC73 were in the cropped zone. NA = no data collected.

Groundwater is highly dynamic in tidal wetlands since it is affected by daily tidal forcing. To quantify the extent of short-term fluctuations in groundwater level, we calculated the daily range of groundwater (daily maximum minus minimum value) and tested how that variability was affected by sampling period (pre-versus post-restoration), tide phase (spring versus neap tide periods), and season (wet versus dry season periods). At SFC during the pre-restoration period, daily groundwater range tended to be small, smaller in magnitude than reference high marshes (Figure 4.18). After restoration, however, daily groundwater range increased dramatically at SFC, particularly during the wet season. In both reference high marshes and SFC stations, daily groundwater variability tended to be higher during the wet season and during spring tide periods versus neap tide periods, emphasizing these natural periodic sources of variability in groundwater fluctuations.

Using hierarchical partitioning to quantify the relative importance of drivers for daily groundwater variation, we found that at SFC, effects were dominated by the restoration (Figure 4.19). Tide phase also accounted for some variation in daily groundwater, but much less than restoration. In reference high

marsh stations in contrast, tide phase was the strongest driver of daily groundwater fluctuations while season and pre- versus post-restoration sampling period had relatively minor effects.

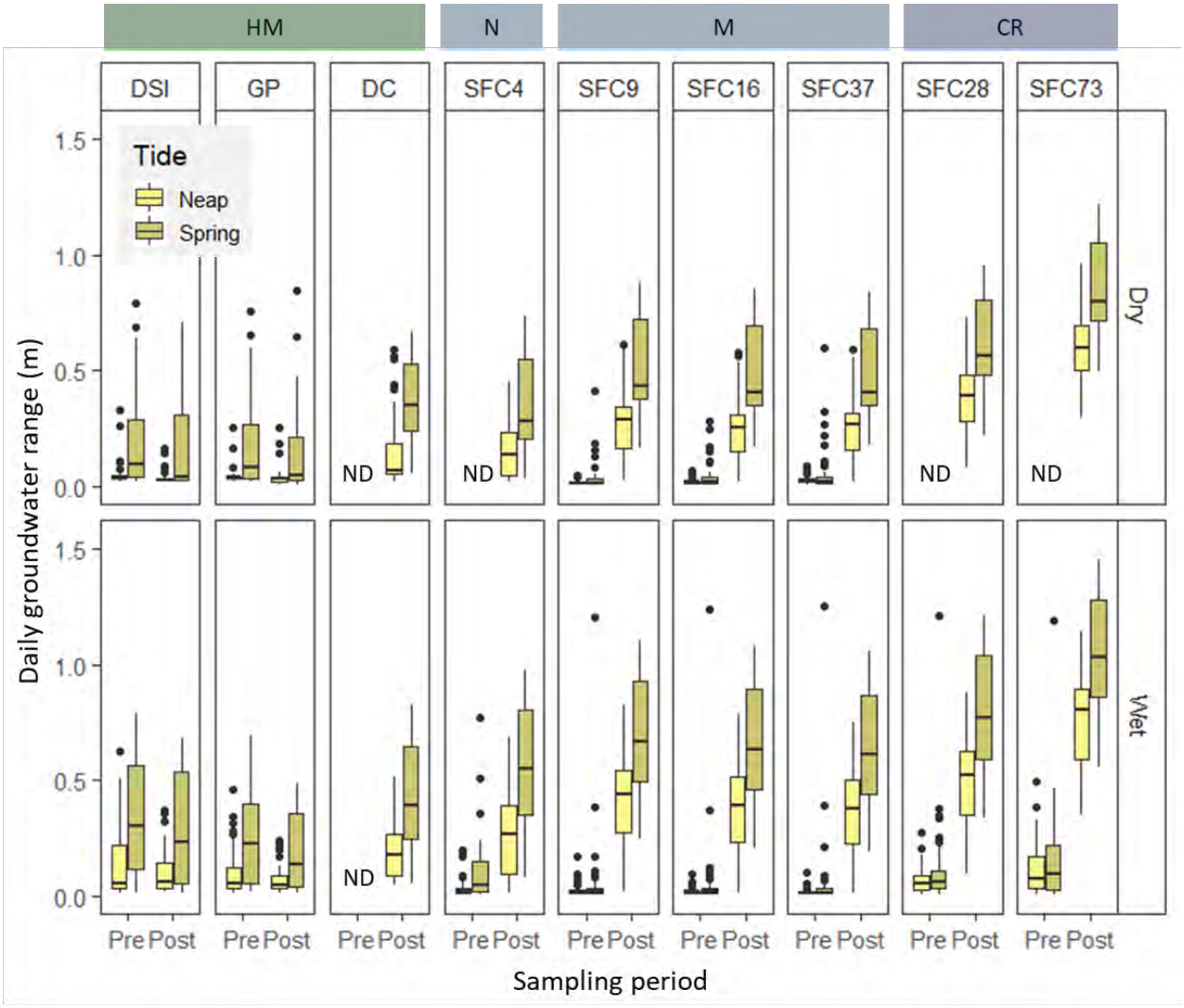

Figure 4.18. Differences in daily groundwater range (max – min groundwater level, in meters) by station, season, sampling period, and tide phase (neap versus spring). HM = reference high marsh stations; N = SFC north zone; M = SFC middle zone; CR = SFC cropped zone. ND = no data.

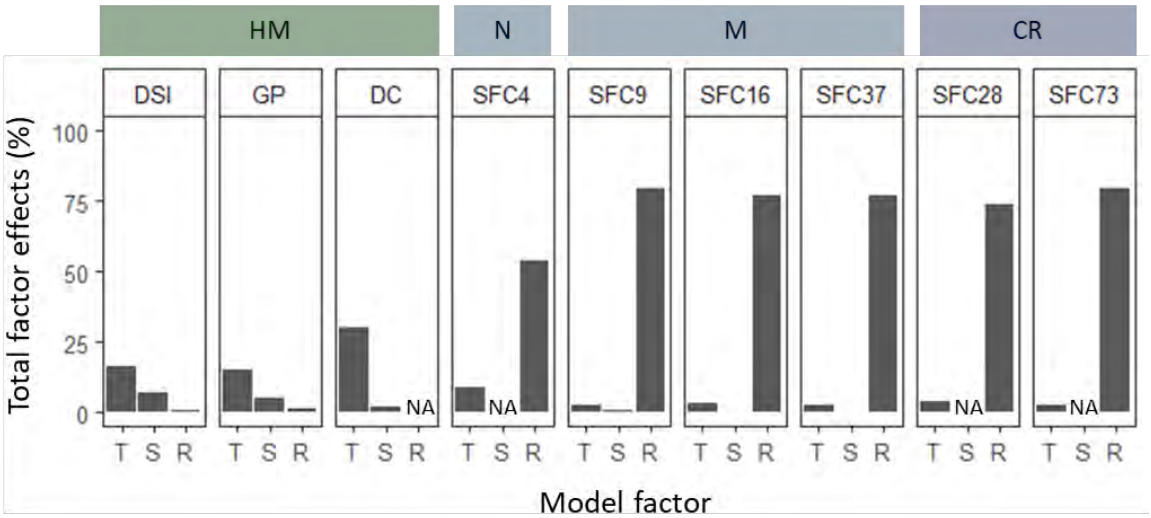

Figure 4.19. Percent variance in daily groundwater range accounted for by three factors: monthly tide phase (T), season (S), and pre- versus post restoration sampling period (R). Bars for each factor show the percent change in model R^2 due to their combined independent and joint effects, a measure of relative "importance". HM = reference high marsh stations; N = SFC north zone; M = SFC middle zone; CR = SFC cropped zone. NA = not applicable (not included in the model).

Groundwater temperature and salinity. We monitored groundwater temperature and salinity only during the post-restoration monitoring period (2018) using a second set of shallower groundwater wells positioned no more than a meter away from the deeper wells where we measured groundwater level. Wet season groundwater temperatures generally ranged between 5-10 °C and were similar between the three reference high marsh stations and all six stations at SFC (Figure 4.20). This range of temperatures was also very similar to wet season temperatures in water flooding channels at SFC and the Dry Stocking Island reference station (Figures 4.8-4.10). During the dry season, groundwater temperatures increased to between approximately 12-20 °C at all stations in the study, with slightly warmer temperatures at several of the SFC stations. Thus groundwater remained a few degrees cooler than channel temperatures during the summer of 2018 (Figures 4.8-4.10).

Groundwater salinity varied between SFC and reference sampling stations more than temperature (Figure 4.21). During the wet season, two reference high marshes (Dry Stocking Island and Doty Creek) generally had oligohaline (0.5-5 ppt) conditions, while Goose Point high marsh was in the oligohaline to low mesohaline (5-18 ppt) range. Doty Creek, in particular, was a small wetland in a narrow coastal drainage that likely had substantial freshwater input. SFC stations varied considerably in salinity during the post-restoration period from fresh to oligohaline groundwater at SFC73 near Nolan Slough to mesohaline groundwater at SFC 9, SFC16, and SFC37, all in the middle zone. Salinities tended to increase at all stations during the dry season, although variability during this four month period was remarkably high (June conditions may have still been relatively fresh due to spring-time precipitation). The most saline sites were DSI and GP reference marshes and SFC73. Station SFC4 in the north zone had the lowest salinity among SFC stations during the dry season, with values ranging from oligohaline to low mesohaline conditions.

Combining temperature and salinity data into bivariate plots illustrated how overall groundwater conditions shifted over the course of the wet and dry seasons during the early post-restoration monitoring period (Figure 4.22). During the dry season from June to September, groundwater temperature remained fairly constant but salinity increased considerably by September. During the wet season, groundwater cooled and gradually became fresher from December to March. By March, there was a relatively distinct

separation in salinity among SFC stations: stations SFC28 and SFC73 in the cropped zone were oligohaline while middle zone stations tended to be mesohaline.

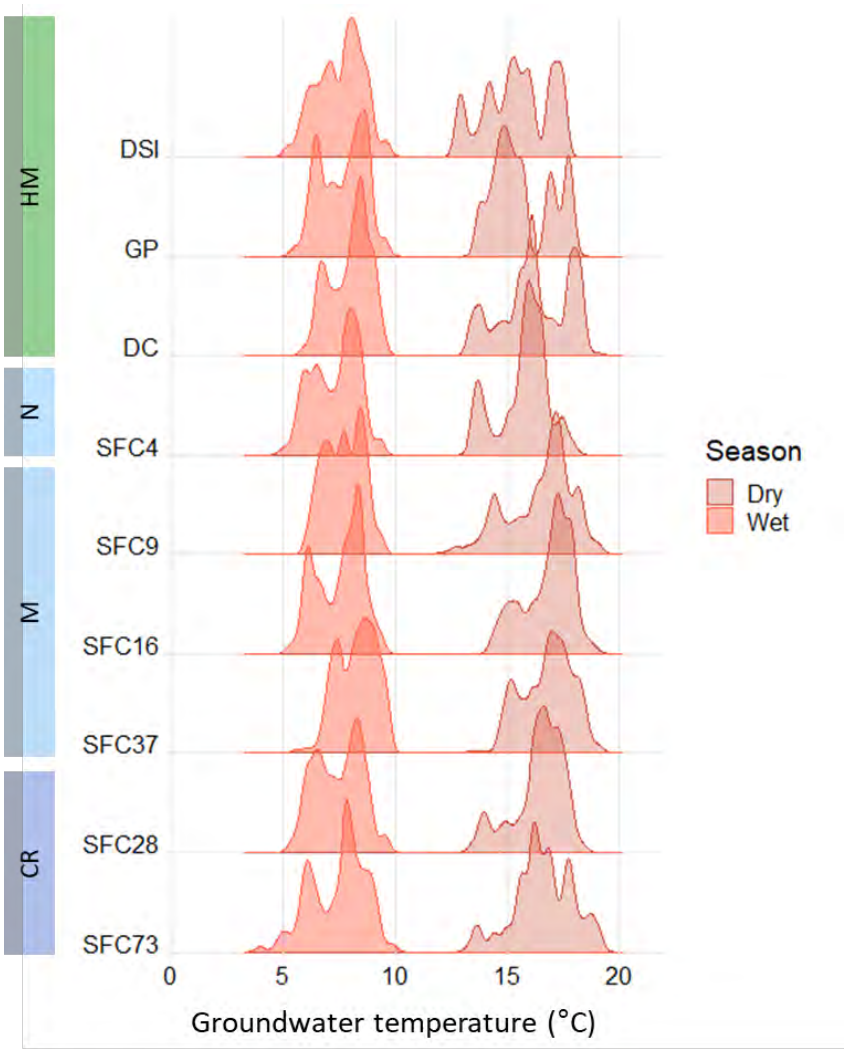

Figure 4.20. Smoothed frequency distribution of groundwater temperature during wet (winter) and dry (summer) seasons for the post-restoration monitoring period in three reference high marsh stations and six SFC stations. The height of each curve is proportional to the number of observations at a given temperature. Distributions are based on all 15 minute values when the groundwater was high enough to immerse the logger positioned at the bottom of the rooting zone.

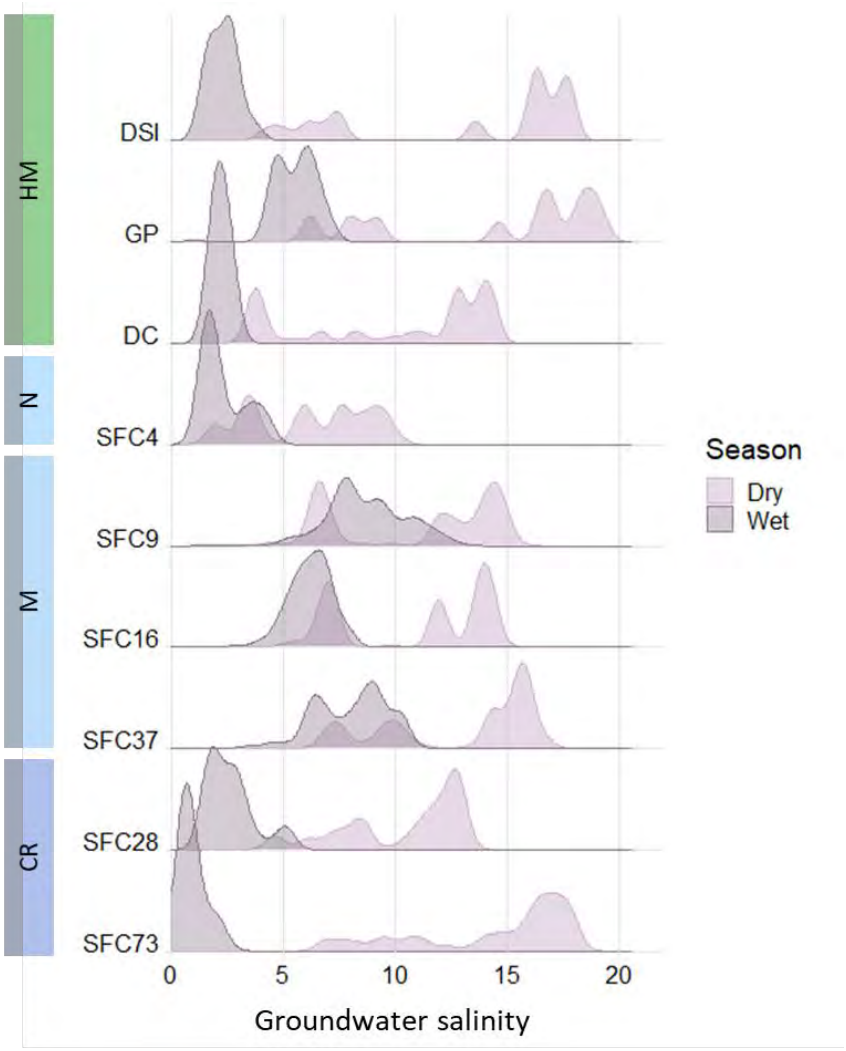

Figure 4.21. Smoothed frequency distribution of groundwater salinity during wet (winter) and dry (summer) seasons for the post-restoration monitoring period in three reference high marsh stations and six SFC stations. The height of each curve is proportional to the number of observations at a given salinity. Distributions are based on all 15 minute values when the groundwater was high enough to immerse the logger positioned at the bottom of the rooting zone.

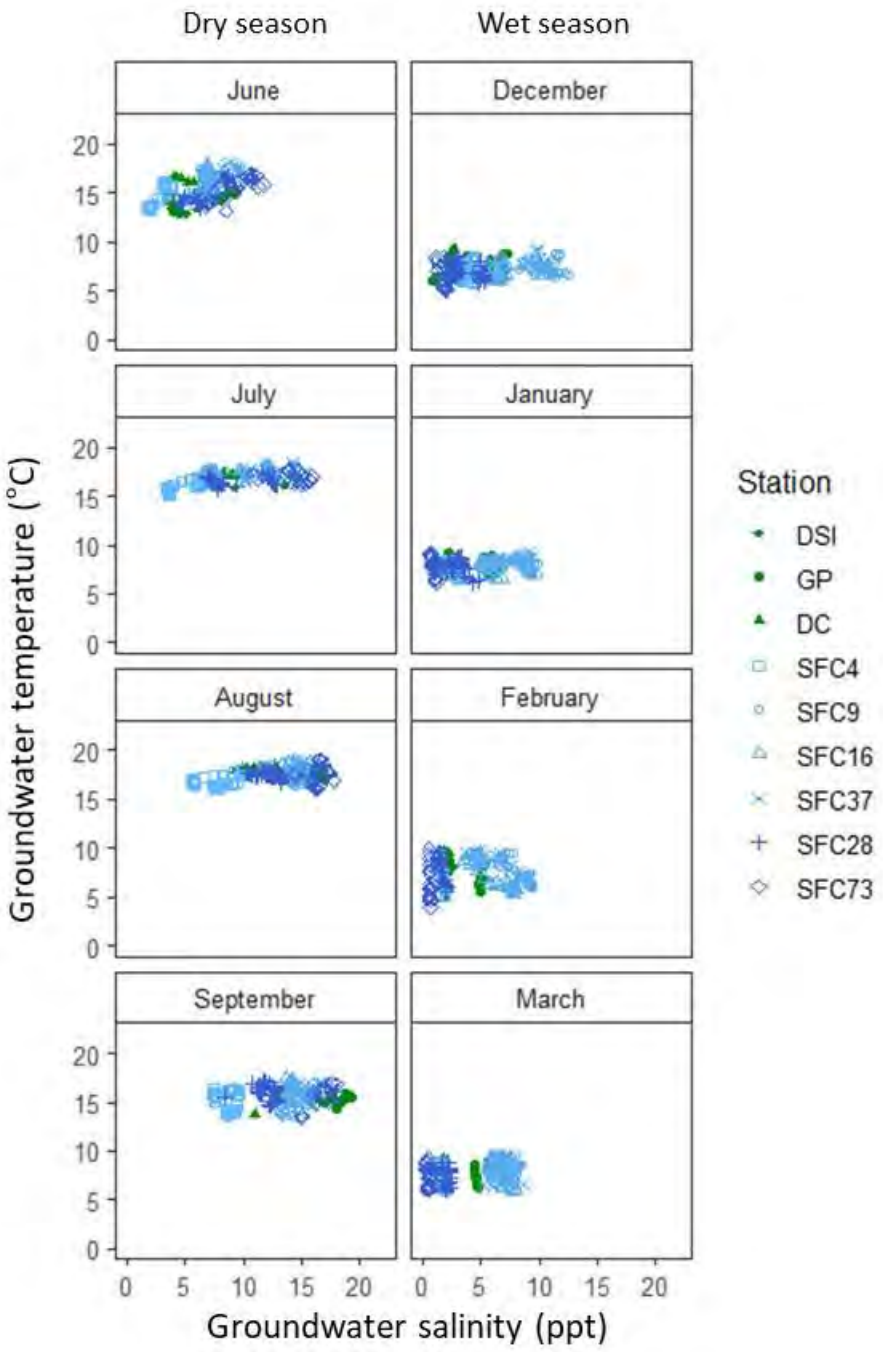

Figure 4.22. Monthly and seasonal differences in groundwater temperature and salinity conditions during the post-restoration monitoring period in three reference high marsh stations (green symbols) and six SFC stations (blue symbols). Each point represents a daily mean salinity and temperature value.

Groundwater conditions are expected to have important effects on tidal wetland vegetation, benthic invertebrate communities, soil microorganisms and soil biogeochemistry, and thus yield important information when included in wetland monitoring. For instance, saltier groundwater may lead to lower productivity in vascular plants (DeLaune et al. 1987, Janousek et al. 2020). Our stations were not numerous enough at SFC to draw strong linkages between vegetation composition and groundwater salinity, but the

spatial variation we observed in groundwater salinity across the site following restoration is consistent with our more vegetation sampling. For example, after restoration more freshwater-acclimated plants tended to persist in the north zone (represented by station SFC4 which was the freshest of all SFC groundwater stations), while pre-restoration plants in the middle zone were rapidly replaced by brackish tidal wetland species in the middle and cropped zones which had higher dry season salinities (see Chapter 5 for vegetation results).

Citations

Alvarez MdP, Carol E, Hernández MA, Bouza PJ. 2015. Groundwater dynamic, temperature and salinity response to the tide in Patagonian marshes: Observations on a coastal wetland in San José Gulf, Argentina. Journal of South American Earth Sciences 62:1-11.

Bottom DL, Jones KK, Cornwell TJ, Gray A, Simenstad CA. 2005. Patterns of Chinook salmon migration and residency in the Salmon River estuary (Oregon). Estuarine, Coastal and Shelf Science 64:79-93.

Bridgeland, WT, Brophy LS, van de Wetering S, So KJ, van Hoy R, Lowe RW, and Ledig DB. 2017. Ni-les'tun tidal wetlands restoration project: Planning, implementation, and lessons learned. U.S. Department of Interior, Fish and Wildlife Service, Region 1, Biological Technical Publication FWS/BTP-R1015-2017, Washington, DC.

Brophy LS, van de Wetering S, Ewald MJ, Brown LA, Janousek CN. 2014. Ni-les'tun tidal wetland restoration effectiveness monitoring: Year 2 post-restoration (2013). Institute for Applied Ecology, Corvallis, OR.

Brophy LS, Brown LA, Ewald MJ. 2015. Waite Ranch baseline effectiveness monitoring: 2014. Prepared for the Siuslaw Watershed Council, Mapleton, OR. Institute for Applied Ecology, Corvallis, OR.

Brophy LS, Brown LA, Ewald MJ, Peck EK. 2017. Baseline monitoring of Wallooskee-Youngs restoration site, 2015, Part 2: Blue carbon, ecosystem drivers and biotic responses. Institute for Applied Ecology, Corvallis, OR.

DeLaune RD, Pezeshki SR, Patrick Jr. WH. 1987. Response of coastal plants to increase in submergence and salinity. Journal of Coastal Research 3:535-546.

Fofonoff NP, Millard Jr. RC 1983. Algorithms for computation of fundamental properties of seawater. UNESCO Technical papers in marine science No. 44.

Janousek CN, Dugger BD, Drucker BM, Thorne KM. 2020. Salinity and inundation effects on productivity of brackish tidal marsh plants in the San Francisco Bay-Delta Estuary. Hydrobiologia 847:4311-4323.

Lawrence PJ, Smith GR, Sullivan MJP, Mossman HL. 2018. Restored marshes lack the topographic diversity found in natural habitat. Ecological Engineering 115:58-66.

Lee II, H, Brown CA. (eds). 2009. Classification of regional patterns of environmental drivers and benthic habitats in Pacific Northwest estuaries. U.S. EPA, Office of Research and Development, National Health and Environmental Effects Research Laboratory, Western Ecology Division. EPA/600/R-09/140.

Magnusson A, Hilborn R. 2003. Estuarine influence on survival rates of Coho (*Oncorhynchus kisutch*) and Chinook salmon (*Oncorhynchus tshawytscha*) released from hatcheries on the U.S. Pacific coast. Estuaries 26:1094-1103.

Mueller P, Schile-Beers LM, Mozder TJ, Chmura GL, Dinter T, Kuzyakov Y, de Groot AV, Esselink P, Smit C, D'Alpaos A, Ibáñez C, Lazarus M, Neumeier U, Johnson BJ, Baldwin AH, Yarwood SA, Montemayor DI, Yang Z, Wu J, Jensen K, Nolte S. 2018. Global-change effects on early-stage decomposition processes in tidal wetlands – implications from a global survey using standardized litter. Biogeosciences 15:3189-3202.

Price MHH, Connors BM, Candy JR, McIntosh B, Beacham TD, Moore JW, Reynolds JD. 2019. Genetics of century-old fish scales reveal population patterns of decline. Conservation Letters e12669.

Schile LM, Callaway JC, Parker VT, Vasey MC. 2011. Salinity and inundation influence productivity of the halophytic plant *Sarcocornia pacifica*. Wetlands 31:1165-1174.

Temmerman S, Bouma TJ, Govers G, Lauwaet D. 2005. Flow paths of water and sediment in a tidal marsh: Relations with marsh developmental stage and tidal inundation height. Estuaries 28:338-352.

USACE 2000. Installing monitoring wells/piezometers in wetlands. Wetlands Regulatory Assistance Program. ERCD TN-WRAP-00-02.

Wagner RJ, Boulger Jr RW, Oblinger CJ, Smith BA. 2006. Guidelines and standard procedures for continuous water-quality monitors – Station operation, record computation, and data reporting. US Geological Survey Techniques and Methods 1-D3. 51 pp.

Wallace KJ, Callaway JC, Zedler JB. 2005. Evolution of tidal creek networks in a high sedimentation environment: A 5-year experiment at Tijuana Estuary, California. Estuaries 28:795-811.

Walsh C, MacNally R. 2015. Package 'heir.part'. CRAN package documentation.

Wilson AM, Evans T, Moore W, Schutte CA, Joye SB, Hughes AH. 2015. Groundwater controls ecological zonation of salt marsh macrophytes. Ecology 96:840-849.

Chapter 5: Vegetation change

Christopher Janousek and Laura Brophy

Key findings

- Prior to restoration, the SFC site had high cover of non-native plant species, especially reed canarygrass.
- Total plant cover tended to decline at SFC two years following tidal restoration with an increase in bare space.
- Before restoration, plant species diversity was highest in high reference marsh, intermediate in SFC wetlands, and lowest in low reference marsh. After restoration, plant diversity tended to increase at SFC.
- At the plant alliance level, the overall coverage of both native and non-native plant alliances decreased at SFC, while bare space increased.
- By 2020, four years following restoration, patches of native species including Lyngbye's sedge were common throughout the lower elevation, more-southerly zones at the site.

Introduction

In emergent tidal marshes, scrub-shrub tidal wetlands, and forested tidal wetlands, vascular plants are foundation species that play a central role in wetland structure and processes. Plants provide physical habitat for other wetland organisms (Smith et al. 2014), are key components of estuarine food webs and carbon fluxes (Maier and Simenstad 2009; Cragg et al. 2020), and affect wetland soil deposition (Leonard and Luther 1995). Diverse types of vegetated tidal wetlands are present in the Pacific Northwest (PNW), occurring across a range of salinities and inundation levels, and comprising a variety of vegetation types from succulent and halophyte-dominant emergent marshes, to grass and sedge-dominated marshes, to tidal swamps dominated by shrubs or trees. Common plant groups in PNW tidal wetlands include grasses, sedges, rushes, forbs, shrubs, and trees. Many species are tolerant of brackish or saline conditions.

The distribution, abundance, and productivity of plant species in tidal wetlands is controlled by biological processes including seed dispersal and germination, plant growth, interactions between species, and herbivory, as well as the estuarine physical environment (Keammerer 2011, Bertness 1991, Janousek and Folger 2014). Spatial differences in wetland inundation and salinity in particular affect plant composition in least-disturbed wetlands (Watson and Bryne 2009, Janousek and Folger 2014). However, these important controlling factors may be substantially altered in former tidal wetlands that have been diked and cut off from regular tidal inundation. Once separated from tidal influence, former tidal wetlands may have fresher soils and highly altered patterns of inundation (see Chapters 2,4).

Degraded tidal wetlands often have very different plant assemblages than least-disturbed wetland ecosystems due to changes in hydrology, land management practices, and soil biogeochemistry (Jones et al., in review). In the Pacific Northwest, non-native species with an affinity for fresher and/or drier soil conditions such as the invasive reed canarygrass (*Phalaris arundinacea*) may become abundant in diked wetlands (Brophy 2009, Diefenderfer et al. 2016). In former tidal wetlands that have been altered for agricultural uses, desirable cropped or foraged species may be maintained in place of native species.

Restoring the full suite of ecosystem functions and services provided by tidal wetlands, including native biodiversity requires recovery of plant cover, abundance, and species composition to levels that are similar to least-disturbed reference systems. Differences in inundation and salinity as well as temporal development of wetland soils, are expected to lead to vegetation development that mimics native systems. However, the pace and degree to which vegetation development is restored may depend on levels of habitat disturbance, pre-restoration plant composition, site elevation, and other characteristics of the impounded wetland and its estuary and watershed. Because of the large size of the SFC restoration project site in Tillamook Bay and zone-specific differences in management type, elevation, and salinity, across the project area, the project offered a valuable opportunity to examine how land use could impact tidal wetland vegetation development.

Monitoring objectives. In this chapter we report on pre-and early post-restoration percent cover, composition, and species richness of plants in the Southern Flow Corridor project and reference marshes in Tillamook Bay. To assess spatial and temporal differences in vegetation, we used both standard quadrat and vegetation mapping methods that encompass plot and landscape-level spatial scales. We addressed several questions in our analyses: (1) how did plant cover, composition, species richness, and assemblage composition change following removal of dikes at SFC? (2) Did vegetation composition differ among major land-use/land-cover zones at SFC before and after restoration? (3) Was early vegetation change within the SFC site following restoration linked to wetland surface elevation?

Materials and methods

Post-restoration monitoring used the same methods as baseline monitoring and are described in the SFC Effectiveness Monitoring Plan (Brophy and van de Wetering 2014) and the baseline monitoring report (Brown et al. 2016b).

Quadrat sampling. We sampled vegetation cover, composition, and richness during summer 2014 (pre-restoration period) and summer 2018 (post-restoration period) in replicate quadrats distributed throughout SFC and reference sites using the same methods. We distributed plots randomly within five land-use/land-cover zones at SFC (north, middle, south, cropped, grazed), and in low and high reference marshes, with sample sizes per zone somewhat proportional to the total land area of each zone (Table 5.1, Figure 5.1).

At each plot we made a visual estimate of the percent cover of all emergent vascular plant species and of bare ground and other cover classes (e.g., wood) in a 1.0 m^2 quadrat. Total cover of all classes summed to 100% within a quadrat. In plots with overhanging plants (typically trees, shrubs, or vines), we included this additional vegetation layer, so that total plant cover exceeded 100% in these cases. We identified plants to the species level when possible, with a small number of plants identified to only the genus or family level, or left unidentified. Species nomenclature follows Jaster et al. (2017) except that we treated pickleweed (*Sarcocornia perennis*) as *Salicornia pacifica* following Piirainen et al. (2017). Using a RTK-GPS rover, we measured the elevation of the wetland surface at the edge of each vegetation plot (see Chapter 2).

Table 5.1. Number of vegetation plots sampled (and analyzed) in each zone within SFC and reference wetlands. The same number of plots were evaluated in 2014 and 2018.

Wetland zone	Total area (ha)	Pre-restoration management history	Number of plots
Low reference marsh (LM)	8.2	Generally unmanaged	19
High reference marsh (HM)	8.7	Generally unmanaged	23
SFC North zone (N)	16.6	Mainly non-tidal, seasonal freshwater wetland, mix of emergent marsh and forested wetland	20
SFC Middle zone (M)	65.6	Non-tidal seasonal freshwater wetland, mainly emergent marsh. Some remnant tidal channels.	56
SFC South zone (S)	5.5	Freshwater mitigation site for about 2 decades prior to restoration	8
SFC Cropped zone (CR)	42.8	Area subdivided into actively managed fields with varying numbers of cropped fields by year	45
SFC Grazed zone (GR)	8.6	Seasonal cattle grazing	8

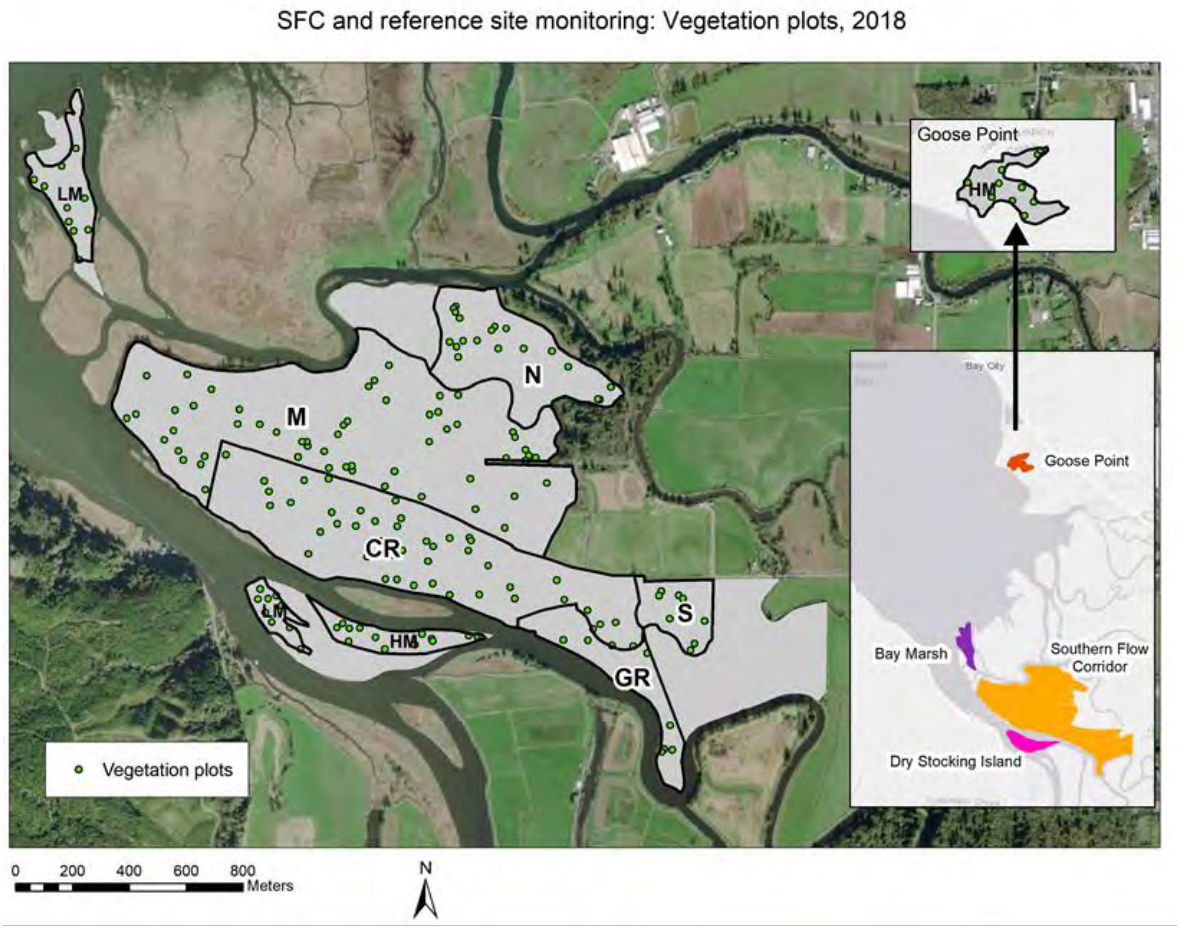

Figure 5.1. Distribution of vegetation quadrats sampled in 2014 and 2018 at SFC and reference tidal wetlands. HM = reference high marsh, LM = reference low marsh; N = SFC north zone, M = SFC middle zone, CR = SFC cropped zone, S = SFC south zone, GR = SFC grazed zone. Background image: ESRI World Imagery.

In 2018 we used a Garmin handheld GPS to navigate back to the location of plots sampled in 2014 (post hoc comparison of more precise RTK-GPS measurements showed that 91% of plots were relocated to within 5 meters of the original location and 98% of plots were located to within 8 m). We determined post-restoration species cover and richness in each plot as in 2014.

Using percent cover data, we determined several metrics of vegetation assemblage structure at each plot. We computed total vascular plant cover (all species, including living and dead biomass), total native species cover, total non-native species cover, and plant species richness. Generally, we classified plants as native or non-native based on Jaster et al. (2017). However, as some taxa we encountered have ambiguous native status in Oregon, or include both native and non-native subspecies, which we did not distinguish in the field. We treated reed canarygrass (*Phalaris arundinacea*) and water foxtail (*Alopecurus geniculatus*) as non-native and common rush (*Juncus effusus*) as native (Brown et al. 2016b, USDA 2019), but for other generally uncommon plants with ambiguous status, we did not include these species in total native or total non-native plant cover estimates (they were however included in total plant cover and species richness). Although we did generally not distinguish between living and dead biomass in percent cover estimates, in 2018 we estimated this for reed canarygrass cover in each plot.

We tested for differences in total plant cover, total native species cover, total non-native species cover, and plot-level species richness among zones (low reference marsh, high reference marsh, five SFC zones) with one-factor ANOVA before and after restoration separately. We used one factor Kruskall-Wallis non-parametric tests where variances where heteroscedastic (Levene's test). We also examined differences in cover between sampling periods and between SFC and reference wetlands for several common PNW estuarine species: *Carex lyngbyei*, a dominant in least disturbed low marshes; *Deschampsia cespitosa*, a dominant in mature mid to high marshes; *Potentilla anserina*, a common species in least-disturbed high marshes; and *Phalaris arundinacea*, a dominant plant at SFC and other disturbed coastal wetlands (Janousek and Folger 2014).

To assess vegetation change over time, we quantified differences in plant metrics between sampling events by computing the mean (and 95% confidence intervals) difference in values between paired 2014 and 2018 plots for each zone. We regarded confidence intervals that do not overlap zero as indicating a significant change in vegetation metrics between sampling periods, with positive values showing greater post-restoration cover or diversity. We also tested whether zones differed in their degree of post-restoration change with one-factor ANOVA.

Since tidal elevation is a major driver of vegetation characteristics in least-disturbed tidal wetlands in Oregon (Janousek and Folger 2014), and it potentially impacts the development of plant assemblages in restored wetlands as well, we tested for relationships between pre-restoration wetland surface elevation (z*) and the degree of change in total, native, and non-native plant cover; and plot-level species richness between 2014 and 2018 sampling periods.

We used multivariate methods to further examine differences in vegetation composition by sampling period, between SFC and reference marshes, and between zones within SFC. To visualize differences in plant composition, we used non-metric multidimensional scaling (NMDS) on plant cover data for common species. We excluded species that occurred at less than 3% frequency in the combined 2014 and 2018 data set, leaving 25 species (and bare ground) in the analysis. We conducted the NMDS in R package "vegan" using function "metaMDS" which runs multiple iterations of the ordination to find an optimum global solution. In the ordination, species percent cover data were square-root transformed and Wisconsin double standardized prior to computation, and pair-wise differences among all plots were determined as a matrix of Bray-Curtis dissimilarities (Oksanen 2015). We tested for differences in composition before and after restoration for each zone separately with permutational ANOVA (PERMANOVA) using the "adonis" function in package "vegan".

Finally, we examined differences in total species richness (gamma diversity) between sampling periods and wetland zones with species accumulation curves and by computing the Chao statistic with small sample size correction, an estimate of minimum expected species diversity based on species

frequencies in each data set (Chiu et al. 2014). For species accumulation curves, we converted percent cover data to a matrix of presence-absence scores and computed 95% confidence intervals using function "specaccum" in package "vegan." When curves reach a horizontal asymptote, it suggests that all species richness has been accounted for by the sampling effort. Asymptotes were rarely attained in our dataset, but non-overlapping confidence intervals in diverging curves still indicate significant differences in gamma diversity. We constructed species accumulation curves for low and high reference marshes, and for three SFC zones that had relatively large sample sizes (N, CR, M). We estimated the Chao statistic and its standard error using function "specpool" in "vegan".

Vegetation mapping. To evaluate differences in vegetation composition at the landscape scale at SFC, we also mapped the distribution and extent of distinct plant assemblages at the SFC and reference sites during the 2014 and 2018 sampling periods with aerial photography and field reconnaissance. Vegetation mapping methods were the same in 2014 and 2018, but the resolution of the aerial images differed. In 2014, mapping used publicly-available 2009 NAIP images (0.5m resolution); whereas the 2018 images were obtained via a custom aerial mission by Eagle Digital Imaging, Inc. (Corvallis, OR), with a ground sampling distance of 15 cm (6 in). Images were acquired at low tide on June 2, 2018 using a 90° camera angle and onboard GPS was used for automated georeferencing. Products were delivered as 33 individual tiles (MrSID format) and as two image mosaics (TIF format) covering SFC and reference sites.

As described in the SFC Effectiveness Monitoring Plan (Brophy and van de Wetering 2014) and baseline monitoring report (Brown et al. 2016b), vegetation mapping focused on pastures and lowlands west of the confluence of Dougherty and Hoquarten Sloughs and did not generally include forested or scrub-shrub wetlands on the SFC site, so these shrub and forested areas were not mapped in detail. However, we spent some field time characterizing the major canopy dominants (trees and shrubs) within the forested wetlands, and also used aerial photo interpretation to assist the final mapping.

In both 2014 and 2018, vegetation mapping covered some areas within SFC that were otherwise not monitored (namely, the far northwest and southeast portions of SFC) for soils or vegetation composition in quadrats. The northwest area (north of Blind Slough, adjacent to the Wilson River, and west of the Blind Slough tide gates) was omitted from monitoring because it already had muted tidal influence at baseline and thus was distinctly different from the rest of the SFC site. The southeast area (upper reaches of Nolan Slough) could not be monitored at baseline due to active cattle grazing. However, it was possible to map vegetation in both areas, so this was done for completeness.

Preliminary review of the 2018 aerial images and vegetation plot data for the reference sites (Bay Marsh, Dry Stocking Island, and Goose Point) showed that the composition and extent of plant communities had not changed substantially since the baseline monitoring in 2014. Therefore, vegetation was not mapped at the reference sites in 2018. Field reconnaissance is recommended for future monitoring events, and re-mapping is recommended when that reconnaissance shows substantial change in the composition or extent of plant communities.

In August 2018, the project site was traversed on foot to correlate field vegetation with patterns in the aerial photographs. Aerial photographs were printed for field use at a scale of approximately 1:3000, with a UTM grid overlay. Map units (plant associations, described below) were delineated in the field on the aerial printouts. In the office, digital vegetation maps were created in ArcGIS 10.3 by georeferencing the field maps and tracing the map unit boundaries into the GIS at a scale of 1:1000; the polygon size threshold was about 0.1 ha (0.25 ac). After map unit attribution as described below, the resulting vegetation map was saved as a shapefile (SFC_2018_vegmap_20200609_FINAL.shp).

As in 2014, we did not attempt to digitize water features such as channels and ponds. However, to improve estimates of the area occupied by vegetation types, we did digitize the lower portions of a few large channels. Ponded water could not be accurately mapped, as the area of ponding varied greatly across the tide cycle. However, the substrate under most ponded areas was bare ground, which was mapped. As in 2014, we did not map vegetation on dikes (which were upland). We also did not map areas behind setback dikes (which were outside the restoration area).

Following the National Vegetation Classification Standard (The Nature Conservancy 1994), we used a two-level hierarchical vegetation classification scheme. Each map unit was attributed with a plant association and an alliance. Alliances, the coarser level, were described by a single major dominant species that characterized a larger area. Plant associations represented fine gradations of dominant species; as during baseline monitoring, we divided these to reflect small differences in community composition. This two-level classification allows flexibility in tracking future vegetation change. We also mapped bare ground, which generally had less than about 20% vegetation cover.

We characterized alliances as native-dominated or non-native-dominated, based on the alliance's major dominant species. The percent cover of native species versus non-native species varied at finer spatial scales within these alliances, but the native/non-native attribute provides a broader overview of changes in dominance of native and non-native vegetation. These changes were summarized by calculating the change in area between 2014 and 2018 for each alliance, providing an indication of vegetation transitions at SFC at a broad scale. Change in area was not calculated for major channels since these were not consistently mapped (see below). Change in area was also not calculated for unmapped areas, since these generally reflected mapping boundaries and construction activities rather than ecological changes.

Restoration caused a very noticeable decline in condition of two of the site's predominant species: the non-native invasive reed canarygrass, and native coastal willow. Our alliance-level classification reflects this decline. Areas in good condition (healthy plants) were classified as "reed canarygrass" and "coastal willow" respectively. Areas in poor condition were classified as "reed canarygrass - dead/dying" and "coastal willow - unhealthy/dead". We did not subdivide plant associations in this way, to avoid generating an unwieldy number of associations.

Results and discussion

Plant cover in vegetation plots. Before restoration, total plant cover ranged from 91 to 119% in SFC and reference marsh zones, with the cropped zone having lower cover than the north and middle zones at SFC ($\chi^2 = 31.8$, df = 6, $P < 0.0001$; Figure 5.2A). Following restoration, differences in total cover among zones were more pronounced ($\chi^2 = 82.9$, df = 6, $P < 0.0001$; Figure 5.2B). Cover remained high in low and high reference marsh and in the north and south zones at SFC but declined to 35-66% in the other zones at SFC. Bare ground and wrack was particularly common in the cropped zone where there was significant die back of plant cover following restoration. Before restoration, bare ground was 0.1% at SFC, but increased to 34.5% in the post-restoration monitoring period. Comparing the 2014 to 2018 change in total plant cover across zones, there was a trend towards declining cover in all SFC zones with significant declines in plant cover in the north, middle and cropped zones (Figure 5.2C).

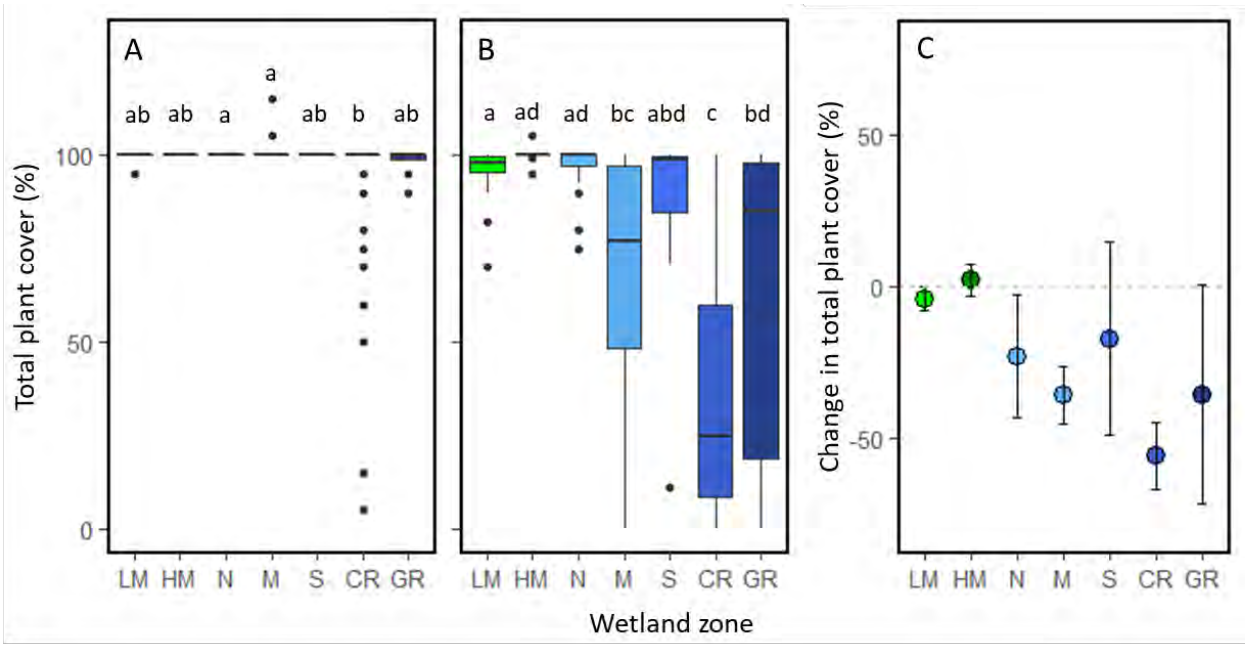

Figure 5.2. Total plant cover in reference marshes and SFC zones during pre- (A) and post-restoration (B) sampling periods. Boxplots in this and subsequent figures show median cover (horizontal bars), interquartile range (upper and lower edges of boxes), 1.5 times the interquartile range (whiskers), and outliers (points). Bars sharing the same letters were not significantly different. (C) Change (± 95% confidence intervals) in total plant cover by between 2014 and 2018 (positive values indicate an increase in cover in the post-restoration period).

Prior to restoration, native plant cover was lower at SFC (5-49%) compared to low reference (80%) and high reference marsh (77%) ($\chi^2 = 67.5$, df = 6, $P < 0.0001$; Figure 5.3A). SFC areas had high cover of non-native species such as reed canarygrass (*Phalaris arundinacea*) before restoration. Following restoration, native plant cover was even lower in SFC zones than before restoration ($\chi^2 = 86.7$, df = 6, $P < 0.0001$; Figure 5.3B), likely because of the increase in bare space as existing vegetation died off, but it remained high in low and high reference marsh. Native cover significantly declined after restoration in only the middle zone at SFC, but there were trends toward declining native cover in the north and south zones as well (Figure 5.3C).

Before restoration, non-native plant cover was higher in SFC zones compared to low and high marsh reference sites ($F_{6,171} = 19.5$, $P < 0.0001$; Figure 5.4A). Reed canarygrass was particularly common at SFC prior to restoration, while native species typical of PNW wetlands were common in the reference sites. High non-native cover at SFC prior to restoration was expected, since the site was in agricultural use, and this is consistent with observations from other diked pastures within the Pacific Northwest. For instance, cover of non-native pasture grasses was high prior to restoration at the Ni-les'tun and Wallooskee-Youngs restoration sites in the Coquille River and Lower Columbia River estuaries (Brophy and van de Wetering 2012, Brophy et al. 2017). These established non-native species can persist for a number of years following restoration, as was observed at the Ni-les'tun project (Brown et al. 2016a) and in restored oligohaline sites on the Skagit Delta (Clifton et al. 2018). Non-native cover declined markedly in several SFC zones following restoration, especially in the cropped and grazed zones (Figure 5.4B,C), and differed significantly by land-cover/land-use zone ($\chi^2 = 43.4$, df = 6, $P < 0.0001$).

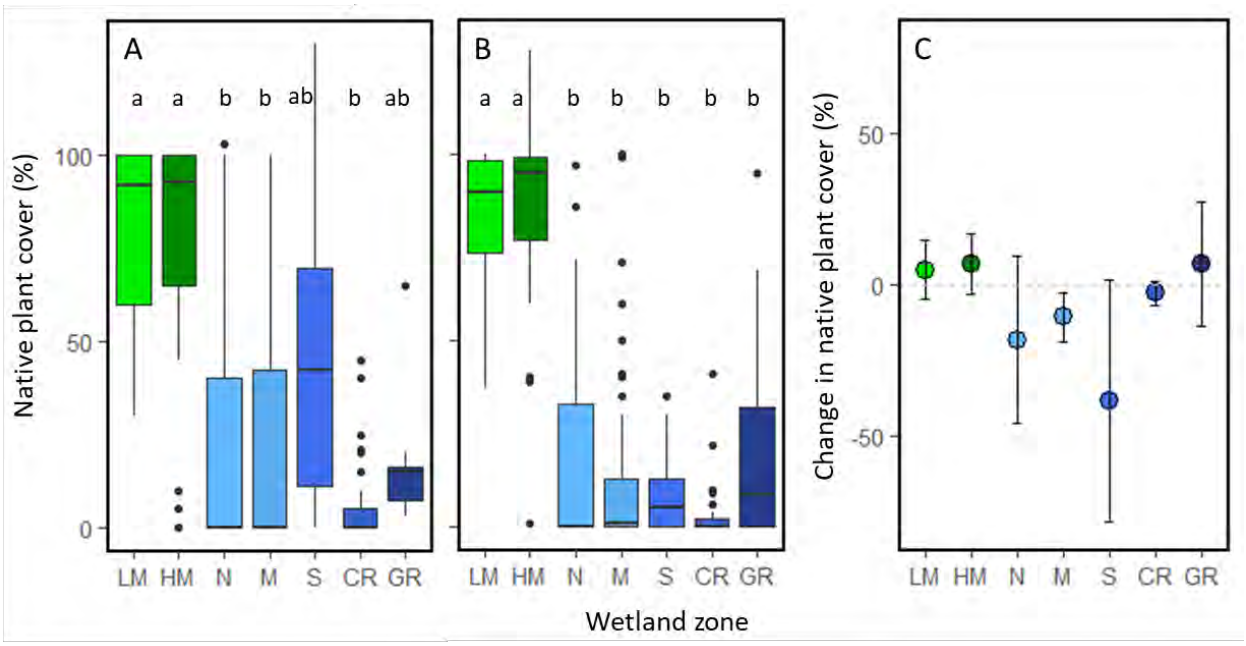

Figure 5.3. Native plant cover in reference wetlands and SFC land-cover/land-use zones before (A) and after (B) restoration. Bars sharing the same letters were not significantly different. (C) Change (± 95% confidence intervals) in native plant cover by zone between 2014 and 2018. See Table 5.1 for an explanation of wetland zones.

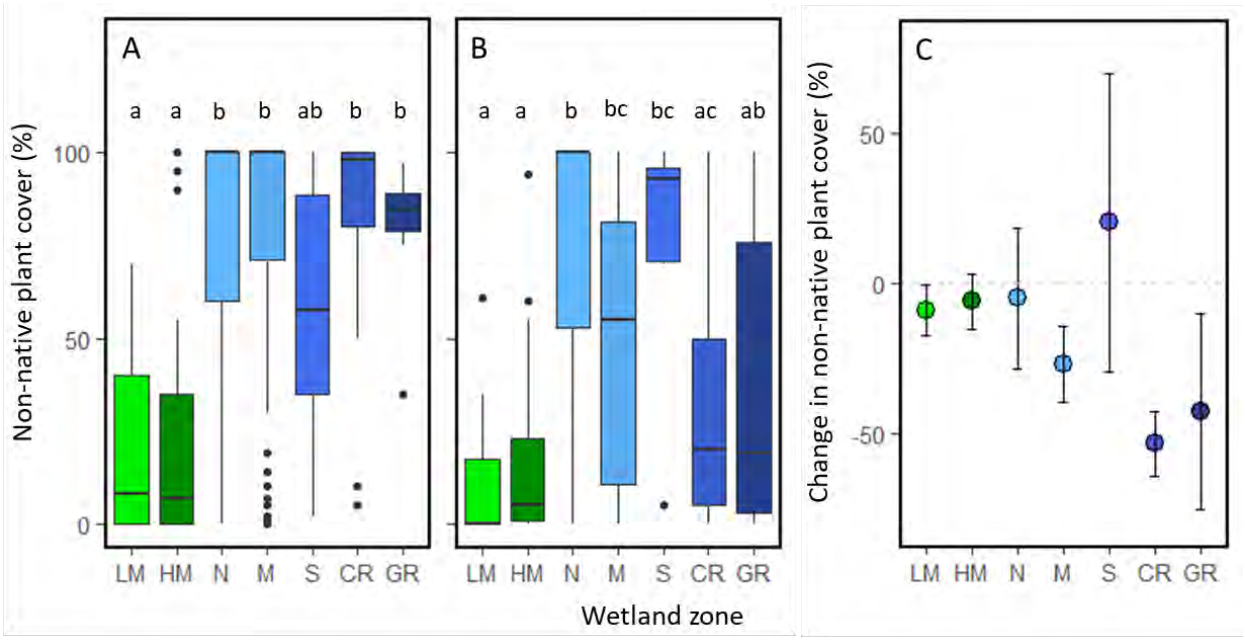

Figure 5.4. Differences in non-native plant cover in reference and SFC wetlands before (A) and after (B) restoration. Bars sharing the same letters were not significantly different. (C) Mean change (± 95% confidence intervals) in non-native plant cover by zone between 2014 and 2018.

Pre- to post-restoration change in total and non-native plant cover varied to some degree with elevation, but the data were highly variable with little explanatory power in the model (total cover: R^2_{adj} = 0.13, P < 0.001; non-native cover: R^2_{adj} = 0.08, P < 0.001; Figure 5.5). Change in native species cover was not related to wetland elevation (native cover: R^2_{adj} = -0.01, P = 0.81). Living reed canarygrass declined markedly at SFC after restoration (Figure 5.6).

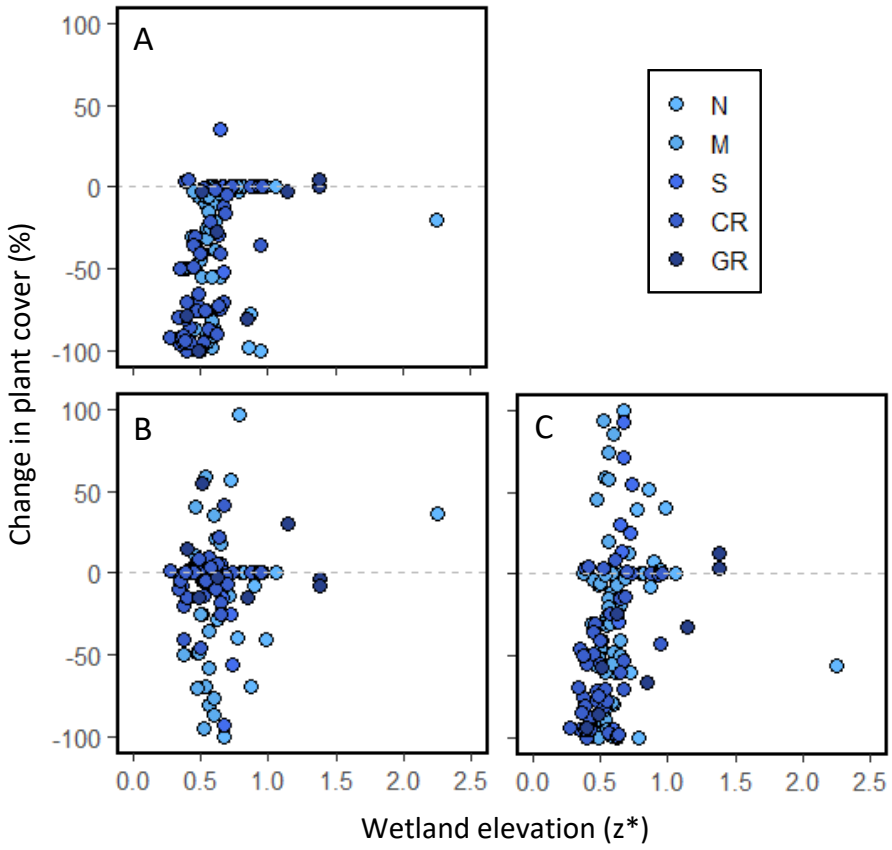

Figure 5.5. Change in (A) total native cover, and (B) total native plant cover, and (C) total non-native plant cover at SFC between pre- and post-restoration periods as a function of wetland surface elevation (z*).

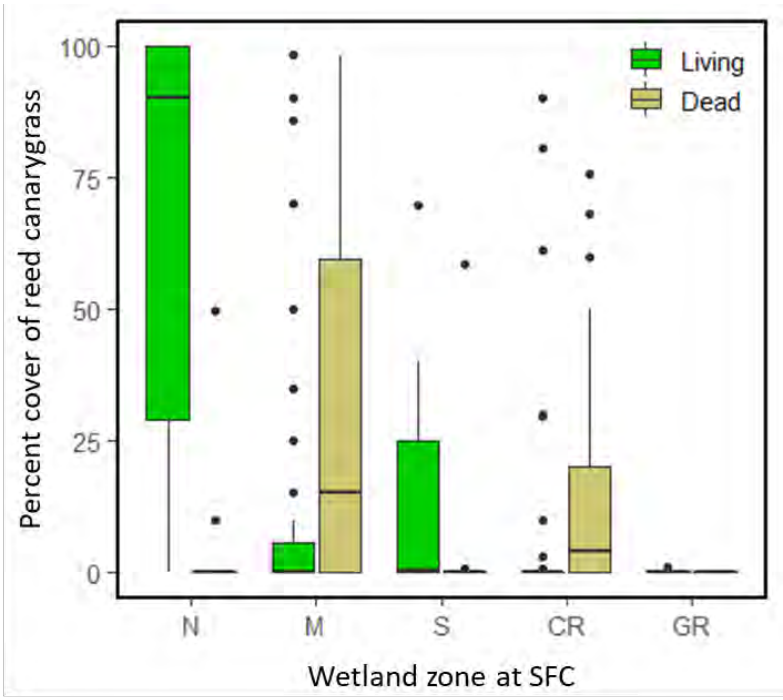

Figure 5.6. Percent cover of living and dead reed canarygrass by land-use/land-cover zone at SFC in the post-restoration sampling period (2018). Living versus dead cover of this species was not distinguished quantitatively in 2014, but the latter was probably minimal.

Species composition and diversity in plots. In the quadrats sampled in 2014 and 2018, we encountered 68 taxa of vascular plants (angiosperms, gymnosperms, non-seed plants) with 61 identified to the species level (Table 5.2). Most plants we encountered were emergent grasses, sedges, rushes or forbs, but the data set also included eight woody shrub and tree species including Sitka spruce (*Picea sitchensis*), twinberry (*Lonicera involucrata*), and willows (*Salix* spp.). Several species were present in 2014 plots, but not in 2018 and vice versa, although all common species in the data set were observed during both sampling periods.

Common plant species in Oregon tidal wetlands such as Lyngbye's sedge, tufted hairgrass, creeping bentgrass, and Pacific silverweed showed major differences in abundance between low reference marsh, high reference marsh, and pooled SFC land-cover/land-use zones (Table 5.2, Figure 5.7).

Table 5.2. Average cover of vascular plants, bare ground, and other cover classes (e.g., wrack) in low reference marsh (LM), high reference marsh (HM), and the Southern Flow Corridor restoration project (SFC) during the pre- (2014) and post-restoration (2018) monitoring periods. Values in black indicate species presence, including "0.0%" values that rounded to zero cover, but were present. Values in grey indicate that the species was completely absent. N = native; NN = non-native; NA = not applicable.

				Pre-restoration cover (%)			Post-restoration cover (%)		
Species	Family	Code	Native status	LM	HM	SFC	LM	HM	SFC
Bare ground	NA	NA	NA	0.5		0.1	4.6	1.2	34.5
Achillea millefolium	Asteraceae	AchMil	NN	0	7.0	0	0	4.2	0
Agrostis stolonifera	Poaceae	AgrSto	NN	19.5	3.3	6.9	10.6	3.4	6.8
Alnus rubra	Betulaceae	AlnRub	N	0	0	0.2	0	0	0
Alopecurus geniculatus	Poaceae	AloGen	?N	0	0	0	0	0	0.5
Alopecurus pratensis	Poaceae	AloPra	NN	0	0	9.3	0	0	0.0
Angelica lucida	Apiaceae	AngLuc	N	0	0	0	0	0.0	0
Anthoxanthum odoratum	Poaceae	AntOdo	NN	0	0	0	0	0	0.1
Athyrium filix-femina	Athyriaceae	AthFil	N	0	0	0.1	0	0	0
Atriplex prostrata	Amaranthaceae	AtrPro	N	0	6.9	0	0	0.3	0.9
Callitriche stagnalis	Plantaginaceae	CalSta	NN	0	0	0	0	0	0.1
Carex lyngbyei	Cyperaceae	CarLyn	N	78.5	0	0	80.5	0	0.3
Carex obnupta	Cyperaceae	CarObn	N	0	1.9	9.0	0	1.9	3.4
Cirsium arvense	Asteraceae	CirArv	NN	0	0	0	0	0	0.0
Cirsium vulgare	Asteraceae	CirVul	NN	0	1.7	0.2	0	0	0
Cotula coronopifolia	Asteraceae	CotCor	NN	0	0	0	0	0	1.5
Deschampsia cespitosa	Poaceae	DesCes	N	0	26.3	0	0	33.1	0.4
Distichlis spicata	Poaceae	DisSpi	N	0	0	0	0	0.0	0
Eleocharis palustris	Cyperaceae	ElePal	N	0	0.1	0.1	2.7	0.0	0.9
Eleocharis parvula	Cyperaceae	ElePar	N	0	0	0	0	0	0.7
Elymus repens	Poaceae	ElyRep	NN	0	0	0	0	0	0.0
Epilobium ciliatum	Onagraceae	EpiCil	N	0	0.2	0.3	0	0	0.0
Festuca rubra ssp. *juncea*	Poaceae	FesRub	N	0	3.3	0	0	0.0	0
Galium trifidum	Rubiaceae	GalTri	N	0	1.1	0	0	0.1	0
Glyceria x *occidentalis*	Poaceae	GlyOcc	NN	0	0.0	0	0	0	0.0
Heracleum maximum	Apiaceae	HerMax	N	0	1.3	0	0	0.1	0
Holcus lanatus	Poaceae	HolLan	NN	0	0.0	1.3	0	0	0.1
Hordeum brachyantherum	Poaceae	HorBra	N	0	0.0	0	0	0.1	0.0
Impatiens capensis	Balsaminaceae	ImpCap	NN	0	0.0	5.3	0	0	0
Isolepis cernua	Cyperaceae	IsoCer	N	0	0.0	0	0	0	0.0
Juncus balticus ssp. *ater*	Juncaceae	JunBal	N	0	9.3	0	0.0	8.8	0.3
Juncus bufonius	Juncaceae	JunBuf	N/NN	0	0.0	0	0	0	0.8
Juncus effusus	Juncaceae	JunEff	N	0	0.0	3.2	0	0	0.0
Lonicera involucrata var. *ledebourii*	Caprifoliaceae	LonInv	N	0	0.0	0.3	0	0.9	0
Lotus corniculatus	Fabaceae	LotCor	NN	0	0.0	1.5	0	0	0.4
Lupinus sp.	Fabaceae	Lup	N	0	0.0	0	0	0	0.1
Lysimachia maritima	Primulaceae	LysMar	N	0	0.0	0	0	0.0	0
Malus fusca	Rosaceae	MalFus	N	0	0.0	0	0	0.3	0
Oenanthe sarmentosa	Apiaceae	OenSar	N	0	0.3	1.9	0	1.1	0.2
Phalaris arundinacea	Poaceae	PhaAru	NN	0	11.1	47.4	0	6.0	35.9
Picea sitchensis	Pinaceae	PicSit	N	0	0	0	0	2.6	0

Table 5.2. Continued.

				Pre-restoration cover (%)			Post-restoration cover (%)		
Species	Family	Code	Native status	LM	HM	SFC	LM	HM	SFC
Polygonum aviculare	Polygonaceae	PolAvi	N/NN	0	0	0	0	0.0	0.0
Potentilla anserina	Rosaceae	PotAns	N	0.9	17.7	2.7	0	26.5	1.4
Ranunculus repens	Ranunculaceae	RanRep	NN	0	0	1.5	0	0	0
Ranunculus scleratus	Ranunculaceae	RanScl	N/NN	0	0	0	0	0	0.0
Rubus bifrons	Rosaceae	RubBif	NN	0	0	0.9	0	0	0.0
Rubus laciniatus	Rosaceae	RubLac	NN	0	0	0.5	0	0	0
Rumex conglomeratus	Polygonaceae	RumCon	NN	0	0.1	0.0	0	0	0.2
Rumex crispus	Polygonaceae	RumCri	NN	0	0	0	0	0	0.0
Rumex fueginus	Polygonaceae	RumFue	N	0	0	0	0	0	0.0
Rumex sp.	Polygonaceae	Rum	NA	0	0	0	0	0	0.0
Salix hookeriana	Salicaceae	SalHoo	N	0	0	1.3	0	0	0.8
Salix sitchensis	Salicaceae	SalSit	N	0	0	1.5	0	0	0
Salix sp.	Salicaceae	Salix sp	NA	0	0	0	0	0	0.0
Sambucus racemosa var. *arborescens*	Adoxaceae	SamRac	N	0	0	0.8	0	0	0.0
Sarcocornia perennis	Amaranthaceae	SarPer	N	0	0.1	0	0	0	0
Schedonorus arundinaceus	Poaceae	SchAru	NN	0	0	4.2	0	2.9	2.6
Schoenoplectus pungens	Cyperaceae	SchPun	N	0.5	0	0	0	0	0
Senecio minimus	Asteraceae	SenMin	NN	0	0	0	0	0.1	0
Sonchus oleraceus	Asteraceae	SonOle	NN	0	0	0	0	0.7	0.1
Spergularia canadenisis var. *occidentalis*	Caryophyllaceae	SpeCan	N	0	0	0	0	0	0.0
Symphyotrichum subspicatum	Asteraceae	SymSub	N	0	2.7	0	0	6.2	0
Triglochin maritima	Juncaginaceae	TriMar	N	0	5.4	0	1.6	1.7	0.0
Typha latifolia	Typhaceae	TypLat	N	0	0	0.4	0	0	2.5
Vicia nigricans var. *gigantea*	Fabaceae	VicNig	N	0	0.2	0	0	0	0
UnkD	Asteraceae	UnkD	NA	0	0	0	0	0.0	0
UnkR	Poaceae	UnkR	NA	0	0	0	0	0	0.0
Unk S	Unknown	UnkS	NA	0	0	0	0	0	0.0
Misc Bryophyta	NA	Bry	NA	0	0	0	0	1.3	0.0
Bare ground	NA	NA	NA	0.5	0	0.1	4.6	1.2	34.5
Other cover classes	NA	NA	NA	0	0	3.1	0	0.3	5.1

Low marsh reference wetlands were dominated in both sampling years by Lyngbye's sedge (*Carex lyngbyei*) and creeping bentgrass (*Agrostis stolonifera*). Other species occurring in low marsh plots included arrowgrass (*Triglochin maritima*), Olney's three-square (*Schoenoplectus pungens*), Pacific silverweed (*Potentilla anserina*) and common spikerush (*Eleocharis palustris*). High reference marsh plots included a greater diversity of species, with relatively high cover of tufted hairgrass (*Deschampsia cespitosa*), Pacific silverweed, Baltic rush (*Juncus balticus*), reed canarygrass, and yarrow (*Achillea millefolium*).

Both before and after restoration, reed canarygrass had the highest average cover of any vascular plant species at SFC (Table 5.2), however its overall cover declined somewhat (from 47% to 36%) after restoration. Although reed canarygrass remained relatively abundant in 2018, a high fraction of cover we observed in plots was dead (Figure 5.6), especially in the middle and cropped zones. These dead stands are expected to gradually be removed as decomposition proceeds. Indeed in areas of SFC during the 2018 sampling, we commonly observed wrack consisting of reed canarygrass, and observed even further decline towards the southern end of the site in 2020. Relatively healthy living stands of reed canarygrass persisted in both 2018 and 2020 in the north zone of the site which tended to have fresher soils (Figure 2.12).

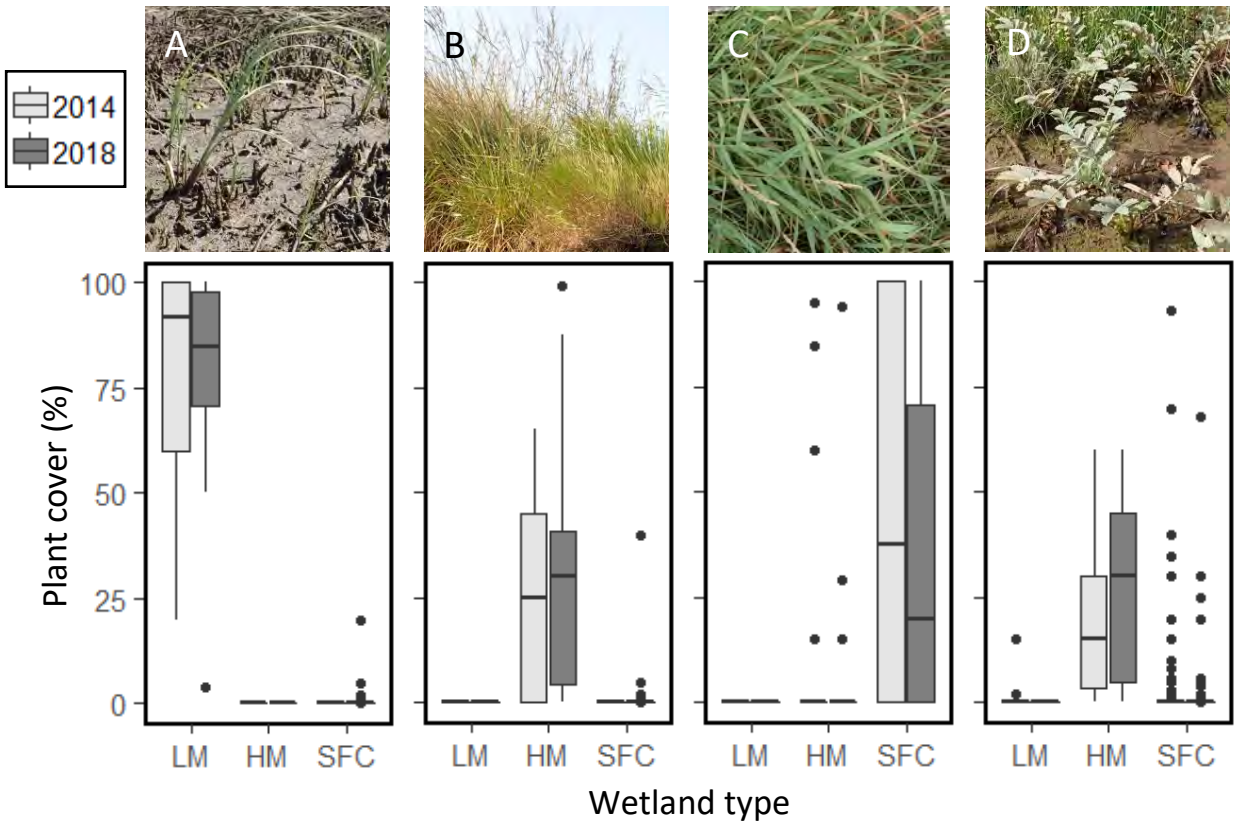

Figure 5.7. Cover of selected common estuarine plant species in the Tillamook Estuary in reference low marsh (LM), reference high marsh (HM) and at SFC (all land-use/land-cover zones pooled) for pre- and post-restoration sampling periods. A. *Carex lyngbyei* (native), B. *Deschampsia cespitosa* (native), C. *Phalaris arundinacea* (invasive), D. *Potentilla anserina* (native). See Figure 5.1 for a key to symbols.

Other relatively common species at SFC in the pre-and post-restoration sampling periods included creeping bentgrass, meadow foxtail (*Alopecurus pratensis*), slough sedge (*Carex obnupta*), jewelweed (*Impatiens capensis*), and tall fescue (*Schedonorus arundinaceus*). All of these species, except creeping bentgrass, declined in cover following restoration of tidal hydrology at the site. Creeping bentgrass can commonly be observed in both least-disturbed and restored tidal wetlands in the PNW (Frenkel and Morlan 1991, Adamus 2005, Brophy et al. 2014, Brown et al. 2016a, Janousek et al. 2019).

We analyzed differences in overall plant composition between SFC and reference wetlands in both monitoring periods with non-metric multidimensional scaling and PERMANOVA. For both years, there was a distinct difference in species composition between reference low and reference high marsh (Figure 5.8A) with the former dominated by Lyngbye's sedge, and the latter a more diverse mix of species. Composition in these zones did not change markedly between sampling years (low marsh: $F_{1,36} = 1.1$, $P = 0.30$; high marsh: $F_{1,44} = 1.2$, $P = 0.31$). In general, the NMDS mapping suggested that SFC plots had intermediate composition between reference wetland types and other SFC plots showing unique combinations of species. However, composition shifted to varying degrees in all SFC zones following restoration (north zone: $F_{1,36} = 2.6$, $P = 0.05$; middle zone: $F_{1,110} = 11.2$, $P \leq 0.001$; south zone: $F_{1,14} = 2.3$, $P = 0.06$; cropped zone: $F_{1,88} = 32.0$, $P \leq 0.001$; grazed zone: $F_{1,14} = 3.6$, $P = 0.004$), with all zones trending closer to low marsh than to high reference marsh (Figure 5.8B).

At the plot-level, plant species richness differed between SFC land-use/land-cover zones and reference wetlands during the pre-restoration ($F_{6,171} = 19.0$, $P < 0.0001$), and post-restoration monitoring periods ($F_{6,171} = 9.1$, $P < 0.0001$). Before restoration, most SFC zones (N, M, S and CR) had lower richness, comparable to diversity in low reference marsh, while the grazed zone and reference high marsh had higher richness (Figure 5.9A). Overall patterns were similar in the post-restoration monitoring period (Figure 5.9B), with the middle zone and reference high marsh showing evidence of increases in species richness (Figure 5.9C). Change in species richness between 2014 and 2018 was not correlated with wetland elevation ($R^2_{adj} = -0.01$, $P = 0.99$; Figure 5.10).

We examined total site-level richness (gamma diversity) with species accumulation curves for low and high reference marshes and for three SFC zones that had larger numbers of sample plots. Species richness was four- to five-fold higher in high reference marshes than in low reference marsh (Figure 5.11). Intermediate levels of richness were observed in three of the SFC zones (north, middle, cropped). In the middle and cropped zones, diverging confidence intervals suggested that richness was higher in the post-restoration monitoring period than before restoration. However, we also noted somewhat higher richness in HM during post-restoration monitoring, suggesting that rarer species could possibly have been better detected in the post-restoration monitoring. Extrapolating from observed species richness to estimated total species richness by zone with Chao's estimator (Chiu et al. 2014), there were similar differences between zones and between sampling periods (Table 5.3). High reference marsh had greater expected species richness than low marsh (in both sampling periods). In the three SFC zones evaluated, expected species richness was higher in the post-restoration monitoring period than before restoration (however, note relatively high standard errors). This is likely due to die-back of the pre-restoration dominants such as reed canarygrass that formed a monoculture throughout much of SFC before restoration, and its replacement with brackish-tolerant colonizing plants (Figure 5.10 and discussion below).

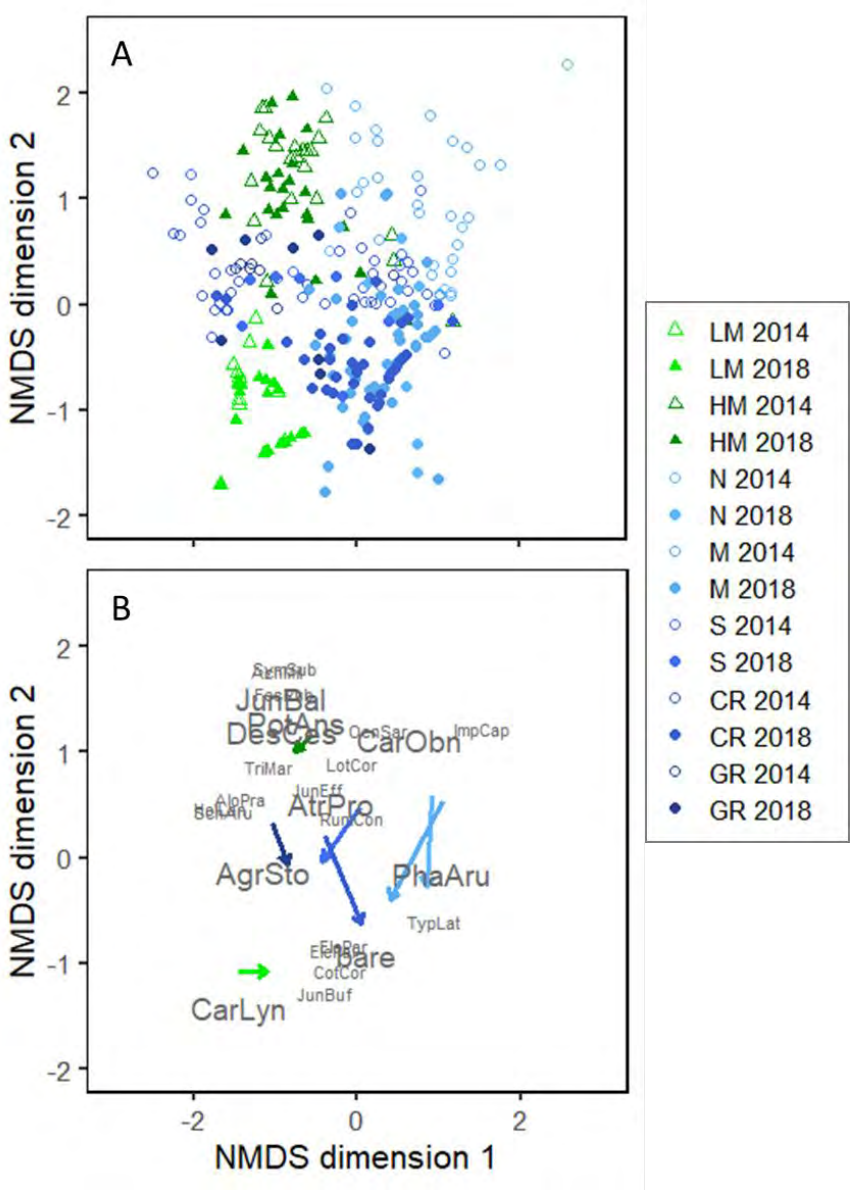

Figure 5.8. Differences in species composition between zones and monitoring periods with non-metric multidimensional scaling analysis (NMDS). (A) All plots were sampled in both the pre-restoration sampling event (2014; open symbols) and post-restoration sampling event (2018; filled symbols). Green points represent reference wetland plots and blue points represent SFC plots. (B) Same NMDS results as in A, but showing directional change in the centroid of each wetland zone from 2014 to 2018 with arrowheads, and the two dimensional position of plant species used in the analysis. Species in larger font had a frequency of occurrence of ≥10% in the dataset, while species in smaller font had a frequency of occurrence <10%. Species codes are in Table 5.2; bare = non-vegetated ground.

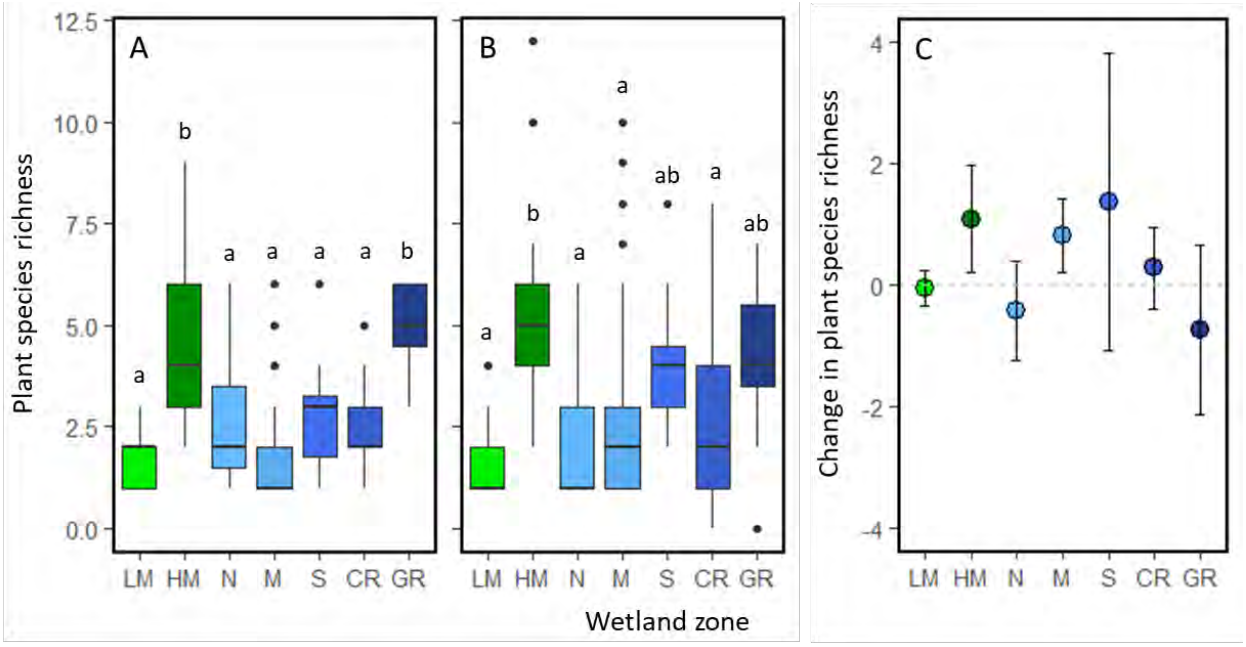

Figure 5.9. Differences in plant species richness in reference and SFC wetlands before (A) and after (B) restoration. Bars sharing the same letters were not significantly different. Panel (C) shows change (± 95% confidence intervals) in species richness by zone between 2014 and 2018.

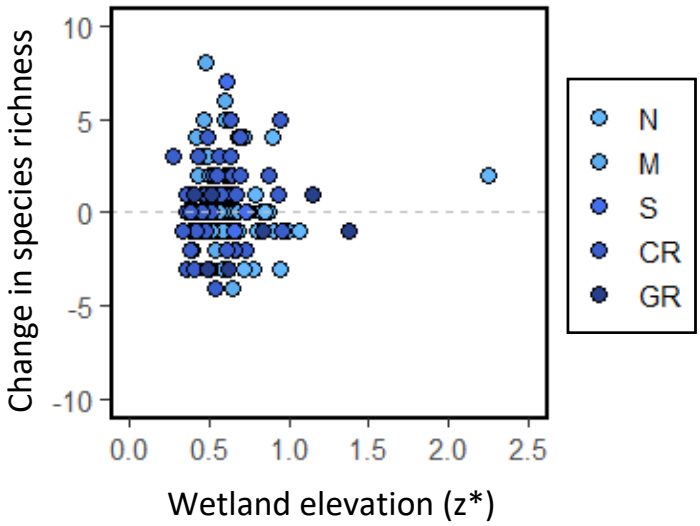

Figure 5.10. Change in plot-level plant species richness at SFC between pre- and post-restoration periods as a function of wetland surface elevation.

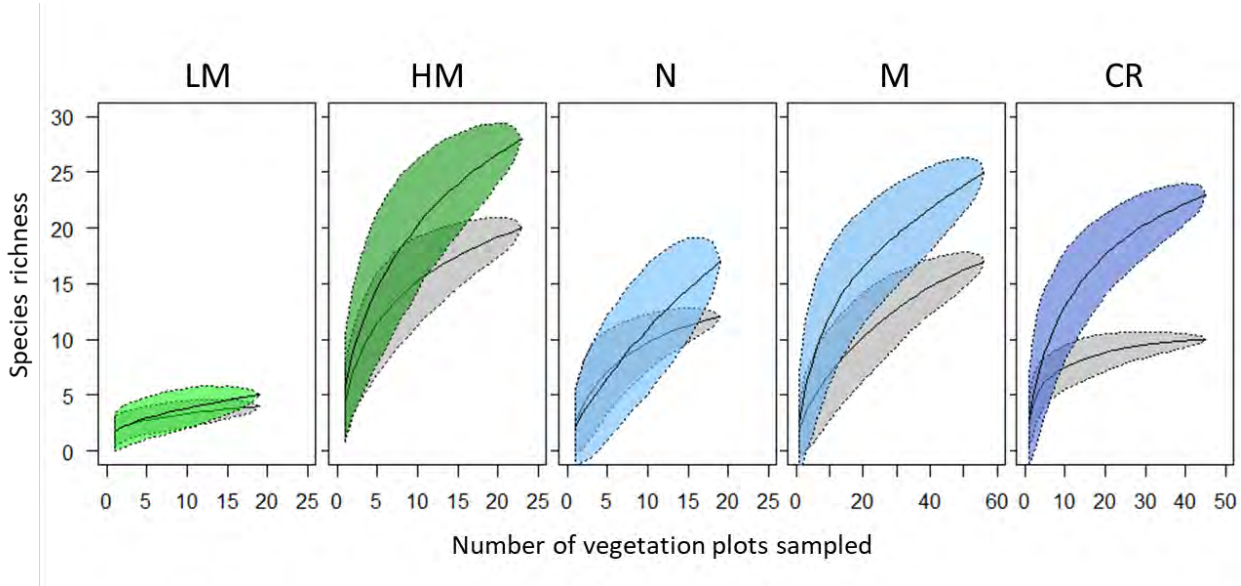

Figure 5.11. Cumulative species richness in reference low and high marsh and several SFC zones with species accumulation curves during pre- and post-restoration sampling periods. Polygons show 95% confidence intervals. We did not conduct analyses for zones with small sample sizes (S and GR zones).

Table 5.3. Estimated total species richness (gamma diversity) for reference marshes and SFC zones in 2014 and 2018. Statistics are Chao's estimate of minimum species richness based on the frequency of singletons and doubletons in the data set for each zone (Chiu et al. 2014). The south and grazed zones were not evaluated due to their relatively small sample sizes.

Wetland zone	2014 Chao estimate ± SE	2018 Chao estimate ± SE
Low reference marsh (LM)	4.5 ± 1.3	6.9 ± 3.6
High reference marsh (HM)	25.7 ± 6.2	34.5 ± 5.7
SFC North zone (N)	13.1 ± 1.7	85.2 ± 79.2
SFC Middle zone (M)	25.0 ± 8.1	84.4 ± 69.8
SFC South zone (S)	NA	NA
SFC Cropped zone (CR)	10.5 ± 1.3	35.0 ± 12.9
SFC Grazed zone (GR)	NA	NA

Vegetation mapping. Before restoration, non-native vegetation alliances occupied the majority of SFC (112 ha, 61% of the site; Table 5.4), whereas native alliances occupied about 54 ha (29% of the site). After restoration, the area of both native and non-native alliances decreased substantially, primarily due to an increase in bare ground (Figure 5.12). Bare ground increased from zero in 2014 (no mapped bare ground) to about a fifth of the site (39 ha) in 2018 (Table 5.4; Figure 5.13). The increase in bare ground was primarily due to dieback of the diked site's formerly dominant vegetation (particularly reed canarygrass), which was intolerant of the increased salinity and inundation after restoration. However, soil disturbance by machinery operations during restoration was also a factor (Figure 5.12).

Figure 5.12. Example of bare ground at SFC in 2018, showing the impacts of soil disturbance by earthmoving machinery, which was extensive in this area.

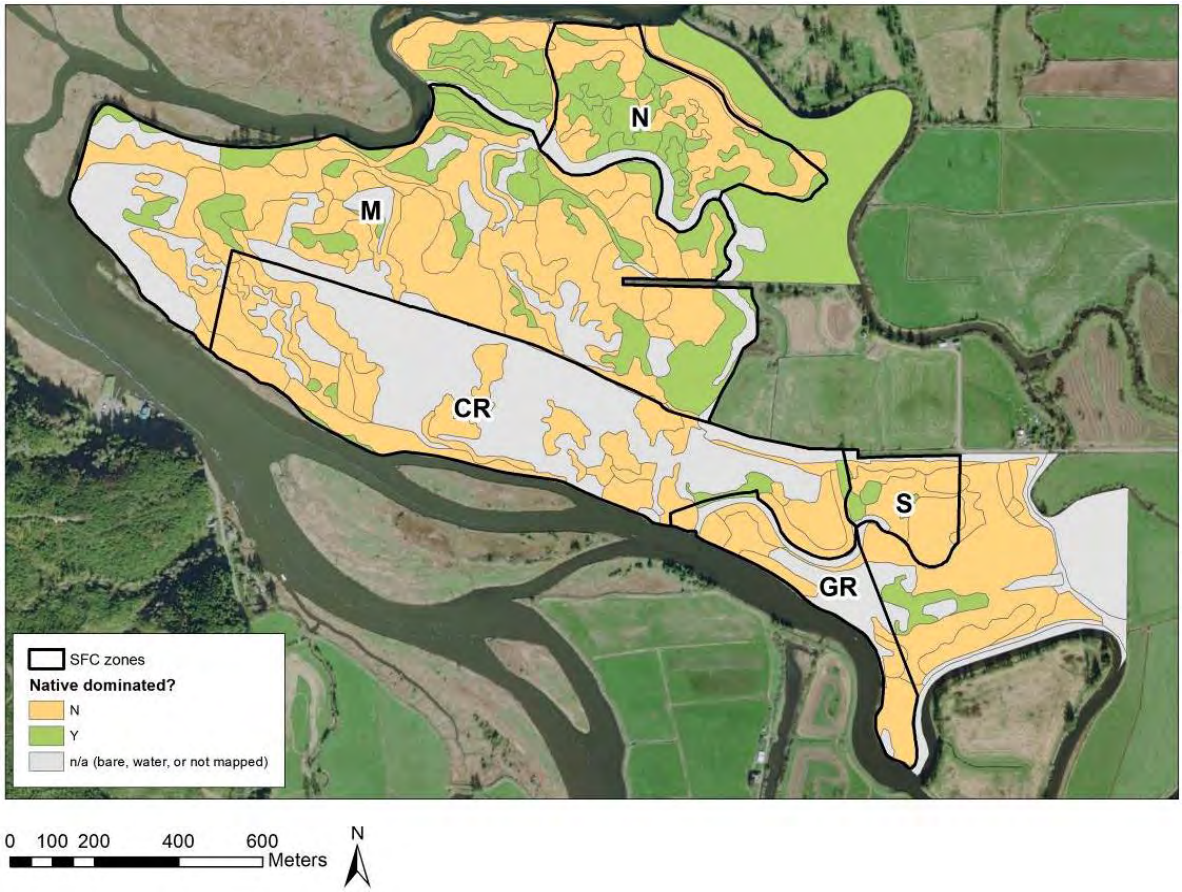

Figure 5.13. Native-dominated (green) vs. non-native-dominated (orange) plant communities at SFC in 2018. Bare ground and unmapped areas are gray (see Figure 5.14 for details). Background image: ESRI World Imagery.

Table 5.4. Total area of native-dominated, non-native-dominated vegetation, and bare ground at SFC before (2014) and after restoration (2018). Green rows indicate increased area; yellow rows indicate decreased area.

Vegetation type	2014 area (ha, %)	2018 area (ha, %)	Change between 2014 and 2018 (ha, %)
Native-dominated	53.59 (29.1%)	40.50 (22.1%)	- 13.09 (-24.4%)
Non-native dominated	111.59 (60.6%)	88.45 (48.3%)	- 23.14 (-20.7%)
Bare ground	0.00 (0.0%)	39.36 (21.5%)	+ 39.36 (NA*)
Upland/not mapped	18.85	14.80	NA**
Total	184.03	183.11	

* Percent change could not be calculated for bare ground, because no bare ground was mapped in 2014.
** Percent area/change was not calculated for the unmapped area because it is not meaningful (see "Methods").

The area of native- versus non-native-dominated vegetation and bare ground varied by land-cover/land-use zone at SFC (Table 5.5). Zones with a relatively high proportion of native-dominated vegetation included the north zone, where substantial areas were occupied by willow; and areas outside the regularly monitored zones ("Other" in Table 5.5), which were predominantly forested (Sitka spruce alliance). As observed in vegetation plots (Figure 5.2), plant cover was lowest (that is, bare ground was particularly prevalent) in the cropped zone in 2018 (Figure 5.13), but the SFC site overall showed a decrease in plant cover (increase in bare ground) from 2014 to 2018 (Table 5.4).

Table 5.5. Area of native-dominated, non-native-dominated vegetation, and bare ground by SFC land-cover/land-use zone in 2018.

Vegetation type	North	Middle	South	Cropped	Grazed	Other	Total
Native-dominated	7.15	13.63	0.60	1.08	0.13	17.91	40.50
Non-native dominated	7.76	36.58	4.42	19.01	4.90	15.78	88.45
Bare ground	1.72	15.37	0.50	22.75	3.59	10.23	54.16
Total	16.63	65.58	5.52	42.83	8.63	43.92	183.11

Across the entire SFC site, the most prominent shift in vegetation from 2014 to 2018 observed in the vegetation mapping was the decline in extent and condition of reed canarygrass (Table 5.6; Figure 5.6). The extent of the healthy reed canarygrass alliance dropped from 82.2 ha in 2014 to 7.8 ha in 2018, a 91% reduction. About half of the area that was occupied by healthy reed canarygrass in 2014 had shifted to bare ground in 2018 (39 ha) and about half had declined sharply in condition (2018 alliance "reed canarygrass – dead/dying", 41 ha). This landscape-level change in the mapped data was consistent with the very high proportion of dead reed canarygrass observed in vegetation plots in the middle and cropped zones (Figure 5.6).

Other prominent shifts at SFC at the alliance level included a strong increase in the area of the non-native creeping bentgrass alliance; an increase in areas dominated by the brackish-tolerant Pacific silverweed; declines in the non-native pasture grasses tall fescue and meadow foxtail, and a decline in area and condition of coastal willow (Table 5.6). These changes are consistent with the increased salinity and inundation after restoration at SFC (Chapters 2 and 4).

The large extent of dead and dying reed canarygrass in 2018 (Table 5.6, Figure 5.6) indicated the still-dynamic condition of vegetation at SFC. We expect these areas to transition over the next few years to the brackish-tolerant species seen on the lower parts of the site, particularly Lyngbye's sedge. Qualitative observations in the cropped zone in 2020 indicate that Lyngbye's sedge and dwarf spikerush (*Eleocharis parvula*) were becoming common. The 7.32 ha of unhealthy or dead coastal willow also indicated the site's dynamic conditions in 2018. Observations in summer 2020 suggest that willow is continuing to decline across most of the site due to increasing salinity, but since this species can tolerate some salinity (Brophy 2009), it may continue to persist in the fresher parts of the site (e.g., near Hall Slough).

Table 5.6. Area of each vegetation alliance at SFC before (2014) and after restoration (2018). Green rows indicate alliances showing major increases in area; yellow rows indicate major decreases in area.

Vegetation alliance	2014 area (ha)	2018 area (ha)	Change between 2014 and 2018 (%)
Reed canarygrass - dead/dying	0.00	40.68	NA[1]
Bare ground	0.00	39.36	NA[1]
Creeping bentgrass	0.14	35.97	+25,883%
Sitka spruce	23.17	20.97	-9%
Reed canarygrass – healthy	82.18	7.77	-91%
Coastal willow - unhealthy/dead	0.00	7.32	NA[1]
Pacific silverweed	0.00	3.70	NA[1]
Tall fescue	17.52	3.23	-82%
Coastal willow - healthy	17.11	2.74	-84%
Creeping spikerush	0.39	1.76	+356%
Lyngbye's sedge	1.37	1.29	-6%
Toad rush	0.00	1.29	NA[1]
Slough sedge	6.64	0.62	-91%
Common cattail	3.19	0.79	-75%
Perennial ryegrass	0.00	0.64	NA[1]
Meadow foxtail	8.81	0.16	-98%
Upland/not mapped	14.35	7.43	NA[2]
Major channels	4.50	7.37	NA[2]
Total	184.03	183.11	-1%

[1] Change in area could not be calculated for alliances with zero area in 2014 or 2018.
[2] For channels and unmapped areas, % change was not calculated (see "Methods").

The spatial distribution of alliances at SFC showed striking patterns in 2018 (Figure 5.14). Bare ground and creeping bentgrass predominated on the south side of the site in the cropped and grazed zones, whereas in the middle zone, dead and dying reed canarygrass predominated. In the north zone, native species such as Sitka spruce and coastal willow were widespread, but there were also substantial areas of healthy reed canarygrass. These vegetation patterns were driven by spatial variability in ecosystem drivers such as salinity, as well as physical site changes associated with past land uses (Janousek et al. 2020). Such spatial variability in ecosystem drivers and the resulting biota illustrates the importance of site stratification in monitoring (Simenstad et al. 1991).

The spatial variability across the SFC site was also evident in the large differences among zones in the area of each alliance (Table 5.7). Prior to restoration, the reed canarygrass alliance was found across

the vast majority of the cropped and middle zones (Brown et al. 2016b). In 2018, the cropped zone had no remaining healthy reed canarygrass and only 3 ha of dead/dying reed canarygrass; the rest of the formerly healthy reed canarygrass was gone, replaced by bare ground and creeping bentgrass. By contrast, the middle zone, at a slightly higher elevation and with less saline soils, still had over 35 ha of dead and dying reed canarygrass (Table 5.7); and the north zone, which tended to have the least saline soils two years after restoration (Figure 2.12), still had nearly 5 ha of healthy reed canarygrass in 2018.

Table 5.7. Area occupied by each vegetation alliance at SFC, by land-use/land-cover zone, in the post-restoration sampling period (2018).

	Area (ha)						
Alliance	North	Middle	South	Cropped	Grazed	Other*	Total
Reed canarygrass - dead/dying	1.83	35.28	0.44	3.04		0.08	40.68
Bare ground		13.79		21.43	2.55	1.59	39.36
Creeping bentgrass	1.04	1.14	2.76	14.93	2.82	13.28	35.97
Sitka spruce	2.10	5.50	0.27	0.20		12.91	20.97
Reed canarygrass - healthy	4.89		1.19			1.69	7.77
Coastal willow - unhealthy/dead	2.11	4.88	0.33	0.00			7.32
Pacific silverweed	1.12	0.71				1.88	3.70
Tall fescue			0.02	1.05	2.08	0.08	3.23
Coastal willow	1.67	0.58				0.49	2.74
Creeping spikerush				0.47	0.13	1.16	1.76
Lyngbye's sedge		0.48		0.41		0.41	1.29
Toad rush		1.29					1.29
Slough sedge		0.09				0.53	0.62
Common cattail	0.15	0.11				0.53	0.79
Perennial ryegrass						0.64	0.64
Meadow foxtail		0.16					0.16
Major channels	1.72	1.47	0.14	0.04	0.90	3.09	7.37
Upland/not mapped		0.11	0.35	1.28	0.14	5.55	7.43
Total	16.63	65.58	5.52	42.84	8.63	43.92	183.11

* "Other" indicates vegetation mapping areas outside the monitoring zones.

At the finest mapping scale (highest-resolution), we classified the SFC mapped area into 34 map units, which included 31 plant associations and 3 land cover classes (Figure 5.14, Appendix Tables A5.1, A5.2). The 3 non-association land cover map units were bare ground, lower sections of major channels (mapped to allow visualization of changes in these most dynamic channels over time), and unmapped areas. The unmapped areas included uplands and areas that were mapped in 2014, but were not included in the 2018 post-restoration vegetation mapping because they are located behind new setback dikes.

Of the 31 mapped plant associations, about half (14) were groupings of species within the two alliances that occupied the largest area at SFC (Appendix Tables A5.1 and A5.2): reed canarygrass (8 associations; map units 20-27) and creeping bentgrass (6 associations; map units 1-6). These alliances contained many associations because their dominant species (reed canarygrass and creeping bentgrass) are adapted to a wide variety of site conditions, and thus occur by a wide variety of co-dominants. For example, creeping bentgrass dominated in areas that had been cropped or grazed before restoration,

excavated dike removal areas, and compacted equipment tracks and former roadways. Because of the varying physical conditions (ecosystem drivers) across these different areas, co-dominants within creeping bentgrass associations ranged from pre-restoration pasture dominants that persisted on higher ground and in fresher portions of the site (e.g. reed canarygrass and velvetgrass), to early salt-marsh colonizers such as brass buttons and toad rush (in the lower-elevation and more saline areas), to early-established stands of typical salt marsh dominants such as Lyngbye's sedge and tufted hairgrass (particularly near the Trask and Tillamook Rivers). Similarly, co-dominants within reed canarygrass associations included native freshwater wetland species such as slough sedge and Pacific silverweed; pasture species such as birdsfoot trefoil; and brackish-tolerant colonizers such as creeping bentgrass and brass buttons.

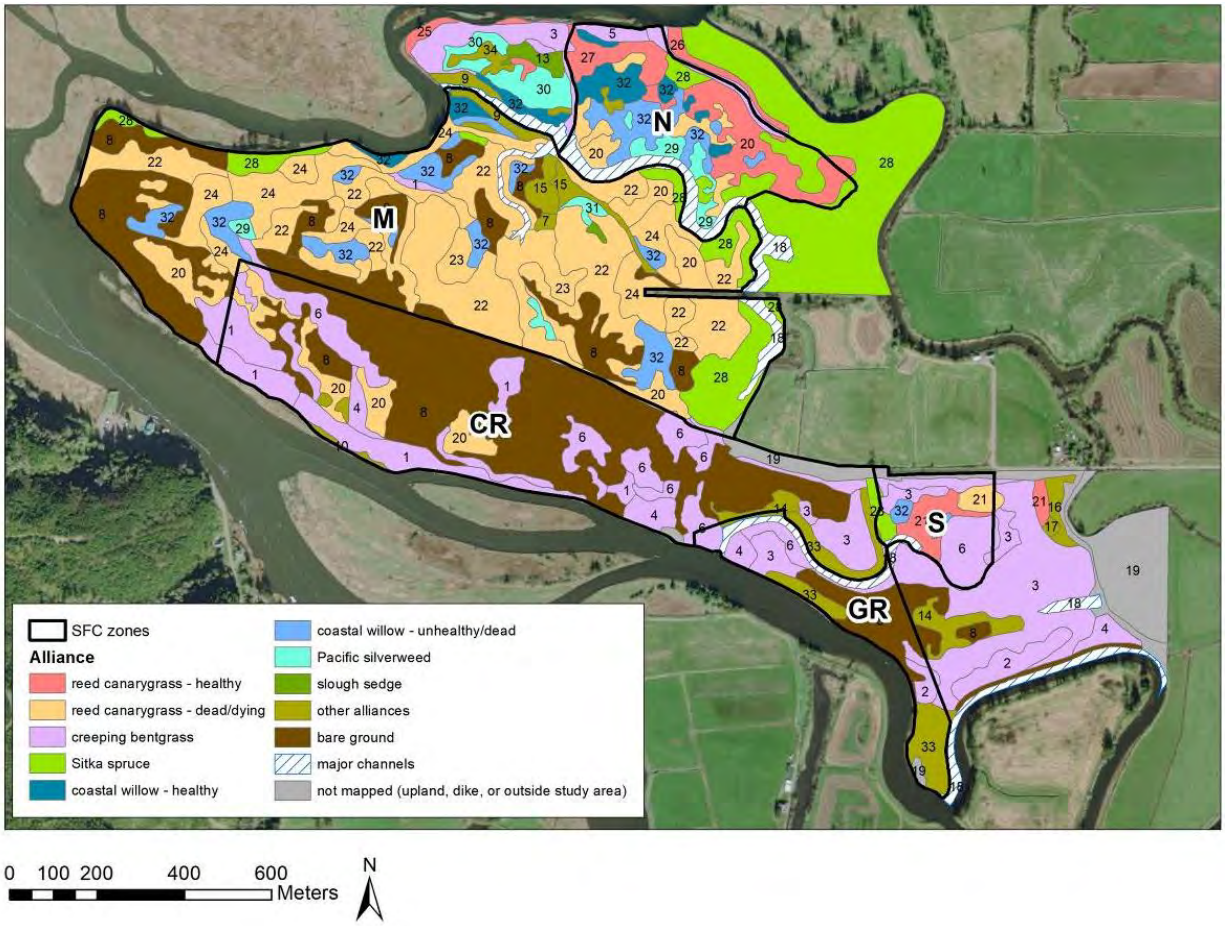

Figure 5.14. Vegetation alliances and associations at SFC mapped during the post-restoration monitoring period (2018). Colors indicate alliances (see legend), and labels indicate associations (see Appendix, Table A5.1). Small polygons are not labeled; for a complete map, a GIS shapefile is available from the second author. Background image: ESRI World Imagery.

Besides reed canarygrass and creeping bentgrass associations, only two other plant associations occupied more than 2 ha at SFC: Sitka spruce-dominated associations, and coastal willow-dominated associations (Appendix, Table A5.1). The Sitka spruce forested wetlands occupied the same area as before restoration -- about 21 ha, primarily on the east side of the site along upper Blind Slough and near Hall Slough. The portions of these forested wetlands closest to Hall Slough appear to remain similar to their condition prior to restoration, probably maintained by freshwater inflows in this area. However, the forested wetlands on upper Blind Slough have declined in condition, with most of the understory shrubs

now dead, and many of the spruce in poor condition (Figure 5.15). This is most likely due to the increased salinity and inundation with the restoration of tidal flows (see Chapter 4). Future monitoring is recommended to determine whether brackish-tolerant trees and shrubs can establish and persist with the new salinity and inundation regimes at the site. Vegetation mapping using remote data (e.g., aerial photos) is recommended for tracking these changes, since the shrub and forested areas are difficult to access and potentially dangerous due to falling trees.

Figure 5.15. South margin of forested wetlands along upper Blind Slough in the middle zone in August 2018, showing dead understory shrubs and poor condition of Sitka spruce due to increased salinity and inundation after restoration. Photo by L. Brophy.

The remaining 18 associations mapped in 2018 occupied less than 3 ha each and were represented by only a handful of polygons; these collectively occupied 13.5 ha (7.3% of the mapped area) (Appendix, Table A5.1). We were able to map these areas in more detail because of the high-resolution aerials; their mapping will allow more detailed tracking of change in the future.

Overall patterns of vegetation development. Our observation of early vegetation change at SFC is consistent with reports of vegetation succession in other PNW tidal wetland restoration projects. Together these studies from across the region suggest a common pattern of plant succession (Figure 5.16). Prior to restoration, many sites are initially occupied by species found in disturbed pastures or freshwater wetlands, including invasive reed canarygrass (Frenkel and Morlan 1991, Thom et al. 2002, Borde et al. 2012, Woo et al. 2018). Once dikes are breached or completely removed as part of hydrologic restoration, there is fairly rapid loss of pasture and freshwater wetland species followed by an increase in bare ground (Thom et al. 2002, Davis et al. 2018, Brown et al. 2016a). Subsequent colonization by annual and then by perennial species characteristic of low-elevation brackish and salt marsh such as pickleweed (*Salicornia pacifica*), salt grass (*Distichlis spicata*), and brass buttons (*Cotula coronopifolia*) is then observed after several years (Frenkel and Morlan 1991, Cornu and Sadro 2002, Thom et al. 2002, Davis et al. 2018). Finally, plants characteristic of middle or high-elevation tidal marshes such as tufted hairgrass begin to recruit years later (Cornu and Sadro 2002, Thom et al. 2002). In freshwater or lower salinity areas within estuaries, restored sites may eventually support woody species such as Sitka spruce, twinberry, and crab apple (*Malus fusca*), developing into scrub-shrub or forested tidal swamps in place of emergent marshes.

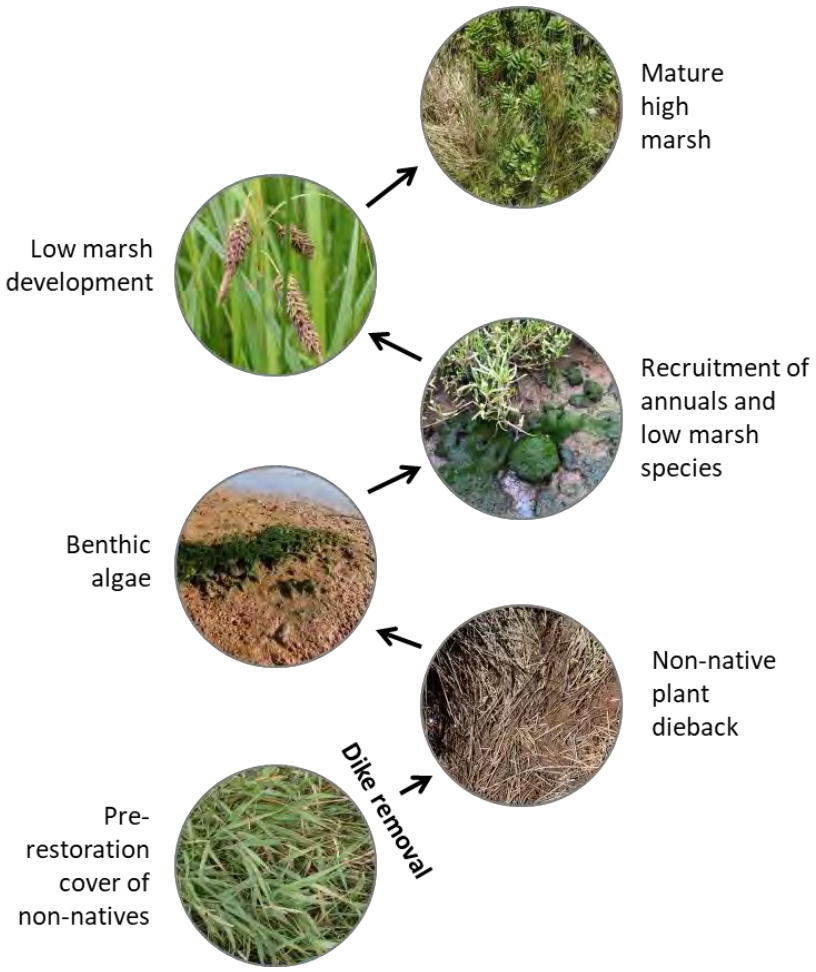

Figure 5.16. General conceptual model of vegetation change in PNW tidal wetland restoration projects based on observations in this study and others (e.g., Frenkel and Morlan 1991, Cornu and Sadro 2002, Thom et al. 2002, Borde et al. 2012, Woo et al. 2018).

Vegetation change over time in PNW restoration sites may be closely tied to important physical gradients present in estuarine wetlands, including elevation. For instance, Brophy et al. (2014) noted that the decline in non-native tall fescue after restoration proceeded more slowly in higher elevation areas of a project site in the Coquille Estuary. Outside the PNW, Eertman et al. (2002) also found that lower elevation areas with greater inundation gained typical tidal marsh species more rapidly than drier areas. At SFC we observed that lower-elevation areas tended to lose more of their existing plant cover in the very early stage of vegetation development (Figures 5.2, 5.5; Janousek et al. 2020). Since these areas also tended to increase more in soil salinity and pH than other areas following restoration (Chapter 2), we hypothesize that frequent tidal inundation was a major driver of initial vegetation loss and replacement with bare space (Janousek et al. 2020).

Given that SFC has relatively low elevation and strongly brackish (mesohaline) tides inundate even the easternmost reaches of the site in summer (see Chapter 4), we suggest that recovery of native tidal wetland vegetation will occur fairly rapidly across much of the site, consistent with observations from

several other west coast tidal restoration projects (Frenkel and Morlan 1991, Grismer et al. 2004). In fact, qualitative observations of vegetation in the cropped and middle zones during summer 2020 showed that many patches of native species including tufted hairgrass, dwarf spikerush, common spikerush, and Lyngbye's sedge were becoming well established at the site (Figure 5.17). Other colonizing vegetation included non-native brass buttons (which may eventually be outcompeted by native species), golden dock (*Rumex maritimus*, an uncommon native tidal marsh forb), and some occurrences of typical high marsh species such as Pacific silverweed, yarrow, and Douglas aster (*Symphyotrichum subspicatum*).

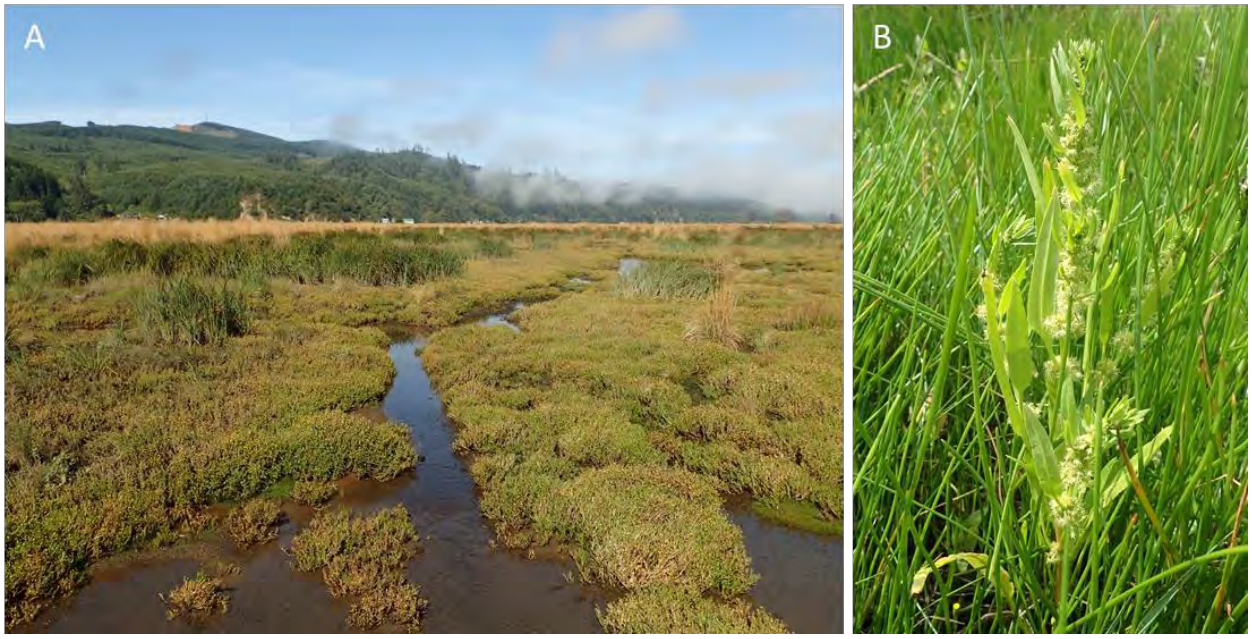

Figure 5.17. Examples of vegetation observed at SFC during August 2020, four years after restoration of tidal inundation at the site. (A) Assemblages present in the cropped zone, including brass buttons (foreground), Lyngbye's sedge (taller dark green patches), and tufted hairgrass (background). (B) Golden dock growing in a patch of native common spikerush in the middle zone.

Since wetland surface elevation at much of SFC may remain relatively low for up to several decades, in the near term, vegetation communities similar to nearby reference low marshes may develop. These assemblages are likely to be dominated by Lyngbye's sedge, but may also include substantial cover of creeping bentgrass on slightly higher ground. The site does contain some topographic heterogeneity, however, with higher elevation areas which could support other species. Broad-scale development of plant species composition at SFC that more closely resembles complex assemblages of high marshes such as Dry Stocking Island and Goose Point may take several decades or more.

Some areas of SFC, particularly the north zone, which is somewhat higher and fresher than other areas at SFC, may change more slowly than the cropped or middle zones. The die-back and replacement of large patches of reed canarygrass may take some time as large healthy stands of this species were still observed in some locations at SFC in 2020, four years following restoration of tidal hydrology (Figure 5.18). Clifton et al. (2018) found that non-native vegetation present before restoration in some PNW brackish wetlands persisted following restoration activities as it competed with native species.

Figure 5.18. Persistence of reed canarygrass at SFC in the north zone in August 2020 (background).

As vegetation development continues at the site, it will be important to monitor a variety of parameters including total cover, native species cover, species richness, and species composition. Information on species composition is particularly important because it will help managers evaluate the relative success of native and non-native species and help researchers and managers link rates of important wetland functions such as sediment accretion or wildlife support to specific plant species or assemblages.

Citations

Adamus PR, Larsen J, and Scranton R. 2005. Wetland Profiles of Oregon's Coastal Watersheds and Estuaries. Part 3 of a Hydrogeomorphic Guidebook. Report to Coos Watershed Association, US Environmental Protection Agency, and Oregon Department of State Lands, Salem, OR.

Bertness MD. 1991. Interspecific interactions among high marsh perennials in a New England salt marsh. Ecology 72:125-137.

Borde AB, Cullinan VI, Diefenderfer HL, Thom RM, Kaufman RM, Zimmerman SA, Sagar J, Buenau KE, Corbett C. 2012. Lower Columbia River and estuary ecosystem restoration program reference site study: 2011 restoration analysis. Pacific Northwest National Labs report PNNL-21433, Richland WA.

Brophy LS, van de Wetering S, Ewald MJ, Brown LA, Janousek CN. 2014. Ni-les'tun tidal wetland restoration effectiveness monitoring: year 2 post-restoration (2013). Institute for Applied Ecology, Corvallis, OR.

Brophy LS. 2009. Effectiveness monitoring at tidal wetland restoration and reference sites in the Siuslaw River Estuary: A tidal swamp focus. Report to Ecotrust, Portland, Oregon. Green Point Consulting, Corvallis, OR.

Brophy LS, Brown LA, Ewald MJ, Peck EK. 2017. Baseline monitoring at Wallooskee-Youngs restoration site, 2015, Part 2: Blue carbon, ecosystem drivers and biotic responses. Institute for Applied Ecology, Corvallis, OR.

Brown LA, Ewald MJ, and Brophy LS. 2016a. Ni-les'tun tidal wetland restoration effectiveness monitoring: Year 4 post-restoration (2015). Corvallis, Oregon: Estuary Technical Group, Institute for Applied Ecology, Corvallis, OR.

Brown LA, Ewald MJ, Brophy LS, van de Wetering S. 2016b. Southern Flow Corridor baseline effectiveness monitoring: 2014. Estuary Technical Group, Institute for Applied Ecology, Corvallis, OR.

Chiu C-H, Wang Y-T, Walther BA, Chao A. 2014. An improved nonparametric lower bound of species richness via a modified Good-Turing frequency formula. Biometrics 70:671-682.

Clifton BC, Hood WG, Hinton SR. 2018. Floristic development in three oligohaline tidal wetlands after dike removal. Ecological Restoration 36:238-251.

Cornu CE, Sadro S. 2002. Physical and functional responses to experimental marsh surface elevation in Coos Bay's South Slough. Restoration Ecology 10:474-486.

Cragg SM, Friess DA, Gillis LG, Trevathan-Tackett SM, Terrett OM, Watts JEM, Distel DL, Dupree P. 2020. Vascular plants are globally significant contributors to marine carbon fluxes and sinks. Annual Review of Marine Science 12:469-497.

Davis MJ, Ellings CS, Woo I, Hodgson S, Larsen K, Nakai G. 2018. Gauging resource exploitation by juvenile Chinook salmon (*Oncorrhynchus tshawytscha*) in restoring estuarine habitat. Restoration Ecology 26:976-986.

Diefenderfer HL, Borde AB, Sinks IA, Cullinan VI, Zimmerman SA. 2016. Columbia Estuary Ecosystem Restoration Program: Restoration design challenges for topographic mounds, channel outlets, and reed canarygrass. PNNL-24676, final report prepared for the Bonneville Power Administration, Portland, Oregon by the Pacific Northwest National Laboratory, Sequim, Washington and Columbia Land Trust, Vancouver, WA.

Eertman RHM, Kornman BA, Stikvoort E, Verbeek H. 2002. Restoration of the Sieperda tidal marsh in the Scheldt Estuary, The Netherlands. Restoration Ecology 10:438-449.

Frenkel RE, Morlan JC. 1991. Can we restore our salt marshes? Lessons from the Salmon River, Oregon. The Northwest Environmental Journal 7:119-135.

Grismer ME, Kollar J, Syder J. 2004. Assessment of hydraulic restoration of San Pablo marsh, California. Environmental Monitoring and Assessment 98:69-92.

Janousek CN, Folger C. 2014. Variation in tidal wetland plant diversity and composition within and among estuaries: assessing the relative importance of environmental gradients. Journal of Vegetation Science 25:534-545.

Janousek CN, Thorne KM, Takekawa JY. 2019. Vertical zonation and niche breadth of tidal marsh plants along the northeast Pacific coast. Estuaries and Coasts 42:85-98.

Janousek CN, Bailey SJ, Brophy LS. 2021. Early ecosystem development varies with elevation and pre-restoration land use/land cover in a Pacific Northwest tidal wetland restoration project. Estuaries and Coasts 44:13-29.

Jaster T, Meyers SC, Sundberg S (eds) 2017. Oregon Vascular Plant Checklist, v.1.7

Leonard LA, Luther ME. 1995. Flow hydrodynamics in tidal marsh canopies. Limnology and Oceanography 40:1474-1484.

Maier GO, Simenstad CA. 2009. The role of marsh-derived macrodetritus to the food webs of juvenile Chinook salmon in a large altered estuary. Estuaries and Coasts 32:984-998.

Oksanen J. 2015. Multivariate analysis of ecological communities in R: vegan tutorial.

Simenstad, CA, Tanner CD, Thom RM, Conquest L. 1991. Estuarine Habitat Assessment Protocol. UW-FRI-8918/-8919 (EPA 910/9-91-037), Rep. to U.S. Environ. Protect. Agency - Region 10. Wetland Ecosystem Team, Fish. Res. Inst., University of Washington, Seattle, WA.

Smith KR, Barthman-Thompson L, Gould WR, Mabry KE. 2014. Effects of natural and anthropogenic change on habitat use and movement of endangered salt marsh harvest mice. PLoS ONE 9:e108739.

Thom RM, Zeigler R, Borde AB. 2002. Floristic development patterns in a restored Elk River estuarine marsh, Grays Harbor, Washington. Restoration Ecology 10:487-496.

Woo I, Davis MJ, Ellings CS, Nakai G, Takekawa JY, de la Cruz S. 2018. Enhanced invertebrate prey production following estuarine restoration supports foraging for multiple species of juvenile salmonids (*Onchorhynchus* spp.). Restoration Ecology 26:964-975.

Chapter 6: Finfish abundance and migration

Stan van de Wetering and Maxwell Tice-Lewis

Key findings

- Abundance of juvenile chinook salmon (age-0) increased six-fold in SFC after restoration, to a level about twice that of the mainstem river reference areas. By contrast, chinook abundance in the mainstem rivers decreased during the post-restoration period. We attribute the increase in chinook abundance at SFC to the restoration process.
- Juvenile chum (age-0) were absent from SFC before restoration, but their abundance increased greatly after restoration, reaching about six times that of river reference areas and ten times that of age-0 chinook within SFC. We saw little change in chum abundance at the reference rivers. We attribute the increase in SFC chum abundance to the restoration process.
- Age-0 coho were present at SFC both before and after restoration, but their abundance did not change much.
- Staghorn sculpin increased in abundance at SFC following restoration, while three-spined stickleback declined.
- Tidal migration monitoring suggested that juvenile chinook and chum were residing within SFC across multiple tidal cycles, if not continuously, suggesting that the recovering SFC site is providing consistent nursery habitat for these species.
- Age-0 coho, which prefer still water habitats, reduced their use of the lower SFC channel habitats that were previously located close to the pre-restoration tide gates.

Introduction

Research from Pacific Northwest estuarine systems has demonstrated that estuaries provide habitats critical to a number of juvenile salmonids during their early life history (Greene and Beamer 2012, Brophy et al. 2014, Jones et al. 2014). Our aim within the present study was to assess changes in fish abundance and migratory behavior at SFC before and after restoration and to compare patterns with tidal channels in reference areas in southern Tillamook Bay. Based on prior experience in other Oregon estuaries (Brophy et al. 2014, van de Wetering et al. 2008, van de Wetering et al. 2009) we anticipated encountering a handful of species that predominantly use the high and low marsh tidal channel network for juvenile rearing. These species include chinook salmon (*Oncorhynchus tshawytscha*), chum salmon *(Oncorhynchus keta)*, coho salmon *(Oncorhynchus kisutch)*, steelhead trout (*Oncorhynchus mykiss)*, cutthroat trout (*Oncorhynchus clarkia)*, shiner perch (*Cymatogaster aggregata)*, staghorn sculpin (*Leptocottus armatus)*, prickly sculpin (*Cottus asper)*, and starry flounder (*Platichthys stellatus)*. Pacific herring *(Clupea pallasii),* and eulachon (*Thaleichthys pacificus)* are also found in these habitats but for shorter periods of time.

In more saline regions of PNW estuaries, larvae and juveniles from additional species such as Northern anchovy, surf smelt, and various rockfishes are found (van de Wetering, unpublished data, Siletz, Alsea and Coquille estuaries). Because the SFC site is located in a more brackish region of Tillamook Bay and some of the above species are encountered at lower rates than others, we focused on a subset of species age groups for our SFC site analysis. We measured fish distribution, abundance, and tidal migration

patterns at the SFC site and nearby reference sites to allow for an assessment of restoration efficacy through analysis of species response patterns. We analyzed data using a before-after-control-impact (BACI) framework. We focused our restoration site (SFC) sampling efforts in remnant tidal channels and constructed ditches and our reference site sampling efforts across the broader mainstem river habitats that provide migration corridors for the SFC site.

Materials and methods

Low tide fish distribution and abundance. We sampled fish distribution and abundance using low tide seine sampling. Sampling was focused on the lower low tide of the daily tidal cycle, as fish found during lower low tides typically remain in that habitat during the period when they are most susceptible to mortality, therefore expressing a preference for residency in that habitat. Sampling focused on the months of March through August in both 2014 (pre-restoration monitoring period), and 2018 (post-restoration monitoring period), when juvenile salmonids are most abundant in Oregon estuaries (Brophy et al. 2014, van de Wetering et al. 2009, van de Wetering and French. 2008). There were five sub-watersheds monitored at SFC: Blind Slough, Nolan Slough, Trib 1, Northwest Ditch and Trib 2 (note this is a different location from the Trib 2 station monitored for channel morphology). Within each SFC location, we longitudinally stratified seine samples across the lower reach of the monitoring sub-watershed (Figure 6.1). Northwest Ditch was used as a sampling site in 2014 but was no longer a viable site in 2018 and was replaced by Trib 2 for post-restoration sampling. We determined Trib 2 was appropriate as a post-restoration replicate of Northwest Ditch due to the close proximity of the two sites and relative to its geographic position within the restored marsh. Reference sampling was conducted at five locations distributed across an expected salinity and temperature gradient in the Trask and Wilson Rivers, and located adjacent to one of the four SFC restoration sampling locations (Figure 6.1).

We sampled mainstem rivers as reference sites instead of tidal sub-basin channels because it was not possible to find high marsh channel reference habitats comparable to the SFC site when sub-basin size, geography and human disturbance patterns were considered (see Chapter 3 for differences in reference high marsh and SFC tidal channel morphology). Additionally, our past experience has shown that to generate capture rates that allow for reasonable statistical inferences to be made, fish densities have to be at levels commonly found in the mainstem rivers (Brophy et al. 2014, van de Wetering et al. 2009, van de Wetering and French 2008). Rivers such as the Tillamook, Trask, Wilson, Kilchis, and Miami that drain into Tillamook Estuary provide migration corridors for salmonids. Other species that use the river channels as corridors include non-salmonids that typically spawn, rear, and migrate through the upper portion of an estuary; shiner perch is one example. The river channel habitats are therefore the fish supply source for the SFC site and thus allow us to better determine what changes observed during the post-restoration period can be attributed to the restoration itself, as opposed to changes in fish abundance across the broader set of rivers that spill into Tillamook Estuary and or ocean habitats.

Within each SFC sample location, six samples were taken with each sample consisting of a single seine set. All seine samples across the SFC locations were 10 m in length with a maximum of 10 m in width, or the width of the wetted channel if it measured less than 10 m. SFC location seine sample depths averaged 0.1 m ranging from 0.05 to 1.5 m. Along mainstem rivers (reference sites), we targeted six samples at each of the three river reference locations. Mainstem reference samples consisted of a seine set that measured 10 m in length and varied slightly in width, averaging five meters, with an average max depth of 1.5 m and minimum depth of 0 m. Because there were four SFC locations and three reference locations, we analyzed the data as an unbalanced design. Year 2014 reference site sample size was 109 while that in 2018 was 130. Year 2014 restoration site sample size was 136 while that in 2018 was 133. Sampling at all monitoring locations was standardized by taking all samples during the morning lower low slack tide, using the same net for each location, and sampling the same surface area each time. During the

dryer portions of the year there were instances within the four SFC restored sub-basins when fewer than six samples were gathered due to lack of water in the channel during low tide.

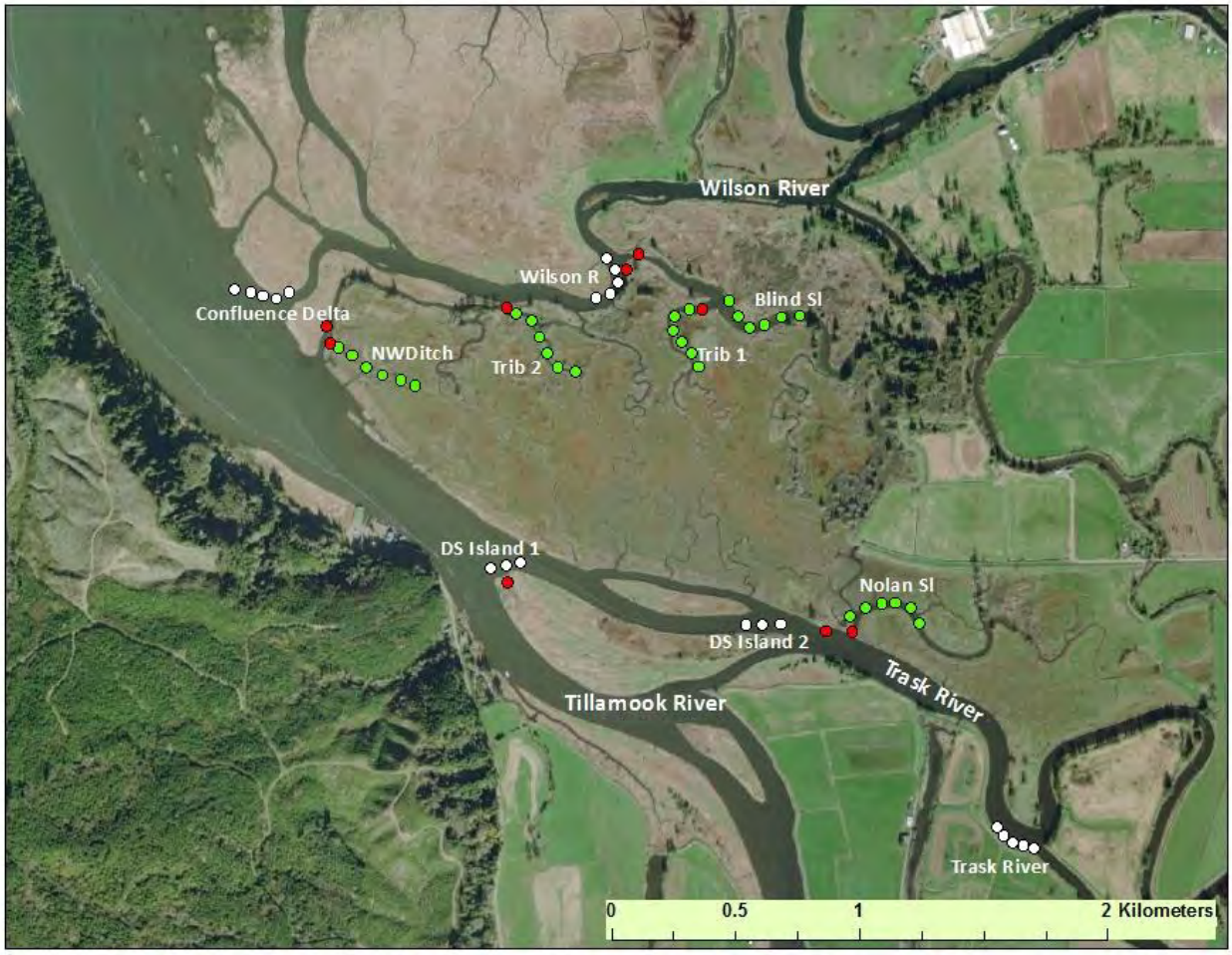

Figure 6.1. Seine and camera (fish migration) sampling sites during pre- and post-restoration. Points represent individual sample sites. Colors are as follows: Green = SFC channel seining, white = river reference seining, red = fish migration.

We used the count data for each species age-class group only during periods when the species was present. This resulted in varying numbers of total samples available for analysis among species age-class groups. Age-1+ cutthroat trout and age-0 and age-1+ starry flounder were not evaluated due to their limited numbers (Table 6.2). We normalized raw counts to produce a capture rate ("CPUE" or count per unit effort), then performed statistical analyses of this metric (referred to as "abundance") as described below. At SFC and reference sampling stations, we combined all locations for each age-class species group rather than examining each of the four restoration sub-basins individually. Although this increased the potential for variation based on habitat characteristics among the four sub-basins, it also increased power within the analysis and provided a more easily understood summary of patterns observed.

To determine if fish species abundances changed at the SFC site following restoration, we used two-way ANOVA consistent with a BACI design. We tested the interaction term (site x sampling period) to identify whether a restoration effect occurred, distinct from any differences in fish abundance due to time (sampling period). For statistical modeling, each species age-class group monthly sample event was considered to be independent and was treated as a replicate. We analyzed abundance (CPUE), but

because the underlying seine data were composed of counts, we used generalized linear models appropriate for count data (i.e., Poisson, Negative Binomial). Initial distributions indicated a high prevalence of zero-counts and overdispersion for all species observed, but at varying degrees. Both zero-hurdle and zero-inflated negative binomial models were considered; however, we could not determine whether a separate underlying process influenced the zero-counts, a requirement for those models (for zero-hurdle, see Mullahy 1986; for zero-inflation, see Lambert 1992). Instead, individual species were modeled using negative binomial distributions, which are known to handle zero-inflation and over-dispersion better than a Poisson distribution, which assumes a dispersion parameter of "1" and a mean that equals the variance (Zeileis et al. 2008).

We fit negative binomial general linear models (GLMs) and conducted type-III ANOVAs to determine whether the interaction effect was statistically significant. For some species age groups, regardless of model type, the overdispersion and zero-inflation were too severe to allow for modeling. In these cases, formal statistical analyses were not used, instead we provide qualitative habitat-based results of species occurrence patterns. Analyses for Prickly Sculpin were not carried out due to inconsistencies in field identification during pre-restoration. No analyses were carried out for age-0 and age-1+ Starry flounder and age-1+ cutthroat trout due to their low numbers (Tables 6.2 and 6.3).

Fish migration patterns. We examined fish migration patterns before (2014) and after (2018) SFC restoration activities including dike and tide gate removal and channel reconstruction. Because age-0 Chinook were present in our 2014 seine samples at much greater numbers than any other salmonid species-age class found at the reference locations, they were designated as the target species for tidal migration evaluations. Age-0 Chinook were present by March, peaked in May, and began to decrease in number during June. Based on this pattern, we chose the months of May and June as migration sampling months. Migration samples were gathered during two consecutive days in both May and June. For comparability, sampling during May and June was timed for the same portion of the monthly tidal cycle so fish experienced the same tide heights and timing of the daily cycle. Our target sample tide cycle began with an early morning lower low followed by a 1.8 m (6 ft) late morning lower high, followed by a late afternoon higher low. Two daily tidal cycles were sampled during each sample month.

SFC tidal migration sampling occurred inside the mouth of four sub-basin channels sampled for fish abundance (Blind Slough, Nolan Slough, Northwest Ditch and Trib 2) (Figure 6.1). Northwest Ditch was used as a sampling site in 2014 but was no longer a viable site in 2018 and was replaced by Trib 2 for post-restoration sampling (Figure 6.1). We determined Trib 2 was appropriate as a post-restoration substitute for Northwest Ditch due to the close proximity of the two sites to one another relative to the reference sites used and its geographic position within the restored marsh. Sampling during the pre-restoration period at tide gate locations occurred approximately 10 m inside the upstream end of the tide gate pipe itself. This resulted in the commonly occurring tide pipe "headwater pool" to be positioned immediately downstream of the camera sampling transect. We monitored fish migration behavior using a "fence" of cameras (sampling transect) positioned perpendicular to the channel (Figure 6.2). Fyke nets were used to narrow channel widths during pre-and post-restoration sampling. Fyke nets were positioned across the more shallow sloped portions of the channel's bed at sample sites. The overall width of the sampling sites during post-restoration was greater due to the channel restoration actions (excavation) and thus resulted in more unsampled habitat when compared to pre-restoration.

We sampled in reference channels along the banks of the Wilson and Trask rivers (Figure 6.1). Reference marsh sub-basin sampling (Dry Stocking Island channel) occurred at the downstream-most point in the channel, where the channel spilled into the mainstem Trask River. Guide nets running from the bank toward the thalweg were used to concentrate and direct migrating fish toward the camera sampling transect (Figure 6.2). Sampling transects consisted of a set of poles (stations) positioned in a line perpendicular to water flow. Each station had four cameras mounted to the pole.

A

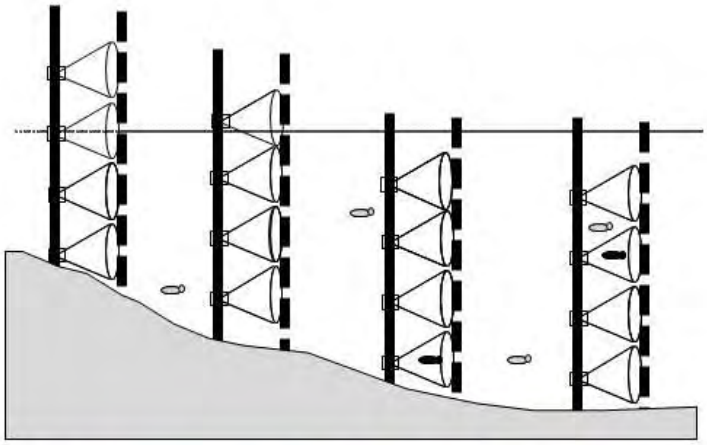

B

C

Figure 6.2. Field sampling of fish movement. (A) Example camera sampling transect showing each station pole and field of depth pole as well as each camera's conical field of view where fish are and are not counted (black versus grey) for migration analysis. (B) Pre-restoration Northwest Ditch tide gate pool sample site. (C) Nolan Slough post-restoration partially fyked channel sample site.

Camera stations at all locations (SFC and reference sites) were placed in a maximum water depth of 0.2 m during the morning lower low tide. Cameras were set at 0.2, 0.5, 0.8, and 1.1 m vertically above

the channel bottom. For the mainstem river reference locations, greater bank slope generally resulted in greater sampling depths. Station number differed during pre- and post-restoration due to the increased width in the restored channels. Camera station number increased from one to three from pre- and post-restoration for Blind and Nolan sloughs. There was no change in station number for Trib 2.

Count data were generated from review of the underwater video (Figure 6.3). All fish were enumerated within a field of view that was 0.04 m^2 with a depth of field of 0.31 m as defined by PVC posts placed in front of each camera station (Figure 6.2). Counts were recorded on a minute-by-minute basis, by species age-class and lumped into 30 minute bins for analysis. Ten percent of the video reviewed by an individual reviewer was "re-read" and validated by two additional reviewers. Counts from sampling periods at each camera were summed over each day across a combination of location type (SFC or reference sites), location, date, station, camera position, and tide direction during the sampling day.

Figure 6.3. Example sampling data gathered using videography. The four views represent different cameras located at different elevations off the channel bed within the same sampling station (pole).

As with fish abundance data, we analyzed site sampling [illegible] by sampling period [illegible] effects on [illegible] with pre- and post-restoration [illegible] impact of marsh restoration on fish movement [illegible] derived from camera data:

1. Net movement, calculated as the difference between all fish swimming upstream and all fish swimming downstream for a camera sample.
2. Maximum use, calculated as the maximum of the net movement for a particular camera sample.
3. Total movement, calculated as the sum of the absolute value of fish moving upstream and the absolute value of fish moving downstream for a camera sample.

The first metric, *net movement*, is used to describe the net number of fish moving in a unidirectional manner upstream or downstream within the SFC channels or along the river's bank. *Net movement* is calculated by subtracting all fish swimming downstream from all fish swimming upstream. Below we provide net movement data from an Oregon Estuarine monitoring site (Figure 6.4). The chart shows a dominant unidirectional migration during the full sampling period resulting in a net movement of (+) 190 (final cumulative count). In this example downstream migration occurs during the observation period but sums to less than the upstream migration at the end of the sampling period.

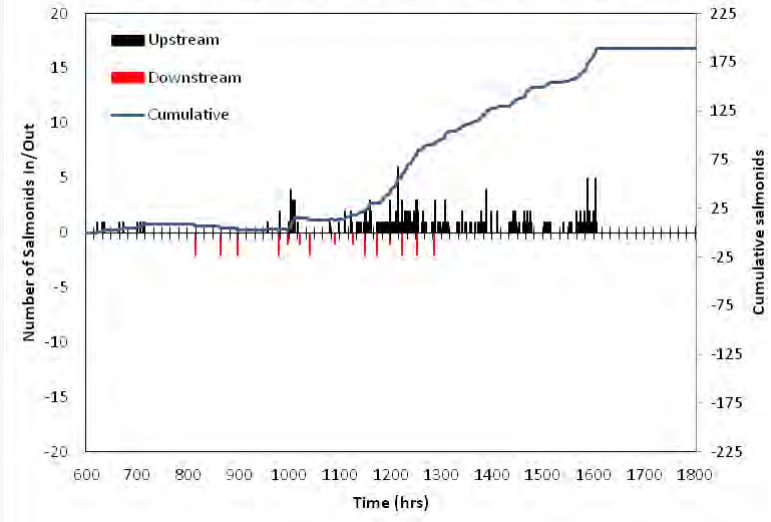

Figure 6.4. Example data (Coquille Estuary 2013) showing a fish migration pattern wherein the *net movement* is a positive number (describing the upstream migration).

The second metric, *maximum movement*, is different in that is assists us in understanding whether fish are utilizing key habitats near the sampling location and moving in a bidirectional manner upstream or downstream between those key habitats. We provide an example of this below in Figure 6.5. In our example the majority of fish are migrating downstream during the period of 0600 hrs to 0930 hrs. This morning migration results in a cumulative value that is (-) 85 at time 1000 hrs. During the period of 1000 hrs to 1600 hrs the cumulative line moves to a value of (+) 10. The *net movement* estimate is (+) 10 and does not represent the extent of fish use in those habitats near the sampling location because it does not capture the large group of fish that moved both downstream and upstream across the full sampling period. The *maximum movement* metric captures this pattern of habitat use.

The third metric, *total movement*, assists us with understanding how many of the observed fish are utilizing only that habitat that immediately surrounds the sampling cameras – the few feet upstream and downstream of the camera sampling transect. Fish that hold in one area throughout a tidal cycle typically move a short distance (one meter) upstream and downstream to capture prey items. This feeding foray behavior results in high upstream and downstream counts that are uniform across time opposed to continuous or pulse unidirectional counts (Figure 6.5). An estimate of net movement when fish are expressing this local feeding foray behavior would result in a low number suggesting limited fish use occurred – upstream and downstream counts would cancel one another. We provide an example of this below in Figure 6.6. In our example the majority of fish are migrating upstream and downstream in a continuous manner during the period of 1000 hrs to 1600 hrs. This migration results in a net movement (cumulative value) of (+) 5 at time 1800 hrs. The net movement estimate of (+) 5 does not represent the extent of fish use in those habitats because it does not capture the large number of fish that remained near the sampling transect carrying out local feeding forays. The *total movement* metric captures this pattern of habitat use.

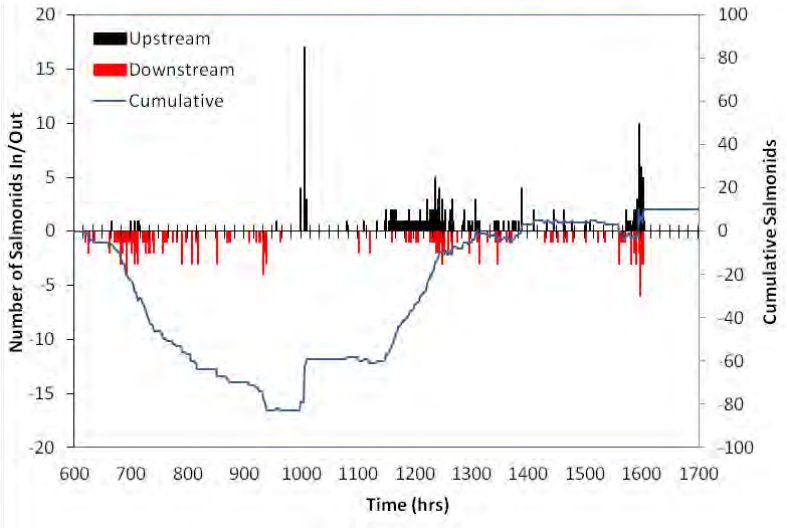

Figure 6.5. Example data (Coquille Estuary 2013) showing a fish migration pattern wherein the *net movement* is (+) 10 (final value for cumulative line) but the *maximum movement* value is 95 (the difference between the lowest (-85) and highest (+10) point on cumulative line).

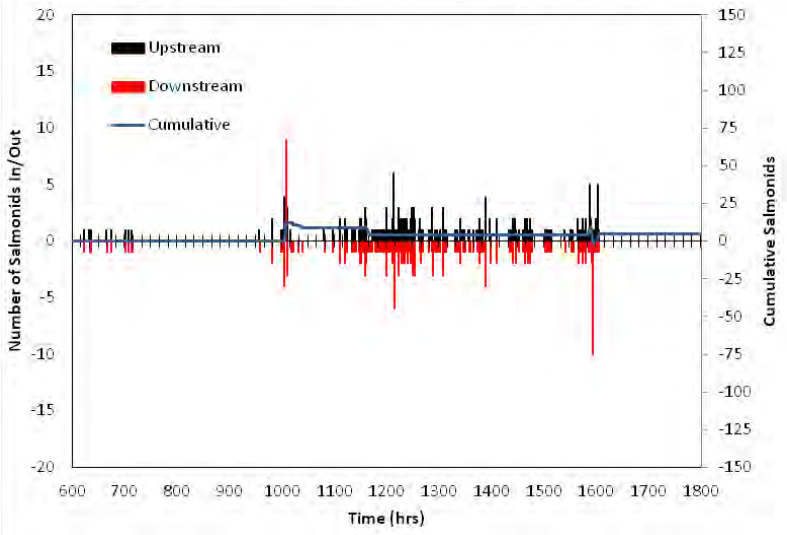

Figure 6.6. Example data (Coquille estuary 2013) showing a fish migration pattern wherein the *net movement* was (+) 5 (final value for cumulative line) but the *total movement* value was 419 (absolute value of all in and out migration counts).

We sampled three locations at SFC: Blind Slough, Nolan Slough, and Northwest Ditch 2014 /Trib 2 2018. Two of the four original reference sites monitored (2014) were utilized for the present analysis: mainstem Wilson River at Blind Slough and mainstem Trask River at Nolan Slough. The first reference site dropped from the analysis was located on the Wilson River close to the Trib 2 and Northwest Ditch sites. After careful consideration, it was excluded due to habitat differences between the two larger river sites, which could result in different levels of fish usage, confounding interpretation of analyses. The second reference site dropped from the main analysis was Dry Stocking Island because it was a small high marsh channel habitat with less tidal exchange and therefore migration patterns were expected to be strongly different. Despite these concerns, we did run models including these sites, and achieved a similar conclusion to the model results that excluded these sites.

We considered four species groups for analysis of tidal migration: salmonids (*Oncorhynchus* spp.), three-spine stickleback (*Gasterosteus aculeatus*), shiner perch (*Cymatogaster aggregata*), and cottids (staghorn sculpin, (*Leptocottus armatus)* and prickly sculpin, (*Cottus asper*). Video reviewing efficacy was at times reduced by reduced visibility and influenced the video reviewers' ability to differentiate individual species characteristics (for instance pattern of parr marks), so salmonid and cottid species could not be reliably identified to the species level. Thus, these taxa were grouped at the family level for analysis. Many more individuals were enumerated during the video review process than what we used for our analysis: Our count method for the analysis utilizes a depth of field measurement of 0.31 m but fish passing at distances greater than 0.31 m from the cameras can be viewed and are counted separately (Table 6.1). The efficiency of these additional count groups varies with tidal conditions and is why we exclude those counts from our formal analyses. A total of 96,784 fish were counted across the pre- and post-restoration period with 68,075 (70%) being used in our analysis (Table 6.1).

Table 6.1. Total fish counted (video analysis) during the pre- and post-restoration migration sampling periods for within and beyond the count zone, as well as those fish determined to be milling and not migrating through the sampling cells.

	Within count zone	Beyond count zone	Milling	**Total**
Salmonid	13,182	3,591	2,197	**18,970**
Three-spine stickleback	47,012	4,758	3,923	**55,693**
Shiner perch	4,381	9,344	1,130	**14,855**
Cottids	1,672	302	603	**2,577**
Unknown	1,828	2,503	358	**4,689**
Total	**68,075**	**20,498**	**8,211**	**96,784**

The effects of site, sampling period, and their interaction on the three fish movement variables was determined using linear models and Type-III 2-way ANOVAs. For each species and movement metric, a linear model was produced and model fits were assessed using standard diagnostic plot and normality test procedures. When species-metric residual distributions did not meet standard assumptions of normality, data transformation was investigated. If the transformed data did not violate ANOVA assumptions, linear models were run. In the event the transformation did not improve normality and heteroscedasticity, raw non-transformed data were used in the models. Only those fish observed within the 0.04 m^2 habitat sample cells were used for analyses while those observed outside this field of view were not. Model output represents mean fish migration for those habitat cells sampled and does not represent total site abundance estimates for the metrics modeled. Because camera station number differed across the two years we used an unbalanced design for our analysis.

Results and discussion

Low tide fish distribution and abundance. We observed several species across the late winter through late summer sampling period. Monthly data (raw counts, Tables 6.2 and 6.3) suggested several of those species had periods of peak use of tidal channels at SFC. Age-0 chinook were present in all months sampled (March through August). Chum (age-0) and coho were present in March, April and May, with age-0 coho use extending into June. Pacific staghorn sculpin and three-spined stickleback were present during all months sampled. Prickly sculpin were present in April through August. Age-0 and age-1 shiner perch were present in July and August. Cutthroat numbers were too low to determine the peak months of use.

Table 6.2. Raw (unstandardized) sample counts by species age-class and month in reference site samples.

	Age-0 Chinook		Age-0 Coho		Age-1+ Coho		Age-0 Chum		Age-1 Cutthroat	
	2014	2018	2014	2018	2014	2018	2014	2018	2014	2018
Mar	0	16	13					69	2	
Apr	51	49	66	476	33		78	485		
May	616	173	30		57	36		7		
June	222	140	1	1					2	3
July	166	28							5	
Aug	90	18								2

	Pacific Staghorn Sculpin		Prickly Sculpin		Three-Spined Stickleback		Age-0 Shiner Perch		Age-1+ Shiner Perch		Age-0 Starry Flounder		Age-1+ Starry Flounder	
	2014	2018	2014	2018	2014	2018	2014	2018	2014	2018	2014	2018	2014	2018
Mar	29	112			6	5					3		4	6
Apr	50	129		1	67	17					4		14	8
May	538	973		3	25	25						17	3	2
June	123	658		37	83	24		1		72	10	33	4	3
July	193	525		24	39	7	108	1612	193	536	6	23	10	1
Aug	88	297	33	12	1	1	344		30		37		2	

Table 6.3. Raw (unstandardized) sample counts by species age-class and month in SFC site samples.

	Age-0 Chinook		Age-0 Coho		Age-1+ Coho		Age-0 Chum		Age-1+ Cutthroat	
	2014	2018	2014	2018	2014	2018	2014	2018	2014	2018
Mar	2	124	1	24	131	1		620		
Apr	1	70	97	821	231	13		2190		
May	0	590	244		4	59		14		
June	0	71	160	10						
July	0	24								2
Aug	0	8				1				3

	Pacific Staghorn Sculpin		Prickly Sculpin		Three-Spined Stickleback		Age-0 Shiner Perch		Age-1+ Shiner Perch		Age-0 Starry Flounder		Age-1+ Starry Flounder	
	2014	2018	2014	2018	2014	2018	2014	2018	2014	2018	2014	2018	2014	2018
Mar	7	34		2	535	32								2
Apr	592	49		9	765	410								1
May	11	766		123	2974	6325								7
June	2	1123		250	3266	6893		8	1	142		7		
July	5	937	21	361	8056	647		445		251		2		2
Aug	3	931	16	191	3375	234								

We analyzed age-0 chinook abundance for the period of March through August. In SFC channels, Age-0 chinook abundance was relatively low (many zero counts occurred) during the pre-restoration

period, but abundance increased about six-fold during the post-restoration period, reaching about double that of river reference locations during the same year (Figure 6.7). At the reference locations, age-0 chinook abundance was higher and more variable during the pre-restoration sampling period than during the post-restoration period. The negative binomial model resulted in a significant interaction term (site and sampling period) ($\chi^2 = 185.37$, df = 1, $P < 0.001$), indicating the increase in abundance at SFC was likely due to the restoration.

Age-0 chum abundance was analyzed for March and April due to the large number of zero count samples in May. Negative binomial modeling failed due to the low sample size (two sampling months) and large number of zero counts. In SFC channels, chum increased from zero during pre-restoration to the second-highest abundance for any fish species observed at SFC post-restoration (Figure 6.7). By contrast, chum abundance at reference locations was relatively unchanged from pre- to post-restoration sampling. Post-restoration chum abundance at SFC was about six times that of the reference locations. There was clearly a restoration effect for age-0 chum salmon, even though our model could not be used to demonstrate it.

Age-0 coho abundance was analyzed for the period of March through June. Age-0 coho abundance increased from the pre- to post-restoration sampling period in both the reference and SFC channels (Figure 6.7). There was no significant interaction between site and sampling period in the negative binomial model ($\chi^2 = 1.54$, df = 1, $P = 0.21$); thus, our model did not demonstrate an effect of restoration on age-0 coho abundance.

Age-1+ coho abundance was analyzed for the period of March, April and May. Age-1+ coho counts decreased during the post-restoration period for both the reference and SFC channels (Figure 6.7). The variance associated with both the reference and SFC channels was high during the pre-restoration period and reduced during the post-restoration (Figure 6.7). The negative binomial model interaction term (site and sampling period) was non-significant ($\chi^2 = 0.0089$, df = 1, $P = 0.92$); thus, our model did not demonstrate an effect of restoration on age-1+ coho abundance.

Staghorn sculpin (all ages lumped) abundance was analyzed for the period of March through August. Staghorn sculpin abundance increased in both reference and SFC channels during the post-restoration period (Figure 6.7). There was a significant interaction between sampling period and site, with a greater increase in abundance for the SFC channels ($\chi^2 = 9.72$, df = 1, $P < 0.01$); this suggests the increase was due to the restoration.

Three-spined stickleback (all ages lumped) abundance was analyzed for the period of March through August. Three-spined stickleback abundance was low in reference channels and several times higher in the SFC channels during both pre- and post-restoration sampling (Figure 6.7). Abundance dropped in the SFC channels during the post-restoration period. The negative binomial model resulted in a significant interaction term (site and sampling period) ($\chi^2 = 8.55$, df = 1, $P < 0.05$), suggesting the decrease in abundance at SFC was the effect of the restoration.

Age-0 shiner perch were analyzed for the period of June and July. Age-0 shiner perch abundance in reference and SFC channels was relatively low during the pre-restoration sampling period and increased at both restoration and reference locations during the post-restoration sampling period (Figure 6.7). Abundance increased more in the reference channels compared to the SFC channels following restoration. Use of a statistical model to determine an interaction term between restoration and period failed due to small sample sizes and a larger number of zero counts.

Age-1+ shiner perch were analyzed for the period of June and July. As with the age-0 year class, age-1+ shiner perch counts increased from the pre-to post-restoration period at both SFC and reference locations (Figure 6.7). Counts in the reference channels increased at a rate similar to those observed in the restoration channels during post-restoration. Use of a statistical model to determine an interaction term between restoration and period failed due to small sample sizes and a large number of zero counts.

Our models suggest that restoration at SFC led to a statistically significant increase in the abundance of age-0 chinook, age-0 chum, and staghorn sculpin and a decrease in three-spined stickleback.

The abundance of coho and other fish species did not appear to change substantially at SFC due to restoration activities. Our ability to detect an effect from restoration using statistical models was in large part dependent upon the seasonal distribution of each species, which is driven by their life histories. Species that use lower riverine and upper estuarine habitats for limited periods of time create challenges for sampling design and sample intensity; it can be difficult to achieve sample sizes large enough to detect change despite variability. Species that have a greater temporal and spatial distribution allow for an improved analysis due to reduced zero counts and reduced count variability. The lower variance in the age-0 chinook, age-0 chum, three-spined stickleback and staghorn sculpin counts demonstrates their greater temporal distribution and more even spatial distribution across the SFC restored channels. The significant site-by-sampling period interactions for some of these same species suggests a strong preference for the SFC restored channels as rearing habitat.

Chinook salmon contribute substantially to the Pacific Northwest coastal economy (Radke 1996, Swedeen et al. 2019). The states of Alaska, Washington, Oregon, California, and Idaho take part in joint harvest planning and regulations through the Pacific States Marine Fisheries Commission, with a goal of ensuring this species is available for harvest across its full range. The North Pacific Fisheries Commission consults with the Pacific States Marine Fisheries Commission regarding habitat and harvest. Awareness of the importance of Pacific Northwest estuarine habitat to salmonid life history, survival, and resilience has risen greatly in recent years, but for decades, these organizations suffered from a lack of recognition of the role of estuaries (Bottom et al. 2005). Our results demonstrate the large SFC site has already restored a significant amount of preferred chinook and chum habitat previously lost during the early expansion of settlement in the Tillamook Estuary.

The increase in age-0 coho at the reference and SFC locations during post-restoration was likely due to increased spawning and rearing numbers in the river systems of the Tillamook Bay watershed (Oregon Department of Fish and Wildlife 2021). When comparing abundance for reference versus restoration channels, age-0 coho were approximately five-fold greater in SFC channels during the pre-restoration monitoring period and only two-fold greater during post-restoration (Figure 6.7). The variability in age-0 coho catch per unit effort increased during the post-restoration period for both the reference and restoration channels (Figure 6.7).

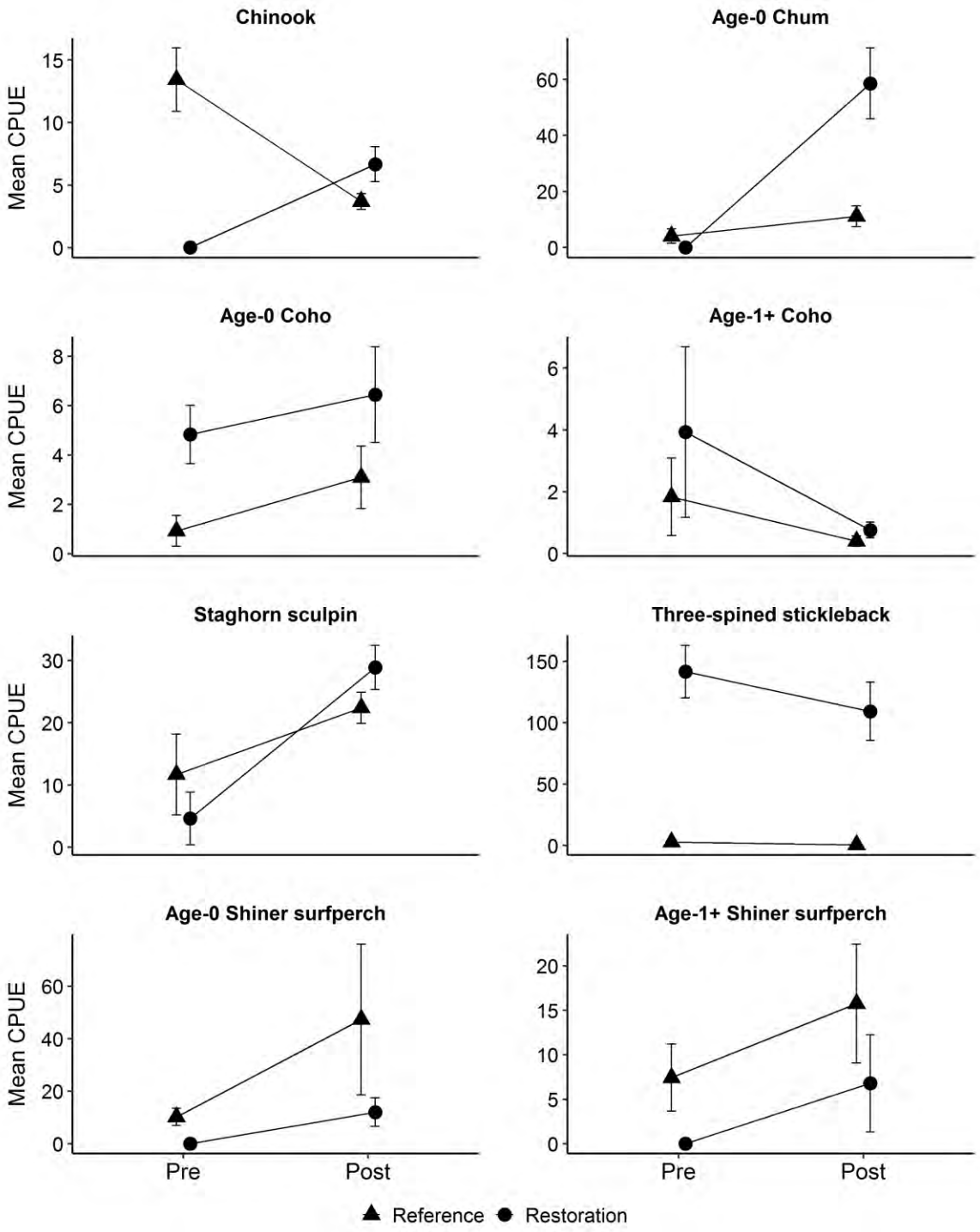

Figure 6.7. Mean abundance (CPUE or count per unit effort) for those species observed at reference and restoration (SFC) sites during 2014 pre-restoration (Pre) and 2018 post-restoration (Post) periods (means ± SE).

Our past experience when working with age-0 coho in Oregon estuaries is that this species age-class prefers low-velocity low- salinity habitat when available within a broader suite of estuarine habitats. Miller and Sadro (2003) found a common age-0 coho seasonal migration pattern in South Slough, Oregon, with fish migrating downstream into the cool, low-salinity mid-estuary habitats during the early spring season followed by an upstream migration back to cool, fresh or low-salinity tributary habitats as the low

flow summer season arrived. Jones et al. (2014) also recognized the importance of these habitats to age-0 coho in the Salmon River, Oregon. A few examples of low-velocity, low-salinity habitats are beaver dam ponds associated with a freshwater source near head-of-tide within a marsh; habitat behind failed tide gates associated with small (less than 4th order) freshwater sub-basins; and the more modern muted tidal regulator gates that allow some (limited) juvenile fish ingress and egress but result in less tidal exchange and thus lower average tidal velocities. Older existing failing tide gates and newer muted tidal regulator gates can allow for limited passage (within a given tide), but this limited passage is consistent (month to month) during the winter and spring storm season. The use of these gated habitats by age-0 coho is typically limited to the cool wet season due to the reduced water availability and increase in water temperature during the dry season.

High flow events associated with winter storms often result in age-0 coho being 'flushed' out of freshwater streams located higher in the stream network and nearer to spawning habitats. The low-gradient, low-velocity, limited tidal exchange habitat preference expressed by age-0 coho in least-disturbed and disturbed tidal habitats can result in highly variable abundance because the preferred habitat is not uniformly distributed across the landscape (Brophy et al. 2014, van de Wetering et al. 2009, van de Wetering and French 2008). Pools associated with failing tide gates and dredged ditches can provide adequate habitat in disturbed tidal marshes while beaver dam pools can provide habitat in least disturbed tidal marshes. When assessing fish use at SFC we tested for changes in those habitats within the diked landscape and positioned within the hydrologic influence of the failing tide gates. For this reason our seine sampling design was cost-effective and efficient for several species, but challenging for juvenile coho salmon.

Despite the failure of our models to detect a restoration effect on coho abundance, we believe age-0 coho abundance at the SFC site has increased during post-restoration and that the site is now providing preferred coho rearing habitat. To demonstrate this within the present study, we would have had to increase sample size by two or three-fold and broaden the geographic area to include a much greater percentage of the pre-restoration SFC site. Much of that geographic area could not be sampled during the pre-restoration period due to many historic channels being dry and many currently restored channels not yet created (excavated). In addition, costs would have been much greater. With completion of the SFC project, three separate rivers now feed the SFC restored channel system in a more direct manner (Figure 6.1). The complex network of marsh channels restored within the SFC site has resulted in many distributary channels connecting multiple low elevation sub-basins containing preferred age-0 coho habitat in their upper reaches (see Figure 1.2). Additional presence/absence data from this inner network area, when considered alongside our abundance counts for the outer network sites, suggests the SFC project has increased age-0 coho rearing capacity within the broader Tillamook Basin.

Tidal migration patterns. First we present the summarized counts without taking into consideration the extent of variability within each sample day and across sample days and months: It is important to note that migration patterns can be highly variable and thus acquiring multiple samples (sites and sample days) improves the error around the estimate. The summarized results for maximum use (peak migration count) show a pattern of reduced migration for juvenile salmonids, three-spined stickleback and cottids for both restoration and reference sites during post-restoration (Table 6.4). The pattern for shiner perch is similar for the two periods (Table 6.4).

Table 6.4. Summed counts (all sites and all days) for the *maximum movement* metric for different species groups assessed. Restoration (SFC) sample locations are Blind Sl and Nolan Sl; reference sample locations are Wilson R, DSI and Trask R.

Species	Pre-restoration	Post-restoration
Age-0 Salmonids		
Blind Sl	1873	161
Nolan Sl	212	109
Wilson R	360	95
DSI	29	66
Trask R	235	91
Three-spine stickleback: all ages		
Blind Sl	5112	183
Nolan Sl	5557	376
Wilson R	969	673
DSI	21	15
Trask R	821	383
Cottids: all ages		
Blind Sl	52	21
Nolan Sl	4	1
Wilson R	5	0
DSI	513	227
Trask R	21	0
Shiner perch: all ages		
Blind Sl	30	100
Nolan Sl	2	269
WIlson R	5	13
DSI	87	90
Trask R	97	72
All Combined		
Blind Sl	7067	465
Nolan Sl	5775	755
Wilson R	1339	781
DSI	650	398
Trask R	1174	546

Maximum use movement. Mean maximum use counts decreased following restoration at SFC for both juvenile salmonids and three-spined stickleback (Figure 6.8). Counts at reference sites remained the same for salmonids and increased slightly for three-spine stickleback for the post-restoration sampling period (Figure 6.8). A significant site-by-sampling period interaction was observed for both salmonid ($F = 9.42$, $df = 1$, $P < 0.01$) and three-spined stickleback ($F = 23.00$, $df = 1$, $P < 0.001$) maximum movement, indicating that restoration activities led to decreased maximum fish movement at SFC.

Both the shiner surfperch and cottid mean maximum use differed very little between restoration-period groups and was close to zero (Figure 6.8). A high prevalence of zeros and high variability among non-zero counts resulted in violations of standard ANOVA modeling assumptions. For these reasons we only describe the above qualitative patterns in the data.

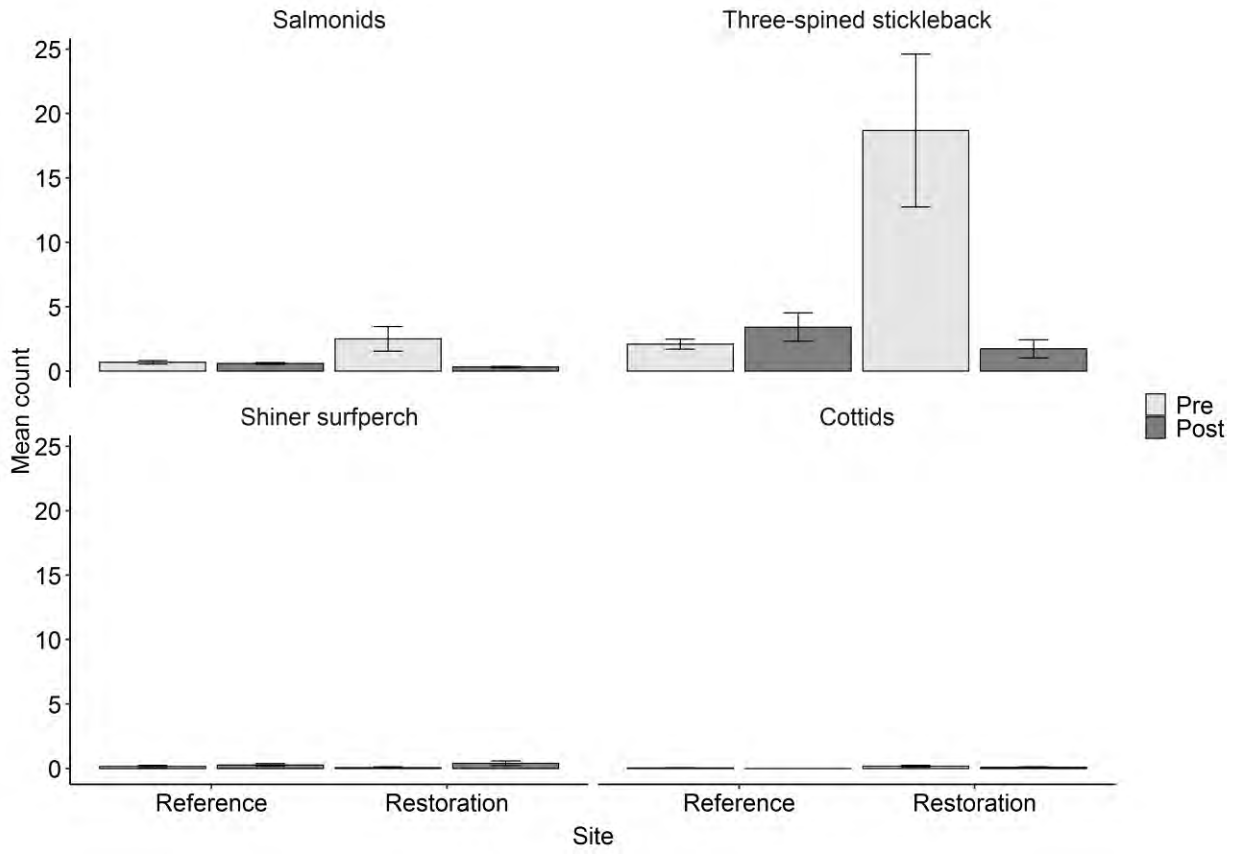

Figure 6.8. Modeled mean maximum movement count per habitat cell for salmonids, three-spined stickleback, shiner surfperch, and cottids in reference and restored tidal channels during pre- and post-restoration sampling periods. Negative values indicate movement out of channels.

Total Movement. Mean total movement counts decreased following restoration for both juvenile salmonids and three-spined stickleback (Figure 6.9). Total movement in the reference sites remained similar for salmonids and increased slightly for three-spine stickleback in the post-restoration sampling period. There was a significant interaction between site and sampling period for total movement for juvenile salmonids ($F = 5.48$, $df = 1$, $P < 0.050$) and three-spine stickleback ($F = 31.90$, $df = 1$, $P < 0.001$) indicating the number of fish that held in the area of the channel mouths during pre-restoration period had been reduced.

Both the shiner surfperch and cottid mean total movement differed very little between restoration-period groups and was close to zero (Figure 6.9). A high prevalence of zeros and high variability among non-zero counts resulted in violations of standard ANOVA modeling assumptions. For these reasons we only describe the above qualitative patterns in the data.

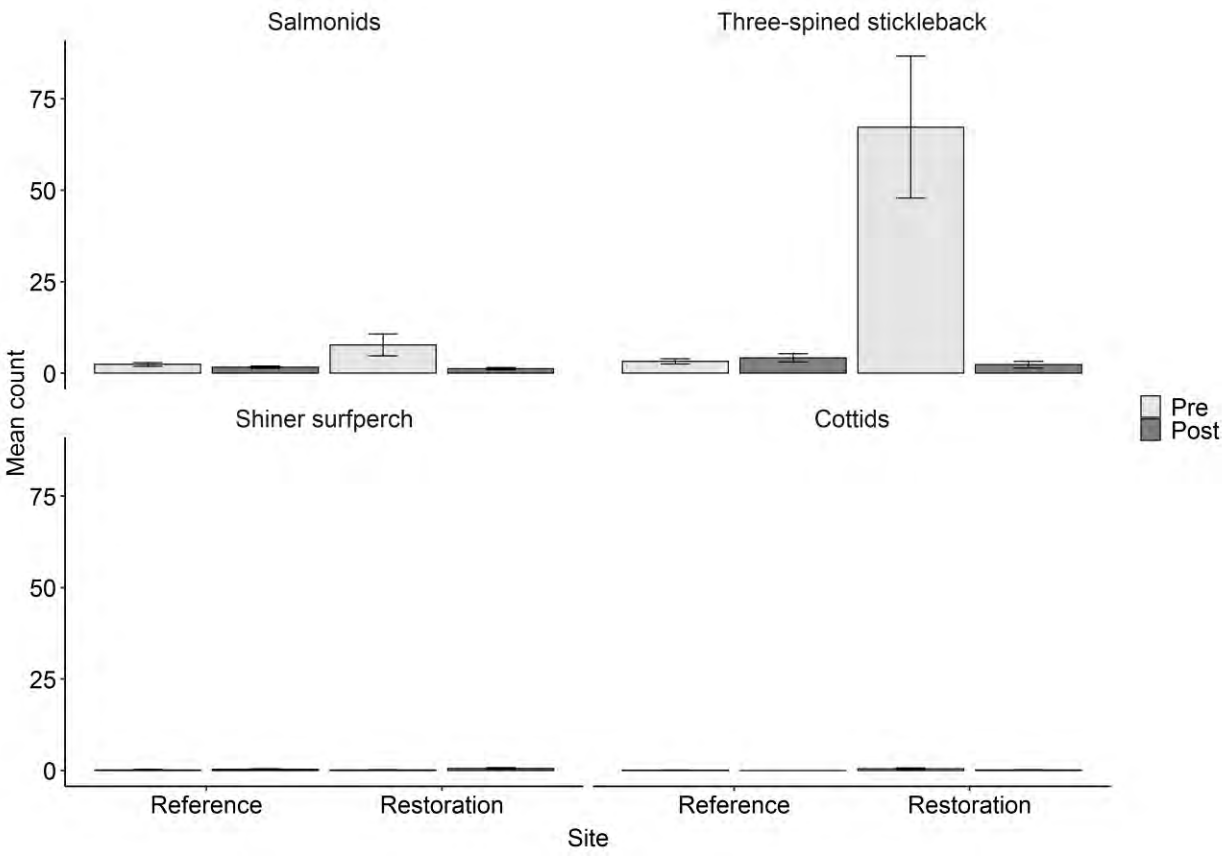

Figure 6.9. Modeled mean total movement count per habitat cell for salmonids, three-spined stickleback, shiner surfperch, and cottids in reference and restored tidal channels during pre- and post-restoration sampling periods. Negative values indicate movement out of channels.

Net movement. We analyzed mean net movement of salmonids with a weighted simple linear model using the raw data. Mean salmonid net movement differed little between reference and SFC channels with all but one value being positive (Figure 6.10), suggesting small numbers of salmonids entered and exited the SFC channels during the tidal cycles we monitored during both sampling periods. The interaction between site and sampling period was not significant ($F = 0.12$, $df = 1$, $P = 0.73$) due to the low magnitude of the differences observed in salmonid net movement means.

Mean net movement for three-spined stickleback was analyzed with a weighted simple linear model using the raw data. Pre-restoration stickleback net movement at SFC sites was negative (out of restored site channels), but highly variable. Following restoration, net stickleback movement was positive at SFC, but very close to zero (Figure 6.10). Reference sites showed a minor increase in upstream migration from post-restoration to pre-restoration periods, but less than at SFC sites. Despite this, there was no significant interaction between site and sampling period, likely due to the amount of variability observed in the pre-restoration SFC mean net movement ($F = 0.48$, $df = 1$, $P = 0.49$).

Both the shiner surfperch and cottid mean net movement differed very little between restoration-period groups and was close to zero (Figure 6.10). We attempted a mean net movement analysis for shiner surfperch and cottids using a weighted simple linear model. A high prevalence of zeros and high variability among non-zero counts resulted in violations of standard ANOVA modeling assumptions. For these reasons we only describe the above qualitative patterns in the data.

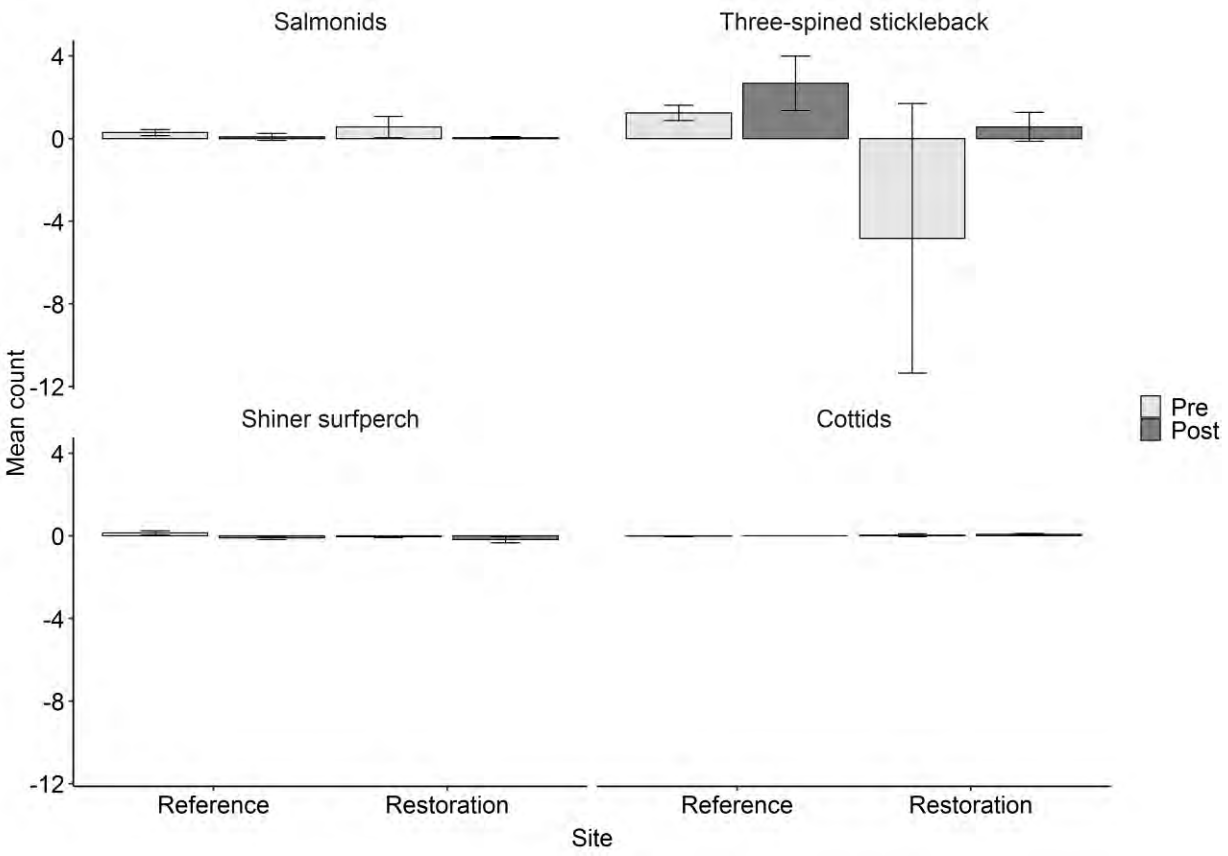

Figure 6.10. Modeled mean net movement count per habitat cell for salmonids, three-spined stickleback, shiner surfperch, and cottids in reference and restored tidal channels during pre- and post-restoration sampling periods. Negative values indicate movement out of channels.

Juvenile salmonid behavior observed in the Wilson and Trask rivers highlighted the absence of consistent larger migration patterns upstream or downstream during either the flood or ebb tide (Figures 6.8-6.10). We suggest this is because tidal velocities in these reaches are limited and the energy required to retain a position within in a given habitat cell is limited, and because fish density is low and prey-resources are readily available reducing the need for competitive behaviors such as searching out new habitats for additional food resources. Our video reviewers noted slower swimming speeds and extensive feeding behavior during review of the Wilson and Trask river migration data when compared to mainstem river habitats we have monitored in other estuaries (Brophy et al. 2013, van de Wetering et al. 2009, van de Wetering and French 2008). The results for two of the three migration metrics showed significant decreases in salmonid movement from pre- to post-restoration sampling. Because age-0 coho but no age-0 chinook were present in the SFC site during pre-restoration and the restoration resulted in elimination of the SFC channel mouth preferred habitat (low velocity with limited tidal exchange), we suggest the reduced salmonid migration was a result of 1) age-0 coho using slow water habitats more internally within the SFC site; 2) generally lower age-0 chinook densities throughout the three river confluence area during post-restoration so fewer fish were available to migrate; and 3) because the majority of the migrants sampled were age-0 chinook, the behavior they exhibited within the river reference habitats was repeated within the SFC channels, i.e. limited movement.

Three-spined stickleback behavior observed in the Wilson and Trask rivers demonstrated a tendency for this species to move in an upriver direction across the full daytime tidal cycle (Figure 6.8 and 6.10). This species' behavior was similar when observed within the SFC site. Maximum movement was

positive, therefore demonstrating a peak in migration occurred with movement into the channel at some point during the full tidal cycle. Total movement was high relative to the other species demonstrating fish moved both up-channel and down-channel during sampling. Net movement was negative, but the error for the estimate was high suggesting the true mean could have been nearer to zero. Taken together, these three metrics allow us to understand how this species moved from the tide-gate pool up-channel into the pre-restoration habitat and returned to the tide-gate pool by the completion of the tidal cycles sampled. The observations for the reference sites during post-restoration show either a slight increase or a similar value to that observed during pre-restoration. Observations at SFC for the three metrics during post-restoration suggest reduced migration and thus a reduced use of the restored habitat by this species, resulting in a large shift in the tidal channel community.

In Oregon tidal wetlands we have observed the influence of local habitat characteristics on finfish migration behavior during tidal cycles in a few common ways (Brophy et al. 2013, van de Wetering et al. 2009, van de Wetering and French 2008). Important factors include local peak flow velocities during the rising and falling tides, and water depths during the lower and higher low tides within the daily cycle. We have concluded higher velocities can result in increases in migration both into (against) the tidal current as well as with the tidal current. We commonly observe fish drifting with the flooding or ebbing tidal current during peak velocity periods resulting in migration into or out of channels. This has occurred where habitat volume is being increased or decreased, as the tide floods and ebbs, respectively. Lower or limited tidal velocities have been shown to result in lower migration rates regardless of the migration direction. At some sites we have observed fish feeding on drifting prey items as they migrate into the slower current of an ebbing tide flowing out of a marsh channel network. We have also observed migration into slower tidal currents when fish are moving out of a marsh channel network and into a mainstem river after holding within the marsh during the prior low tide period. Additional habitat characteristics that influence fish migration behavior include the presence of low tide refugia. We define low tide refugia as pool or glide habitat that is greater than or equal to 0.31 m in depth at low tide. In past studies we have observed more limited migration out of the marsh channel network and into mainstem river habitats when this condition is met (Brophy et al. 2013, van de Wetering et al. 2009, van de Wetering and French 2008).

Although the above summary describes a widely varying set of migration patterns, our observations have suggested habitat type (marsh channel network and adjacent mainstem river) and quality are directly associated with the patterns observed. The three metrics we use to evaluate tidal migration patterns allow us to better assess the finfish community's response to the available habitat. In past studies (Brophy et al. 2014) we have used the three migration metrics together with abundance data to provide an overall picture of fish habitat use patterns. For instance, when large numbers of fish were present (a high value for total movement) but the net movement and net maximum movement were limited, we concluded there was a consistent group of fish present within the camera station habitat unit (i.e., pool, riffle, glide, etc.) itself and those fish moved (feeding and schooling) throughout that habitat area across the full tidal cycle. Conversely, when both net and maximum use counts were high at the end of the tidal cycle, we concluded there was an overall migration farther into the full channel network throughout the flood tide with fish remaining inside the channel network, beyond the sampling transect habitat unit, at the end of the tidal cycle – i.e. they remained in the tidal marsh habitat during the low tide period. These results have then been supported by higher counts observed during low tide seine sampling for abundance. Low tide residence is more common when adequate pool depths are available within the tidal wetland habitat and or when the low tide remains at a higher level (> 0.31m) overall (van de Wetering, unpublished data, Coquille, Siuslaw, Alsea, Yaquina, Siletz, and Nestucca estuaries, 2000-2020).

The SFC site presents a set of conditions that is different from those we have observed in past projects. Three rivers form a confluence adjacent to the SFC site. Substrates in these mainstem rivers are composed of larger grain sizes than the smaller channels internal to the SFC wetlands. Moreover, temperature and salinity patterns at SFC in the southern portion of the Tillamook Estuary are somewhat different from other Oregon estuaries that we have monitored during prior projects. The broad shallow

habitat results in a stronger mixing of saline and fresh waters resulting in a more limited salt wedge adjacent to the SFC channel network earlier in the spring season (Brophy et al. 2013, van de Wetering et al. 2009, van de Wetering and French. 2008). Finally, tidal velocities are lower in the mainstem river habitats that feed the SFC tidal marshes when compared to those we have observed in the Coquille, Little Nestucca, Siletz, and Alsea rivers (unpublished data). Salmon spawning habitats occur relatively close to the SFC site when compared to many other sites we have studied in Oregon. For this reason, newly emerged fry occur each year in the mainstem river habitats adjacent to the SFC site. These young of the year are commonly found in lower velocities and shallow (< 2 ft) habitats compared to juveniles that have been rearing in the system for several months.

We suggest the increase in juvenile Chinook and chum abundance observed in the seine sampling at SFC, taken together with the tidal migration and channel morphology results, indicates that the SFC restoration has already resulted in the creation of preferred juvenile salmonid rearing habitat. We also suggest the low velocity failing tide gate pool habitat used by coho during pre-restoration has been effectively replaced by a much greater volume of low velocity preferred habitat located across the upper portions of all the restored SFC sub-basins (Figure 6.3). We expect SFC to provide an ever-increasing volume of rearing habitat and thus carrying capacity for various native species as the restoration process continues during the next several decades. We suggest that continued morphological evolution of the restored channel network will continue to allow for increased fish use over time, and that rates of use will continue to increase due to greater habitat availability. Improved juvenile fish food resource availability will also occur as channel sediment scouring is reduced and benthic macroinvertebrate habitat is improved (see Chapter 7).

Citations

Bottom DL, Simenstad CA, Burke J, Baptista AM, Jay DA, Jones KK, Casillas E, Schiewe MH. 2005. Salmon at River's End: the Role of the Estuary in the Decline and Recovery of Columbia River salmon. U.S. Dept. Commerce, NOAA Technical Memo. NMFS-NWFSC-68.

Brophy LS, van de Wetering S, Ewald MJ, Brown LA, Janousek CN. 2014. Ni-les'tun Tidal Wetland Restoration Effectiveness Monitoring: Year 2 Post-restoration. Estuary Technical Group. Institute for Applied Ecology, Corvallis, OR.

Greene C, Beamer EM. 2012. Monitoring Population Responses to Estuary Restoration by Skagit River Chinook salmon. NOAA Annual Report. Fish Ecology Division, Northwest Fisheries Science Center, East Seattle, WA.

Jones KK, Cornwell TJ, Bottom DL, Campbell LA, Stein S. 2014. The Contribution of Estuary-Resident Life Histories to the Return of Adult Oncorhynchus kisutch. Journal of Fish Biology 85:52-80.

Lambert D. 1992. Zero-Inflated Poisson regression, with an Application to Defects in Manufacturing. Technometrics 34:1-4.

Miller BA, Sadro S. 2003. Residence Time and Seasonal Movements of Juvenile Coho Salmon in the Ecotone and Lower Estuary of Winchester Creek, South Slough, Oregon. Transactions of the American Fisheries Society 132:546–559.

Mullahy J. 1986. Specification and Testing of Some Modified Count Data Models. Journal of Econometrics 33:341-65.

Oregon Department of Fish and Wildlife. 2021. Adult Salmonid Inventory and Sampling Project.

Radtke H, Davis SW. 1996. The Cost of Doing Nothing: the Economic Burden of Salmon Declines in the Columbia River Basin. The Institute for Fisheries Resources, Northwest Regional Office. Eugene, OR.

Swedeen P, Batker D, Radtke H, Boumans R, Willer C. 2019. An Ecological Economics Approach to Understanding Oregon's Coastal Economy and Environment. Meyer Memorial Trust. Audubon Society of Portland.

van de Wetering S, French R, Hall A, Smith B. 2009. Fisheries Restoration Efficacy Monitoring Report for the Little Nestucca USFWS Coastal Refuge property. Confederated Tribes of Siletz Indians. Siletz, OR.

van de Wetering S, French R. 2008. Tidal Fish Migration Patterns in Winchester Creek. Confederated Tribes of Siletz Indians. Siletz, OR.

Zeileis A, Kleiber C, Jackman S. 2008. Regression models for count data in R. Journal of Statistical Software 27:1-25.

Chapter 7: Benthic macroinvertebrates

Stan van de Wetering and Maxwell Tice-Lewis

Key findings

- Total abundance of benthic macroinvertebrates was higher during the 2018 sampling period than in 2014; this increase was observed at both the SFC site and the reference sites.
- Benthic macroinvertebrate diversity increased at two of three SFC reaches and decreased at one SFC reach. Parallel diversity shifts were seen at the nearby reference sites, suggesting these changes may have been driven by environmental factors.
- SFC populations of benthic macroinvertebrates may have dispersed to nearby mainstem river reference sites, complicating abundance and diversity comparisons.
- After restoration, macroinvertebrate species composition at SFC shifted toward the communities found at reference sites.

Introduction

When tidal hydrology and salinity are restored to a tidal wetland with a history of diking and water control, significant shifts in habitat structure and energetics commonly occur. These include channel scour and fill, new channel formation, changes in sediment grain size, and shifts in seasonal and daily salinity of tidal waters (Hood 2002, D'Alpoas 2007, So et al. 2009, Brophy et al. 2014). These shifts in benthic habitats have been shown to result in changes in both abundance and diversity of benthic macroinvertebrates (Gray 2005, Brophy et al. 2014, Howe et al. 2014). As described in Chapter 6, salmonids are keystone species in the Pacific Northwest that are often the main focus when federal and state funds are used to restore aquatic habitats (Pacific Coastal Salmon Restoration Fund 2000, Oregon Plan for Salmon and Watersheds 1997). Juvenile salmon utilize a diverse suite of food resources present in tidal wetland habitats during a portion of their life cycle, and these prey assemblages therefore have long been a point of interest to the salmon recovery community (Higley 1981, Healey 1982, Duffy et al. 2010, David et al. 2015).

We conducted a before-after-control-impact (BACI) study of benthic macroinvertebrate communities at SFC and reference wetlands to increase our understanding of how benthic invertebrate abundance, composition, and diversity in tidal channels responded to the restoration actions. We examined changes in major taxa abundance and composition as well as several metrics of taxonomic diversity. In addition, we aimed to improve our understanding of how these invertebrate communities potentially support juvenile salmonids through prey resource availability.

Materials and methods

We conducted benthic sampling in June, based on past data on seasonal change in species diversity and abundance for the Coquille River Estuary (Brophy et al. 2014). We sampled the same SFC study channel reaches used for fish sampling: Nolan Slough, Blind Slough, and Trib 1, a tributary to Blind Slough (Figure 7.1). Only those portions of the channel that remained inundated during the mean low tide

during spring flow conditions were sampled. Within the three SFC channel reaches, the thalweg was the target sample area. Samples were stratified longitudinally across the full fish abundance sampling areas (Figure 7.1). We sampled three reference sites (Trask River near Nolan Slough, Wilson River near Blind Slough and Dry Stocking Island near Nolan Slough). Sampling methods at river locations were similar to wetland channel locations, except that the edge of the channel thalweg was targeted since deeper areas were inaccessible. At both SFC and reference sites, we collected ten samples at equal intervals along the full length of each monitoring reach with a coring device measuring 80 mm in diameter (0.005 m^2) and 40 mm deep (approximate volume of 254 cm^3).

Taxonomic identification. Benthic macroinvertebrate samples were identified and enumerated by Invertebrate Ecology, Inc. (Moscow, ID) in 2014 and Ecoanalysts (Moscow, ID) in 2018. The taxonomic resolution of identification varied across years, which could affect diversity metrics; therefore, we conservatively combined species at the family level for diversity metric analyses.

Figure 7.1. Benthic macroinvertebrate sampling reaches at SFC (green) and reference channel reaches (white). All reaches were sampled in 2014 and 2018.

Abundance and diversity metrics. Statistical analysis of abundance data from single season sampling events will logically provide fewer insights than multiple season sampling due to the complexity of widely varying species life history traits such as reproductive cycles and dispersal rates. Biotic factors such as annual and seasonal stream flow patterns can affect habitat availability and thus abundance (Konrad et al. 2008). Shifts in stream bed scour and fill rates can create additional limits to interpreting single season species abundance patterns (Schwendel et al. 2011). Although species abundance can

fluctuate among seasons and across years, relative abundance data limited to a single season provides an understanding of the presence or absence of key species and species groups. These patterns are in turn useful in interpreting broader shifts in habitat availability and measures of community diversity (Barbour et al. 1998). Observations of shifts in species groups that use specific habitats provide a means of measuring change in habitat over time. Measures of community diversity provide additional useful insights in determining the overall health (ecological condition) of the restored habitats because as habitat diversity and health increases so does benthic macroinvertebrate diversity (Barbour et al. 1998).

We used abundance data to examine the presence or absence of key species and species groups associated with potential shifts in habitat. We used measures of community diversity to determine the overall health of the SFC habitat early in the restoration process. We characterized benthic invertebrate diversity with four related diversity metrics: (i) simple taxonomic richness, (ii) Shannon-Weiner index, (iii) exponential Shannon diversity, and (iv) exponential Simpson diversity. We chose to use multiple metrics to measure diversity as a means to resolve inherent issues associated with each metric, discussed further below (Gotelli and Chao 2013). Evaluating all four metrics, rather than a single metric, provided a more robust assessment of diversity trends.

Simple taxonomic richness (*S*) is the number of unique taxa (families) for each sample. Because richness does not account for differences in evenness (relative abundances of taxa) in a sample, (Gotelli and Chao 2013), we also calculated three additional diversity metrics that account for evenness by differential weighting of rare species.

The Shannon-Weiner index (H_{Sh}), or the Shannon index, is an index of diversity calculated as

$$H_{Sh} = -\sum_{i=1}^{S} p_i \, log p_i$$

where *S* is the total number of taxa in a sample and p_i is the relative abundance of the *i*th species. Shannon index considers both taxa number and relative abundance, but is not a linear measure of diversity (a sample with a Shannon index value of 4 is *not* twice as diverse as a sample with a Shannon index of 2). As *S* approaches infinity, the Shannon index behaves asymptotically. Because of this nonlinearity issue, we also calculated the effective number of taxa per sample using two additional indices, which do behave linearly: exponential Shannon index, calculated as exp(H_{Sh}) and exponential Simpson index, exp(H_{Si}). Effective diversity equates to the number of taxa required in a sample to obtain a value of the Shannon index and Simpson index respectively (MacArthur 1965, Jost 2006). Exponential Shannon and Simpson are also known as Hill numbers of differing orders (Hill 1973), solved for by the equation,

$$^{q}D = \left(\sum_{i=1}^{S} p_i^q \right)^{1/(1-q)}$$

According to Jost (2006), *q* is the order of diversity. As *q* increases, rare species in a sample are weighted to smaller degrees. Simple richness equates to *q* = 0, exponential Shannon equates to *q=1* and exponential Simpson equates to *q = 2*. Simple richness weights all taxa equally, whereas exponential Simpson puts more weight on common species. We calculated diversity metrics in R v. 3.6.1 using the "vegan" package v. 2.5-6 (Oksanen et al. 2013).

Statistical analyses. We used general linear models (R package "lme4" v. 1.1-25) and 2-way ANOVAs (R package "car" v. 3.0-10) to analyze differences between sample reaches at SFC and reference channels and sampling period (pre- versus post-restoration), and their interaction for each of the four diversity metrics. We conducted analyses by channel reach; unlike the fish analyses, we did not pool SFC or reference reaches. We took this approach because of observed habitat differences that seemed likely to

impact the invertebrate species assemblages found at individual reaches, such as differences in channel substrate composition, sediment scour rates, and influences from variable agricultural practices (nutrient input) in the Tillamook, Trask and Wilson river systems. Since salinity can affect macroinvertebrate habitats, we also examined salinity patterns during the pre- and post-restoration sampling periods (see Chapter 4).

Results and discussion

Abundance. A total of 25,391 benthic invertebrate specimens were collected and identified during 2014 and 2018. Twenty-six percent of the specimens were identified to genus while the remainder were identified to family level only. Major taxa included amphipods, insects (Coleoptera, Diptera), nematode worms, and annelid worms (Oligochaeta, Polychaeta) (Figures 7.2-7.5). Total abundance for all taxa increased at all sampled reaches (SFC and reference) from the pre-restoration to post-restoration sampling period (Figures 7.3-7.5 and Table 7.1). For simplicity, we present the abundance data for each SFC channel reach in comparison to the adjacent mainstem river reference reach only; Blind Slough and Trib 1 were compared to the Wilson River, and Nolan Slough was compared to the Trask River.

The largest shifts in community composition were an increase in the family *Corophiidae* (Amphipoda) in all SFC and reference reaches after restoration (Figures 7.3, 7.4, 7.5), and a decrease in the family *Chironomidae* (Diptera) in all SFC and reference reaches except Trib 1 (Figures 7.3 and 7.4). We suggest the change in the abundance of these two taxa was a response to the restoration. The decrease in chironomid abundance was likely due to removal of pre-restoration SFC channel sediments that had high organic matter and increases in water velocities due to tidal restoration within SFC (see Chapter 3; Pender 1986, Frouz et al. 2003, Bridgeland et al. 2017). In addition, pre-restoration chironomid abundance at SFC may have been high enough that these insects were dispersing from SFC and colonizing the local Wilson and Trask River reference reaches, resulting in increased abundance. In support of this hypothesis, chironomids were absent in the high marsh reference reach at Dry Stocking Island (DSI) (Appendix Figure A7.1) and had low abundance (mean = 2.5) at the reach monitored at the confluence of the Wilson and Trask rivers (2014 only, data not shown). The Trask River reference, DSI and Wilson River confluence reaches are 0.2, 0.7, and 1.7 km respectively downstream of the mouth of Nolan Slough while the Wilson River confluence site is 1.2 km downstream of the mouth of Blind Slough (Figure 7.1).

Chironomids typically complete their life cycle over one year (Pender 1986), making them more susceptible to annual and seasonal shifts in hydrologic patterns that influence scour and fill of channel substrates. Changes in chironomid abundance were different however in the Trib1 channel reach at SFC. During the pre-restoration period tidal exchange rarely occurred in this tributary due to the condition of its collapsed tide pipe, so less water was available in this channel's network. During post-restoration sampling we observed an increase in low tide ponded water associated with the channel's low terraces and on the marsh surface adjacent to the channel's network. These small ponded areas offered increased habitats preferred by chironomids during post-restoration and could be the driving factor in their increasing abundance after restoration.

The increased abundance of amphipods at all three SFC reaches following restoration is similar to our observations at the Ni-les'tun restoration site in the Coquille River Estuary (Brophy et al. 2014). At the Ni-les'tun site, we observed immediate colonization of restored tidal channels by amphipods, with abundances exceeding all other benthic taxa. Amphipods can reproduce several times within a season (Ericksen 1968, Desmond et al. 2002), giving them a competitive edge over other species entering habitats undergoing physical and chemical changes, such as occurs with dike and tide gate removal and the introduction of daily tidal flushing. However, it is notable that amphipods also increased at the Wilson and Trask reference reaches (but not at DSI). The post-restoration increase in amphipod abundance at the

Wilson and Trask River reference reaches may have been due to dispersal of amphipods from SFC channel reaches once those sites were rapidly colonized.

Other notable pre- to post-restoration shifts in benthic macroinvertebrate communities at SFC included increases in crustaceans (isopods and cumaceans) and omnivorous polychaetes (Nereididae) that prey on crustaceans in some channel reaches. In addition, we observed decreases in oligochaetes

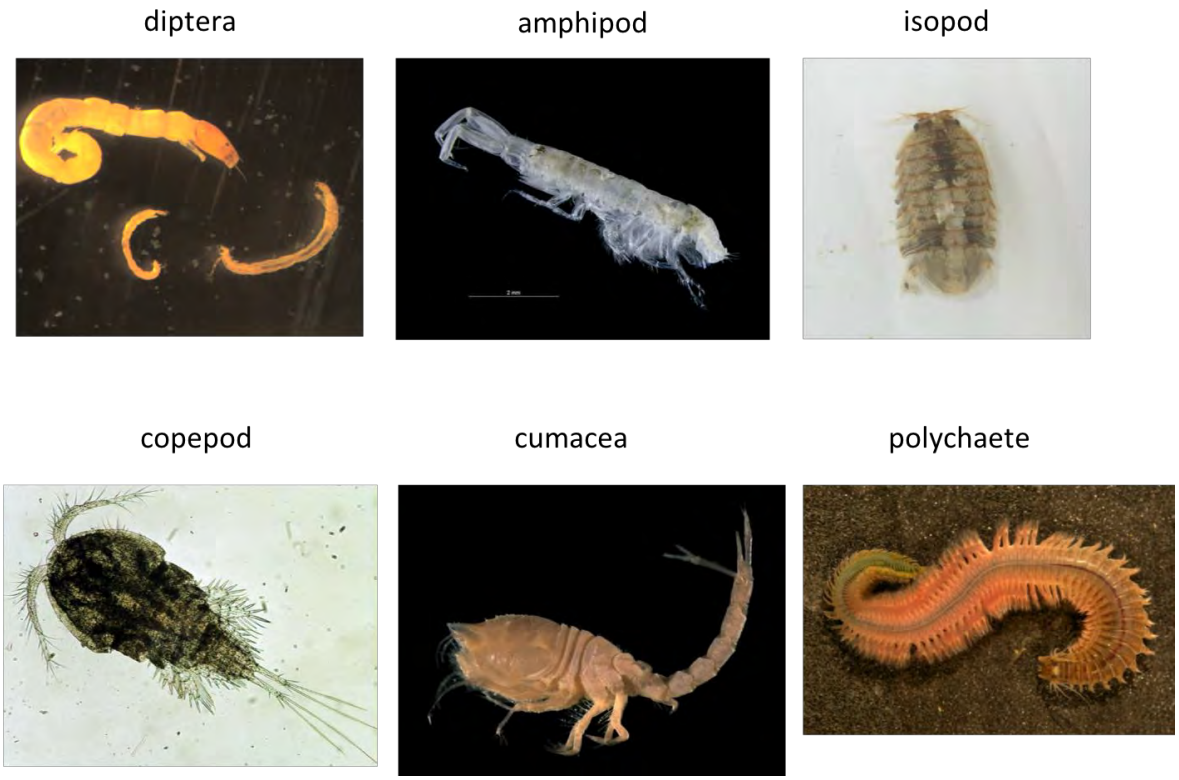

Figure 7.2. Examples of common benthic macroinvertebrate taxa found at the SFC and reference sites. Diptera image by E. Hayes-Pontius used under CC BY-SA 3.0 license; isopod image by Columbo2 used under CC BY-SA 3.0 license; copepod image is in the public domain; amphipod image and cumacea image and polychaete image by H. Hillewaert used under CC BY-SA 4.0 license.

(Naididae) that are soft-sediment detritivores, and increases in polychaetes (the non-native Ampharetid, *Hobsonia florida*) that are infaunal deposit feeders (Figures 7.3 – 7.5) in some reaches at SFC. Lastly, the New Zealand mud snail (an invasive gastropod) remained at similar densities in Nolan Slough before and after restoration, but increased in Blind Slough, and was newly found in relatively high abundance at Trib 1 during the post-restoration sampling (Figures 7.3-7.5). This species has been documented at other sites across Oregon and the lower Columbia River (Benson et al. 2020).

Patterns of benthic invertebrate community change observed in restored SFC channel reaches are very similar to the responses we observed at year two on the 202 ha Ni-les'tun restoration project on the Coquille River (Brophy et al. 2014). As described above, at Ni-les'tun the amphipod *Corophium* quickly colonized the site and dominated the year two post-restoration community. Polychaetes, molluscs, and crustaceans were also strongly represented in restored tidal channels at the Ni-les'tun site at year two (Brophy et al. 2014).

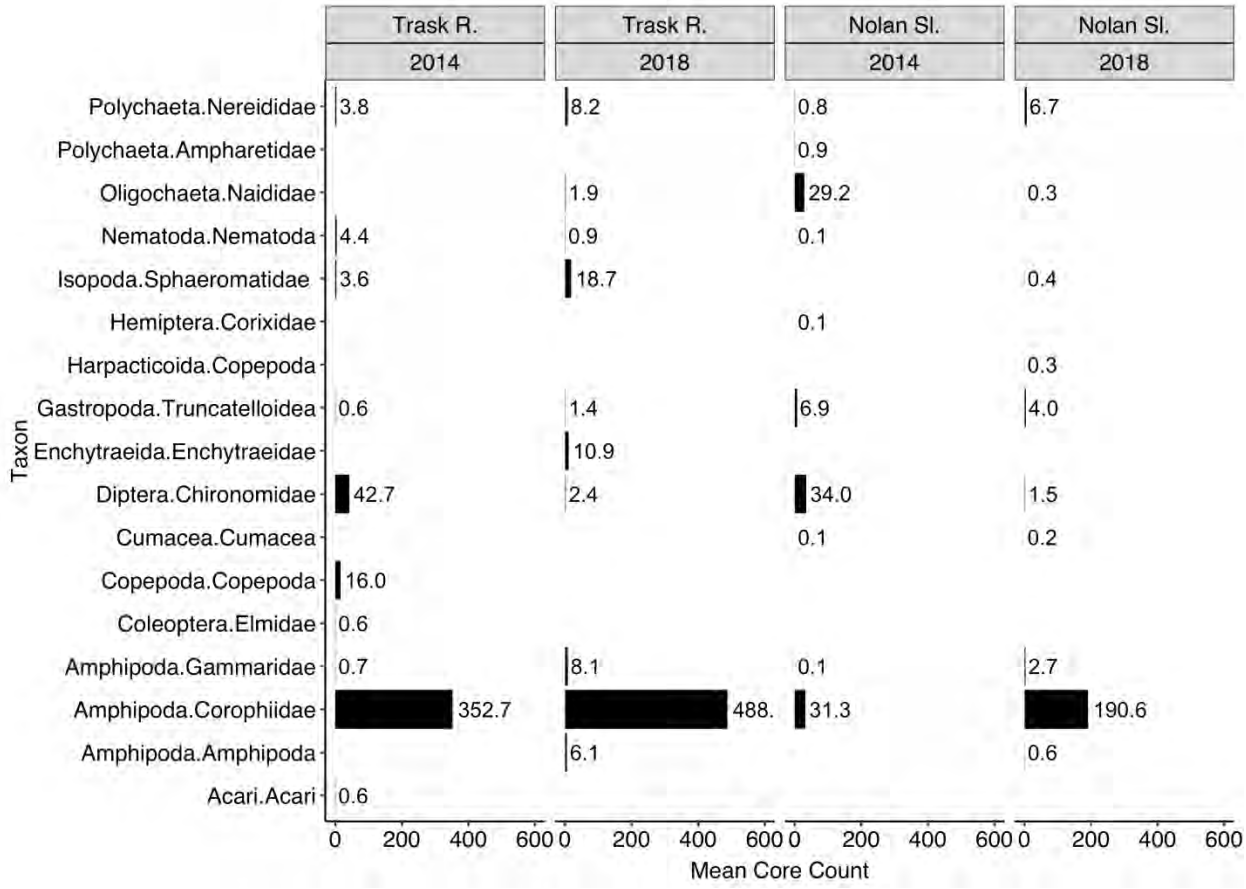

Figure 7.3. Mean abundance (counts/core) by channel reach for the ten most abundant benthic macroinvertebrate taxa in Nolan Slough and the closest reference site (Trask River) for the pre-and post-restoration sampling periods.

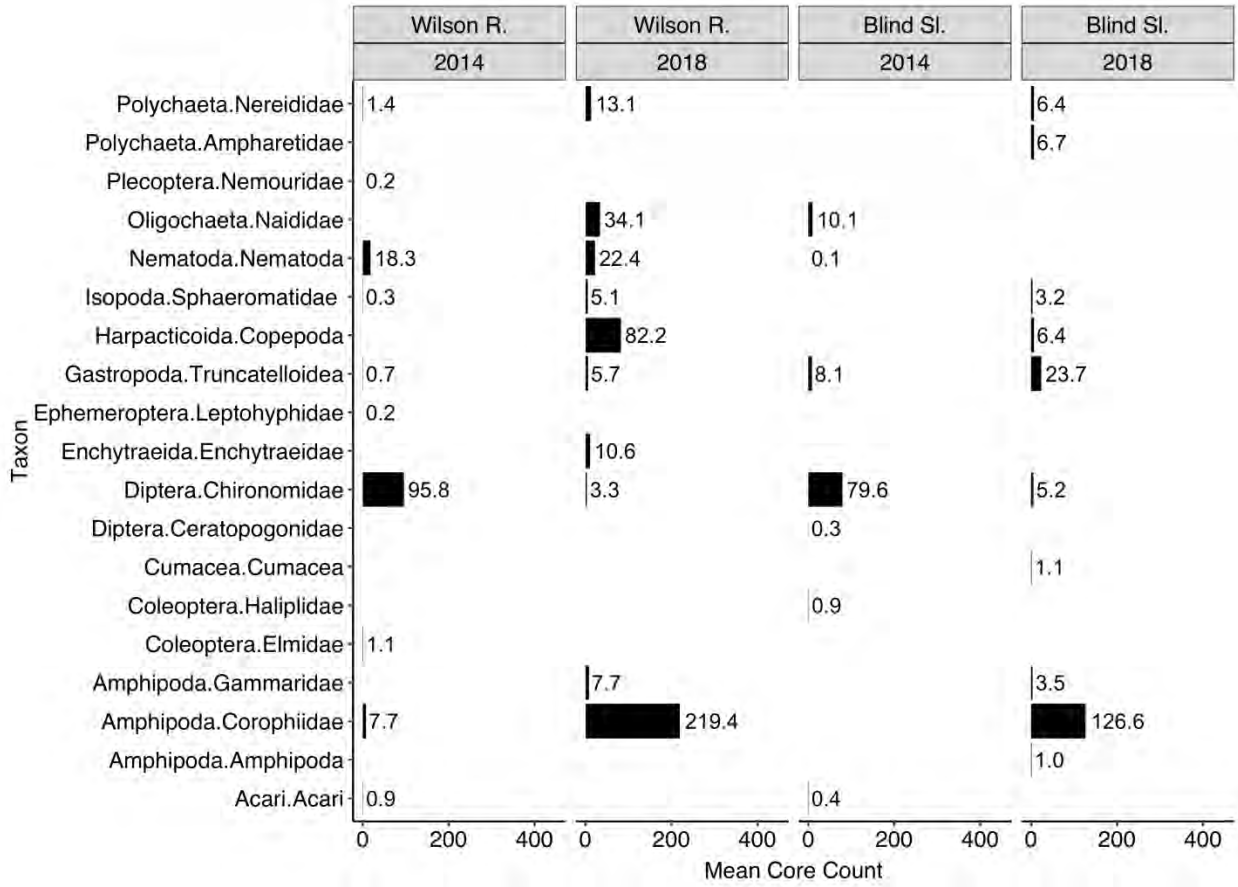

Figure 7.4. Mean abundance (counts/core) by channel reach of the ten most abundant benthic macroinvertebrate taxa in Blind Slough and the nearby reference channel reach (Wilson River) during the pre- and post-restoration sampling periods.

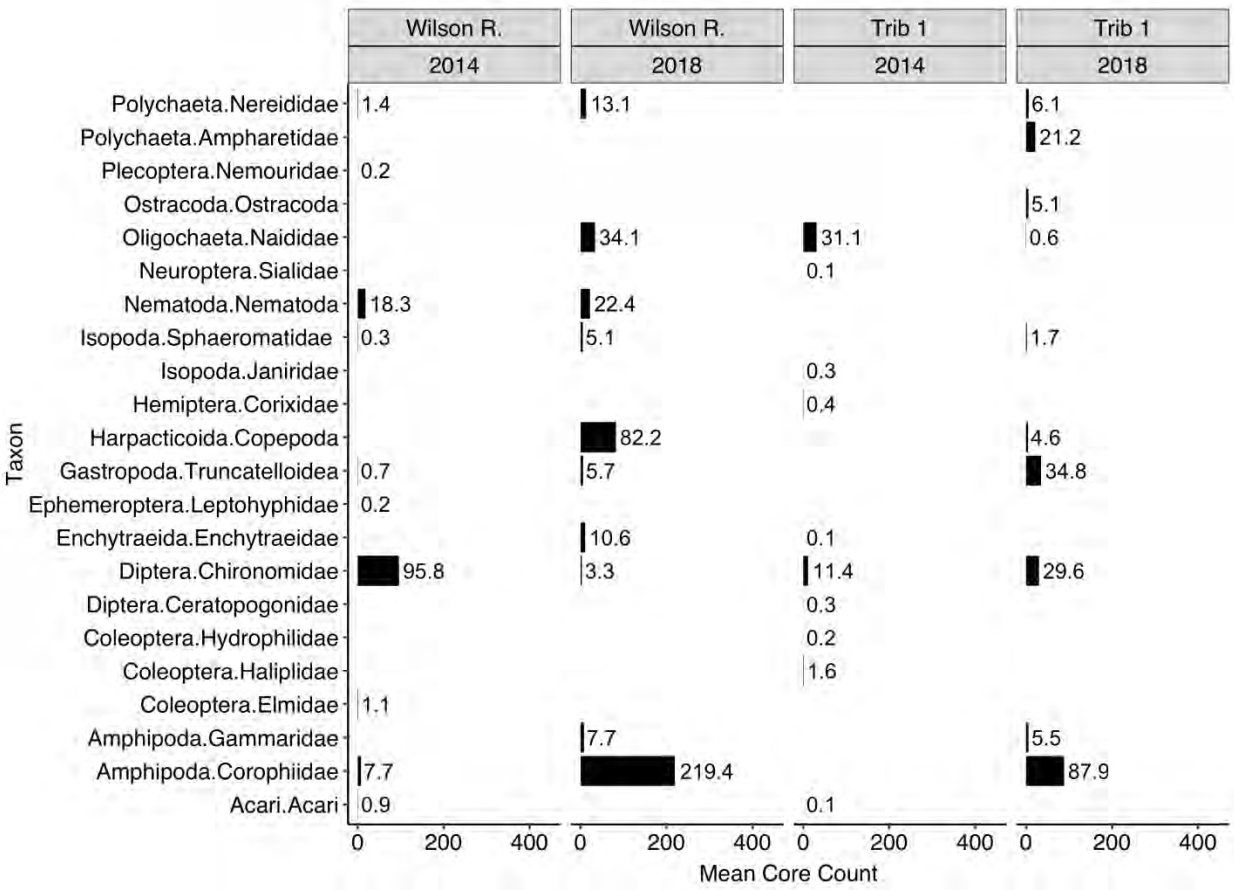

Figure 7.5. Mean abundance (counts/core) by channel reach of the ten most abundant benthic macroinvertebrate taxa at Trib 1 and the nearby reference channel reach (Wilson River) during the pre- and post-restoration sampling periods.

Table 7.1. Total abundance of benthic macroinvertebrates at each SFC and reference sampling reach by sample year.

	Wilson R.	Trask R.	DSI	Blind Sl.	Trib 1	Nolan Sl.	Total
2014	1,269	4,262	793	995	457	1,037	8,813
2018	4,077	5,480	1,098	1,863	1,986	2,074	16,578

Taxon diversity. Measures of benthic invertebrate diversity in SFC channel reaches varied by channel, with Blind Slough and Trib 1 having greater diversity after restoration while Nolan Slough decreased in diversity (Figures 7.6-7.9). Diversity in Blind Slough increased because of increased taxon richness and evenness -- that is, a more even distribution across taxa (Figure 7.4). Trib 1 diversity increased because of increased evenness (Figure 7.5), while Nolan Slough diversity decreased because of decreased evenness (Figure 7.3). Interestingly, each change in diversity at SFC was paralleled by a similar enough change in diversity at the closest reference channel reach (Figures 7.6-7.9), that we cannot conclude that the restoration action caused the SFC changes; instead these changes may have been due to broader environmental changes affecting both SFC and reference reaches.

Analysis of variance (ANOVA) indicates that the Blind Slough and Trib 1 reaches within SFC showed post-restoration increases in diversity that were not significantly different from the increases at the Wilson River and DSI reference reaches (Table 7.2). Although the post-restoration diversity decrease at Nolan

Slough was significantly different from all reference reaches (Table 7.2), the composition of the macroinvertebrate community at Nolan Slough became more similar to the nearby Trask River reference reach after restoration (Figure 7.3).

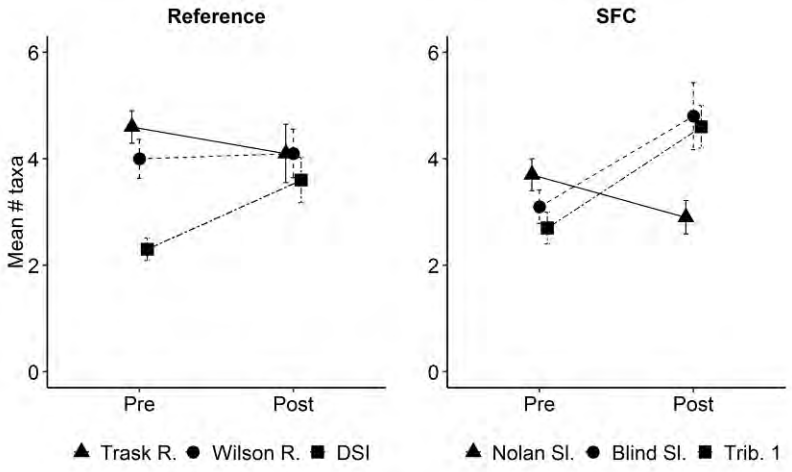

Figure 7.6. Benthic macroinvertebrate taxonomic richness at reference and SFC (restoration) channel reaches during pre-restoration (2014) and post-restoration (2018) sampling periods (mean ± SE).

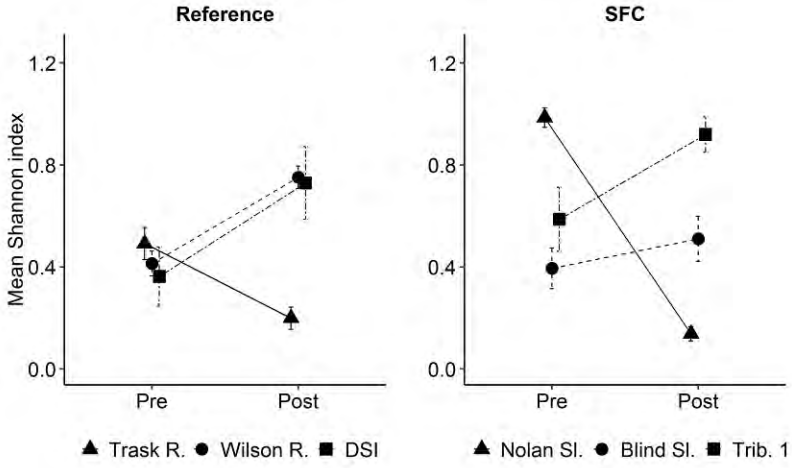

Figure 7.7. Shannon-Weiner index for benthic macroinvertebrate diversity at reference and SFC (restoration) channel reaches during pre-restoration (2014) and post-restoration (2018) sampling periods (mean ± SE).

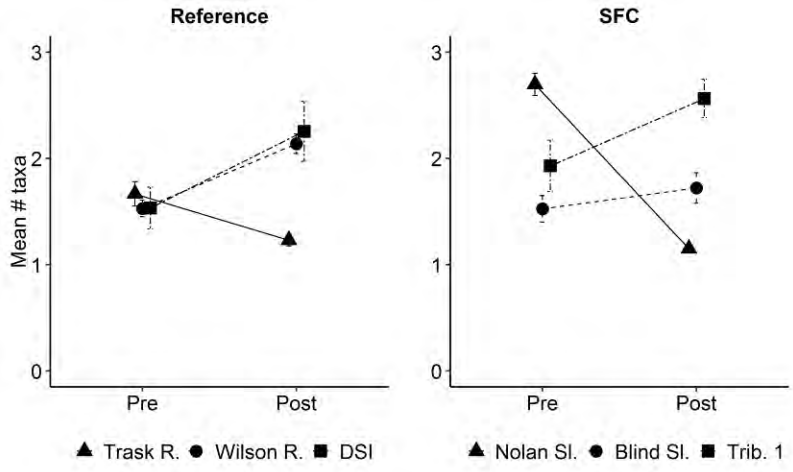

Figure 7.8. Exponential Shannon-Weiner index for benthic macroinvertebrate diversity at reference and SFC (restoration) channel reaches during pre-restoration (2014) and post-restoration (2018) sampling periods (mean ± SE).

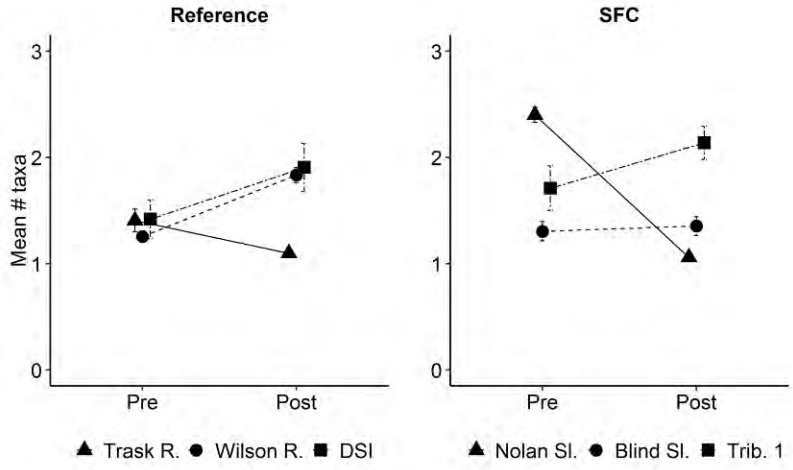

Figure 7.9. Benthic macroinvertebrate community mean exponential Simpson index at reference and SFC (restoration) channel reaches during pre-restoration (2014) and post-restoration (2018) sampling periods (mean ± SE).

Table 7.2. Pairwise comparisons of change in diversity between SFC and reference reaches. A plus sign indicates there was a statistically significant (P<0.05) change in diversity between the reference and SFC reach. A full table of ANOVA results is shown in Appendix Table A7.1.

Trask R. reference

	Nolan Sl.	Blind Sl.	Trib 1
Simple richness		+	+
Shannon index	+	+	+
Exponential Shannon	+	+	+
Exponential Simpson	+	+	+

Wilson R. reference

	Nolan Sl.	Blind Sl.	Trib 1
Simple richness			+
Shannon index	+		
Exponential Shannon	+		
Exponential Simpson	+	+	

DSI reference

	Nolan Sl.	Blind Sl.	Trib 1
Simple richness	+		
Shannon index	+		
Exponential Shannon	+		
Exponential Simpson	+		

Collectively, our results for benthic invertebrate abundance and diversity show a change in taxonomic composition within SFC channels following restoration, with composition shifting towards that of least-disturbed tidal marsh channels and river reference reaches (Gray 2005, Brophy et al. 2014, present study DSI site). Nanami et al. (2005) and Degraer (2008) have shown that grain size and sediment type affect estuarine benthic macroinvertebrate community structure. While evaluating tidal wetland restoration in the Coquille Estuary in southern Oregon, Brophy et al. (2014) noted anecdotal evidence suggesting that a shift from smaller to larger channel bottom sediment grain sizes at year two post-restoration may have influenced the composition of the benthic community. Restoration of tidal inundation at SFC may have flushed out fine-grained, organic-rich sediments from channels which negatively affected insects but favored amphipods. We expect the recovery process of channel scour, fill, and sediment sorting to continue and to create additional change in species composition while simultaneously increasing species diversity.

The effects of salinity on benthic macroinvertebrate communities in estuarine habitats is well-documented (Odum 1988). Brophy et al. (2014) reported that the salinity gradient in a Coquille River high marsh affected the benthic macroinvertebrate community across the full channel network. Because there are no internal freshwater sources feeding the SFC site channel network, the seasonal salinity patterns at the site are the result of precipitation and freshwater river outflows mixing with the mesohaline or polyhaline tidal waters from the bay. Incoming tides pass over the sand bars formed where the rivers enter the bay and penetrate the tidal channels within SFC (Figure 7.1). During the pre-restoration monitoring period, mesohaline salinities were observed in the SFC channel reaches during the dry season (see Chapter 4 Trib 1; additional August grab sample data not provided herein), probably due to the leaky tide gates at

all SFC sample reaches. Using the results from SFC Trib 1 (see Chapter 4) pre-restoration peak salinities were probably lower in Blind and Nolan Sloughs when compared to Wilson River and Trask Rivers, respectively, for the same period. We have observed mesohaline dry season salinities, probably due to leaky tide gates and seasonal evaporation, at diked sites in the Nestucca and Yaquina estuaries (unpublished data) as well as the Coquille Estuary (Brophy et al 2014). Following restoration the SFC Trib 1 channel showed a seasonal salinity shift from ~10 ppt to ~20 ppt during the peak of the dry season (see Chapter 4). If structural or flow characteristics were to change at SFC (e.g., channels deepen, sea level rises, or dry season river flows decrease), mesohaline salinities in the SFC channel network would be expected to occur for longer periods with the possibility of salinities rising well into the polyhaline range. Greater salinity would be expected to result in a species shift within the SFC benthic macroinvertebrate community, but the dominant groups observed during the post-restoration period (amphipods, polychaetes and crustaceans) would likely remain abundant.

The post-restoration decrease in benthic community diversity at the Trask River reference reach was not observed at the Wilson River and DSI reaches; this highlights the challenge of identifying appropriate reference sites for restoration monitoring, and the value of having multiple reference sites in restoration monitoring. We expected to see greater differences in taxa in the river channel reaches versus the SFC reaches due to differences in sediment grain sizes, but this did not seem to be supported by the data; SFC channel taxa became more similar to river reference taxa during post-restoration. The changes we observed in benthic community diversity at the Trask River reference reach might be attributable to interannual variation in flow regimes (such as increased bed scour during storm events) and or the long history of agricultural runoff in the Tillamook Basin (State of Oregon 2001). However environmental factors such as flow regime are less defensible when the results for the Wilson River and Dry Stocking Island are considered.

Higley et al. (1981) found amphipods to be a dominant prey item in the stomachs of chinook salmon, staghorn sculpin, and shiner surfperch sampled in a tidal creek and a tidal slough within the Siletz River Estuary located on the central Oregon coast. Duffy et al. (2010) observed large portions of juvenile Chinook salmon stomach contents to be composed of amphipods, polychaetes, and crustaceans in both nearshore and offshore samples gathered from the Puget Sound. More recently, David et al. (2015) described foraging by juvenile salmon in several Oregon and Washington estuaries, noting a diverse array of benthic macroinvertebrates consumed by juvenile salmon. Those most commonly found were dipterans (insect of greatest proportion), amphipods, crustaceans, and insects other than Diptera. In SFC channels, we observed increased counts of Corophiid amphipods, Nereid polychaetes, and crustaceans (isopods and cumaceans) following restoration. Our results, taken together with previous studies examining juvenile salmonid diets, indicate that there was increased prey resource availability in SFC channels following restoration, and that SFC channel reaches now provide improved habitat quality for juvenile salmonid species. Additionally, past research (Beamish et al. 2004, Duffy and Beauchamp 2011) has suggested that marine survival increases when growth rates increase during the juvenile salmonid's estuarine rearing period. Therefore, we suggest that the large SFC site may have the potential to eventually affect marine survival rates of local salmonid stocks.

The potential influence of the restoration at SFC on benthic macroinvertebrate abundance and composition downstream of the mouths of Blind and Nolan Sloughs is of particular interest. Although such influence may have made it harder to detect post-restoration change, these results suggest the restored SFC site may be exporting benthic macroinvertebrates to nearby channels. If export is occurring and is increasing abundance and diversity within mainstem river habitats adjacent to the SFC site, then the SFC site could provide additional benefits (increased carrying capacity and survival rates) to the broader fish community across the confluence area. Understanding food web resources in estuarine environments is a challenging process (Deegan and Garrit 1997). More recent research has continued to improve our understanding of the complex factors that drive food web variability within and across estuaries (Nordstrom et al. 2014, Arndt and Burnside 2015, Nelson et al. 2015, Howe et al. 2017) as well as the

challenges with defining spatial-scale connectivity in these environments (Vinagre et al. 2017). Basal food resources exported from tidal wetland habitats have varying availability to estuarine consumers in part based on the spatial patterns of a given consumer's rearing or resident habitat and factors such as fluvial discharge (Syvitski et al. 2005, Howe et al. 2017). If future monitoring data continue to suggest there is a correlation between production of benthic macroinvertebrates in SFC channels and populations in nearby mainstem river habitats, restoration practitioners, ecologists, and resource users would be able to more accurately assign the values and benefits these SFC high marsh habitats provide to Tillamook Bay estuarine species more broadly.

It is important to note that sampling in the present study occurred only two years after the removal of the dikes and tide gates at SFC, at the beginning of the site's long-term restoration trajectory. Channel substrates and annual and seasonal hydrologic variability are key drivers of benthic macroinvertebrate community abundance and composition in tidal marsh habitats (Odum 1988). Therefore, the community responses we documented here are expected to change further over time, both in the near and long-term. Comparing future measurements of SFC and reference channel benthic invertebrate communities with pre-restoration data and these early post-restoration results will help document the long-term effects of tidal wetland restoration on fish prey availability.

Citations

Arndt S, Burnside W. 2015. Effects of nutrient limitation on the dynamics of an estuarine food web. https://www.researchgate.net/publication/228772204.

Barbour MT, Gerritsen J, Snyder BD, Stribling JB. 1998. Rapid Bioassessment Protocols for Use in Streams and Wadeable Rivers: Periphyton, Benthic Macroinvertebrates, and Fish, 2nd ed. EPA 841-B-99-002.

Beamish RJ, Mahnken C, Neville CM. 2004. Evidence that reduced early marine growth is associated with lower marine survival of coho salmon. Transactions of the American Fisheries Society 133:26–33.

Benson AJ, Kipp RM, Larson J, Fusaro A, 2020. *Potamopyrgus antipodarum* (Gray JE, 1853): U.S. Geological Survey, Nonindigenous Aquatic Species Database, Gainesville, FL.

Brophy LS, van de Wetering S, Ewald MJ, Brown LA, Janousek CN. 2014. Ni-les'tun Tidal Wetland Restoration Effectiveness Monitoring: Year 2 Post-Restoration (2013). Estuary Technical Group. Institute for Applied Ecology. Corvallis, OR.

David AT, Simenstad CA, Cordell JR, Toft JD, Ellings CS, Gray A, and Berge HB. 2015. Wetland loss, juvenile salmon foraging performance, and density dependence in Pacific Northwest estuaries. Estuaries and Coasts 39:767–780.

D'Alpoas A, Lanzoni S, Marani M, Rinaldo A. 2007. Landscape evolution in tidal embayments: Modeling the interplay of erosion, sedimentation, and vegetation dynamics. Journal of Geophysical Research 112:1-17.

Death, RG. 2008. Effects of Floods on Aquatic Invertebrate Communities. In: Aquatic Insects: Challenges to Populations. (eds) Lancaster J, Briers RA. CAB International, Wallingford, UK. p. 103–121.

Deegan LA, Garrit RH. 1997. Evidence for spatial variability in estuarine food webs. Marine Ecology Progress Series 147:31-47.

Degraer S, Verfaillie E, Willems W, Adriaens E, Vincx M, Van Lancker V. 2008. Habitat suitability modeling as a mapping tool for macrobenthic communities: An example from the Belgian Part of the North Sea. Continental Shelf Research 28:369-79.

Desmond JS, Deutschman DH, Zedler JB. 2002. Spatial and temporal variation in estuarine and invertebrate assemblages: Analysis of an 11-year data set. Estuaries 25:552-569.

Duffy ED, Beauchamp D, Sweeting RM, Beamish RJ, Brennan JS. 2010. Ontogenetic diet shifts of juvenile chinook salmon in nearshore and offshore habitats of Puget Sound. Transactions of the American Fisheries Society 139:803-823.

Duffy E, Beauchamp DA. 2011. Rapid growth in the early marine period improves marine survival of chinook salmon, *Onchorhinchus tshawytscha*, in Puget Sound, Washington. Canadian Journal of Fisheries and Aquatic Sciences 68:232-240.

Eriksen CH. 1968. Aspects of the limno-ecology of *Corophium spinicorne* Stimpson (Amphipoda) and *Gnorimosphaeroma oregonensis* (Dana)(Isopoda). Crustaceana 14:1-2.

Frouz J, Matena J, Ali A. 2003. Survival strategies of Chironomids (Diptera: Chironomidae) living in temporary habitats: A review. European Journal of Entomology 100:459-465

Gotelli NJ, Chao A. 2013. Measuring and Estimating Species Richness, Species Diversity, and Biotic Similarity from Sampling Data. The Encyclopedia of Biodiversity. In: Levin SA (ed) Encyclopedia of Biodiversity, 2nd ed., vol 5. Academic Press, Waltham MA, p. 195-211.

Gray A. 2005. The Salmon River Estuary: Restoring Tidal Inundation and Tracking Ecosystem Response. PhD dissertation, University of Washington, Seattle, WA.

Healey MC. 1981. Juvenile Pacific Salmon in Estuaries: The Life Support System. Estuarine Comparisons. Proceedings of the Sixth Biennial International Estuarine Research Conference, Gleneden Beach, Oregon, November 1-6, 1981. Kennedy VS. (ed) Academic Press, p. 315-341.

Hill MO. 1973. Diversity and evenness: A unifying notation and its consequences. Ecology 54:427-32.

Higley DL, Holton RL. 1981. A Study of Invertebrates and Fishes of Salt Marshes in Two Oregon Estuaries. Miscellaneous report No. 81.5. U.S Army Corps of Engineers. Coastal Engineering Research Center. Fort Belvoir, VA.

Hood WG. 2002. Application of landscape allometry to restoration of tidal channels. Restoration Ecology 10:213–222.

Howe E, Simenstad CA, Toft JD, Cordell JR, Bollens SM. 2014. Macroinvertebrate Prey Availability and Fish Diet Selectivity in Relation to Environmental Variables in Natural and Restoring North San Francisco Bay Tidal Marsh Channels. San Francisco Estuary and Watershed Science 12:1-45.

Howe E, Simenstad CA, Ogston A. 2017. Detrital shadows: Estuarine food web connectivity depends on fluvial influence and consumer feeding mode. Ecological Applications 27:2170–2193.

Jost L. 2006. Entropy and diversity. Oikos 113:363-75.

Konrad CP, Brasher AMD, May JT. 2008. Assessing streamflow characteristics as limiting factors on benthic invertebrate assemblages in streams across the Western United States: Freshwater Biology 53:1983–1998.

MacArthur RH. 1965. Patterns of species diversity. Biological Reviews 40:510-33.

Nanami A, Saito H, Akita T, Motomatsu KI, Kuwahara H. 2005. Spatial distribution and assemblage structure of macrobenthic invertebrates in a brackish lake in relation to environmental variables. Estuarine, Coastal and Shelf Science 63:167-76.

National Ocean and Atmospheric Administration. 2000. Pacific Coastal Salmon Recovery Fund.

Nelson, JA, Deegan, Garrit, R. 2015. Drivers of spatial and temporal variability. Marine Ecology Progress Series 533:67-77.

Nordström MC, Currin CA, Talley CA, Whitcraft CR, Levin LA. 2014. Benthic food-web succession in a developing salt marsh. Marine Ecology Progress Series 500:43–55.

Odum EP. 1988. Comparative ecology of tidal freshwater and salt marshes. Annual Review in Ecological Systems 19:147-76.

Oksanen J, Blanchet FG, Kindt R, Legendre RP, Minchin PR, O'hara RB, Simpson GL, Solymos P, Stevens MH, Wagner H, Oksanen MJ. 2013. Package 'vegan'. Community Ecology Package, version 2:1-295.

Oregon Department of Environmental Quality. 2001. Tillamook Bay Watershed Total Maximum Daily Load (TMDL). https://www.oregon.gov/deq/Data-and-Reports/Pages/Publications.aspx.

Oregon Watershed Enhancement Board. 1997. Oregon's Plan for Watersheds. https://www.oregon.gov/oweb/resources/Pages/opsw.aspx.

Pender LCV. 1986. Biology of freshwater Chironomidae. Annual Review of Entomology 31:1-23

So K, van de Wetering S, Van Hoy R, Mills J. 2009. An Analysis of Reference Tidal Channel Plan Form Characteristics for the Ni-les'tun Unit Restoration. U.S. Fish and Wildlife Service Pacific Northwest Regional Office.

Syvitski J, Kettner A, Correggaiari A, Nelson B. 2005. Distributary channels and their impact on sediment dispersal. Marine Geology 222-223:75-94.

Vinagre C, Costa MJ, Dunne JA. 2017. Effect of spatial scale on the network properties of estuarine food webs. Ecological Complexity 29:82-92.

Willson MF, Halupka KC. 1995. Anadromous fish as keystone species in vertebrate communities. Conservation Biology 9:489-97.

Chapter 8: Mosquito abundance at SFC

Scott Bailey

Key findings

- Captures of mosquito larvae were generally low at SFC throughout the study with peak abundance in spring before restoration.
- Adult mosquito captures were low at SFC before and after restoration and were dominated by two *Culex* species.
- The primary species of concern, *Aedes dorsalis*, was not observed at SFC during the study period.

Introduction

The Southern Flow Corridor (SFC) project aimed to restore numerous tidal wetland functions by reintroducing tidal flows where they were previously excluded. As noted in earlier chapters of this report, plants and animals all respond to the resulting physical changes at the restoration site and community compositions shift accordingly. In some tidal wetland restoration projects, an undesirable consequence of changes to hydrology resulting from restoration is substantially increased numbers of mosquitoes, particularly salt-tolerant species such as *Aedes dorsalis*. Many mosquito species that occur in coastal watersheds can act as vectors to diseases that affect humans and other animals, particularly viral diseases (Goddard et al. 2002). These include Western equine encephalitis, St Louis encephalitis, West Nile Virus, and many others. As a result, mosquito population outbreaks are a public health concern in addition to being very unsettling for residents and visitors as well as domestic pets, livestock, and wildlife. Compared to other species widespread in the western U.S., including *Culex (Cx.) tarsalis* and *Cx. pipiens, Aedes dorsalis* does not appear to be an important vector for diseases of primary concern (Kramer et al. 1998, Goddard et al. 2002). However, it is a strong flier known to move long distances to forage; females prefer humans and other large mammals for blood meals; and they feed relentlessly, during both day and night (Gjullin and Eddy 1972, Belton 1983). While outbreaks of some other species may pose greater public health risks through disease transmission, an outbreak of *Aedes dorsalis* remains incredibly problematic for communities where they occur.

A. dorsalis is “one of the most important and widespread species in the Northwest,” and it “breeds naturally in brackish or salt-water marshes and is also one of the most abundant and troublesome species in irrigated areas and in flooded grasslands” (Gjullin and Eddy 1972). This species breeds in pools of water that remain stagnant for at least 4-5 days; in tidal wetlands these conditions are met at elevations between the lower high tides of the month and the higher high tides (Bridgeland et al. 2017). Outbreaks at tidal wetland restoration projects have occurred elsewhere, including the Ni-les’tun restoration project at Bandon Marsh National Wildlife Refuge on the southern Oregon coast (USFWS 2014) and Napa River Estuary north of San Pablo Bay, in California (W. Maffei, pers. comm.). The outbreak at Bandon began shortly after restoration construction ended, whereas at Napa River problems began several years after project work was completed. The Ni-les’tun project was the first estuarine project in Oregon to experience such dramatic shifts in mosquito populations, and it disrupted the quality of life of nearby residents and visitors and created management concerns for the US Fish &

Wildlife Service and others. The mosquito problem at Ni-les'tun was resolved using an Integrated Marsh Management program that included mosquito monitoring, spraying with a very specific larvicide (*Bacillus thuringiensis*), and excavation of over 24 miles of additional tidal channels (Bridgeland et al. 2017). Although an increase in mosquito numbers has not been apparent at other recent tidal wetland restoration projects in Tillamook Bay (Miami Wetlands - S. Bailey, pers. obs., Kilchis Preserve - The Nature Conservancy, pers. comm.), given its size and proximity to urban Tillamook, the Bandon experience prompted us to include mosquitoes as part of the SFC monitoring effort.

Like other parameters detailed in this report, we sampled for larval and adult mosquitoes before and after the restoration of tidal flows at the SFC project. However, mosquito monitoring differed from other work reported in this document in several important ways. First, the distribution of sample sites was limited, generally to the eastern side of SFC and the sites sampled were not randomly selected from all available restored areas. Second, we did not follow a modified BACI sampling design because no trapping was completed at reference sites. Our fourfold goals for mosquito sampling were to: 1) identify adult mosquito species present at SFC and provide some understanding of their relative abundances, 2) assess the status of larval rearing at the site, 3) determine whether the project resulted in apparent changes in mosquito composition, abundance, and reproduction, and 4) recommend an approach for future mosquito monitoring.

Materials and methods

Prior to sampling, we toured the restoration site with Wes Maffei, General Manager of the Napa County Mosquito Abatement District (NCMAD) in American Canyon, California. Our objective was to get insights into mosquito ecology and behavior from a recognized expert, identify good sites for larval and adult trapping, and discuss sampling methodologies and strategy.

Based on the above visit and continued consultation with W. Maffei, we established six larvae/adult sampling stations during the pre-restoration sampling period (2015). All locations were chosen because they appeared likely to have mosquitoes present (particularly larvae, whose presence indicate that a site is being used for reproduction not just adult foraging) during baseline conditions and were expected to remain relatively accessible following restoration activities planned for 2016 (Figure 8.1).

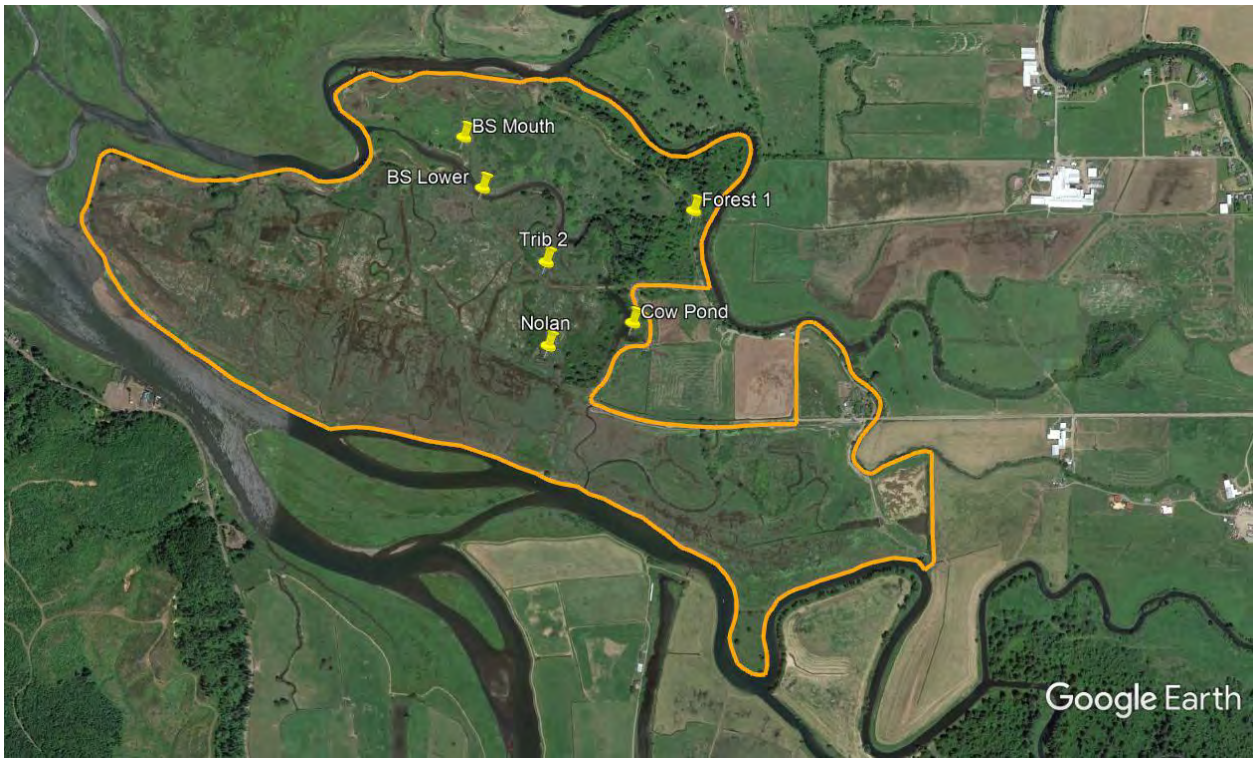

Figure 8.1. Mosquito sampling stations in 2015 and 2017. The area outlined in orange indicates the primary portion of the SFC project restored to tidal influence in 2016. Imagery from Google Earth, © 2020 Google. Data, SIO, NOAA, U.S. Navy, NGA, GEBCO.

Prior to restoration, we began sampling in March 2015 and continued approximately bi-weekly through July. We also completed one sampling bout in October and two in November (Table 8.1). During 2017 and 2018 (during- and post-restoration periods) we focused our efforts on the period from May through September, again sampling approximately bi-weekly (Figure 8.2). We used the same six sampling stations established in 2015 during the 2017 sampling season. However, the author of this chapter was involved in an automobile accident in 2018 and was unable to perform field work for this study. As a result, we used volunteer labor to gather mosquito data. To facilitate access for our volunteers, we altered most locations for the 2018 sampling season: we used one of the original sampling locations (Forest 1) and established five new stations (Figure 8.3). Three of the new stations were at the SFC restoration site, each within 400 m of a previously used station. The remaining two stations were approximately 2,000 m southeast of the SFC restoration site. These were located at a separate portion of the SFC project where dikes were removed, a new setback dike was built, and contaminated soils were removed and/or capped (no other parameters covered in this report were monitored at this area). This portion of the SFC project was closer to the urban center of Tillamook and, as a result, these two stations were closer to residential, commercial, and industrial properties (and associated infrastructure) than the other stations.

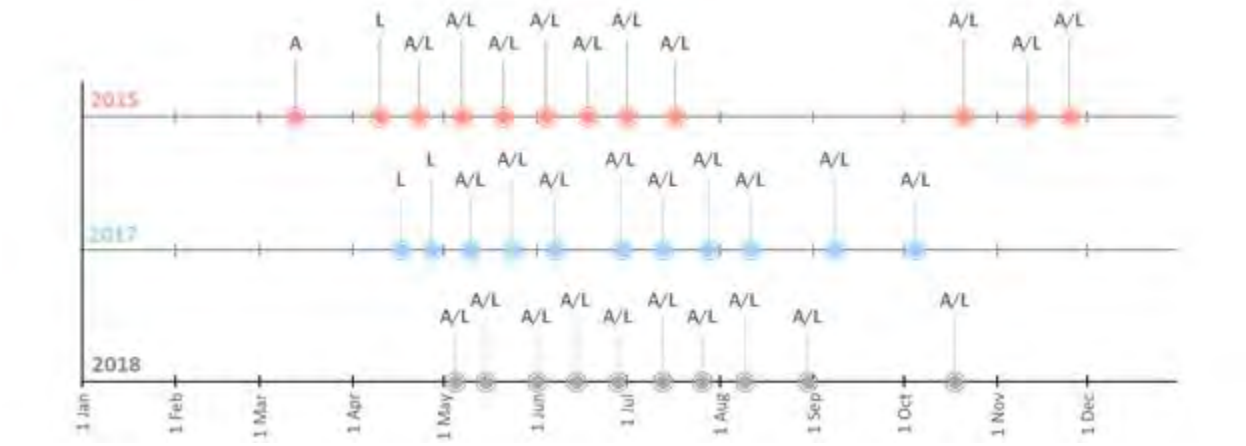

Figure 8.2. Sampling dates for mosquito adults (A) and larvae (L) at SFC during 2015, 2017 and 2018.

Larval sampling. We sampled for larval mosquitoes on 12 occasions during 2015, 11 occasions in 2017, and 10 occasions in 2018 (Figure 8.2). During each sampling session, we dipped for larvae at shallow water bodies in proximity to each of the six adult trapping stations and often at waterbodies encountered travelling among stations. In addition, we visually searched for larval mosquitoes at waterbodies encountered while traversing the site. At the regular stations, we sampled primarily within remnant natural channels, drainage ditches, and/or associated lateral impoundments with nearly perennial water (but water levels varied), but also at small ephemeral pools that were stormwater and/or tidally fed. Sporadically sampled water bodies were often small, ephemeral stormwater/tidal impoundments, but we also sampled in nearby channels and adjacent flooded areas.

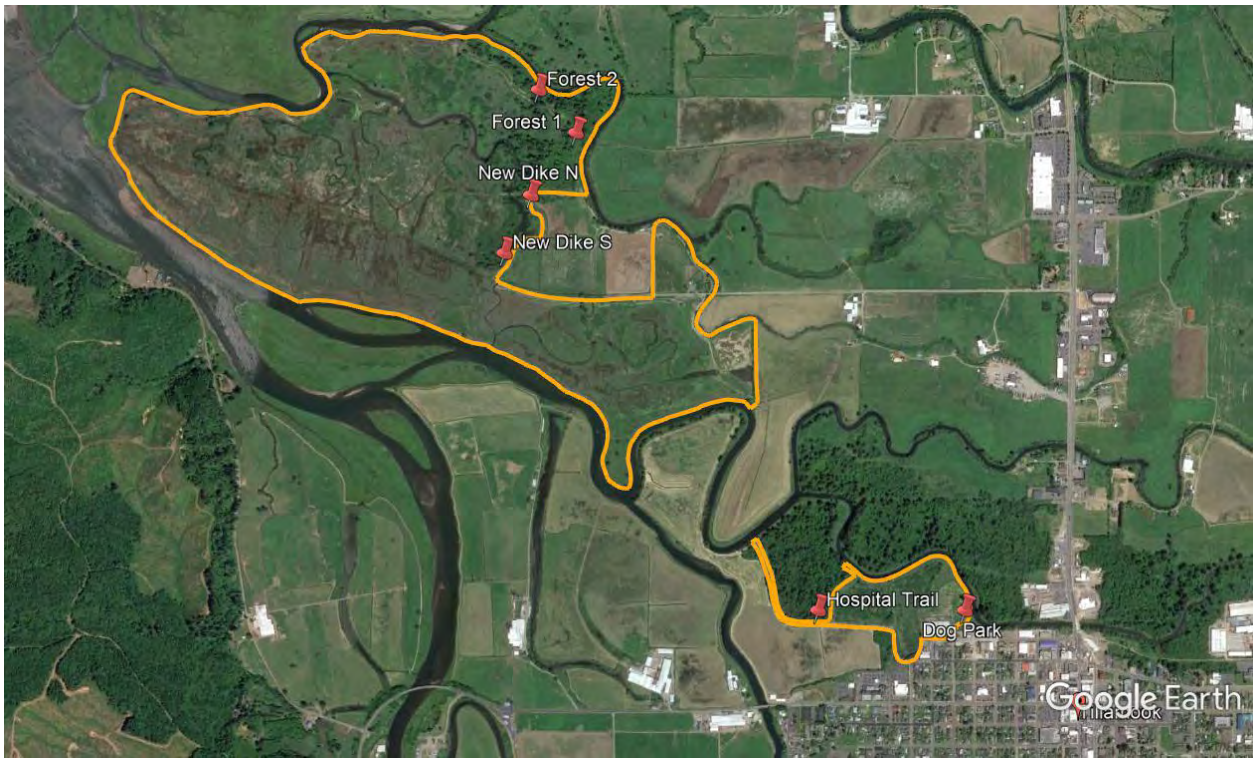

Figure 8.3. Mosquito sampling stations sampled during 2018. Imagery from Google Earth, © 2020 Google. Data, SIO, NOAA, U.S. Navy, NGA, GEBCO.

In 2015, all sampling was completed upstream of dikes and tide gates separating the SFC site from Tillamook Bay. Most of the water bodies sampled had muted tidal signatures due to leakage/breaches in the dikes, but some were primarily stormwater fed and disconnected from direct tidal exchange. In 2017 and 2018, we sampled within remnant natural channels, constructed channels and drainage ditches, and in small pools in the adjacent floodplains. Our 2018 larval sampling sites were subject to direct tidal exchange. Water levels and salinities varied with the tide cycle and rainfall patterns (although not all sampling sites were regularly inundated with tidal flows).

During all sampling sessions, we used a 350 ml dipper mounted to a 1m handle (Figure 8.4) to capture larvae within the water column. In areas within the water bodies where larvae would likely occur (along the margins, often in association with overhanging vegetation), we plunged the dipper into the water column, quickly removed it and carefully inspected the contents each time it was withdrawn. At the six repeat sampling stations, we collected nine dips during each visit in waterbodies that were available near the station (typically these dips were spread among more than one water body because each was small). The number of dips at other potentially suitable areas for larvae encountered while walking varied, but was thorough for the size of the water body. When larvae were captured, we used a bulb dropper to transfer them from the dipper into labeled vials containing 95% isopropanol. Upon returning from the field, we refreshed the isopropanol and stored the vials in a cool, dark place until they could be shipped for identification. For each sampling bout, we measured water depth with markings on the handle of our larvae dipper, measured temperature and salinity with an Omega CDH-93 handheld meter, and recorded general weather information. We also noted incidental observations of fishes and other potential predators within the sampled water bodies.

Adult sampling. At the six standard stations, we sampled for adult mosquitoes 11 times during 2015, nine times during 2017, and 10 times during 2018 (Figure 8.2). We used Center for Disease Control (CDC) traps baited with CO_2 (dry ice), and hung the traps from limbs so the trap intake was typically 0.75 – 1.5 m above ground in wind-protected areas among trees, shrubs and other vegetation (Figure 8.5). We deployed traps in the afternoon and retrieved them the following morning (15-18 hour deployments). We avoided deploying traps on days that were exceptionally windy or rainy. When we retrieved each trap, we immediately removed the mesh collection bag, added a paper label, and placed the bag inside the CO_2 container until all field work scheduled for that day was complete (to euthanize the contents). We recorded weather and noted the condition of the sampling equipment (e.g., whether dry ice remained or the fan still functioned, etc.) at each sample site.

Upon completion of field work, sample bags were placed in a freezer until the contents could be sorted. For sorting, we emptied the bags one at a time onto a large, light colored work surface, separated adult mosquitoes from other insects, and placed mosquitoes and a paper label into small glass vials. To minimize potential for spoilage, we limited the maximum number of individuals in each vial to approximately 20 and dried the contents of all vials by placing them in a warm oven (50-75 ^{o}C) for 20-30 minutes before inserting a cotton ball (above the mosquitoes, but not pressing down on them) and capping the vials. We stored capped vials in a freezer until they could be shipped for identification.

Species identification. Two to three times during each sampling season, we carefully packaged vials of larvae and adults and shipped them overnight to Wes Maffei at NCMAD for identification. He identified all individuals to the lowest taxonomic level possible, identified sex for adult specimens, and returned the results via email. Maffei was able to identify most individuals to species, but some were only identifiable to genus because they were incomplete specimens that lacked key diagnostic characteristics.

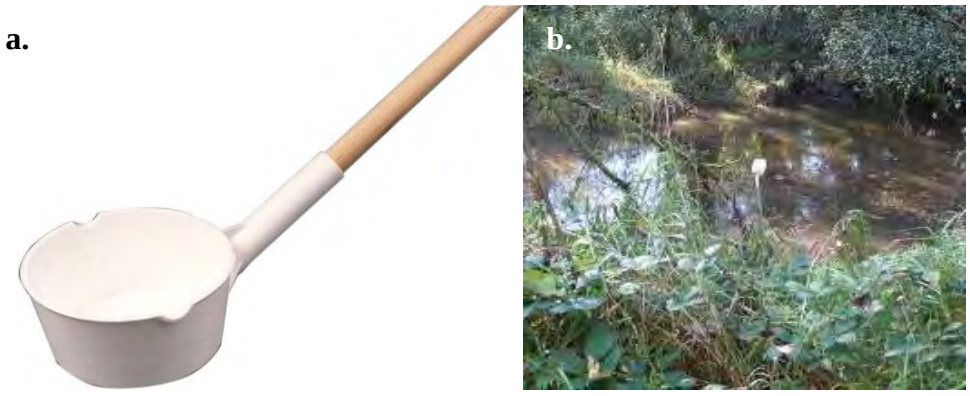

Figure 8.4. (a) Mosquito dipper used for larval sampling. (b) Mosquito dipper standing upright in vegetation at one of the SFC sampling stations.

Data analysis. We captured larval mosquitoes during only a few sampling trips over the course of this study and, as a result, there was little data on larval mosquitoes to analyze. We compiled the total number of individuals captured during each sampling trip by species but performed no further analysis of the larval data. To index the efficacy of each of our adult trapping stations, we calculated annual trap success for each station by dividing the number of samples containing mosquitoes by the total number of sample trips.

Raw data for adult mosquitoes received from NCMAD provided total captures by species at each sampling station for each sampling date. As noted above, we completed a different number of sampling bouts during each of the three sample years and the length of the sampling season and level of effort during some months varied among years. Therefore, to standardize results for comparisons we calculated catch-per-unit effort (i.e., catch per trap night) plus 95% confidence intervals for each sample year. We did this for each species by dividing total captures by total trap nights (i.e., total number of nights traps were deployed times the number of traps deployed per night [for example 11 nights x 6 traps per night = 66 trap nights]). We performed this calculation for all data from each sample year and for a subset of the data from May, June and July of each year. For this period, we had similar sampling efforts during each of the three years. For the 2018 data set, we completed these calculations with data from all six sample stations and with a data set that excluded the two stations that were located away from the SFC restoration site (since these two stations were closer to the Tillamook urban area than other stations).

Figure 8.5. CDC trap hung from a tree limb during trapping to collect adult mosquitoes at the SFC site.

Results and discussion

Larval mosquitoes. In 2015, prior to SFC restoration, we captured 268 larvae with nearly all collected during three spring sampling bouts – peak captures were in late April and very few occurred after early May (Table 8.1). We captured larvae at only half of the six repeat sampling stations (BS Mouth, Forest and Cow Pond). We dipped fewer than 10 larval mosquitoes combined (including pupae) from aquatic habitats at these three stations. Instead, we captured most larvae (260) within a series of shallow, ephemeral, rainwater-fed pools encountered while walking between stations in a freshwater wetland in an area loosely bounded by the Nolan, Cow Pond and Trib 2 stations (Figure 8.1). Larvae were abundant in these pools from mid-April to early-May, but the area dried by May 20 (after rain became less frequent) and remained dry for the duration of our 2015 sampling (even following summer rain events).

All larvae captured in 2015 (264) were identified as *Aedes aboriginis*, but we did collect four *Culiseta* (Ca.) sp. larvae in November probably representing *Ca. inornata*. *A. aboriginis* larvae captured in April and May were in a series of shallow (<20 cm), cool (<17^{o}C), freshwater (rain fed) pools (salinity <0.5 PPT) (Table 8.1). As noted above, larvae were abundant throughout this series of pools during this time. Superficially, all larvae observed in this area appeared to be the same species. The few *A. aboriginis* larvae captured in June 2015 were in muted tidal channels at the Forest and BS Mouth stations. Two of the three specimens from Forest and the single specimen from BS Mouth were pupae. During these captures, the Forest station had shallow (<15 cm), warm (19.4^{o}C), freshwater conditions, and BS Mouth had shallow (<20 cm), very warm (26.1^{o}C), mesohaline waters (6.2 ppt). *Culiseta* larvae captured in November were dipped from shallow (<15 cm), cold (10.6^{o}C), oligohaline (0.9 ppt) water in an alcove in the upper portion of Blind Slough.

Table 8.1. Number of mosquito larvae collected and habitat conditions during each sampling date in 2015 (prior to restoration). For dates with captures, water conditions at stations where no larvae were present are reported in parentheses.

Sample date	Number of larvae captured	Species	Capture location	Water temp (°C)	Water salinity (ppt)	Water depth (cm)
10-Apr	52	*Aedes aboriginis*	Freshwater pools, forest	9.5 - 12.3 (11.2 - 14.1)	0.1 - 0.2 (0.1 - 0.9)	10 – 20 (10 - 30)
22-Apr	167	*Aedes aboriginis*	Freshwater pool	16.5 (15.2 - 22.6)	0.1 (0.0 - 0.6)	5 – 10 (5 - 30)
6-May	40	*Aedes aboriginis*	Freshwater pool	9.6 (11.0 - 13.9)	0.1 (0.1 - 2.5)	5 – 10 (5 - 30)
21-May	0	-	-	15.0 - 17.3	0.1 - 2.0	5 - 35
4-Jun	0	-	-	17.0 - 28.3	0.2 - 2.4	10 - 35
18-Jun	4*	*Aedes aboriginis*	Forest, mouth of Blind Slough	19.4 - 26.1 (21.8 - 34.6)	0.4 - 6.2 (0.2 - 13.4)	10 – 20 (5 - 25)
1-Jul	0	-	-	16.8 - 25.2	0.3 - 9.6	5 - 20
16-Jul	0	-	-	17.9 - 23.2	0.9 - 14.6	5 - 25
21-Oct	0	-	-	15.6 - 16.4	5.0 - 12.4	5 - 25
11-Nov	4	*Culiseta* sp. (probably *Ca. inornata*)	Cow pond	10.6 (10.3 - 11.7)	0.9 (0.3 - 3.8)	5 – 15 (5 - 35)
25-Nov	0	-	-	5.6 - 6.3	0.1 - 0.3	10 - 80

* 3 pupae and 1 late instar larvae

Outside of the spring period, we did not capture larvae in most of the sampling completed in 2015. During spring and November sampling bouts, water at these stations ranged from 0.1 to 13.4 ppt, but was most commonly ~0.1 to 2.5 ppt. During summer and early-fall, salinities ranged from fresh to mesohaline (0.1 to 14.6 ppt) but were most often moderately mesohaline (~8.0 to 13.0 ppt) because most of our pre-restoration larval sampling sites had muted tidal signatures.

In 2015, we observed potential predators of larval mosquitoes including three-spined stickleback (*Gasterosteus aculeatus*), dragonfly larvae, water beetles, and rough-skinned newts (*Taricha granulosa*). Stickleback were present (and sometimes abundant) in sampled waterbodies at all regular stations (but we did not observe them in the ephemeral pools where most larvae were captured). We observed other potential predators more sporadically (particularly invertebrate predators).

Conditions at the SFC restoration site changed dramatically after fall 2016 when dikes surrounding the site were removed and tidal inundation returned. We did not capture or observe larvae anywhere within the SFC restoration site during either the 2017 or 2018 sampling seasons (Tables 8.2 and 8.3). However, on two separate occasions in 2018 (one in late-June and one in mid-October) we captured larval mosquitoes at one of the newly established stations nearer the Tillamook urban center. We captured a total of 31 individuals in an outfall pool at the terminus of a small, stormwater drainpipe at the Dog Park sampling station (Table 8.3).

Nearly all larvae captured in 2018 (30) were *Ca. incidens*. We captured a single individual of *Aedes* sp. which lacked enough detail to allow it to be keyed to species, but it was not *A. dorsalis*.

The stormwater outfall where we captured these larvae collected runoff from Front Street in Tillamook, discharged into a small pool <1 m^2 in surface area, 20-40 cm deep and heavily shaded by tall, overhanging grass that draped onto the water surface. This feature was constructed as part of the SFC project in an area associated with removal and capping of contaminated soils. When larvae were dipped from this pool, water was cool (15.1 ^oC in June and 11.3 ^oC in October) and nearly fresh (0.5 ppt).

We did not capture larvae in most of the samples collected in 2017 and 2018 (Tables 8.2 and 8.3). Water at these locations during spring ranged from fresh to moderately mesohaline (0.1 to 9.6 ppt), but fresh to oligohaline (~0.0 to 2.5 ppt) conditions were most common. Summer and early-fall salinities ranged from fresh to polyhaline (0.4 to 21.7 ppt) but were typically upper mesohaline (~12.0 to 17.0 ppt).

During these two sampling seasons, three-spined stickleback were widespread (and often abundant) in channels and in pools across the newly reconnected tidal floodplain. We also observed juvenile salmonids and other fishes (e.g., shiner perch [*Cymatogaster aggregata*] and other unidentified species) on several occasions. We observed potential invertebrate predators more sporadically. Rough-skinned newts were much less widespread and less often observed than in 2015.

Table 8.2. Number of mosquito larvae collected and habitat conditions during each sampling date in 2017. Water conditions at stations where no larvae were present are reported in parentheses.

Sample date	Number of larvae captured	Species	Capture location	Water temp (°C)	Water salinity (ppt)	Water depth (cm)
13-Apr	0	-	-	(9.3 - 12.3)	(0.0 - 0.2)	(10 - 100)
27-Apr	0	-	-	(11.5 - 13.7)	(0.0 - 0.1)	(10 - 100)
9-May	0	-	-	(16.9 - 28.1)	(0.1 - 0.2)	(5 - 40)
23-May	0	-	-	(13.6 - 23.0)	(0.1 - 0.8)	(5 - 75)
7-Jun	0	-	-	(14.6 - 18.2)	(0.1 - 2.4)	(5 - 40)
29-Jun	0	-	-	(18.7 - 26.6)	(0.9 - 8.2)	(5 - 20)
13-Jul	0	-	-	(18.9 - 23.4)	(0.5 - 10.5)	(5 - 30)
28-Jul	0	-	-	(17.2 - 20.7)	(5.3 - 17.6)	(5 - 35)
11-Aug	0	-	-	(18.1 - 21.8)	(9.1 - 18.4)	(5 - 40)
8-Sep	0	-	-	(18.3 - 21.0)	(12.5 - 21.7)	(5 - 30)
5-Oct	0	-	-	(11.7 - 13.3)	(5.2 - 12.9)	(5 - 30)

Table 8.3. Number of mosquito larvae collected and habitat conditions during each sampling date in 2018. For dates with captures, water conditions at stations where no larvae were present are reported in parentheses.

Sample date	Number of larvae captured	Species	Capture location	Water temp (°C)	Water salinity (ppt)	Water depth (cm)
5-May	0	-	-	(12.5 - 24.9)	(0.1 - 0.9)	(5 - 40)
1-Jun	0	-	-	(17.4 - 30.2)	(0.3 - 6.4)	(5 - 45)
14-Jun	0	-	-	(14.4 - 19.0)	(0.4 - 9.6)	(5 - 20)
28-Jun	6	*Culiseta incidens* (5), *Aedes* sp. (1)*	Dog park	15.1 (14.2 - 15.4)	0.4 (0.3 - 9.1)	20 (5 - 30)
13-Jul	0	-	-	(17.4 - 24.8)	NA	(5 - 15)
25-Jul	0	-	-	(23.4 - 29.5)	(13.4 - 18.6)	(5 - 15)
8-Aug	0	-	-	NA	NA	NA
30-Aug	0	-	-	(17.6 - 28.2)	(0.6 - 14.9)	(5 - 40)
18-Oct	25	*Culiseta incidens*	Dog Park	11.3 (11.8 - 12.4)	0.6 (1.2 - 14.9)	30 (5 - 35)

* Unable to ID to species, but lacked characteristics consistent with *A. dorsalis*

Comparison of pre- and post-restoration larval sampling. Due to our limited sampling effort and sample size, our larval sampling should be considered principally as qualitative data. However, our results suggest that restoration actions at SFC reduced potential larval mosquito habitats and that mosquito reproduction at the site also was also reduced by restoration actions.

As noted earlier, the primary motivation for our mosquito monitoring at SFC was the *A. dorsalis* outbreak that occurred after tidal marsh restoration efforts at Bandon Marsh National Wildlife Refuge along the southern Oregon coast (USFWS 2014), so assessing whether larvae of that species were present before and after restoration actions was an important objective. We did not capture any *A. dorsalis* larvae during this study and, as a result, our limited larval sampling effort suggests that the species was either not reproducing or was at least uncommon at SFC during both the pre-restoration and early post-restoration monitoring periods.

Although *A. dorsalis* was absent from our samples, we captured larvae of *A. aboriginis, Ca. incidens,* and probably *Ca. inornata*. The temporal pattern of their occurrence is consistent with reported information on these species. *A. aboriginis* was captured only during the pre-restoration monitoring period and was abundant only during April. The species occurs primarily in, and adjacent to, forested environments west of the Cascade Range, and its larvae are reported to occupy snow- and rain-fed pools in wooded and semi-wooded environments (Gjullin and Eddy 1972, Belton 1983). The

apparent absence of this species following restoration is to be expected since habitats where we captured its larvae were largely eliminated by restoration of tidal flows across SFC wetlands. *Ca. incidens* and *Ca. inornata* are both species that commonly occur throughout the Pacific Northwest and typically are active during cooler weather from fall through spring (Gjullin and Eddy 1972, Belton 1983). We captured *Culiseta* larvae during both pre-restoration (probably *Ca.* inornata) and post-restoration (*Ca*. *incidens*) sampling, but their numbers were exceptionally low during both periods. Larvae of these species can be found in fresh to polyhaline water in natural pools and anthropogenic features including ditches, containers, and abandoned swimming pools.

Although we caught mosquito larvae during two of the three years that we sampled, the number captured or observed during each of these years was small. At the SFC restoration site where extensive elevation, vegetation, soils, fish, and invertebrate sampling was conducted, we observed and captured larvae only during pre-restoration sampling in 2015. These results suggest that mosquito production at SFC was low prior to restoration and that it may have decreased further following restoration of tidal flows. All larvae captured post-restoration occurred in a single stormwater outfall at the edge of the SFC project site near the town of Tillamook, which differed substantially from most of the wetland areas restored at SFC.

We captured and observed very few larvae in remnant tidal channels, irrigation ditches, or other similar aquatic features during pre-restoration sampling, and none were captured or observed in channel habitats after tidal inundation was restored. During baseline, most larvae were captured in small, ephemeral pools in often densely vegetated emergent freshwater wetland habitats. These aquatic habitats were interspersed among the existing channel system and available during the winter/spring wet period. During drier summer and fall months, these wetland areas dried up and had no remaining surface water. The restoration effort largely eliminated this habitat type within portions of SFC by restoring tidal hydrology. Instead, the early post-restoration landscape supported numerous brackish, shallow pools during low tide within areas that varied from having dense stands of dead and dying plant material, no vegetation, or sparsely re-establishing vegetation (dependent upon location within SFC site, time since construction and other factors). These new tidally influenced aquatic habitats ranged from <1 m^2 to a hectare or more in size at low tide and were part of a contiguous flooded landscape of dozens of hectares during high tides. Mosquito larvae occupied areas where freshwater wetland vegetation was unaffected by construction activities and portions of the site disturbed and denuded by heavy equipment during restoration operations. No larvae were captured or observed in brackish ponded areas and because they were regularly flooded during high tides, they did not provide an environment conducive to mosquito reproduction.

The presence of predators and regular inundation by tides undoubtedly influenced our results. During the pre-restoration sampling period, stickleback were common but largely restricted to channel-type habitats. Post-restoration, it appeared that the channels supported more large schools, and the species was widely distributed and often abundant in the newly available tide pools on the marsh plain. These tide pools generally flooded on a daily basis, thus failing to meet the breeding requirements of *A. dorsalis*. A variety of other fish species also were present during our post-restoration work (see Chapter 7) and were restricted to channel-type habitats during our visits to the site which were timed to occur during low tides.

Our data are insufficient to fully evaluate the effects of restoration actions on water quality at our larval sample sites but do allow us to report general observations (Tables 8.1, 8.2 and 8.3). During all years, water temperatures at our sample stations were highly variable spatially and temporally. Ambient conditions (air temperature, cloud cover, etc.) influenced water temperatures and seasonal variation was apparent. Differences in pool connectivity (and tide phase), shade, and other factors likely also influenced spatial variability in water temperatures at our sample stations. Measured salinity also was quite variable during all years, but its range increased post-restoration. During all years, freshwater and lower-oligohaline conditions dominated in spring and mid- to late-fall (rainy season). During the pre-

restoration sampling period, summer (dry season) conditions ranged from fresh to upper-mesohaline but were typically low- to mid-mesohaline (~6.0 to 14.0 ppt). Post-restoration dry season conditions also were variable, but salinities were higher than during the baseline period, ranging from the upper limit of fresh to polyhaline (0.5 to 21.7 ppt). In early summer oligohaline to moderately mesohaline (~3.0 to 10.0 ppt) waters were common, and mid to upper mesohaline conditions (10.0 to 18.0 ppt) were typical as summer progressed. Before restoration, we observed some stagnant conditions conducive to mosquito reproduction. However, in general leaky tide gates or small dike breaches still provided for a muted tidal signature and water that occurred on much of the site was regularly refreshed with flow from offsite. After dike removal and channel construction/re-connection the influence of off-site flows increased, and we did not observe stagnant conditions.

Adult mosquitoes. In 2015, we captured 170 adult female mosquitoes (and one male *Cx. tarsalis*) during 10 trapping sessions (Table A8.1). Peak captures were in late June and early July with low numbers during earlier and later sampling bouts. We captured adults at each of the six repeat sampling stations with similar frequency (40 to 60 percent trap success), but two stations (BS Lower and Trib 2) accounted for nearly half of all individuals captured (48 percent).

We identified six different mosquito species in three genera in 2015, but one species (*Cx.* [*Cx.*] *tarsalis*) represented 82 percent of all captures (Table A8.1). *Cx. pipiens* accounted for approximately 11 percent of captures, but no other species accounted for >4 percent of captures. Mean captures per trap night by species for all trap nights ranged from 0.02 to 2.12, and *Cx. tarsalis* was the only species that exceeded one individual per trap night (Figure 8.6). Mean captures per trap night by species for sampling bouts in May, June and July ranged from 0.03 to 3.81, and only *Cx. tarsalis* exceeded one individual per trap night (Figure 8.7).

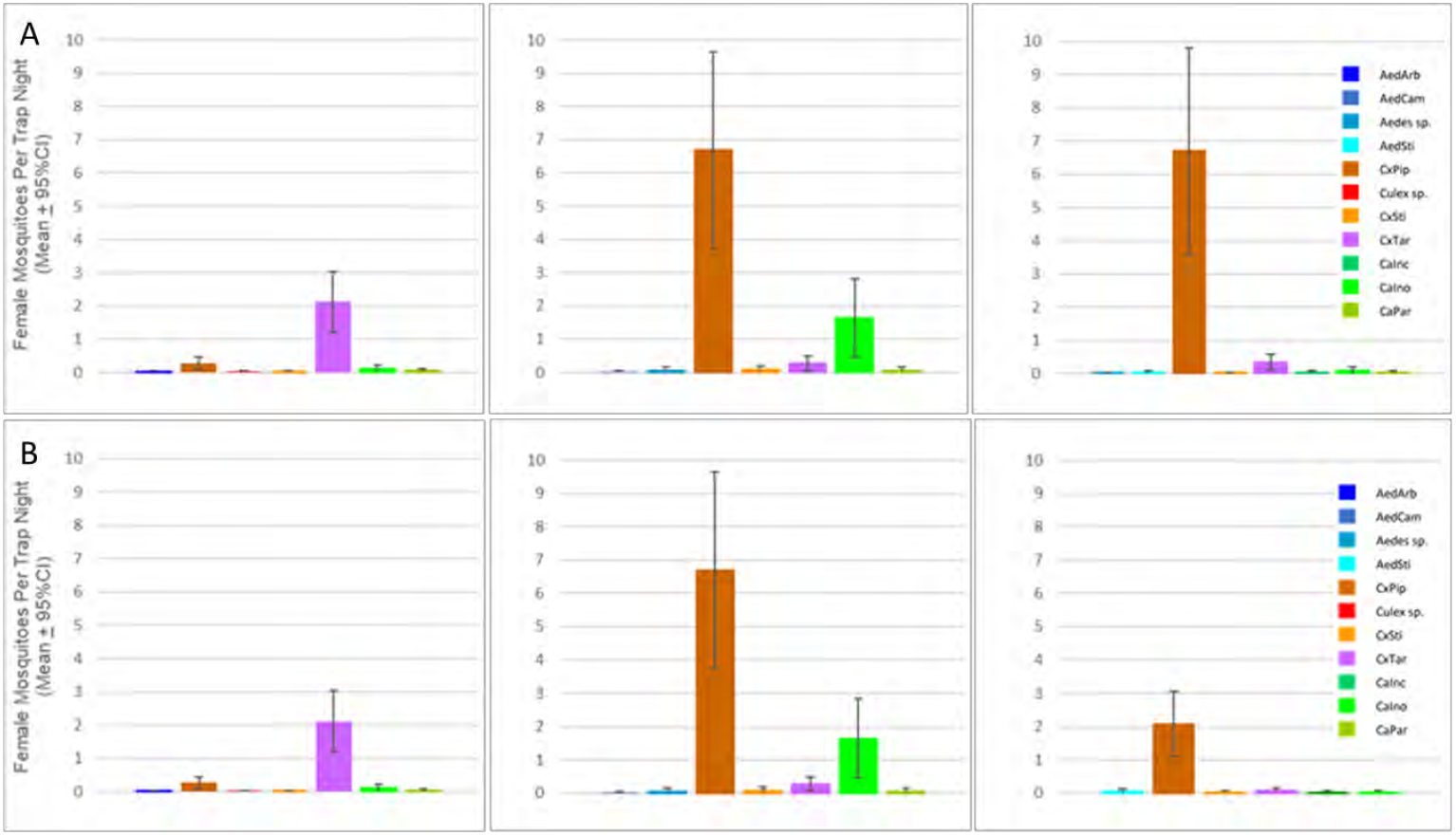

Figure 8.6. Mean adult female mosquito captures per trap night by species for all trapping dates in 2015, 2017 and 2018. A. Data from all trapping stations. B. Excludes data from 2018 Dog Park and Hospital Trail stations. See Tables 8.4-8.6 for capture data.

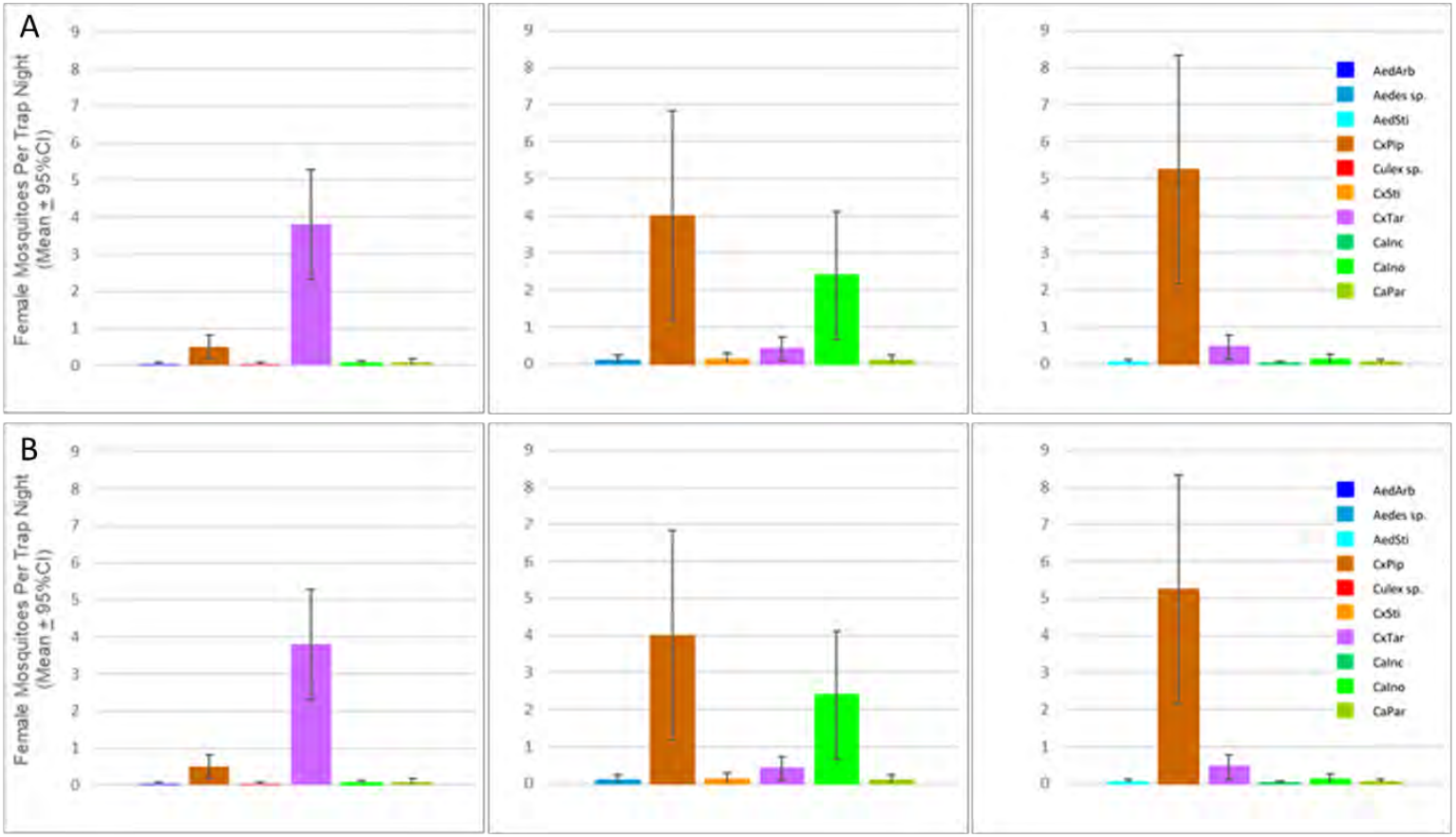

Figure 8.7. Mean adult female mosquito captures per trap night by species for May, June and July trapping dates in 2015, 2017 and 2018. A. Data from all trapping stations. B. Excludes data from 2018 Dog Park and Hospital Trail stations. See Tables 8.4-8.6 for capture data.

We captured 473 adult female mosquitoes (and three male *Aedes* sp. [probably *A. sierrensis*]) during nine trapping sessions in 2017 (Table A8.2). We consistently trapped 50 or more individuals during trapping sessions from late June to early September but captured very few individuals during spring and fall trapping bouts. We captured adults at each of the six repeat sampling stations with similar frequency (56 to 78 percent trap success). However, the total number of individuals captured at each station varied substantially (range = 42 to 150), and one station (Trib 2) accounted for nearly one-third of all captures (31.5 percent).

We identified six different mosquito species in three genera during our work in 2017 (Table A8.2). Two species (*Cx. pipiens* and *Ca. inornata*) represented 76 and 19 percent of all captures, respectively. No other species accounted for >3 percent of captures, and most accounted for less than one percent. Mean captures per trap night by species for all trap nights ranged from 0.02 to 6.69, with only *Cx. pipiens* and *Ca. inornata* exceeding one individual per trap night (Figure 8.6). Mean captures per trap night by species for sampling bouts in May, June and July ranged from 0.08 to 4.00, and *Cx. pipiens* and *Ca. inornata* were the only species exceeding one individual per trap night (Figure 8.7).

We captured 436 adult female mosquitoes (and one male *Cx. pipiens*) during 10 trapping sessions in 2018 (Table A8.3; excluding the Dog Park and Hospital Trail data brings the total number of individuals to 91, with no males). Like previous years, trapping sessions from early June to late August yielded the greatest numbers and we captured few individuals during spring and fall trapping bouts.

We captured adults at each of the six repeat sampling stations. We trapped the greatest number of adult mosquitos at the two newly established stations near urban Tillamook (Dog Park and Hospital Trail) where we trapped adult mosquitoes during 90 percent of trapping sessions at these two stations and they accounted for 79% of all captures (346 total captures). For the four stations at the SFC restoration site, trapping success ranged from 40 to 70 percent. The total number of individuals captured at each station also varied widely (range = 10 to 185).

We identified seven mosquito species in three genera (Table 8.6 – excluding Dog Park and Hospital Trail data drops the total number of species captured to six). Including Dog Park and Hospital Trail data, *Cx. pipiens* represented 92 percent of all captures (and 91 percent of all captures when data from these stations are excluded). No other species accounted for >5 percent of total captures and most accounted for less than one percent.

As noted previously for our 2018 data set, we calculated mean captures per trap night with a data set that included data from Dog Park and Hospital Trail stations and with a data set that excluded these stations. Using data from all stations and from all trap nights, mean captures per trap night by species ranged from 0.02 to 6.69. For the May-July period, mean captures by species ranged from 0.02 to 5.24 per trap night. *Cx. pipiens* was the only species exceeding one individual per trap night during either of these periods (Figures 8.6 and 8.7). With the data set that excluded Dog Park and Hospital Trail stations, captures per trap night (by species) ranged from 0.03 to 2.08 with data from all trapping sessions, and 0.07 to 1.39 captures per trap night for the May, June, and July data set. As above, only *Cx. pipiens* exceeded one individual per trap night.

Comparison of Pre- and Post-restoration Adult Sampling. Trapping is an important tool for monitoring adult mosquitoes. However, factors such as trap design, placement, location, and attractants can greatly influence trapping results (including the number of captures, species trapped, and the reproductive status of individuals captured) and it is important to recognize these factors when interpreting results of mosquito trapping programs (Collier et al. 2006, Henderson et al. 2006, Brown et al. 2014, Hesson et al. 2015). In addition, weather and climate variation can affect mosquito abundance and community composition (Wegbreit and Reisen 2000, Heft and Walton 2008). We believe it is particularly important to highlight this information here. Our study deployed a limited number of adult traps on a small number of trap nights during each of three years, we used only one type of trap and a single attractant and sampled only a portion of the SFC project site. It is possible that we failed to

capture some species that occurred in the area, or it could be that we captured some species at rates greater than their relative numbers. It is also possible that our results are a fair representation of adult mosquitoes present at SFC during the periods in which our traps were deployed. Suffice to say, it is impossible to know for sure whether our trapping results accurately represent the mosquito communities present during the three years of work reported here. In addition, it is unknown what effects weather and climate may have had on mosquito communities during the periods in which we sampled. Based on the above, care must be taken in interpreting our adult trapping results and drawing conclusions based on this work. Regardless, our trapping allows some understanding of mosquito use at SFC during baseline and early post-restoration periods and provides information on a subject that has been little studied in Tillamook County.

The authors have logged numerous hours working at SFC and other tidal wetlands around Tillamook Bay over the past decade (during all seasons). Outside of the contents of adult traps during this study, we observed few adult mosquitoes while working at SFC (and other Tillamook Bay tidal wetlands). Further, we know of no reported outbreaks of mosquitoes from the Tillamook area during the past decade. Our trapping data appear to reflect these observations and paint a picture of an area with typically low numbers of adult mosquitoes patchily distributed across the landscape.

Based on our trap data, both species richness and evenness appear low at SFC. In total we confirmed nine species in our adult trap samples (*Aedes aboriginis, A. campestris, A. sierrensis, A. sticticus, Cx. pipiens, Cx. stigmatosoma, Cx. tarsalis, Ca. incidens, Ca. inornata, and Ca. particeps*) over the course of the study, but no more than seven species were captured during any given sample year (Tables 8.5 - 8.7). Two species were trapped considerably more often than all others, but the dominant species varied among sample years. In 2015 (pre-restoration), *Cx. tarsalis* represented 82 percent of all adult captures but less than five percent of all captures in 2017 and 2018 (during- and post-restoration). Conversely, *Cx. pipiens* accounted for only 11 percent of captures in 2015 but represented 76 and 92 percent of captures in 2017 and 2018, respectively. *Ca. inornata* accounted for 19 percent of captures in 2017, but no other species accounted for >5 percent of captures during any of the three sample years.

Although *Cx. pipiens* was the dominant species captured in both 2017 and 2018, there are interesting differences in our capture results for these two years. For example, captures per trap night was similar for both years when comparing data from all sites and all dates (Figure 8.6A). However, mean captures per trap night in 2017 were considerably greater than in 2018 when comparing data only in the SFC restoration site (Figure 8.6.B). Captures per trap night for *Cx. pipiens* during the May-July period were greater in 2018 than 2017 when using data from all stations (Figure 8.7A). However, the opposite is true when 2018 data from Dog Park and Hospital Trail are excluded (Figure 8.7B). These comparisons suggest that the species may have been more abundant at the SFC restoration site in 2017 than 2018. In addition, it appears that *Cx. pipiens* abundance may have increased as summer progressed during our 2018 sampling effort.

The species we captured all have been documented from the Pacific Northwest and their relative occurrences in our trap data appear consistent with reported information (Gjullin and Eddy 1972, Belton 1983). Species most often captured in our traps are common and often abundant in the west and would be expected from Tillamook County. Those that we captured less often, while known from the PNW, are typically found outside of coastal environments or are uncommon species in general. Some of the species captured are important and well-known pests of humans (e.g., *A. sticticus, Cx. pipiens, Cx. tarsalis*), some are more occasional pests of humans or generally target other hosts (e.g., *A. sierrensis*, *Ca. incidens, Cx. stigmatosoma,*) and the adult biology of some are not well known (e.g., *A. aboriginis, Ca. particeps*). Some are “standing-water mosquitoes'' that breed in permanent or semi-permanent waters over a range of salinities, organic matter content, and level of stagnation/pollution (e.g., *Cx. tarsalis, Cx. pipiens, Ca. incidens, Ca. inornata*), while others prefer floodwaters, rain or

snowmelt pools, tree holes, and other more temporary water sources (e.g., *A. aboriginis, A. sierrensis A. sticticus*).

Population trends in Tillamook County for *Cx. tarsalis* and *Cx. pipiens* are unknown, and it is unclear what caused the shift in relative captures for these species from baseline to early post-restoration. Larvae of these two species are found in a variety of water sources and can occur alongside one another and with other species (including *Ca inornata*). *Cx. tarsalis* are found in standing water in wetlands, irrigated agricultural fields, ditches, borrow pits, sewage treatment and stockyard facilities, ornamental pools, etc., and can tolerate some organic content and pollution and salinities ranging from fresh to brackish. *Cx pipiens* larvae also tolerate a wide range of conditions and are found in settings similar to *Cx. tarsalis.* However, this species tolerates more stagnant waters with high organic content and can become particularly abundant at sewage and manure storage and treatment facilities.

While habitat conditions for larval rearing at SFC changed dramatically from 2015 to 2018, we did not document *Cx. pipiens or Cx. tarsalis* larvae at any time during our study and it seems unlikely that SFC was an important breeding ground for either species. The area surrounding SFC, on the other hand, appears to have provided suitable rearing habitats for both species throughout our study. Dairy operations with grassy pastures, open manure storage and other suitable breeding habitats were common in proximity to SFC, and urban Tillamook provided a wide variety of suitable breeding habitats. Adults of both species are capable dispersers, able to move several miles after emergence to forage and breed (Reisen et al. 1991, Reisen and Lothrop 1995, Ciota et al. 2012). Given the above, it seems likely that most adults of both species captured at SFC reared elsewhere and moved on to SFC while foraging. *Cx. pipiens* can become extremely abundant in urban areas, and this may explain the relatively high number of captures of this species at the Dog Park and Hospital Trail stations in 2018. Both stations are near a variety of potential breeding sites, including agricultural, industrial, and residential properties in or near urban Tillamook and the City of Tillamook wastewater treatment plant. We know of no substantial changes in land use in the area surrounding SFC that might help explain the shift from predominantly *Cx. tarsalis* captures in 2017 to *Cx. pipiens* captures in 2018.

Cx. tarsalis is a common summer mosquito in the PNW. It is an extremely important disease vector in western North America, having been shown to transmit a host of viral diseases including St. Louis Encephalitis, Western Equine Encephalitis and West Nile Virus as well as several strains of avian malaria (Gjullin and Eddy 1972, Belton 1983, Reisen 1993). *Cx. pipiens* is also a common summer mosquito in the PNW and an important viral disease vector, especially for St. Louis Encephalitis and West Nile Virus. *Ca. inornata* is primarily a cool weather mosquito, most often observed in late fall through spring (Gjullin and Eddy 1972, Belton 1983, W. Maffei, pers. comm.). Viral diseases have been isolated from the species, but it is not thought to be a significant human vector.

Conclusions and recommendations

The total number of mosquito larvae captured at SFC before restoration (2015) was low, suggesting that the site provided low-quality larval habitat for mosquitos. Peak larval captures occurred in the spring and only consisted of *A. aboriginis* during that period. We found that larval mosquito captures were even lower during the early post-restoration sampling period (2017 and 2018), indicating that the quality of the site for mosquito production may have declined further following restoration of tidal influence at SFC. We did not capture larvae of either *Cx. tarsalis* or *Cx. pipiens* within SFC during our study, suggesting that adults of these species reared off-site and moved into SFC after emergence from their larval habitats.

We captured more adults during early post-restoration sampling (2017 and 2018) than during baseline monitoring (2015), but the total number of adults captured was small during all years (on average, we captured <50 adults per night during 2017 and 2018 and only 17 per night during 2015).

Two species accounted for a vast majority of adult captures - *Cx. tarsalis* was most common in 2015 and *Cx. pipiens* was most common in 2017 and 2018. Mosquito species diversity was low, and we did not document *A. dorsalis* larvae or adults during our sapling at SFC – a reassuring result, since *A. dorsalis* was the specieswhich became abundant at the Bandon Marsh National Wildlife Refuge following tidal wetland restoration).

While our data suggests that mosquitoes were not abund ant at SFC immediately before or after tidal wetland restoration activities, we recommend continued monitoring efforts for several reasons. First, both *Cx. tarsalis* and *Cx. pipiens* are important vectors of human diseases, and these were by far the most captured species at SFC during our study. Monitoring abundance of larvae and adults both inside and outside SFC may help determine where new mosquitos are being produced and if SFC is a source of adult mosquitos in Tillamook Bay or if it is the final destination for dispersing adults that are produced elsewhere in the estuary or nearby urban and agricultural areas.

Second, at other tidal wetland restoration projects, habitats favorable to *A. dorsalis* reproduction developed a decade or more after restoration actions were implemented (W. Maffei, pers. comm.). Wetland elevations at SFC early post-restoration were largely below mean higher high water (see Chapter 2) and, as a result, after dike removal most of the site was flooded by the tides on a daily basis. This limited the development of potentially suitable standing water habitats for larval mosquitoes during our study. However, as soils continue to accrete and raise the wetland surface elevation at SFC, conditions favorable to *A. dorsalis* reproduction could develop if there are high elevation areas with episodic, standing brackish water.

Finally, we recommend the establishment of a continuous mosquito monitoring program in southern Tillamook Bay that includes a network of replicate monitoring stations inside SFC and in adjacent urban and agricultural areas. Given the public health significance of mosquitoes as disease vectors, it may be possible to include additional project partners to assist with funding and maintaining annual or semi-annual monitoring of mosquito abundance and species composition. We recommend exploring these potential options during subsequent monitoring efforts.

Citations

Belton P. 1983. The Mosquitoes of British Columbia. Handbook No. 41. British Columbia Provincial Museum. Victoria, B.C.

Bridgeland, WT, Brophy LS, van de Wetering S, So KJ, van Hoy R, Lowe RW, and Ledig DB. 2017. Ni-les'tun tidal wetlands restoration project: Planning, implementation, and lessons learned. U.S. Department of Interior, Fish and Wildlife Service, Region 1, Biological Technical Publication FWS/BTP-R1015-2017, Washington, DC.

Brown HE, Paladini M, Cook RA, Kline D, Barnard D, Fish D. 2014. Effectiveness of mosquito traps in measuring species abundance and composition. Journal of Medical Entomology 45:517-521.

Ciota AT, Drummond CL, Ruby MA, Drobnack J, Ebel GD, Kramer LD. 2012. Dispersal of *Culex* mosquitoes (Diptera: Culicidae) from a wastewater treatment facility. Journal of Medical Entomology 49:35–42.

Collier BW, Perich MJ, Boquin GJ, Harrington SR, Francis MJ. 2006. Field evaluation of mosquito control devices in Southern Louisiana. Journal of the American Mosquito Control Association 22:444-450.

Crans WJ. 2016. *Culex pipiens* Linnaeus. Rutgers University New Jersey Agricultural Experiment Station, Center for Vector Biology. Accessed 03/01/2020.

Gjullin CM, Eddy GW. 1972. The mosquitoes of the northwestern United States. Technical Bulletin No. 1447. USDA, Agricultural Research Service. Washington, DC.

Goddard LB, Roth AE, Reisen WK, Scott TW. 2002. Vector Competence of California Mosquitoes for West Nile virus. Emerging Infectious Diseases 8:1385-1391.

Heft DE, Walton WE. 2008. Effects of the El Niño - Southern Oscillation (ENSO) cycle on mosquito populations in southern California. Journal of Vector Ecology 33:17-29.

Henderson JP, Westwood R, Galloway T. 2006. An assessment of the effectiveness of the Mosquito Magnet Pro Model for suppression of nuisance mosquitoes. Journal of the American Mosquito Control Association 22:401-407.

Hesson JC, Ignell R, Hill SR, Östman Ö, Lundström JO. 2015. Trapping biases of *Culex torrentium* and *Culex pipiens* revealed by comparison of captures in CDC traps, ovitraps, and gravid traps. Journal of Vector Ecology 40:158-163.

Kramer LD, Reisen WK, Chiles RE. 1998. Vector competence of Aedes dorsalis (Diptera: Culicidae) from Morro Bay, California, for western equine encephalomyelitis virus. Journal of Medical Entomology 35:1020-1024.

Reisen WK, Milby MM, Meyer RP, Pfuntner AR, Spoehel J, Hazelrigg JE, Webb Jr. JP. 1991. Mark-release-recapture studies with *Culex* mosquitoes (Diptera: Culicidae) in southern California. Journal of Medical Entomology 28:357-371.

Reisen WK. 1993. The western encephalitis mosquito, *Culex tarsalis*. Wing Beats 4:16.

Reisen WK, Lothrop HD. 1995. Population ecology and dispersal of *Culex tarsalis* (Diptera: Culicidae) in the Coachella Valley of California. Journal of Medical Entomology 32:490-502.

USFWS. 2014. Draft Plan and Environmental Assessment for Mosquito Control for Bandon Marsh National Wildlife Refuge. U.S. Fish & Wildlife Service, Bandon Marsh National Wildlife Refuge.

Wegbreit J, Reisen WK. 2000. Relationships among weather, mosquito abundance, and encephalitis virus activity in California: Kern County 1990-98. Journal of the American Mosquito Control Association 16:22-27.

Chapter 9: Greenhouse gas fluxes in restored, reference, and disturbed wetlands

Scott Bridgham, Matthew Schultz, Christopher Janousek, and Laura Brophy

---

Key findings

- Methane emissions at SFC were higher on average than for reference tidal wetlands and diked farm fields, but were within the range of expected values for tidal wetlands.
- Methane emissions at SFC were highly variable but high emissions were observed only under a specific set of environmental conditions (groundwater within 10 to 20 cm of the soil surface, low salinity, warm air temperature, *and* near-neutral pH).
- High methane emissions occurred only when groundwater salinity was below about 5 PSU, considerably lower than the cut-off of about 15 PSU found in recent syntheses of other studies.
- Over 70% of variation in methane emissions could not be explained using the environmental factors we measured because of the complex set of non-linear controls and possibly other controlling factors that were not measured.
- Carbon dioxide emissions were higher when air temperatures were higher and groundwater levels were lower.
- We did not observe significant emissions of nitrous oxide (another potent greenhouse gas) at any of the sites, including former wetlands in agricultural production.

Introduction

There is increasing interest in utilizing the carbon sequestration capacity of both tidal and non-tidal wetlands as a rationale for their restoration, including the potential use of carbon credits as a funding mechanism (Galatowitsch 2009, Murray et al. 2011, Pendleton et al. 2012). Wetlands have, by far, the highest soil carbon sequestration rates per area of any ecosystem type, and tidal wetlands particularly stand out in terms of this ecosystem benefit (Laffoley and Grimsditch 2009, McLeod et al. 2011, Bridgham 2014). While naturally functioning wetlands can sequester and store large quantities of carbon, disturbed wetlands (e.g., those with altered hydrology due to diking and drainage) often lose much of their soil organic matter and elevation due to subsidence (reviewed in Chapter 2). Therefore, restoration of wetland hydrology at disturbed sites may help prevent further oxidation of soil organic matter and may also increase carbon sequestration capacity (Bridgham et al. 2006, Pendleton et al. 2012, Fargione et al 2018, Crooks et al. 2014).

However, the high rate of soil carbon sequestration by wetlands is at least partially offset by their emission of greenhouse gases (GHGs) such as methane (CH_4) and nitrous oxide (N_2O) (Bridgham et al. 2006, Moseman-Valtierra 2012, Windham-Myers et al. 2018, Shiau et al. 2019, Al-Haj and Fulweiler 2020). Over a 100 year time frame with sustained emissions, CH_4 and N_2O have a global warming potential 45 and 270 times greater than carbon dioxide (Neubauer and Megonigal 2015), so even wetlands that efficiently sequester carbon can have a net positive climate warming effect ("radiative forcing") if their CH_4 or N_2O emissions are high (Bridgham et al. 2006, Poffenbarger et al. 2011, Neubauer and Megonigal 2015, Al-Haj and Fulweiler 2020). Natural, disturbed, and restored wetlands are likely to have different biogeochemical conditions that would affect GHG fluxes, such as differences

in hydrology, salinity, soil organic matter content, pH, nutrient availability, and dominant plant communities. However, few studies have examined the effects of these environmental controls on GHG fluxes across different wetland land uses (Cornell et al. 2007, Adams et al. 2012, Pfeifer-Meister et al. 2018, Wollenberg et al. 2018).

The interacting effects of multiple environmental controls may make it difficult to predict emissions of GHGs such as methane from tidal wetlands. Methane is produced under anaerobic conditions by microbes called "methanogens" under anaerobic conditions, and is also consumed by different microbes ("methanotrophs") in the unsaturated aerobic layer of the soil column, so groundwater level is an important control over CH_4 production versus consumption (Bridgham et al. 2013, Turetsky et al. 2014, Al-Haj and Fulweiler 2020). Diked former tidal wetlands often have lower groundwater levels than least-disturbed wetlands (Chapter 4), so restoration of natural tidal hydrology could potentially increase methane emissions by raising groundwater, particularly where salinity is low. This increase could be temporary or longer-term depending on factors such as the development of channel systems in a restored site over time, and the amount of soil compaction due to past agriculture or machinery operations.

Salinity is another important factor controlling methane fluxes in estuaries. Methane production is usually low in saline soils (Megonigal et al. 2004, Bridgham et al. 2013), but there is substantial variation in the relationship between salinity and methane (Poffenbarger et al. 2011, Windham-Myers et al. 2018, Al-Haj and Fulweiler 2020), indicating the importance of other controlling factors. Some studies have found higher CH_4 emissions in soils with high carbon content, but no relationship was found in a global tidal wetland dataset (Al-Haj and Fulweiler 2020 and references therein). Since disturbed wetlands often lose soil organic matter after diking, both disturbed and restored sites may have lower CH_4 emissions than reference wetlands, all else being equal (Cornell et al. 2007). Restoration may reduce soil acidity (Janousek et al. 2021), and many methanogens are intolerant of acidic conditions (Ye et al. 2012), so this could theoretically lead to increased CH_4 emissions following restoration. Finally, plant effects on CH_4 fluxes often vary by species (Laanbroek 2010), so differences in plant community composition and productivity between different wetland types or between pre-and post-restoration periods may affect CH_4 emissions. However, in a global tidal wetland dataset no relationship was found between plant biomass or net ecosystem productivity and CH_4 fluxes (Al-Haj and Fulweiler 2020).

Wetland land use may also affect nitrous oxide fluxes. Nitrous oxide production and consumption pathways are complex, involving multiple microbial processes (Baggs 2011, Butterbach-Bahl et al. 2013) and dependent on multiple environmental factors such as nitrogen availability, soil moisture, temperature, soil organic matter content, oxygen availability, salinity, and pH (Baggs 2011, Moseman-Valtierra 2012, Butterbach-Bahl et al. 2013). As with methane, different wetland land uses likely affect many of these biogeochemical controlling factors, but their overall effect may be difficult to detect, since previous studies have shown that wetlands often have very low, and even negative, N_2O emissions except when they experience anthropogenic nitrogen loading (Moseman-Valtierra 2012).

Carbon dioxide flux when measured in the dark is the sum of above- and below-ground respiration (i.e., ecosystem respiration) due to plants, invertebrates, and microorganisms. Ecosystem respiration is a central component of the total carbon budget for an ecosystem, but it does not include CO_2 uptake due to photosynthesis. Ecosystem respiration also does not include dissolved or particulate exchanges of organic matter in and out of the ecosystem (Chapin III et al. 2011), and therefore it does not equal the net ecosystem carbon balance. Ecosystem respiration is primarily controlled by factors such as plant community composition and biomass, soil organic matter content, temperature, and groundwater level (Chapin III et al. 2011). In wetlands, higher respiration (and thus higher CO_2 emissions) would be expected with greater plant biomass and soil organic matter, and when groundwater levels are lower (Bridgham and Richardson 1992, Bubier et al. 2003, Moffett et al. 2010). Diked former tidal wetlands often have a lower water table compared to least-disturbed tidal wetlands

(Brown et al. 2016, Brophy et al. 2014), which may enhance respiration, but this may be offset by lower soil organic matter content. Many diked former tidal wetlands have subsided enough to become mudflats once they are restored (Adams et al. 2012), so the low vascular plant biomass may lead to low respiration. Thus, as with CH_4 and N_2O fluxes, it is not clear how land use and restoration might affect CO_2 fluxes because of multiple, potentially counteracting, effects of environmental controls on these processes.

With variable land-use/land-cover types across the restoration project and in nearby areas in Tillamook Bay, the SFC restoration project presented a valuable opportunity to investigate the effects of land use, including tidal wetland diking and restoration, on GHG flux in estuarine wetlands. In this study, we addressed the following questions: What is the relative importance of ecosystem drivers such as groundwater level, temperature, and salinity on GHG fluxes in restored tidal wetlands at SFC, nearby least-disturbed tidal wetland reference sites, and adjacent disturbed wetlands (diked pastures) in Tillamook Bay? How do GHG fluxes vary among different wetland classes (least-disturbed, diked, restored)?

Materials and methods

Sample design. We established 12 GHG sampling stations across SFC, reference tidal marshes, and disturbed wetlands (diked pastures, formerly tidal wetlands) near the SFC site. Six sampling stations were spatially distributed across SFC and reflected the diverse pre-restoration land-use/land-cover conditions present throughout the 179 ha restoration site (Figure 9.1, Table 9.1). Prior to restoration in 2016-2017, SFC stations A004, A009, A016, and A037 were in areas of wet abandoned pasture (non-tidal freshwater marsh; “N” and “M” zones) and were dominated by reed canarygrass (*Phalaris arundinacea*) and other species (see Chapter 5). Stations A028 and A073 were in a heavily-ditched cropped area (“CR” zone) managed for hay production before restoration. At the time of sampling in 2017-2018, the northernmost station (A004; “N” zone) was dominated by cattail (*Typha* sp.), while the rest of the stations at SFC were dominated by reed canarygrass and slough sedge (*Carex obnupta*).

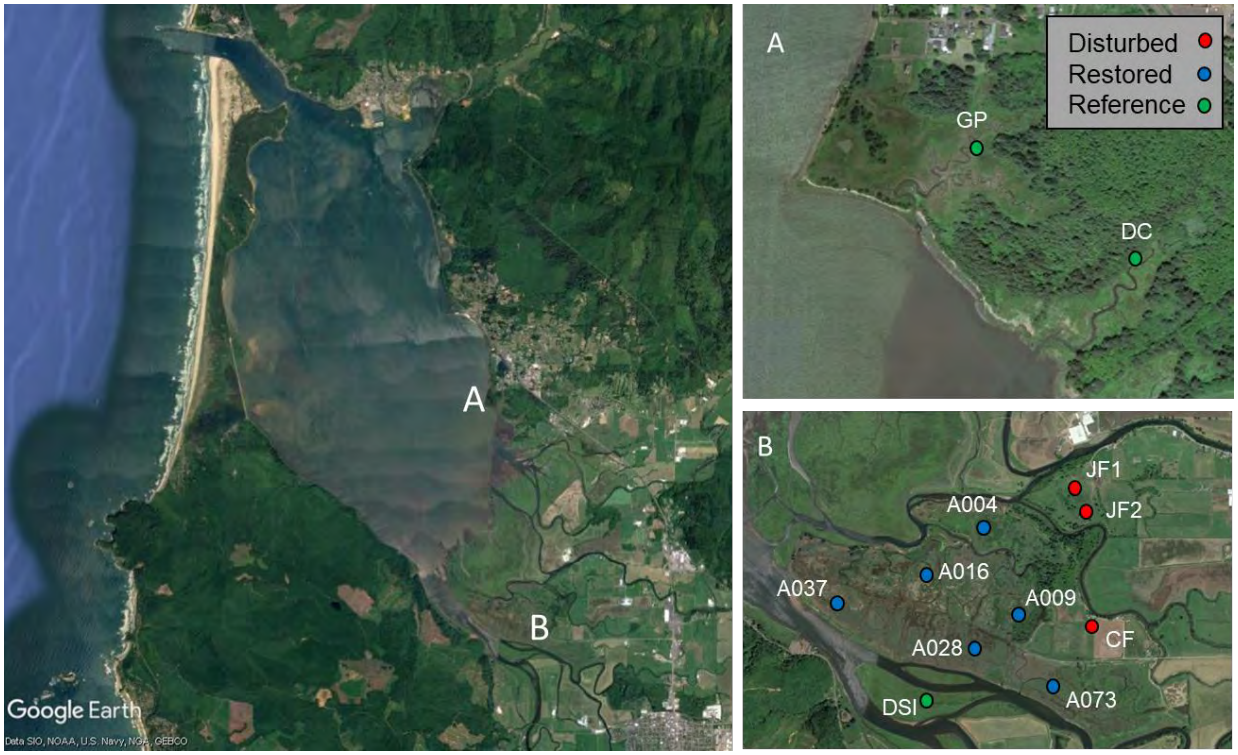

Figure 9.1. GHG sampling stations in Tillamook Bay. Image on the left shows the location of overall sampling sites. At right, areas labeled A on B in the left image are expanded to show locations of the individual disturbed restored, and reference marsh sampling stations. Images from Google Earth, data from SIO, NOAA, U.S. Navy, NGA, GEBCO.

Table 9.1. Greenhouse gas sampling stations, land use type, location (in UTM 10N), and elevation (mean ± standard deviation). Geodetic elevation is in the North American Vertical Datum of 1988 with geoid 12A (NAVD88); standardized tidal elevation (z*) is relative to tidal datums determined at the NOAA Dick Point tidal station in southern Tillamook Bay.

GHG station	Land use type (and zone)	Easting (m)	Northing (m)	Elevation (m, NAVD88)	Elevation (z*)
CF	Disturbed	432174	5035760	2.09 (0.03)	0.66 (0.03)
JF1	Disturbed	432047	5036687	2.25 (0.04)	0.82 (0.04)
JF2	Disturbed	432114	5036525	2.29 (0.03)	0.85 (0.03)
SFC, A004	Restored (N)	431483	5036418	2.20 (0.03)	0.77 (0.03)
SFC, A009	Restored (M)	431675	5035887	1.90 (0.05)	0.48 (0.05)
SFC, A016	Restored (M)	431088	5036147	1.94 (0.05)	0.52 (0.04)
SFC, A028	Restored (CR)	431379	5035698	1.96 (0.03)	0.54 (0.03)
SFC, A037	Restored (M)	430557	5036003	2.03 (0.02)	0.61 (0.02)
SFC, A073	Restored (CR)	431947	5035422	2.32 (0.06)	0.88 (0.06)
Doty Creek (DC)	Reference (HM)	431308	5039695	2.44 (0.03)	0.99 (0.03)
Dry Stocking Isl. (DSI, A043)	Reference (HM)	431170	5035374	2.60 (0.02)	1.15 (0.02)
Goose Point (GP, A068)	Reference (HM)	430956	5039932	2.63 (0.03)	1.18 (0.03)

We established GHG sampling stations at three high marsh reference sites. Two of these stations (Goose Point and Dry Stocking Island) were monitored for elevation, soil accretion, soil composition, shallow groundwater level, groundwater salinity, and vegetation (see Chapters 2, 4, 5). The Doty Creek station was added for this GHG study; groundwater level, groundwater salinity, and elevation were measured here, but not accretion, soils, or vegetation (Chapter 4). Dry Stocking Island (Figure 9.1) is located just south of the SFC restoration. Goose Point and Doty Creek marshes are north of the SFC site (Figure 9.1). Dominant plants at the reference marsh stations were tufted hairgrass (*Deschampsia cespitosa*), Pacific silverweed (*Potentilla anserina*), and creeping bentgrass (*Agrostis stolonifera*).

Bordering the SFC restoration to the north and east are three private farm fields that we used as our disturbed (diked) former tidal wetland sites. These farms were converted from tidal wetlands (Sitka spruce swamp according to Hawes et al. 2018) to agricultural fields through diking and draining in the early 1900's (C. Allen personal communication 2017; J. Thorne personal communication 2017). The southernmost disturbed site (CF) is a farm field that was protected by a setback dike constructed as part of the SFC restoration project. All fields were used for hay production, and fields surrounding stations JF1 and JF2 were also grazed by cattle during the study period.

Gas sampling. At each station we sampled six replicate chambers for greenhouse gas fluxes over the course of a year. In order to avoid trampling that could influence gas release from the soil, we installed three 2.4 m long wood boardwalks at each station with two chamber bases at each end of each boardwalk (Figure 9.2). Bases were left in place in the wetlands throughout the duration of the study. We used two types of chambers made out of PVC in this experiment (28.5 cm diameter by 27 cm height and 39.5 cm diameter by 34 cm height). The chambers excluded light, allowing dark measurements of GHG flux. Sampling occurred eight times from October 2017 to September 2018, corresponding with a period 1-2 years following restoration at SFC, to determine seasonal change and estimate yearly GHG fluxes. We sampled over the complete tidal cycle on each visit for most stations, but this could not be done for three stations because of access issues or because water was too deep with our fixed chamber bases. A floating chamber was crafted by adhering Styrofoam to the exterior of the chamber to sample GHG at high tide on September 29-30, 2018 at these three stations. We compared GHG fluxes with low tide measurements from approximately one month earlier (Aug. 31 - Sept. 2) at these stations to determine if sampling at low tide only significantly biased our estimates.

We measured CO_2, CH_4, and N_2O fluxes within the dark chambers in the field with a portable Fourier-transform infrared (FTIR) gas analyzer (Gasmet DX4040, Vantaa, Finland) in a closed-loop configuration. At each chamber, gas concentrations were measured 10 times per second for 10 minutes and averaged every 30 seconds. Values during the first 90 seconds of a measurement were discarded to avoid anomalies in headspace concentrations due to the pressure disturbance of placing the chamber tops on, yielding approximately 17 values per chamber to determine rates. Gas fluxes that did not yield a significant change in concentration ($P < 0.05$) after 10 minutes were below our detection limit and given a value of zero.

Figure 9.2. Field measurements of greenhouse gas emissions: (A) boardwalk, two chamber bases, and small groundwater well installed in high marsh at Dry Stocking Island, and (B) chamber top placement on one of the chamber bases at a disturbed agricultural site. Photos by C. Janousek.

Environmental variables. At each chamber, we took point measurements of air temperature and soil temperature at 10 cm depth during each sampling period when chamber fluxes were measured. We also measured shallow groundwater level, groundwater salinity, and pH in small shallow (30 cm) and deep (85 cm) groundwater wells constructed from 2 cm diameter PVC pipes located next to each boardwalk. We extracted a groundwater sample for analysis in the field with a refractometer and portable pH analyzer. We generally used the shallow wells to obtain the salinity and pH samples, but when groundwater was greater than 30 cm below the soil surface, we used the deeper wells for salinity and pH samples. In addition to these point-in-time measurements, nearby dataloggers recorded groundwater level and groundwater salinity at each GHG station continuously (see Chapter 4).

In September 2018, to assess the correlation between sulfate concentration and salinity, we extracted groundwater from the wells at each boardwalk, passed the sample through a 0.7 µm glass fiber filter, and put it on ice before storing it frozen at the University of Oregon. Soil pore water samples were analyzed by the University of California, Davis Analytical Laboratory for sulfate via ion chromatography.

Six of the twelve gas flux stations had soil carbon and nitrogen content data from an elemental analyzer already available (Peck 2017). At these stations, we averaged all values within the first 15 cm of a 50 cm deep core to estimate percent carbon. At the remaining six stations, we took six 0-15 cm deep replicate soil cores with PVC cores (5 cm diameter, 15 cm length) during the summer of 2018. We removed roots by hand and homogenized the remaining soil by drying for at least 48 hours at 60 °C and grinding with a pestle and mortar. Percent carbon and nitrogen were determined on a Costech Analytical Technologies 4010 elemental combustion analyzer (Valencia, CA, USA).

Statistical analyses. We performed analyses using the R v.3.6.3 statistical package with RStudio 1.2.5042. Given the many zero values in the dataset, CH_4 and N_2O fluxes could not be transformed to approximate a normal distribution, so we used nonparametric statistics to estimate the contribution of environmental predictor variables to GHG fluxes. Classification and Regression Trees (CARTs) and Random Forests are superior to traditional linear techniques in explaining complex, non-linear relationships, such as we observed between GHG fluxes and environmental variables in this study (James et al. 2013). CARTs provide easy visualization using a "tree" structure that shows relationships between the dependent variable (GHG flux in our case) and the explanatory variables (environmental controls). Each "branch" in the tree is based upon the controlling factor that best breaks measurements of the dependent variable into two groups, and this splitting is continuously iterated. The starting point is termed the "root" and the endpoints of the branches are termed "leaves". To keep the model from overfitting the data, the tree is pruned to eliminate nodes that provide little explanatory power. Random forests average over many decision trees and, thus, provide a more robust evaluation of the relative effect of the environmental variables on GHG fluxes. However, random forests improve accuracy at the expense of interpretability, and thus, we used both methods here.

We used the R packages "rpat" to create Classification and Regression Trees (CARTs) and "party" to create tree plots. Independent variables in the CARTs were groundwater level, soil and air temperature, groundwater pH and salinity, soil carbon and nitrogen, and land use type (reference, restored, disturbed). CARTs were pruned by determining the split that provided substantial increases in model correlation (James et al. 2013). We also ranked the importance of environmental predictors on GHG fluxes with random forests generated with the R package "randomForest". The relative importance of the variables was determined by the relative effects of each variable on the mean square error of the model (i.e., the "accuracy" method). The "tuneRF" routine was used to determine the optimal number of variables to sample at each split. Results of the randomForest were summarized with the R package "randomForestExplainer". We also visualized the relationship of individual environmental variables to GHG fluxes with scatterplots and standard parametric least-squares regression using "ggscatter" in the "ggpubr" package.

To test the effect of land use type on GHG fluxes, we used nonparametric Kruskal-Wallis one-way ANOVA with pairwise comparisons performed with Wilcoxon rank sum test using "kruskal.test" and "pairwise.wilcox.test" functions in R. Means and 95% confidence intervals for GHG fluxes by each land use type were calculated by 10,000 bootstrapped iterations of the data using the "infer package". We did this both on point fluxes and on annual fluxes, which were estimated by linearly interpolating measurements between sampling points over the course of the year.

Results

Environmental data. The effects of the restoration on soil and hydrologic properties at SFC are extensively analyzed in Chapters 2 and 4 of this report and in Janousek et al. (2021), and thus are only summarized here in the context of the GHG fluxes.

The three reference stations were all high marshes, with an elevation at or above mean higher high water (Table 9.1) and groundwater that was generally below the surface, even at high tide (Table 9.2). The disturbed stations were diked and partially drained, so their average water depth was greater than 28 cm below the surface, but all experienced substantial periods of saturated soils and sometimes standing water in the rainy season, from about November to May. The restored stations at SFC (with the exception of A073) had much lower elevations than reference stations (Table 9.1) and, therefore, more frequent tidal inundation and higher groundwater (Table 9.2). One restored station in the middle zone (A009) was the only location to have standing water above the wetland surface throughout the year (see

Figure 4.20).

The disturbed pasture stations were all largely freshwater with an average salinity < 1 PSU, as were SFC stations before restoration (Janousek et al. 2020). Following restoration, restored stations increased in salinity to varying degrees based on their location within SFC; salinities were also higher in the summer and fall (see Chapter 4). Station A004 at SFC had the lowest salinity (average 4.7 PSU) of all reference and restored locations, but salinities at these stations ranged from ≤6 to >20 during the sampling period (Table 9.2). All restored and disturbed stations had groundwater pH that was slightly acidic (6.1 to 6.8), but reference marshes tended to have somewhat higher pH (6.8 to 7.3). Surface soils across SFC experienced an increase in pH following restoration of up 1.0 unit (Chapter 2; Janousek et al. 2021). Soil carbon in the surface 15 cm was substantially higher in reference high marshes at Goose Point (average = 30.0%) and Doty Creek (average = 14.9%) than other locations (range of 4.9 to 9.3%). The disturbed sites had somewhat lower soil carbon (4.9 to 5.9 %) than the restored sites (6.4 to 9.3%).

Table 9.2. Physicochemical characteristics at each GHG sampling station. Mean values (+ standard deviation) over the course of a year are shown for point measurements taken when gas emissions were measured. For groundwater depth, positive values indicate surface inundation while negative values indicate groundwater below the soil surface. Some soil carbon and nitrogen data are from Peck (2017) and only site averages are available for these stations.

Site	Land Use	Sample size	Soil temp (°C)	Air temp (°C)	Groundwater depth (cm)	pH	Salinity (psu)	Soil carbon (%)	Soil nitrogen (%)
CF	Disturbed	42	12.4 (3.9)	15.5 (5.4)	-37.0 (26.1)	6.8 (0.4)	0.5 (0.9)	5.8 (0.6)	1.1 (1.0)
JF1	Disturbed	42	12.6 (5.1)	14.1 (5.9)	-29.2 (31.5)	6.6 (0.2)	0.6 (0.9)	4.9 (1.3)	1.0 (0.8)
JF2	Disturbed	42	12.3 (4.5)	12.1 (6.3)	-28.3 (31.8)	6.4 (0.3)	0.4 (0.7)	5.9 (0.8)	1.2 (0.9)
A004	Restored	45	11.5 (3.4)	16.9 (8.8)	-3.8 (11.2)	6.1 (1.0)	4.7 (5.0)	8.6	0.7
A009	Restored	42	12.4 (4.6)	15.2 (6.1)	9.7 (7.0)	6.5 (0.5)	8.0 (7.7)	9.3	0.7
A016	Restored	24	13.8 (4.2)	17.5 (3.6)	5.9 (4.3)	6.4 (0.3)	14.3 (8.2)	8.6 (1.6)	1.5 (0.6)
A028	Restored	24	15.0 (4.0)	16.8 (2.9)	-0.5 (3.1)	6.5 (0.8)	10.8 (9.0)	6.6	0.5
A037	Restored	42	12.4(4.5)	13.8 (4.0)	0.9 (5.1)	6.6 (0.7)	12.9 (8.0)	7.0 (0.5)	1.2 (0.7)
A073	Restored	39	11.7 (4.4)	16.3 (6.9)	-32.5 (26.3)	6.7 (0.5)	9.9 (8.7)	6.4	0.5
DC	Reference	45	12.0 (3.8)	15.1 (6.8)	-19.0 (14.8)	6.8 (0.6)	8.0 (5.1)	14.9 (4.1)	1.5 (0.7)
DSI	Reference	42	11.6 (3.8)	13.8 (5.5)	-37.6 (25.2)	7.1 (0.5)	11.3 (5.3)	7.1	0.5
GP	Reference	42	11.7 (4.1)	13.8 (8.2)	-22.7 (12.2)	7.3 (0.4)	13.9 (5.1)	30.0	2.1

GHG fluxes, methane. Using the controlling factors we measured (groundwater level, soil and air temperature, groundwater pH and salinity, soil carbon and nitrogen, and land use type), the CART model explained 28% of the variation in CH_4 fluxes (Figure 9.3), and the random forests model explained 23% of the variation ($P < 0.001$, Table 9.3). Over 70% of the variability in CH_4 emissions could not be explained by the controlling factors we measured, indicating the complex, nonlinear interaction of the controlling factors and there may be other important, but unmeasured, controlling factors (see Discussion below).

Among the controls we measured, the factors that showed the greatest relationship to GHG fluxes were groundwater level, air temperature, pH, and groundwater salinity (Figure 9.3). Methane fluxes were greatest when groundwater was close to the surface (≥ -1.5 cm) and at warm air

temperatures (> 24.3 °C) (mean = 21.9 μmol m^{-2} min^{-1}). At cooler air temperatures, high CH_4 emissions (mean = 18.9 μmol m^{-2} min^{-1}) still occurred when groundwater and pH were high (water table ≥ 1.5 cm, pH > 7.0) and salinity was low (< 2.5 PSU). Under other conditions CH_4 emissions were quite low (mean < 0.5 μmol m^{-2} min^{-1}). Based upon importance values (Table 9.3) and mean minimum depth of nodes (Appendix, Figure A9.1), the most important environmental variable controlling methane flux was groundwater level, followed by air temperature, soil temperature, and salinity or pH. The model showed that there was an interactive effect of high groundwater levels and warm air temperatures on maximum predicted CH_4 emissions (Figure 9.4).

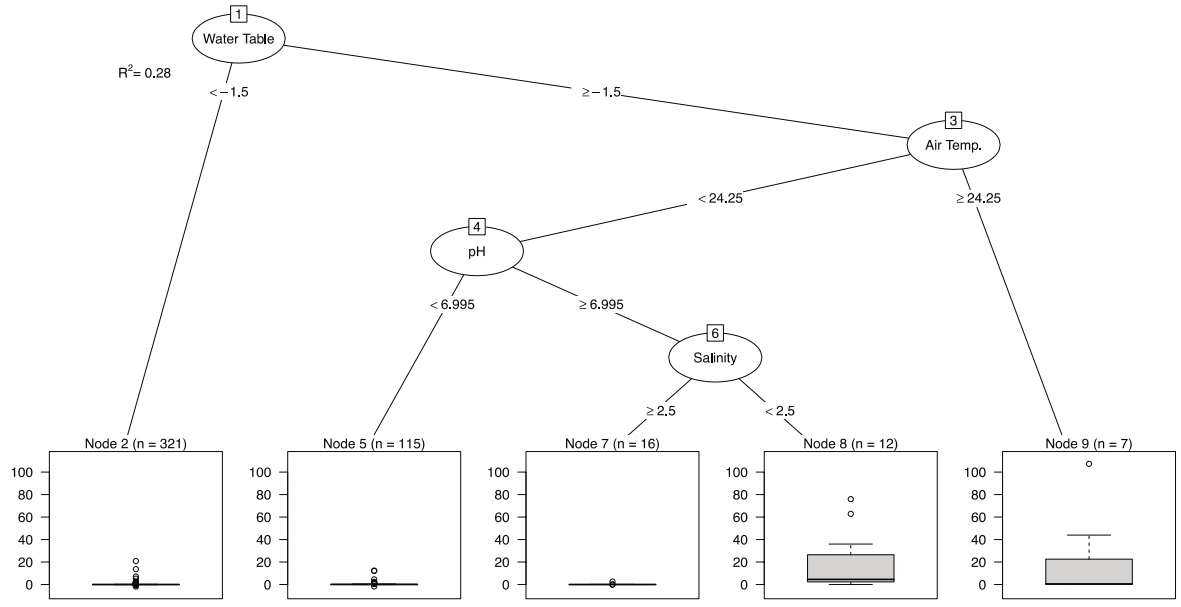

Figure 9.3. Classification and regression tree (CART) model showing the effects of major environmental predictors on CH_4 fluxes in Tillamook Bay wetlands. Top portion of figure shows the tree "branches" which split observations into groups based on the measured environmental controls (groundwater level [water table] in cm relative to soil surface; air temperature in °C; pH; and salinity in PSU). Bottom portion of figure shows a box and whisker plot of CH_4 emissions (μmol m^{-2} min^{-1}) for each group or "node" identified in the model.

Table 9.3. Relative importance of different environmental predictors of three greenhouse gas fluxes as the percent increase in each random forest mean square error when the variable is removed from the model. The top two most important variables for each model are in bold.

	Greenhouse gas		
Environmental Predictor	CH_4	CO_2	N_2O
Groundwater level	**15.7**	**27.7**	5.1
Air temperature	**14.6**	**20.9**	4.8
Soil temperature	13.3	17.2	**6.3**
Groundwater salinity	11.4	16.0	**6.3**
pH	9.1	14.9	-0.4
Land use	5.5	13.9	2.7
Soil carbon	5.5	12.2	3.9
Soil nitrogen	3.8	8.5	1.9
Total % variance explained	22.8	62.2	0.0
Model P-value	< 0.001	< 0.001	0.002

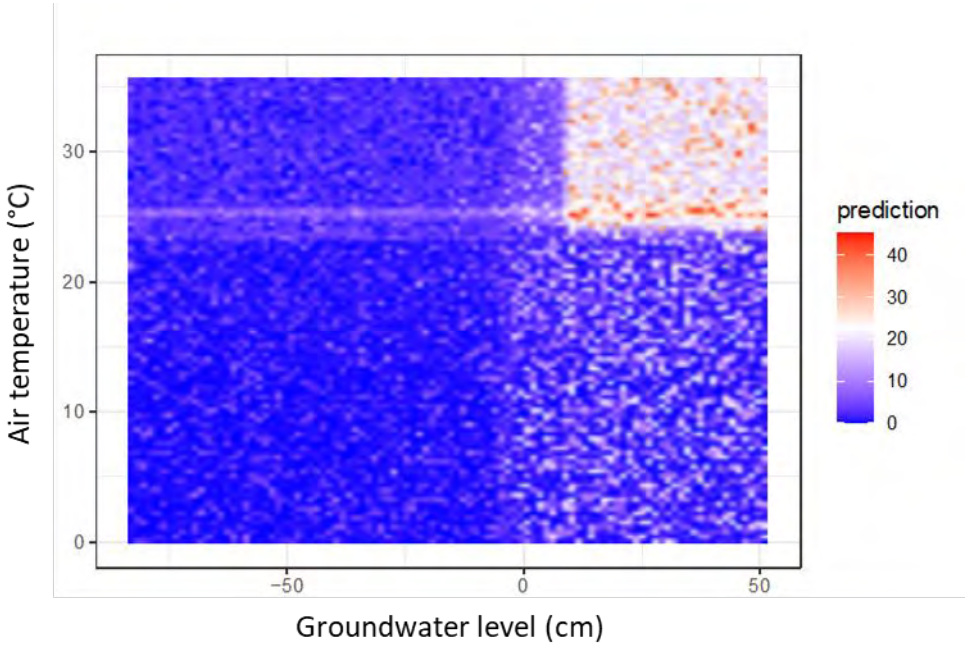

Figure 9.4. Random forest predictions (500 simulations) of instantaneous CH_4 flux (μmol m^{-2} min^{-1}) across gradients of the two most important environmental predictors, air temperature and groundwater level.

Scatterplots between methane and individual environmental drivers (Figure 9.5) demonstrated the highly non-linear and interactive nature of the effect of environmental controls on CH_4 fluxes, and illustrate that the range of favorable conditions for CH_4 emissions is greater than the single cut-off value identified in the CART model. Large CH_4 emissions only occurred when the groundwater level was between -20 and +10 cm, at salinities < 5 PSU, pH > 6.0, and warm temperatures, but low CH_4 fluxes occurred if any of these factors were unfavorable for CH_4 production.

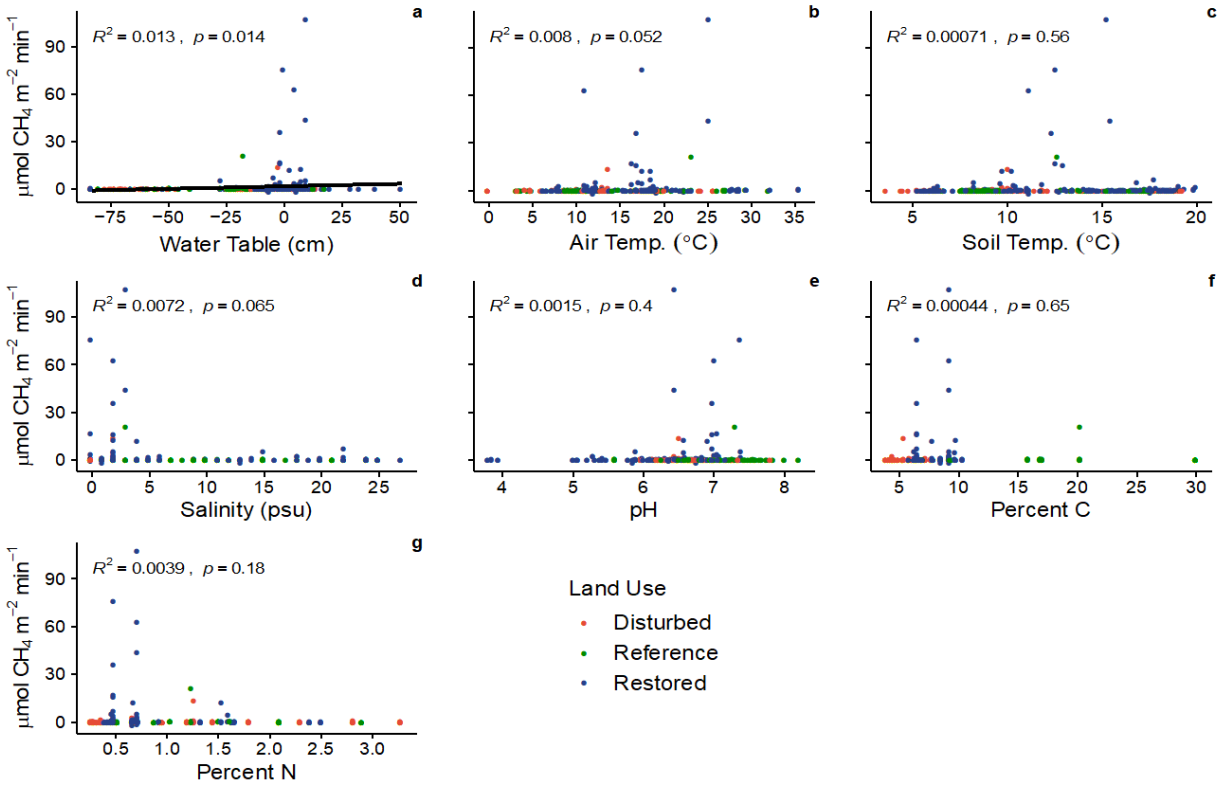

Figure 9.5. Scatterplots of relationships between instantaneous CH_4 fluxes and key environmental variables in Tillamook Bay wetlands including groundwater level ("water table"), air and soil temperature, groundwater salinity and pH, and soil percent carbon and nitrogen.

Restored wetlands had about an order of magnitude greater instantaneous and annual CH_4 fluxes than disturbed and reference wetlands ($P < 0.001$, Table 9.4). However, there was large variation in CH_4 fluxes among restored stations, with station A028 having particularly high emissions and stations A037 and A073 having low emissions (Figure 9.6).

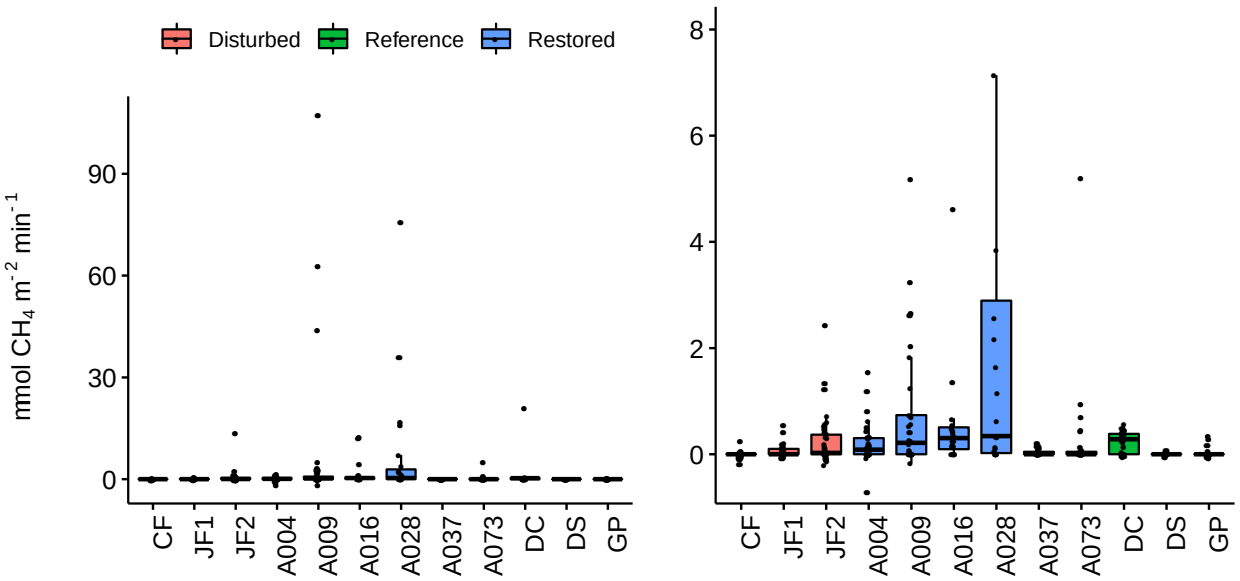

Figure 9.6. Boxplots of methane fluxes in disturbed (diked) former tidal wetlands, reference high marsh, and restored SFC wetlands (dots are individual observations, horizontal line is median, colored area is the upper and lower quartile, whiskers are 1.5 times the interquartile range). Note that the panel on the right has a reduced y-axis to better show the majority of the data points.

Table 9.4. Instantaneous and estimated annual fluxes (mean, median (± 95% confidence limits)) of CH_4, CO_2, and N_2O across land uses using 10,000 bootstrapped estimates. Different letters indicate significant differences among land uses at $P < 0.05$ using Kruskal-Wallis and Wilcoxon rank sum tests.

		Greenhouse gas		
Flux	Land use	CH_4	CO_2	$N_2O \times 10^3$
Instant-aneous (µmol m^{-2} min^{-1})	Disturbed	0.201, 0.000 (0.06, 0.45) b	248, 225 (215, 282) a	3.43, 0.00 (2.2, 4.8) a
	Restored	2.095, 0.048 (0.87, 3.67) a	136, 67 (108, 169) b	7.72, 0.00 (4.7, 10.8) a
	Reference	0.243, 0.000 (0.06, 0.58) b	271, 212 (231, 317) a	-1.85, 0.00 (-7.8, 1.9) b
Annual (mol m^{-2} yr^{-1})	Disturbed	0.111, 0.026 (0.03, 0.25) b	129, 125 (115, 145) a	1.70, 1.52 (1.2, 2.3) b
	Restored	1.509, 0.149 (0.06, 2.54) a	70, 33 (51, 92) b	3.62 , 3.36 (2.3, 5.0) a
	Reference	0.134, 0.000 (0.01, 0.35) b	148, 149 (132, 165) a	-1.01, 0.00 (-4.2, 1.0) c

GHG fluxes, carbon dioxide. The CART model explained 46% of the variation in CO_2 emissions (ecosystem respiration) and showed that fluxes were controlled by an interaction between air temperature and groundwater level (Figure 9.7). Respiration was greatest when the air temperature was greater than 26°C (mean = 654 µmol m^{-2} min^{-1}) and it was almost an order of magnitude lower (mean = 85 µmol m^{-2} min^{-1}) at cooler air temperatures and when groundwater was relatively close to the surface (> -14.5 cm). Intermediate respiration rates occurred at cooler air temperatures and under drier soil conditions, with another cutoff at 9.4°C soil temperature. The random forests model explained 62% of the variation in respiration (Table 9.3) and produced a hierarchy of controlling variables similar to the

CART model. Air temperature or groundwater level were the most important predictive environmental variables depending on the metric used (Table 9.3, Appendix Figure A9.2), followed by soil temperature and salinity. Lower groundwater levels and warmer air temperatures interacted to maximize soil respiration according to the random forest results (Figure 9.8). In individual linear regressions between CO_2 and environmental drivers, respiration was significantly linearly correlated with groundwater level ($R^2 = 0.15$, $P < 0.001$), air temperature ($R^2 = 0.22$, $P < 0.001$), soil temperature ($R^2 = 0.08$, $P < 0.001$), salinity ($R^2 = 0.04$, $P < 0.001$), and percent soil carbon ($R^2 = 0.02$, $P = 0.002$) (Figure 9.9).

Overall, instantaneous and annual soil respiration fluxes in restored wetlands were about half as high as rates in the disturbed and reference wetlands (Table 9.4).

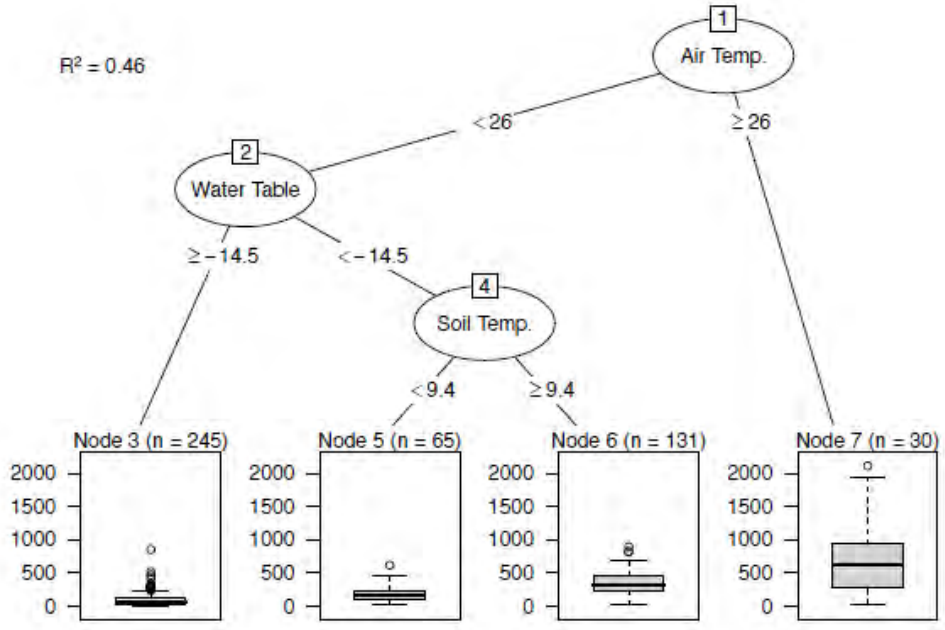

Figure 9.7. Classification and regression tree model showing the effects of environmental predictors on CO_2 fluxes in Tillamook Bay wetlands. Top portion of figure shows the tree "branches" which split observations into groups based on the measured environmental controls (groundwater level [water table] in cm relative to soil surface; air and soil temperature in °C). Bottom portion of figure shows a box and whisker plot of CO_2 emissions (μmol m^{-2} min^{-1}) for each group or "node" identified in the model.

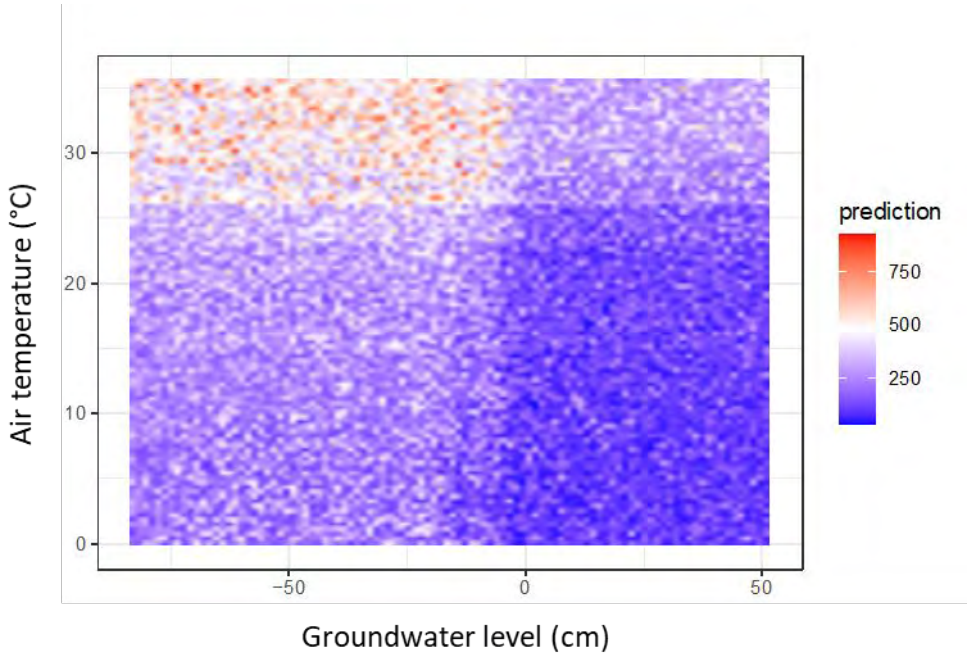

Figure 9.8. Random forest model predictions of instantaneous CO_2 flux rates (µmol m^{-2} min^{-1}) across gradients of the two most important environmental predictors, air temperature and groundwater level.

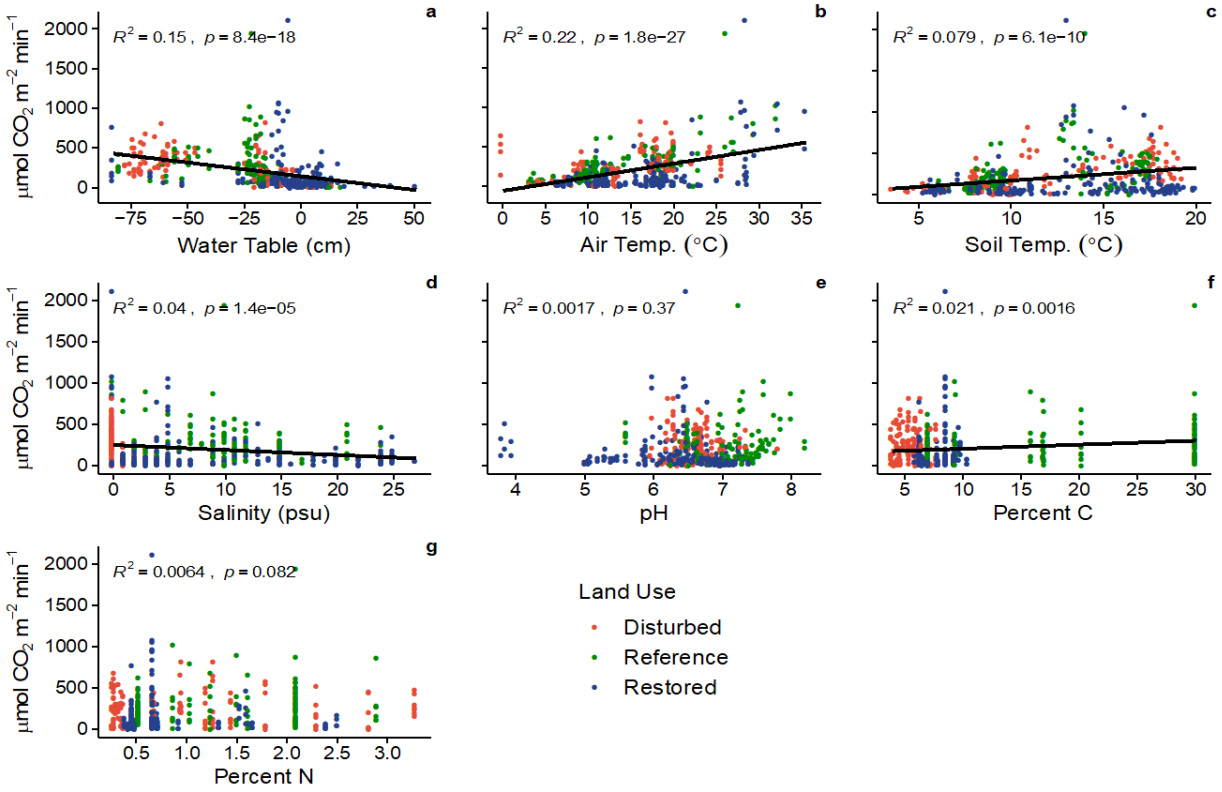

Figure 9.9. Scatterplots of relationships between instantaneous CO_2 fluxes and key environmental variables in Tillamook Bay wetlands including groundwater level ("water table"), air and soil temperature, groundwater salinity and pH, and soil percent carbon and nitrogen.

GHG fluxes, nitrous oxide. N_2O fluxes were low and often below our level of detection and, hence, given a value of zero. In fact, the median flux value was zero. These data show that N_2O fluxes were low across all wetland classes we examined, suggesting that in Tillamook Bay wetlands nitrous oxide emissions may be much less important to overall greenhouse gas production than methane. Non-zero N_2O flux values were both positive and negative, indicating both a net flux out of and into the soil, respectively. The CART model explained 21% of the variation in N_2O fluxes (Figure 9.10) but the random forests explained almost no variation (R^2 = 0.0, Table 9.3), indicating that the global fit of the environmental data to the fluxes was very poor. In individual linear regressions, there were significant positive correlations of N_2O fluxes with soil temperature and salinity and negative correlations with pH and percent carbon, although the explanatory power was always very low (R^2 < 0.04, Figure 9.11).

Despite the low N_2O fluxes, we did find significant differences in instantaneous fluxes among land use types, with the reference wetland stations having a flux that was significantly less than the disturbed and restored wetlands (Table 9.4). When rates were annualized, the restored stations had the highest (but still low) positive flux, disturbed sites had a low positive flux, and the flux in reference sites was not significantly different than zero.

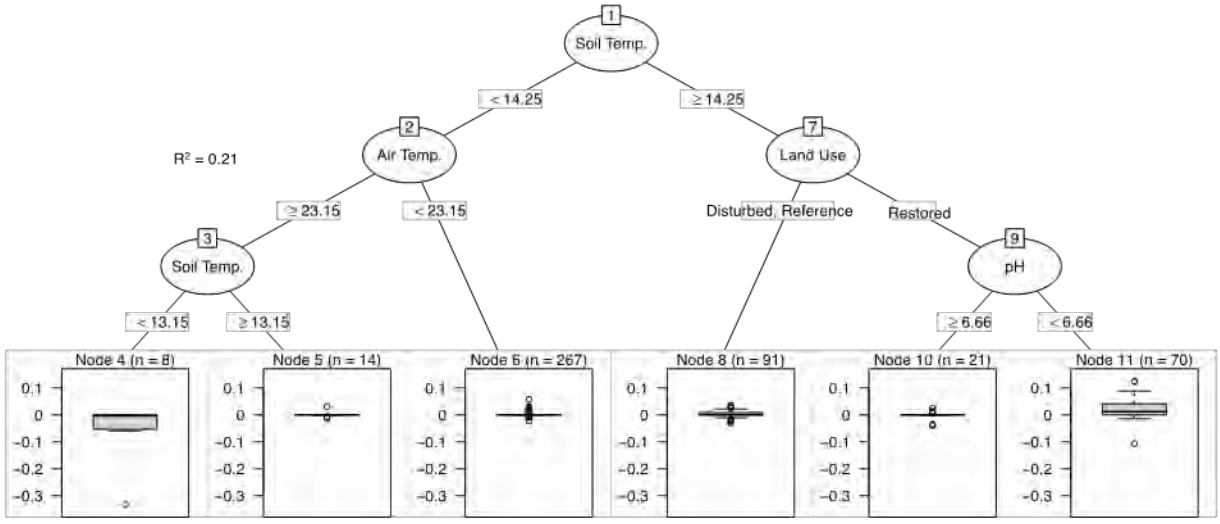

Figure 9.10. Classification and regression tree of the effects of environmental predictors on N_2O fluxes in Tillamook Bay wetlands. Top portion of figure shows the tree "branches" which split observations into groups based on the measured environmental controls (air and soil temperature in °C, land use, and pH). Bottom portion of figure shows a box and whisker plot of N_2O emissions (μmol m^{-2} min^{-1}) for each group or "node" identified in the model.

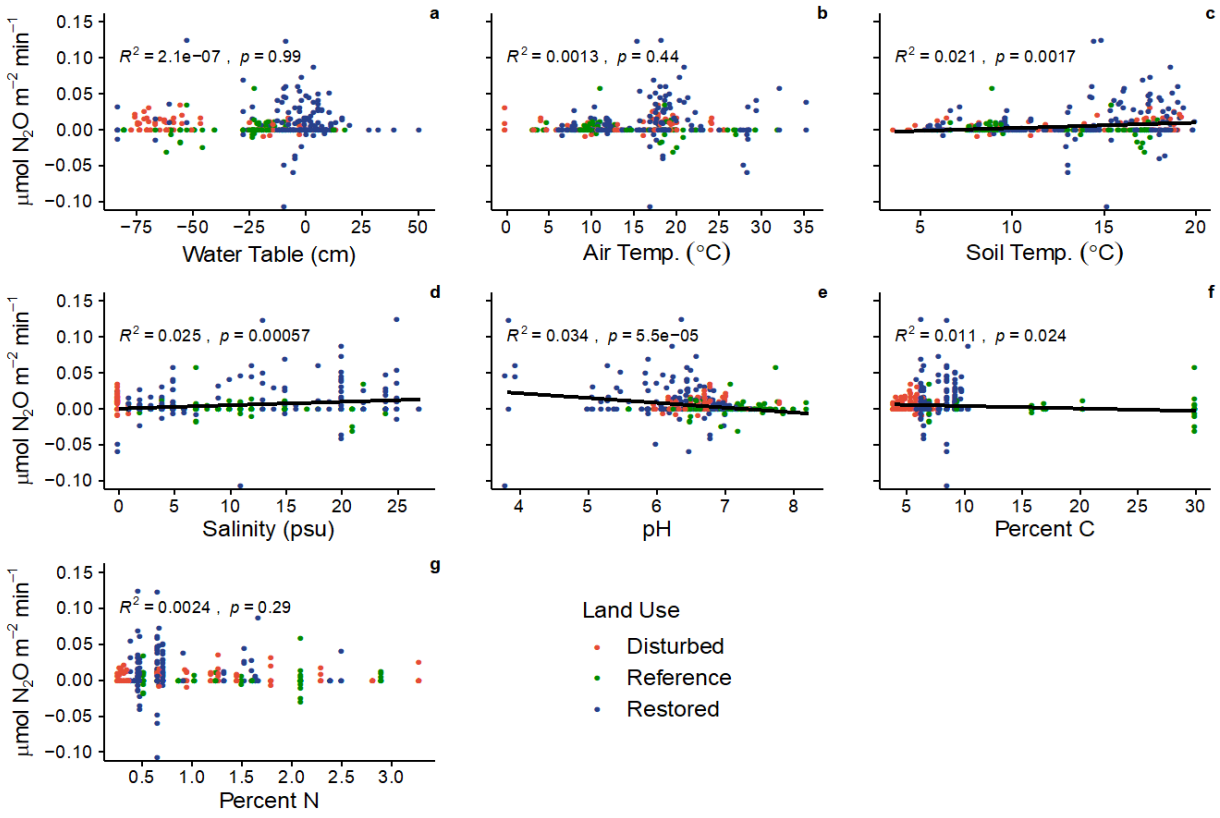

Figure 9.11. Scatterplots of instantaneous N_2O fluxes versus environmental variables in Tillamook Bay wetlands including groundwater level ("water table"), air and soil temperature, groundwater salinity and pH, and soil percent carbon and nitrogen.

GHG fluxes, high tide sampling. Three sites (DC, A004, and A073) were normally not sampled at high tide during the year-long sampling due to access challenges (see Methods above), so we used a floating chamber to sample GHG fluxes on September 29-30, 2018 at high tide and compared them to fluxes at low tide on August 31 – September 2, 2018 (Table 9.5). Carbon dioxide fluxes were significantly lower at high tide for all three stations. There was a non-significant trend of lower CH_4 and N_2O fluxes at high tide in two of three of the stations.

Table 9.5. Greenhouse gas fluxes sampled on August 31 – Sept. 2, 2018 (Aug.) at low tide and September 29-30, 2018 (Sept.) at high tide at one reference high marsh station and two restored locations. The average (± standard error) for the gas fluxes from six chambers are shown along with the corresponding mean environmental conditions. Asterisks indicate that fluxes on the two sampling dates were significantly different at $0.01 < P < 0.05$ with a Wilcoxon rank sum test.

		Greenhouse gas flux (μmol m^{-2} min^{-1})			Soil temp	Air temp		Groundwater salinity
Station	Period	CH_4	CO_2	$N_2O \times 10^3$	(°C)	(°C)	Groundwater depth (cm)	(psu)
DC	Aug (low tide)	0.275 (0.09)	311 (27)*	2.06 (2.0)	17.4	18.6	-20.6	15
	Sept (high tide)	0.002 (0.03)	7.9 (2.5)	0.00 (0.00)	15.2	22.3	14.7	12.7
A004	Aug (low tide)	0.193 (0.08)	262 (61)*	28.2 (31)	14.5	16.9	-8.3	12
	Sept (high tide)	0.0159 (0.02)	17.9 (2.0)	2.03 (2.03)	14.5	22.0	33.3	17.3
A073	Aug (low tide)	0.000 (0.00)	140 (48)*	30.6 (20)	15.7	17.9	-59.3	25
	Sept (high tide)	0.000 (0.00)	21.5 (6.9)	2.0 (2.0)	14.8	23.1	7.0	20.0

Discussion

In this study we sampled GHG fluxes in newly restored tidal wetlands in the SFC project in Tillamook Bay, Oregon one to two years after restoration. We compared fluxes with adjoining disturbed wetlands (diked former tidal wetlands) that remained in agricultural production, and with nearby high marsh reference wetlands, to better understand the effects of land use and tidal restoration on GHG fluxes. The large SFC project has gradients of important environmental factors such as salinity and elevation that are typically expected to have a large effect on GHG fluxes in estuarine wetlands, so we also examined physicochemical controls of GHG fluxes across the whole dataset. In general, we found that among the environmental controls we measured, groundwater level and air temperature had the largest effect on GHG fluxes across the sites we studied. Groundwater levels in particular differed among land uses, resulting in differences in GHG flux among wetland types.

Methane. Typically CH_4 is the GHG of greatest concern in wetland restoration because of its high atmospheric warming potential and because some wetlands emit large amounts of this gas (Bridgham et al. 2006, Neubauer and Megonigal 2015), particularly when salinity is low (Poffenbarger et al. 2011).

A recently-published synthesis (Al-Haj and Fulweiler 2020) provides context on CH_4 emissions at our sites relative to other global wetlands. The average CH_4 emission at our high marsh reference sites (0.24 μmol m^{-2} min^{-1}) was only one-tenth the global average for salt marshes in Al-Haj and Fulweiler (2.45 μmol m^{-2} min^{-1}; calculated from data in the paper). Many studies remove individual fluxes below a defined cut-off point, which we defined as zero to avoid biasing our estimates upwards, and this may at partially explain our lower emission rates. At SFC, average CH_4 emission (2.10 μmol m^{-2} min^{-1}) was similar to the salt marsh average in Al-Haj and Fulweiler. Both our study and the global synthesis found a large range in flux values, with the median emission an order of magnitude lower than the mean, indicating that relatively few observations were responsible for elevating mean methane emissions. Al-Haj and Fulweiler found that salinity and distance from the equator (a surrogate for temperature) were the only significant environmental predictors of CH_4 fluxes in salt marshes across their global dataset, although both had no more than modest predictive strength ($r = -0.49$ and -0.36, respectively).

In the Tillamook Bay wetlands we investigated, CH_4 emissions could only be partially predicted with the CART and random forest models ($R^2 = 0.29$ and 0.23, respectively) using the environmental

controls we measured. This illustrates the complex, nonlinear controls affecting the production of this gas, its transport within the soil, and its consumption (Blodau 2002, Megonigal et al. 2004, Bridgham et al. 2013). Of the environmental variables we measured, groundwater level and air temperature were the most important predictors of CH_4 fluxes, with pH, groundwater salinity, and soil temperature being of secondary importance (Figure 9.3). High fluxes occurred when all or most of the following conditions were met: groundwater was near the soil surface, the air was warm, pH was about neutral, and salinity was low. Several significant correlations between CH_4 fluxes and different environmental drivers (Figure 9.5) further emphasize that there is likely no single master controlling variable on methane emissions in these wetlands, and that low fluxes can occur when one variable favors high methane emission (e.g., high groundwater table) but other conditions do not.

Groundwater level has a well-documented effect on methane fluxes (Bridgham et al. 2013). Higher groundwater levels provide a greater sub-surface anaerobic zone beneath the soil surface for the production of methane and a reduced zone in the soil column between the water table and air for methane oxidation. In addition, soil temperature was correlated with CH_4 fluxes in this dataset, and higher fluxes occurred during the spring and summer. In addition to the direct effect of temperature on methanogens, warmer temperatures have a positive effect on organic matter decomposition, and thus supply more organic matter substrates for use by methanogens (Reddy and DeLaune 2008, Bridgham et al. 2013, Hopple et al. 2020). Most methanogens prefer near-neutral pH conditions, and pH has been shown in other studies to be a strong predictor of CH_4 production (Ye et al. 2012, Bridgham et al. 2013).

The effect of salinity on CH_4 fluxes is of particular interest because diking often converts tidal wetlands to less saline conditions (Chapter 2), and local managers or restoration practitioners may be able to choose where to focus their wetland restoration efforts along the salinity gradient of an estuary. Salinity is correlated with marine-derived sulfate inputs in estuarine wetlands, and can shift the competitive balance between sulfate-reducing bacteria and methane-producing microorganisms (Megonigal et al. 2004). We analyzed a subset of groundwater samples for salinity and sulfate and found a strong positive correlation in their concentrations ($R^2 = 0.80$, $P > 0.001$, data not shown). In both the CART model (Figure 9.3) and scatterplot analysis (Figure 9.5d), we found that high CH_4 fluxes only occurred below about 5 PSU, under oligohaline or freshwater conditions. This range of salinity conducive to high CH_4 fluxes in Tillamook Bay tidal wetlands is lower than reports from compilations of other estuarine wetlands in the U.S., with those studies indicating a cut-off of about 15 PSU (Poffenbarger et al. 2011, Windham-Myers et al. 2018).

The interacting effects of several environmental factors on methane emissions can be seen in the variability of rates measured between and within different wetland types (Figure 9.6). The restored marshes at SFC had on average the highest instantaneous and annual CH_4 emissions across the study, and there was considerable variability over time and between SFC stations. The high emissions at several of the SFC stations were likely due to their generally high groundwater levels (Table 9.2), which was due to lower elevations at SFC (approximately 0.5 m lower than high reference marshes [Chapter 2; Table 9.1]). Several of the SFC stations with the highest methane fluxes (A009, A016, and A028) had groundwater levels at or above the wetland surface during both wet and dry seasons (Figure 4.20), including station A009 which was continually ponded over the study period. (Station A037 also had high groundwater levels, but may have had lower methane emissions because its groundwater was cooler and somewhat saltier). There were also large differences in CH_4 emissions over the course of the year, consistent with seasonal differences in temperature, groundwater level, and salinity (Table 9.2).

Within reference and disturbed marshes, we also observed substantial variability in CH_4 fluxes. The Doty Creek (DC) reference marsh station for example, had CH_4 emissions that were 50-200 times greater than the other two high marsh sites, probably because it had a higher average groundwater level (it was somewhat lower in elevation than the other high marsh reference stations) and had lower salinity (Table 9.2). Similarly, CH_4 emissions at station JF2 in the disturbed site were nine times higher

than at station JF1, whereas the other, drier disturbed site (CF) had a small net uptake of CH_4. These results suggest that differences in hydrology or other factors over relatively small spatial scales may have large effects on GHG emissions, a situation that requires careful sampling to ensure representative samples that encompass the range of natural variability in wetlands.

Although high methane emissions were observed at some SFC stations during specific conditions, there are several factors that could lead to lower emissions at the site over time. First, since SFC is rapidly accreting sediment (Chapter 2) and is likely to move higher in the tidal frame over the coming decades, CH_4 fluxes may decrease as SFC elevations increase to more closely resemble high reference marshes. Second, as tidal creek networks develop more fully at SFC, there may be better drainage of ponded areas during low tide periods, which could further reduce methane emissions. Conversely, it is possible that warming coastal air and/or soil temperatures with climate change could increase tidal wetland methane emissions.

Carbon dioxide. Dark CO_2 fluxes measure ecosystem respiration, which includes respiration by plants, invertebrates, and micro-organisms. Respiration was reasonably well predicted by the CART and random forest models (R^2 = 0.46 and 0.62 respectively), possibly reflecting a simpler set of ecosystem controls than CH_4 and N_2O (Schimel and Gulledge 1998, van den Pol-van Dasselaar et al. 1998). Respiration was positively influenced by warmer temperatures and lower groundwater levels, which is widely consistent with known controls of plant and microbial respiration (Reddy and DeLaune 2008, Chapin III et al. 2011). Restored marshes had lower instantaneous and annual CO_2 fluxes than disturbed and reference marshes (Table 9.4), likely because of their higher groundwater levels.

Nitrous oxide. Nitrous oxide fluxes measured in this study were low, episodic, and could be positive, negative, or, most often, below the instrument detection limit. Measured ecosystem drivers were at best only weakly correlated with N_2O fluxes (Fig. 9.11). Other research has found that wetlands have low nitrous oxide fluxes unless they have major nitrogen inputs (Moseman-Valtierra 2012). Despite these low and variable fluxes, we did find significant differences between land use types. The reference marshes had the lowest instantaneous and annual fluxes, which were not significantly different than zero (Table 9.4). The restored marsh had significantly higher annual N_2O fluxes. Similarly, restored marshes were found to have higher N_2O fluxes than reference marshes in an English estuary, which was attributed to restored sites having wetter conditions and greater tidal inputs of nutrients (Adams et al. 2012), which is true of our study sites. Experimental flooding of cores from previously diked salt marshes was found to increase N_2O emissions in other estuaries (Blackwell et al. 2010, Wollenberg et al. 2018). Interestingly, the Wollenberg et al. study also found that experimental flooding of cores from a diked and drained salt marsh in eastern Canada showed increased CH_4 emissions and decreased CO_2 emissions, similar to our results in Tillamook Bay.

Tidal cycle variability. Hydrology in estuarine wetlands is tidally-dominated, with effects on both surface inundation and groundwater dynamics on daily, monthly, and seasonal time scales (Chapter 4). These hydrologic changes could affect GHG fluxes. In the three sites where we sampled low and high tide approximately one month apart, there were significantly higher CO_2 fluxes and a trend towards higher CH_4 and N_2O fluxes at low tide (Table 9.5). Soil temperatures were slightly higher at two of the three stations in the low tide sampling, which may partially explain the higher gas fluxes. Additionally, the high solubility of CO_2 may have limited its gaseous emissions from the surface over the short period of measurement. Additionally, all three gases could be consumed by microorganisms in the water column at high tide. It is also important to note that we sampled most sites over a range of tides. Given the limited sampling in the tidal comparison over approximately a month, we feel that the most we can conclude is that there is no evidence that our sampling scheme underestimated GHG fluxes.

Mangement implications and conclusions

GHG fluxes showed high spatial and temporal variability in this study, suggesting that a large sampling effort may be needed to adequately characterize fluxes at restoration sites and in natural wetlands. Managers and researchers may need to consider tradeoffs between sampling more sites to better understand spatial heterogeneity versus frequently sampling a smaller number of sites to better evaluate temporal change over tide cycles and seasons.

Of the environmental factors we measured, high groundwater level (just below, at, or just above the soil surface) related most closely to CH_4 emissions. Shallow ponding at low tide (i.e., groundwater level just above the soil surface) was common in some parts of SFC after restoration, including the areas surrounding stations A009 and A028, which showed the highest CH_4 emissions. This ponding may have been due to several factors: a lack of nearby tidal channels to carry away surface drainage; soil compaction due to machinery operations hindering drainage through the soil column; and/or depressional topographic features (again, likely caused by machinery operations) that impeded drainage at low tide. Least-disturbed tidal wetlands at an elevation similar to SFC, with their intact, high-density tidal channel networks and low bulk density soils, generally have very little surface ponding at low tide.

During restoration design at low-salinity sites managers should consider increasing the density of restored tidal channels as a means of reducing potential methane emissions. Adaptive management to reduce ponding after initial site construction may also be helpful. At SFC, ponding is patchy and further excavation is not recommended, particularly since the higher methane fluxes associated with ponding may be temporary. As the site increases in elevation through accretion and as channel networks develop (including the proliferation of smaller low order channels), wetland drainage may improve, reducing ponding and soil saturation, and thus reducing methane emissions. Additionally, in this study, high methane emissions were not observed when salinity was over 5 PSU. Therefore, another strategy for reducing methane emissions at restoration sites could be to select project sites in higher-salinity regions of an estuary.

A variety of studies of have found higher N_2O fluxes in restored (or simulated restoration) tidal marshes, so it is unknown if the very small, but net positive emissions of this gas will persist over time at SFC. Our data suggested generally low N_2O fluxes across a range of land-use, salinity, and groundwater conditions, and that it is not a large problem under these conditions.

This study examined GHG fluxes soon after restoration, and as described above, GHG flux is likely to change as the site develops. We suggest that future monitoring of wetland development at SFC should incorporate GHG flux measurements to determine changes in emissions over time and to enable estimates of the long-term global warming potential of the SFC project. Together with data on soil accretion rates, soil carbon sequestration rates, and spatial variability in ecosystem drivers such as groundwater level, future data collection will help determine how the SFC site contributes to climate mitigation benefits in Tillamook Bay.

Citations

Adams CA, Andrews JE, Jickells T. 2012. Nitrous oxide and methane fluxes vs. carbon, nitrogen and phosphorous burial in new intertidal and saltmarsh sediments. Science of the Total Environment 434:240-251.

Al-Haj AN, Fulweiler RW. 2020. A synthesis of methane emissions from shallow vegetated coastal ecosystems. Global Change Biology 5:2988-3005.

Baggs EM. 2011. Soil microbial sources of nitrous oxide: recent advances in knowledge, emerging challenges and future direction. Current Opinion in Environmental Sustainability 3:321-327.

Blackwell MSA, Yamulki S, Bol R. 2010. Nitrous oxide production and denitrification rates in estuarine intertidal saltmarsh and managed realignment zones. Estuarine, Coastal and Shelf Science 87:591-600.

Blodau C. 2002. Carbon cycling in peatlands—A review of processes and controls. Environmental Reviews 10:111-134.

Bridgham SD. 2014. Carbon dynamics and ecosystem processes. Pages 185-201 *in* D. P. Batzer and R. R. Sharitz, editors. Ecology of Freshwater and Estuarine Wetlands. University of California Press, Berkeley, CA.

Bridgham SD, Cadillo-Quiroz H, Keller JK, Zhuang Q. 2013. Methane emissions from wetlands: biogeochemical, microbial, and modeling perspectives from local to global scales. Global Change Biology 19:1325-1346.

Bridgham SD, Megonigal JP, Keller JK, Bliss NB, Trettin C. 2006. The carbon balance of North American wetlands. Wetlands 26:889-916.

Bridgham SD, Richardson CJ. 1992. Mechanisms controlling soil respiration (CO_2 and CH_4) in southern peatlands. Soil Biology and Biochemistry 24:1089-1099.

Brophy LS, van de Wetering S, Ewald MJ, Brown LA, Janousek CN. 2014. Ni-les'tun Tidal Wetland Restoration Effectiveness Monitoring: Year 2 Post-restoration (2013). Institute for Applied Ecology, Corvallis, OR.

Brown LA, Ewald MJ, Brophy LS, van de Wetering S. 2016. Southern Flow Corridor baseline effectiveness monitoring: 2014. Institute for Applied Ecology, Corvallis, OR.

Bubier JL, Bhatia G, Moore TR, Roulet NT, Lafleur PM. 2003. Spatial and temporal variability in growing-season net ecosystem carbon dioxide exchange at a large peatland in Ontario, Canada. Ecosystems 6:353-367.

Butterbach-Bahl K, Baggs EM, Dannenmann M, Kiese R, Zechmeister-Boltenstern S. 2013. Nitrous oxide emissions from soils: how well do we understand the processes and their controls? Philosophical Transactions of the Royal Society B Biological Sciences 368:20130122.

Chapin III FS, Matson PA, Vitousek PM. 2011. Principles of Terrestrial Ecosystem Ecology. 2nd ed. Springer, New York.

Cornell JA, Craft CC, Megonigal JP. 2007. Ecosystem gas exchange across a created salt marsh chronosequence. Wetlands 27:240-250.

Crooks S, Rybczyk J, O'Connell K, Devier DL, Poppe K, Emmett-Mattox S. 2014. Coastal blue carbon opportunity assessment for the Snohomish Estuary: The climate benefits of estuary restoration. Report by Environmental Science Associates, Western Washington University, EarthCorps, and Restore America's Estuaries.

Fargione JE, Bassett S, Boucher T, Bridgham S, Conant RT, Cook-Patton SC, Ellis PW, Falcucci A, Fourqurean JW, Gopalakrishna T, Gu BHH, Hurteau MD, Kroeger KD, Kroeger T, Lark TJ, Leavitt SM,Lomax G, McDonald RI, Megonigal JP, Miteva DA, Richardson CJ, Sanderman J, Shoch D, Spawn SA, Veldman JW, Williams CA, Woodbury PB, Zganjar C, Baranski M, Elias P, Houghton RA, Landis E, McGlynn E, Schlesinger WH, Siikamaki JV, Sutton-Grier AE, Griscom BW. 2018. Natural climate solutions for the United States. Science Advances 4:eaat1869.

Galatowitsch SM. 2009. Carbon Offsets as Ecological Restorations. Restoration Ecology 17:563-570.

Hawes SM, Hiebler JA, Nielsen EM, Alton CW, Christy JA, Benner P. 2018. Historical vegetation of the Pacific Coast, Oregon, 1855-1910. ArcMap shapefile, Version 2018_01. Oregon Biodiversity Information Center, Portland State University, Portland, OR.

Hopple AM, Wilson RM, Kolton M, Zalman CA, Chanton JP, Kostka J, Hanson PJ, Keller JK, Bridgham SD. 2020. Massive peatland carbon banks vulnerable to rising temperatures. Nature Communications 11:2373.

James G, Witten D, Hastie T, Tibshirani R. 2013. An Introduction to Statistical Learning with Applications in R. Springer, New York.

Janousek CN, Bailey SJ, Brophy LS. 2021. Early ecosystem development varies with elevation and pre-restoration land use/land cover in a Pacific Northwest tidal wetland restoration project. Estuaries and Coasts 44:13-29.

Laanbroek HJ. 2010. Methane emission from natural wetlands: interplay between emergent macrophytes and soil microbial processes. A mini-review. Annals of Botany 105:141-153.

Laffoley D, Grimsditch GE (eds). 2009. The Management of Natural Coastal Carbon Sinks, Gland, Switzerland.
McLeod E, Chmura GL, Bouillon S, Salm R, Bjork M, Duarte CM, Lovelock CE, Schlesinger WH, Silliman BR. 2011. A blueprint for blue carbon: toward an improved understanding of the role of vegetated coastal habitats in sequestering CO_2. Frontiers in Ecology and the Environment 9:552-560.

Megonigal JP, Hines ME, Visscher PT. 2004. Anaerobic metabolism: linkages to trace gases and aerobic processes. In: Schlesinger WH (ed). Biogeochemistry. Elsevier-Pergamon, Oxford, UK, p.317-424.

Moffett KB, Wolf A, Berry JA, Gorelick SM. 2010. Salt marsh–atmosphere exchange of energy, water vapor, and carbon dioxide: Effects of tidal flooding and biophysical controls. Water Resources Research 46:W10525

Moseman-Valtierra S. 2012. Reconsidering climatic roles of marshes: Are they sinks or sources of greenhouse gases? Pages 1-48 *In* Abreu DC and de Borbón SL, editors. Marshes: Ecology, Management and Conservation. Nova Science Publishers, Inc., New York, NY.

Murray BC, Pendleton L, Jenkins WA, Sifleet S. 2011. Green Payments for Blue Carbon: Economic Incentives for Protecting Threatened Coastal Habitats. NIR11-04, Nicholas Institute for Environmental Policy Solutions, Durham, NC.

Neubauer SC, Megonigal JP. 2015. Moving beyond global warming potentials to quantify the climatic role of ecosystems. Ecosystems 18:1000-1013.

Peck EK. 2017. Competing Roles of Sea Level Rise and Sediment Supply on Sediment Accretion and Carbon Burial in Tidal Wetlands; Northern Oregon, U.S.A. Masters thesis, Oregon State University, Corvallis, OR.

Pendleton L, Donato DC, Murray BC, S. Crooks S, Jenkins WA, Sifleet S, Craft C, Fourqurean JW, Kauffman JB, Marbà N, Megonigal P, Pidgeon E, Herr D, Gordon D, Baldera A. 2012. Estimating global "blue carbon" emissions from conversion and degradation of vegetated coastal ecosystems. PLoS ONE 7:e43542.

Pfeifer-Meister L, Gayton LG, Roy BA, Johnson BR, Bridgham SD. 2018. Greenhouse gas emissions limited by low nitrogen and carbon availability in natural, restored, and agricultural Oregon seasonal wetland. PeerJ 6:e5465.
Poffenbarger HJ, Needelman BA, Megonigal JP. 2011. Salinity influence on methane emissions from tidal marshes. Wetlands 31:831-842.

Reddy KR, DeLaune RD. 2008. Biogeochemistry of Wetlands: Science and Applications. CRC Press, Boca Raton, FL.

Schimel JP, Gulledge J. 1998. Microbial community structure and global trace gases. Global Change Biology 4:745-758.

Shiau Y-J, Burchell MR, Krauss KW, Broome SW, Birgand F. 2019. Carbon storage potential in a recently created brackish marsh in eastern North Carolina, USA. Ecological Engineering 127:579-588.

Turetsky MR, A. Kotowska A, Bubier J, Dise NB, Crill P, Hornibrook ERC, Minkkinen K, Moore TR, Myers-Smith IH, Nykänen H, Olefeldt D, Rinne J, Saarnio S, Shurpali N, Tuittila E-S, Waddington JM, White JR, Wickland KP, Wilmking M. 2014. A synthesis of methane emissions from 71 northern, temperate, and subtropical wetlands. Global Change Biology 20:2183-2197.

van den Pol-van Dasselaar A, Corré WJ, Priemé A, Klemedtsson ÅK, Weslien P, Klemedtsson AS, Oenema O. 1998. Spatial variability of methane, nitrous oxide, and carbon dioxide emissions from drained grasslands. Soil Science Society of America Journal 62:810-817.

Windham-Myers L, Cai W-J, Alin SR, Andersson A, Crosswell J, Dunton KH, Hernandez-Ayon JM, Herrmann M, Hinson AL, Hopkinson CS, Howard J, Hu X, Knox SH, Kroeger K, Lagomasino D, Megonigal P, Najjar RG, Paulsen M-L, Peteet D, Pidgeon E, Schäfer KVR, Tzortziou M, Wang ZA, Watson EB. 2018. Chapter 15: Tidal wetlands and estuaries. Pages 596-648 *In* Cavallaro N, Shrestha G, Birdsey R, Mayes MA, Najjar RG, Reed SC, Romero-Lankao P, Zhu Z, (eds). Second State of the Carbon Cycle Report (SOCCR2): A Sustained Assessment Report. U.S. Global Change Research Program, Washington, DC.

Wollenberg JT, Biswas A, Chmura GL. 2018. Greenhouse gas flux with reflooding of a drained salt marsh soil. PeerJ 6:e5659.

Ye R, Jin Q, Bohannan B, Keller JK, McAllister SA, Bridgham SD. 2012. pH controls over anaerobic carbon mineralization, the efficiency of methane production, and methanogenic pathways in peatlands across an ombrotrophic-minerotrophic gradient. Soil Biology and Biochemistry 54:36-47.

Chapter 10: Conclusions and management recommendations

Christopher Janousek and Laura Brophy

Summary of key findings in the SFC project

Our objective in this research was to document early post-restoration change at SFC across a wide range of physical and biological features as well as examine linkages between these parameters and wetland elevation and pre-restoration conditions. We focused our sampling mainly on *ecosystem drivers* (such as hydrology and salinity) and *structural* features of the site (such as plant cover and soil characteristics), as needed to provide basic information on responses to restoration. We also examined several important functional *processes* at SFC including soil accretion rates, fish behavioral patterns in tidal channels, and greenhouse gas emissions from wetland soils.

Data from the early post-restoration period suggests that there were variable rates of change for different ecosystem components at SFC. For instance, we found large changes in some aspects of wetland hydrology (channel and groundwater water levels), and near-surface soil conditions (salinity and pH) suggesting that these parameters rapidly approached reference wetland conditions. However, we observed slower change in channel morphology, native plant cover, and wetland elevation, indicating that such wetland features make take a number of years, perhaps decades, before they are similar to reference wetlands in Tillamook Bay.

Variable rates of change among ecosystem parameters have been observed in other tidal wetland restoration projects (Simenstad and Thom 1996, Craft et al. 1999, Zedler 2000, Morgan and Short 2002, Nordström et al. 2014, Davis et al. 2018). Removal of dikes and tide gates can result in immediate restoration of natural tidal hydrology (Roegner et al. 2010, Brophy et al. 2014) which provides increased habitat for fish, including salmonids (Roegner et al. 2010). Simenstad and Thom (1996) observed immediate fish use of a small tidal wetland built as a mitigation site on the Puyallup River in the Salish Sea, as well as rapid bird use of un-vegetated flats and vegetated marsh.

In some tidal wetland restoration projects such as created sites for mitigation, wetland soil parameters may be among the slowest to recover (Craft et al. 1999). Tidal wetland diking can lead to loss of soil organic matter and soil compaction, for instance. In contrast to other projects, at SFC we found that surface soils already had organic matter content that was similar to reference tidal wetlands. Additionally, although SFC's soils had lower pH and very low water salinities just before restoration, they quickly became more saline and higher in pH.

Vegetation development is one of the key components of wetland recovery, and is closely tied to wetland soils and geomorphology (Simenstad and Thom 1996). Plant density, cover, and composition impact a range of tidal wetland processes including flow modification, sediment trapping, and organic matter production. Patterns of vegetation change 2-4 years following restoration at SFC were largely consistent with succession observed in other PNW tidal wetland restoration projects. Specifically, we observed rapid loss of freshwater wetland species established during the pre-restoration period such as reed canarygrass, and a major increase in bare ground. In most zones across SFC, species typical of PNW tidal brackish marshes began to establish and spread, although areas of reed canarygrass persisted in the higher-elevation north zone of the project site, which tended to be somewhat higher and fresher than other SFC zones.

As plants continue to re-establish within SFC (native species replacing majority freshwater non-native species), the site's capacity to trap sediment and promote sediment accretion is likely to also

increase (Ward et al. 2003) and functions and services provided by the SFC site may also evolve. For instance, bird composition may change between early succession when unvegetated tide flats are common, and later succession when native marsh plants have become more abundant (Eertman et al. 2002; note we did not monitor bird composition during our study). Changes in resource availability may affect succession of higher trophic levels in tidal marshes (Nordström et al. 2014).

Fish capture data in the project indicated important early-post restoration increases in SFC marsh access. Post-restoration catches of juvenile chinook and chum salmon suggested that hydrologic restoration at SFC resulted in several-fold increases in rearing populations even after observing catch reductions in broader basin wide populations. Additionally, other key estuarine finfish species, although not necessarily increasing at SFC due to the restoration, were found to be present in SFC channels indicating the project is providing important fish habitat in southern Tillamook Bay. Benthic invertebrate communities – an important food source for estuarine fishes – also appeared to show early-post restoration changes at SFC including an increase in amphipod density.

Data on greenhouse gas emissions at SFC and in reference high marsh and disturbed wetlands (diked pastures) provided important insight into how the SFC project may be a source or sink of carbon in Tillamook Bay. The results suggest that groundwater level, salinity, and temperature were important drivers of methane and carbon dioxide emissions in these wetlands, with implications for understanding spatial variability in these gases and how design of future restoration projects could be planned to reduce methane emissions where possible. Sampling also showed that nitrous oxide, another powerful greenhouse gas, was not produced in substantial quantities at the SFC site.

Our data suggest that pre-restoration land-use/land-cover differences and wetland elevation were linked to pre-restoration differences in soils and vegetation, and that these differences led to different degrees of change within the first two years after dike removal. Lower elevation areas inside SFC lost pre-restoration vegetation cover more quickly and had greater increases in soil salinity and pH than higher elevation areas. Consistent with data from other tidal wetlands along the Pacific coast, lower elevation areas at SFC also had high soil accretion rates. Intensive pre-restoration land uses such as cropping may have a large impact on elevation and soil conditions such as those observed in the cropped zone at SFC. In other estuaries, intensive land management for agricultural use has led to land subsidence due to soil compaction and oxidation of peat soils (Drexler et al. 2009).

Monitoring recommendations

Our data from SFC show the value in implementing a full-ecosystem approach to monitoring restored tidal wetland development (when funding and other logistical factors permit) because it allows a broad view of changes at the project site and the ways in which restored site conditions differ from reference wetlands. While measuring wetland processes can be more difficult and costly than measuring simple structural metrics, processes are important because they lend insight into how a restoration project may be supporting different ecosystem functions and services at a landscape scale. The SFC project was an excellent opportunity, for example, to measure how greenhouse gas emissions varied between different wetland land use classes.

Our monitoring program from 2013-2020 encompassed a wide range of ecosystem attributes to better understand abiotic and biological change at the SFC site. Nevertheless, we could not sample all potential metrics of interest, and we therefore necessarily focused more on ecosystem drivers and structural attributes at SFC and reference wetlands, rather than on processes and functions. Pending available resources in future monitoring efforts, additional parameters could be evaluated at SFC or other tidal wetland restoration projects including:

- Rates of wetland elevation change within SFC by use of surface elevation tables (Cahoon et al. 2002) or repeated laser leveling from established benchmarks (Cain and Hensel 2018)
- Spatial and temporal changes in channel and groundwater nutrient concentrations and dissolved oxygen
- Abundance and composition of benthic microalgae and macroalgae (Janousek et al. 2007), which can be key components of tidal wetland food webs and indicators of eutrophication
- Rates of primary productivity by vascular plants, benthic microalgae, and phytoplankton
- Bird abundance, diversity, and use of vegetated and unvegetated areas of SFC
- Changes in trophic pathways (food webs) within SFC and in reference wetlands over time
- Long-term changes in local sea-level, wetland elevation, and subsidence to evaluate if a project site is keeping pace with local rates of sea-level rise

Our data suggested that both pre-restoration conditions and early post-restoration change may have been affected by spatial differences in land-use/land-cover within SFC before dike removal and hydrologic restoration (Janousek et al. 2021). Differences in pre-restoration conditions could have long-term impacts on the speed at which different zones within SFC "recover" (that is, change towards reference wetland conditions). Because of these observations, we recommend an assessment of site heterogeneity prior to initiation of restoration and monitoring. Key drivers of such spatial variability could include gradients of salinity and elevation as well as spatial differences in land use (type and impact intensity), and existing vegetation cover. For instance, leaking tide gates may mean that certain areas of a proposed project have muted tidal exchange, brackish salinities, and higher cover of native plants (Brophy et al. 2014). Such a preliminary assessment was conducted during development of the SFC monitoring plan, and was vital to designing the monitoring activities. If gradients of abiotic drivers and land cover have been identified prior to restoration, sampling can then be stratified within the project site to account for such spatial heterogeneity (as was done at SFC).

Although it was not possible at SFC, we also recommend more than one pre-restoration sampling event before restoration activities proceed if project timelines make that possible. More frequent sampling before and after restoration generally enables more powerful statistical analysis using the traditional before-after control impact (BACI) framework (Smokorowski and Randall 2017). We recognize that this will be challenging, both in terms of funding acquisition and rapid mobilization of sampling teams early in the restoration planning process, but for parameters which are inherently highly variable (e.g., fish abundance), more frequent sampling enables evaluation of normal rates of variability relative to change due to the restoration itself.

We found that for monitoring vegetation, soil parameters, and accretion rates, a randomly-distributed plot approach (as used in this project) may be preferable to transect-based sampling designs. Although the latter can be easier to sample logistically during field work, transect-based sampling designs tend to concentrate sampling in smaller areas and may therefore be less representative of the site(s) overall, especially if sites are large or transects are not positioned randomly within the site or within strata. Transects may often be used to capture elevation gradients present within tidal wetland sites, but sampling stratification by elevation stratum can also be achieved with more random plot distribution. With either randomly-distributed sampling or transect-based designs, researchers have the choice of revisiting exact plots, re-randomizing sampling locations at each sampling event, or using a mixture of both approaches.

We found that sampling more than one type of reference wetland (in our case at SFC we sampled both low and high marsh) helped us better understand changing conditions at SFC after restoration. For instance, measurement of several parameters suggested that SFC more closely resembled low marsh early in its development. High marsh represents the likely pre-diking condition at

SFC, and thus represents a state to which SFC may eventually develop, although it may take several decades or longer for some SFC metrics to reach equivalency with least-disturbed high marsh in Tillamook Bay. To maximize statistical power for determining change in a BACI-framework, Underwood (1994) also recommends inclusion of multiple reference sites when possible. All ecosystems are dynamic (Simenstad and Thom 1996), so sampling several reference wetlands multiple times before and after a restoration intervention helps reveal their range of natural variability, which in turn aids in understanding the changes observed in the restored project. For even greater inferential power, a restoring site could also be compared with unrestored diked sites (former tidal wetlands) in addition to least-disturbed reference sites. This design would improve understanding of the initial impact of diking as well as the effect of restoration.

For hydrologic parameters, we recommend long-term continuous monitoring at representative stations where possible. We partly achieved this with year-long logger deployments in the pre-and post-restoration monitoring periods, but we did not have the resources to continue indefinite monitoring. Because hydrologic time series of long duration can be costly to maintain (sensor maintenance, calibration, and data management) and disturbance and damage to sampling facilities from natural and/or anthropogenic causes can result in data loss, monitoring teams should weigh tradeoffs between number of sample locations, sampling frequency, and sampling duration in restoration projects. Those decisions will also be guided by monitoring objectives and research questions. For routine hydrologic monitoring of less dynamic parameters such as groundwater salinity, it may be more favorable to have lower-frequency sampling extended over longer time periods so that researchers can assess seasonal and inter-annual variability inside and outside the project site. To address high water impacts on a restored site (or how project implementation may change flooding impacts in nearby estuarine areas), it may be desirable to implement seasonal monitoring (winter-spring only) when one is more likely to capture storms or extreme events.

Management recommendations

Tidal wetland restoration project implementation can be guided by a wide range of goals and implemented under a range of funding and logistical constraints, each of which will affect project scope and cost, and the ability to provide resources for scientific monitoring. However, we highlight the importance of monitoring in restoration projects since it serves several critical functions. First implementation monitoring (not included in our scope of work at SFC) evaluates whether project implementation met project design plans. Second, effectiveness monitoring evaluates whether ecosystem structure and function after restoration are meeting project goals, which often includes similarity to least-disturbed reference wetlands. Third, post-restoration monitoring allows evaluation of on-going change at a project site and whether additional interventions ("adaptive management") may be necessary. Examples could include the appearance of non-native species at the site, nuisance species (such as mosquito population increases at the Ni-les'tun project in southern Oregon during the first 2 years after restoration). Finally, high quality monitoring data provide valuable scientific insights that can inform design and implementation of future projects. Lessons learned about sampling type and frequency, unexpected events, and general ecological knowledge of linkages between ecosystem components can be invaluable for planning effective and cost-efficient projects in the future.

Some tidal wetland restoration projects consist of little more than dike removal, although other projects including additional manipulations such as channel excavation, addition of wood to channels and floodplains, and grading of wetland elevation (Cornu and Sadro 2002). Depending on project objectives, active intervention such as extensive channel system construction or grading to create topographic mounds (Diefenderfer et al. 2018) could speed a site's restoration trajectory towards reference conditions, although such engineering may be expensive.

Where possible, we suggest focusing restoration efforts on larger sites like SFC. Large-acreage projects may be more cost effective both for implementation and monitoring due to economies of scale. Additionally, according to well-established species-area relationships, larger projects are likely to host more biodiversity due to the species area relationship (Lomolino 2011) than smaller or fragmented projects. Finally, for restoration projects that are motivated in part by carbon finance mechanisms, larger projects may provide more carbon sequestration potential and thus be more viable in terms of providing returns on investments (Crooks et al. 2020).

In Pacific Northwest tidal wetland restoration projects, vegetation is typically not planted but rather allowed to naturally recruit and establish at a site. As evidenced at SFC, where salinity and pH quickly increase, existing freshwater vegetation may rapidly die back to be replaced by typical estuarine species. In some projects, however, active vegetation management following restoration may be necessary. For example, where the restoration target is shrub or forested wetland, woody plantings are usually needed. In other cases, non-native or invasive plants can persist after restoration of tidal flow in some areas, so active management may be needed to control these plants (Clifton et al. 2018) and facilitate native species establishment.

Citations

Brophy LS, van de Wetering S, Ewald MJ, Brown LA, Janousek CN. 2014. Ni-les'tun tidal wetland restoration effectiveness monitoring: Year 2 post-restoration (2013). Institute for Applied Ecology, Corvallis, OR.

Cahoon DR, Lynch JC, Perez BC, Segura B, Holland RD, Stelly C, Stephenson G, Hensel P. 2002. High-precision measurements of wetland sediment elevation: II. The rod surface elevation table. Journal of Sedimentary Research 72:734-739.

Cain MR, Hensel PF. 2018. Wetland elevations at sub-centimeter precision: exploring the use of digital barcode leveling for elevation monitoring. Estuaries and Coasts 41:582-591.

Clifton BC, Hood WG, Hinton SR. 2018. Floristic development in three oligohaline tidal wetlands after dike removal. Ecological Restoration 36:238-251.

Cornu CE, Sadro S. 2002. Physical and functional responses to experimental marsh surface elevation manipulation in Coos Bay's South Slough. Restoration Ecology 10:474-486.

Craft C, Reader J, Sacco JN, Broome SW. 1999. Twenty-five years of ecosystem development of constructed *Spartina alterniflora* (Loisel) marshes. Ecological Applications 9:1405-1419.

Crooks S, Beers L, Settelmyer S, Swails E, Emmett-Mattox S, Cornu C. 2020. Scoping assessment for Pacific Northwest blue carbon finance projects. Silvestrum Climate Associates, TerraCarbon LLC, Strategic Solutions, LLC and the Institute for Applied Ecology.

Davis MJ, Ellings CS, Woo I, Hodgson S, Larsen K, Nakai G. 2018. Gauging resource exploitation by juvenile Chinook salmon (*Oncorrhynchus tshawytscha*) in restoring estuarine habitat. Restoration Ecology 26:976-986.

Diefenderfer HL, Sinks IA, Zimmerman SA, Cullinan VI, Borde AB. 2018. Designing topographic heterogeneity for tidal wetland restoration. Ecological Engineering 123:212-225.

Eertman RHM, Kornman BA, Stikvoort E, Verbeek H. 2002. Restoration of the Sieperda tidal marsh in the Scheldt Estuary, The Netherlands. Restoration Ecology 10:438-449.

Janousek CN, Currin CA, Levin LA. 2007. Succession of microphytobenthos in a restored coastal wetland. Estuaries and Coasts 30:265-276.

Janousek CN, Bailey SJ, Brophy LS. 2021. Early ecosystem development varies with elevation and pre-restoration land use/land cover in a Pacific Northwest tidal wetland restoration project. Estuaries and Coasts 44:13-29.

Lomolino MV. 2001. The species-area relationship: new challenges for an old pattern. Progress in Physical Geography 25:1-21.

Morgan PA, Short FT. 2002. Using functional trajectories to track constructed salt marsh development in the Great Bay, Estuary, Maine/New Hampshire, U.S.A. Restoration Ecology 10:461-473.

Nordström MC, Currin CA, Talley TS, Whitcraft CR, Levin LA. 2014. Benthic food-web succession in a developing salt marsh. Marine Ecology Progress Series 500:43-55.

Roegner GC, Dawley EW, Russel M, Whiting A, Teel DJ. 2010. Juvenile salmonid use of reconnected tidal freshwater wetlands in Grays River, Lower Columbia River Basin. Transactions of the American Fisheries Society 139:1211-1232.

Simenstad CA, Thom RM. 1996. Functional equivalency trajectories of the restored Gog-Le-Hi-Te estuarine wetland. Ecological Applications 6:38-56.

Smokorowski KW, Randall RG. 2017. Cautions on using the before-after-control-impact design in environmental effects monitoring programs. FACETS 2:212-232.

Underwood AJ. 1994. On beyond BACI: sampling designs that might reliably detect environmental disturbances. Ecological Applications 4:3-15.

Ward KM, Callaway JC, Zedler JB. 2003. Episodic colonization of an intertidal mudflat by native cordgrass (*Spartina foliosa*) at Tijuana Estuary. Estuaries 26:116-130.

Zedler JB. 2000. Progress in wetland restoration ecology. Trends in Ecology and Evolution 15:402-407.

Report appendix

The following appendix includes additional tables and figures supplemental to the main body of the report. Tables and figures are labeled with an "A" followed by a number indicating the chapter to which they correspond (e.g., Table A2.1 corresponds with chapter 2).

Table A2.1. Mean (± SD) of wetland surface elevation measured at vegetation plots in different land-cover/land-use zones at SFC during the pre- (2014) and post-restoration (2018) monitoring periods. Data are presented in a geodetic elevation (NAVD88) and a scaled elevation relative to local tide range (z*).

Wetland	Pre-restoration (2014)			Post-restoration (2018)		
zone	NAVD88 (m)	z*	n	NAVD88 (m)	z*	n
LM	2.09 ± 0.03	0.67 ± 0.03	19	2.08 ± 0.03	0.65 ± 0.03	19
HM	2.69 ± 0.03	1.23 ± 0.02	21	2.64 ± 0.02	1.19 ± 0.02	22
N	2.33 ± 0.08	0.89 ± 0.08	19	2.29 ± 0.03	0.86 ± 0.03	19
M	1.97 ± 0.01	0.55 ± 0.01	56	2.01 ± 0.01	0.59 ± 0.01	54
S	2.09 ± 0.02	0.67 ± 0.02	8	2.15 ± 0.03	0.73 ± 0.03	8
CR	1.95 ± 0.03	0.53 ± 0.03	45	1.99 ± 0.03	0.57 ± 0.03	45
GR	2.38 ± 0.16	0.94 ± 0.16	9	2.42 ± 0.14	0.98 ± 0.13	9

Table A2.2. Vertical soil accretion rates (mean ± SD) measured from 2013-2018 in "a" accretion plots, including the horizontal and vertical position of each plot (measured in 2013). Accretion rate standard deviation was determined when there were two or more replicate cores per plot. Horizontal plot positions are in the UTM coordinate system (zone 10N) and vertical positions are in both NAVD88 and local tide-range-scaled datum, z*.

Plot	Wetland zone	Easting (m)	Northing (m)	NAVD88 (m)	z*	Accretion rate, 2013-2018 (mm yr^{-1})
A001a	N	431451	5036408	2.17	0.75	NA
A002a	N	431464	5036524	2.54	1.09	7.8 ± 1.9
A003a	N	431688	5036400	2.29	0.86	6.8
A004a	N	431484	5036430	2.19	0.76	7.6
A005a	N	431951	5036225	2.29	0.86	6.9
A009a	M	431669	5035881	1.87	0.46	NA
A010a	M	431366	5036167	2.02	0.60	NA
A011a	M	431792	5035854	1.91	0.50	NA
A012a	M	431395	5036171	1.93	0.52	NA
A013a	M	431338	5035887	1.98	0.56	NA
A014a	M	431070	5035987	2.02	0.60	11.3 ± 1.3
A015a	M	431706	5036007	1.96	0.54	NA
A016a	M	431084	5036141	1.96	0.54	NA
A017a	M	430370	5036306	2.04	0.62	NA
A025a	CR	431246	5035871	1.79	0.38	NA
A026a	CR	431511	5035723	1.69	0.29	NA
A027a	CR	431024	5035829	1.79	0.39	NA
A028a	CR	431375	5035709	1.94	0.52	14.8
A029a	CR	431266	5035775	1.79	0.38	NA
A030a	CR	431668	5035523	1.94	0.53	15.4 ± 0.6
A031a	CR	430927	5035941	1.98	0.56	15.2
A037a	M	430563	5035992	1.94	0.53	NA
A040a	HM	431377	5035373	2.68	1.23	2.2 ± 1.2
A041a	HM	431527	5035388	3.05	1.57	NA
A042a	HM	431078	5035375	2.62	1.16	2.3 ± 0.2
A043a	HM	431174	5035388	2.63	1.17	1.2 ± 0.1
A046a	LM	430794	5035523	1.96	0.54	4.6 ± 0.7
A047a	LM	430806	5035439	2.00	0.58	3.9 ± 1.4
A062a	LM	430131	5036711	2.18	0.75	5.8 ± 1.1
A063a	LM	430016	5036970	2.12	0.70	12.4 ± 0.4
A064a	LM	430164	5036813	2.31	0.88	4.9 ± 0.9
A068a	HM	430963	5039941	2.65	1.19	3.3 ± 1.6
A069a	HM	430953	5039900	2.69	1.23	5.1 ± 2.0
A072a	CR	431913	5035478	2.27	0.84	7.5 ± 2.2
A073a	CR	431943	5035414	2.39	0.95	10.3 ± 2.0
A074a	CR	432002	5035358	2.42	0.97	10.0 ± 1.0
A075a	S	432299	5035368	2.17	0.74	7.3
A077a	S	432278	5035338	2.11	0.69	NA

Table A2.3. Vertical soil accretion rates (mean ± SD) measured from 2018-2020 in "b" accretion plots, including the horizontal and vertical position of each plot (measured in 2018). Accretion rate standard deviation was determined when there were two or more replicate cores per plot. Horizontal plot positions are in the UTM coordinate system (zone 10N) and vertical positions are in both NAVD88 and local tide-range-scaled datum, z*.

Plot	Wetland zone	Easting (m)	Northing (m)	NAVD88 (m)	z*	Accretion rate, 2018-2020 (mm yr^{-1})
A001b	N	431449	5036408	2.17	0.75	5.5 ± 1.2
A002b	N	431457	5036525	2.64	1.19	NA
A003b	N	431689	5036403	2.29	0.85	4.5
A004b	N	431481	5036430	2.16	0.73	9.1
A005b	N	431955	5036222	2.32	0.88	3.5 ± 1.4
A009b	M	431677	5035879	2.02	0.60	6.2
A010b	M	431363	5036166	2.15	0.72	NA
A011b	M	431802	5035863	NA	NA	6.3
A012b	M	431399	5036173	1.97	0.56	NA
A013b	M	431338	5035883	2.05	0.63	7.7
A014b	M	431072	5035990	2.03	0.61	NA
A016b	M	431081	5036143	2.02	0.60	8.0 ± 1.7
A017b	M	430370	5036308	2.04	0.62	5.5
A025b	CR	431246	5035874	1.85	0.44	NA
A026b	CR	431513	5035719	1.76	0.36	4.8
A028b	CR	431373	5035705	1.98	0.56	5.9 ± 0.1
A030b	CR	431666	5035525	1.97	0.56	NA
A031b	CR	430924	5035940	2.06	0.64	5.6 ± 0.3
A037b	M	430564	5035995	2.01	0.59	NA
A040b	HM	431374	5035371	2.60	1.15	0.4
A041b	HM	431530	5035386	3.14	1.66	0.0
A042b	HM	431075	5035374	2.61	1.16	0.5 ± 0.7
A043b	HM	431176	5035388	2.62	1.17	1.4 ± 1.6
A046b	LM	430796	5035520	1.98	0.57	6.6 ± 0.1
A047b	LM	430811	5035440	2.09	0.67	2.6 ± 1.0
A062b	LM	NA	NA	NA	NA	4.1
A063b	LM	430012	5036972	2.13	0.70	3.4
A064b	LM	430163	5036809	2.30	0.87	NA
A068b	HM	430965	5039945	2.59	1.14	2.1 ± 1.7
A069b	HM	430957	5039901	2.59	1.14	2.3 ± 1.2
A072b	CR	431916	5035479	2.24	0.81	1.8 ± 0.1
A073b	CR	431945	5035412	2.35	0.91	2.7 ± 2.2
A074b	CR	432006	5035356	2.44	0.99	NA
A075b	S	432298	5035365	2.17	0.74	3.5
A077b	S	432278	5035341	2.16	0.73	6.3 ± 2.5

Table A2.4. Surface soil carbon content, pH, and salinity measured in the vicinity of each "a" accretion plot during the pre-restoration sampling period (2014) and the post-restoration sampling period (2018). NA = no data available.

		Carbon content (%)		pH		Salinity	
Plot	Wetland zone	2014	2018	2014	2018	2014	2018
A001	N	7.1	6.2	5.3	5.3	0.2	3.7
A002	N	6.6	2.8	5.4	5.8	0.2	3.5
A003	N	10.3	8.7	5.0	4.8	0.2	6.4
A004	N	8.8	6.9	5.0	5.2	0.3	3.6
A005	N	4.0	7.7	5.0	5.5	0.1	7.7
A009	M	6.2	7.1	4.7	6.3	0.2	NA
A010	M	13.9	7.9	4.8	5.7	0.1	7.9
A011	M	9.0	NA	5.0	NA	0.1	NA
A012	M	8.1	6.4	5.0	6.2	0.2	NA
A013	M	4.8	5.9	5.1	6.2	0.3	7.6
A014	M	7.9	8.2	5.2	5.6	0.1	9.8
A015	M	5.1	7.0	5.2	5.8	0.1	4.4
A016	M	6.5	10.0	4.8	6.1	0.3	9.5
A017	M	9.0	10.3	5.2	5.9	0.1	17.1
A025	CR	6.2	6.3	5.1	6.7	0.1	23.1
A026	CR	6.1	NA	5.2	NA	0.2	NA
A027	CR	6.3	6.2	5.2	6.1	0.1	NA
A028	CR	6.5	NA	5.2	NA	0.2	NA
A029	CR	8.4	NA	5.3	NA	0.1	NA
A030	CR	9.6	7.1	5.1	5.8	0.1	6.9
A031	CR	11.6	7.5	5.1	5.9	0.1	8.8
A037	M	5.9	8.5	4.7	6.4	0.2	21.2
A040	HM	5.8	6.3	5.3	5.5	5.3	6.1
A041	HM	3.6	3.3	5.6	5.6	0.2	1.5
A042	HM	7.3	7.6	5.3	5.6	5.2	6.5
A043	HM	7.8	6.7	5.7	5.7	8.0	8.5
A046	LM	6.0	7.6	6.2	5.7	8.8	NA
A047	LM	4.1	5.5	5.5	5.6	7.8	8.9
A062	LM	5.7	4.6	5.7	5.7	4.8	8.9
A063	LM	3.5	7.0	6.2	5.6	8.2	7.1
A064	LM	4.6	9.4	5.9	5.4	10.4	17.2
A068	HM	11.3	11.2	6.0	6.2	11.1	7.5
A069	HM	13.7	9.0	6.2	6.3	8.1	11.7
A072	CR	10.1	6.8	5.6	5.6	0.1	5.9
A073	CR	6.5	6.8	5.4	5.2	0.1	6.0
A074	CR	6.3	6.3	5.6	5.3	0.1	4.3
A075	S	5.2	6.4	5.4	5.4	0.2	5.2
A077	S	6.3	6.3	5.4	5.5	0.1	7.2

Table A2.5. Deep-rod benchmarks installed in SFC and in reference wetlands during September 2019. Benchmark locations were measured with a smartphone GPS and are only accurate to about 5m. Future surveying for precise horizontal and vertical positioning of the marks is needed.

Benchmark	Site	Wetland zone	Deep rod length (m)	Easting (m)	Northing (m)	Notes
BM-GP	Goose Pt marsh	HM	4.3	430966	5039937	About 2 meters from groundwater wells at A068
BM-BM	Bay marsh	LM	22.0	430163	5036806	South of two feldspar accretion plots
BM-A073	SFC	CR	22.5	431938	5035419	Near A073 groundwater wells
BM-A028	SFC	CR	19.5	431376	5035714	Near groundwater wells and accretion plots at A028
BM-A010	SFC	M	16.0	431360	5036165	Near two sets of accretion plots at A010 and A012

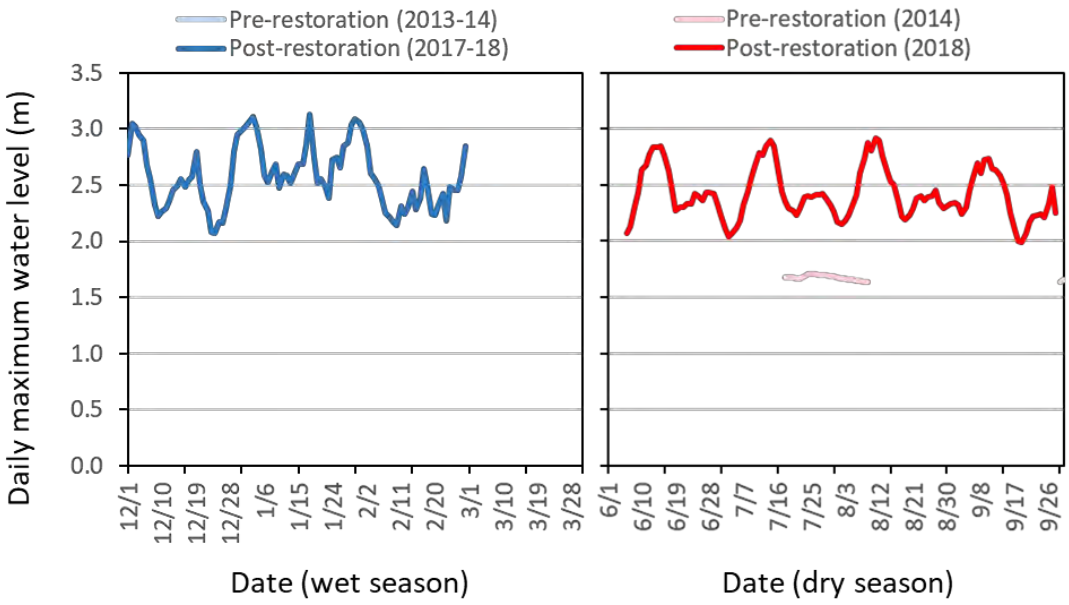

Figure A4.1. Time series of daily maximum water levels (in meters relative to NAVD88) at the upper Blind Slough station inside SFC for the annual wet (Dec-Mar) and dry (Jun-Sep) seasons during the pre- and post-restoration monitoring periods. Water level was only calculated when the sensor was submerged.

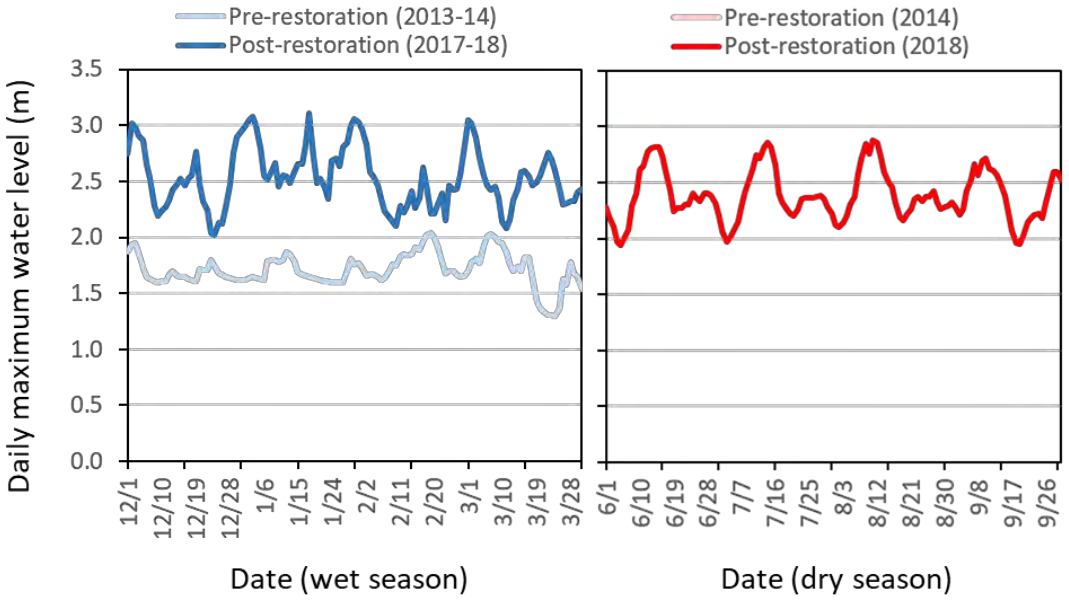

Figure A4.2. Time series of daily maximum water levels (in meters relative to NAVD88) at the upper T1 station inside SFC for the annual wet (Dec-Mar) and dry (Jun-Sep) seasons during the pre- and post-restoration monitoring periods. Water level was only calculated when the sensor was submerged.

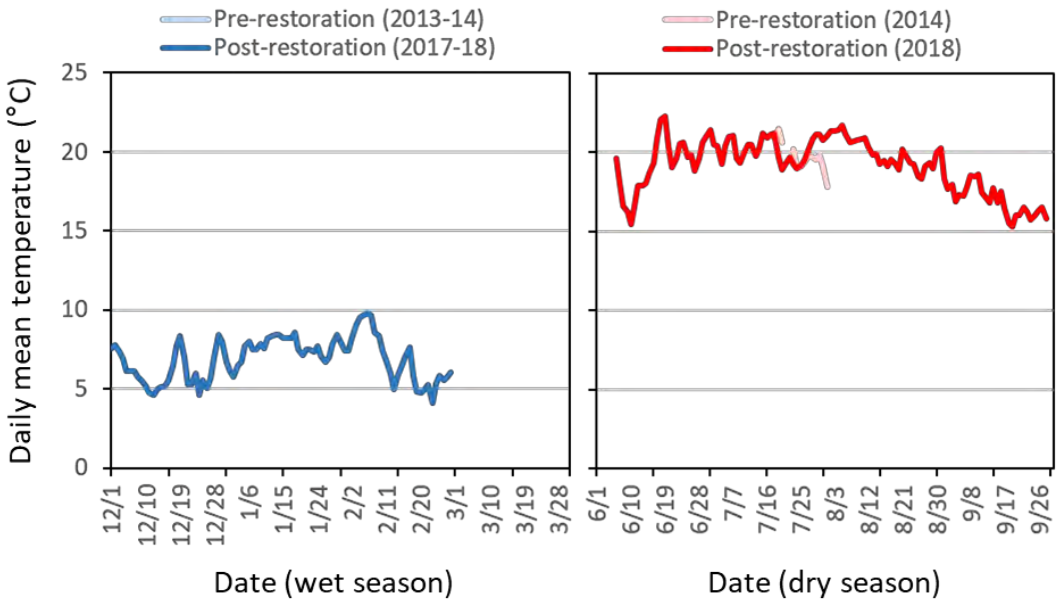

Figure A4.3. Time series of daily average temperature (°C) at the Upper Blind Slough station inside SFC for the annual wet (Dec-Mar) and dry (Jun-Sep) seasons during the pre- and post-restoration monitoring periods. Temperature was only calculated when the sensor was submerged.

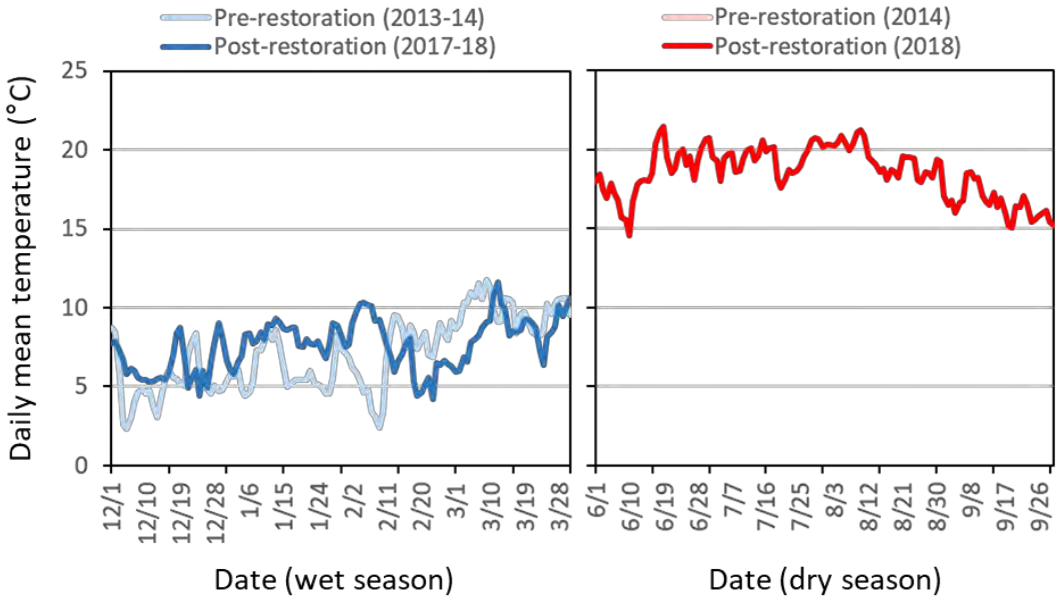

Figure A4.4. Time series of daily average temperature (°C) at the upper T1 station inside SFC for the annual wet (Dec-Mar) and dry (Jun-Sep) seasons during the pre- and post-restoration monitoring periods. Water level was only calculated when the sensor was submerged.

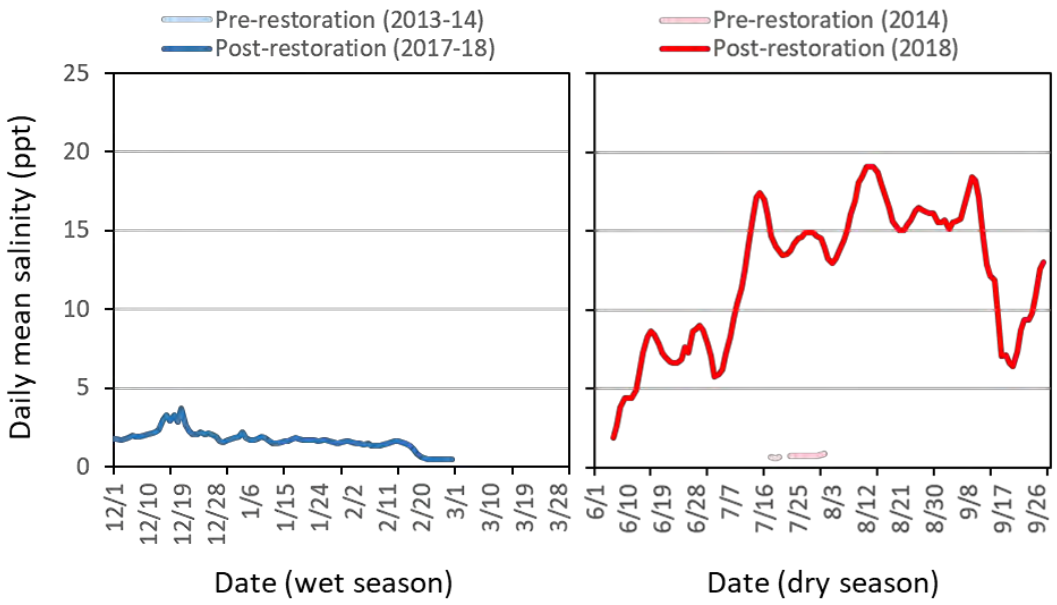

Figure A4.5. Time series of daily average salinity (ppt) at the Upper Blind Slough station inside SFC for the annual wet (Dec-Mar) and dry (Jun-Sep) seasons during the pre- and post-restoration monitoring periods. Salinity was only calculated when the sensor was submerged.

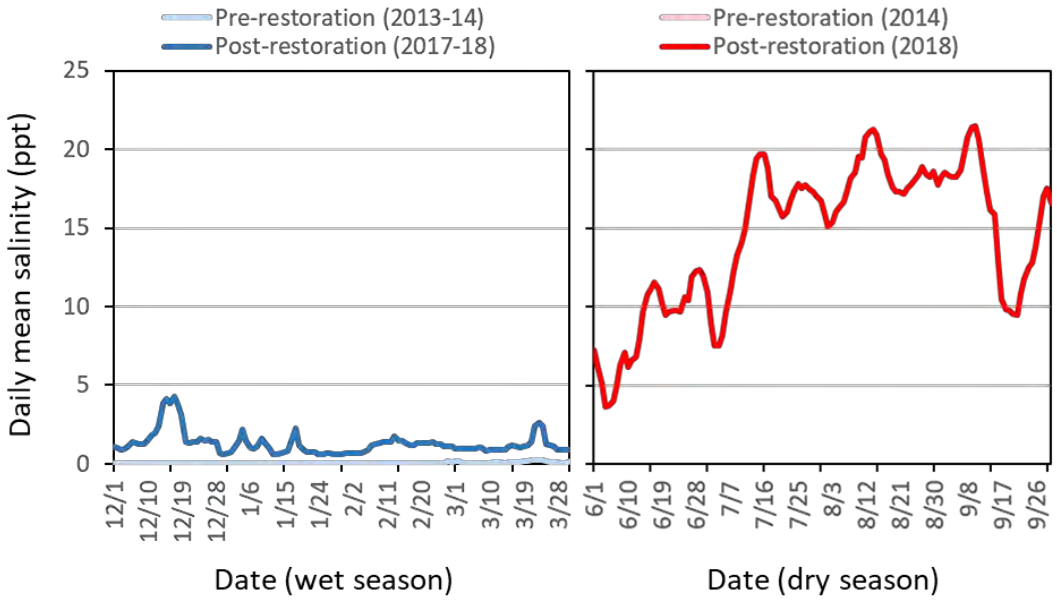

Figure A4.6. Time series of daily average salinity (ppt) at the Upper T1 station inside SFC for the annual wet (Dec-Mar) and dry (Jun-Sep) seasons during the pre- and post-restoration monitoring periods. Salinity was only calculated when the sensor was submerged.

Table A5.1. SFC vegetation map units in 2018, sorted by decreasing area.

Map unit	Association	Area (ha)
8	bare ground	39.36
28	Sitka spruce - red alder / coastal willow - red elderberry - black twinberry - Pacific crabapple - salmonberry	20.97
22	reed canarygrass - slough sedge	19.13
3	creeping bentgrass - creeping spikerush - reed canarygrass	14.55
20	reed canarygrass	12.31
32	coastal willow - black twinberry / reed canarygrass - slough sedge - Pacific silverweed	10.06
24	reed canarygrass - slough sedge - Pacific silverweed - brass buttons	9.21
6	creeping bentgrass - reed canarygrass - (Pacific silverweed)	9.04
19	not mapped	7.43
18	major channels	7.37
1	creeping bentgrass - brass buttons	6.59
23	reed canarygrass - slough sedge - Pacific silverweed	3.33
33	tall fescue - reed canarygrass - creeping bentgrass	3.23
4	creeping bentgrass - velvetgrass	2.24
2	creeping bentgrass - tufted hairgrass	2.21
21	reed canarygrass - creeping bentgrass	2.02
30	Pacific silverweed - Baltic rush- (slough sedge) - (common cattail)	1.88
14	creeping spikerush - brass buttons	1.76
29	Pacific silverweed	1.48
27	reed canarygrass - birdsfoot trefoil	1.43
5	creeping bentgrass - toad rush	1.35
15	toad rush - brass buttons	1.29
9	Lyngbye's sedge	0.88
34	common cattail - Pacific silverweed - (slough sedge) - (reed canarygrass)	0.79
26	reed canarygrass - soft rush - birdsfoot trefoil	0.62
13	slough sedge - Pacific silverweed - Baltic rush - common cattail	0.53
16	perennial ryegrass	0.52
25	reed canarygrass - Baltic rush	0.41
31	Pacific silverweed - common cattail	0.34
10	Lyngbye's sedge - creeping bentgrass	0.22
11	Lyngbye's sedge - tufted hairgrass - creeping bentgrass	0.19
7	meadow foxtail - Pacific silverweed	0.16
17	perennial ryegrass - birdsfoot trefoil	0.12
12	slough sedge	0.09
	Total	183.11

Table A5.2. SFC vegetation map units in 2018, sorted by map unit number.

Map unit #	Association	Area (ha)
1	creeping bentgrass - brass buttons	6.59
2	creeping bentgrass - tufted hairgrass	2.21
3	creeping bentgrass - creeping spikerush - reed canarygrass	14.55
4	creeping bentgrass - velvetgrass	2.24
5	creeping bentgrass - toad rush	1.35
6	creeping bentgrass - reed canarygrass - (Pacific silverweed)	9.04
7	meadow foxtail - Pacific silverweed	0.16
8	bare ground	39.36
9	Lyngbye's sedge	0.88
10	Lyngbye's sedge - creeping bentgrass	0.22
11	Lyngbye's sedge - tufted hairgrass - creeping bentgrass	0.19
12	slough sedge	0.09
13	slough sedge - Pacific silverweed - Baltic rush - common cattail	0.53
14	creeping spikerush - brass buttons	1.76
15	toad rush - brass buttons	1.29
16	perennial ryegrass	0.52
17	perennial ryegrass - birdsfoot trefoil	0.12
18	major channels	7.37
19	not mapped	7.43
20	reed canarygrass	12.31
21	reed canarygrass - creeping bentgrass	2.02
22	reed canarygrass - slough sedge	19.13
23	reed canarygrass - slough sedge - Pacific silverweed	3.33
24	reed canarygrass - slough sedge - Pacific silverweed - brass buttons	9.21
25	reed canarygrass - Baltic rush	0.41
26	reed canarygrass - soft rush - birdsfoot trefoil	0.62
27	reed canarygrass - birdsfoot trefoil	1.43
28	Sitka spruce - red alder / coastal willow - red elderberry - black twinberry - Pacific crabapple – salmonberry	20.97
29	Pacific silverweed	1.48
30	Pacific silverweed - Baltic rush- (slough sedge) - (common cattail)	1.88
31	Pacific silverweed - common cattail	0.34
32	coastal willow - black twinberry / reed canarygrass - slough sedge - Pacific silverweed	10.06
33	tall fescue - reed canarygrass - creeping bentgrass	3.23
34	common cattail - Pacific silverweed - (slough sedge) - (reed canarygrass)	0.79
	Total	183.11

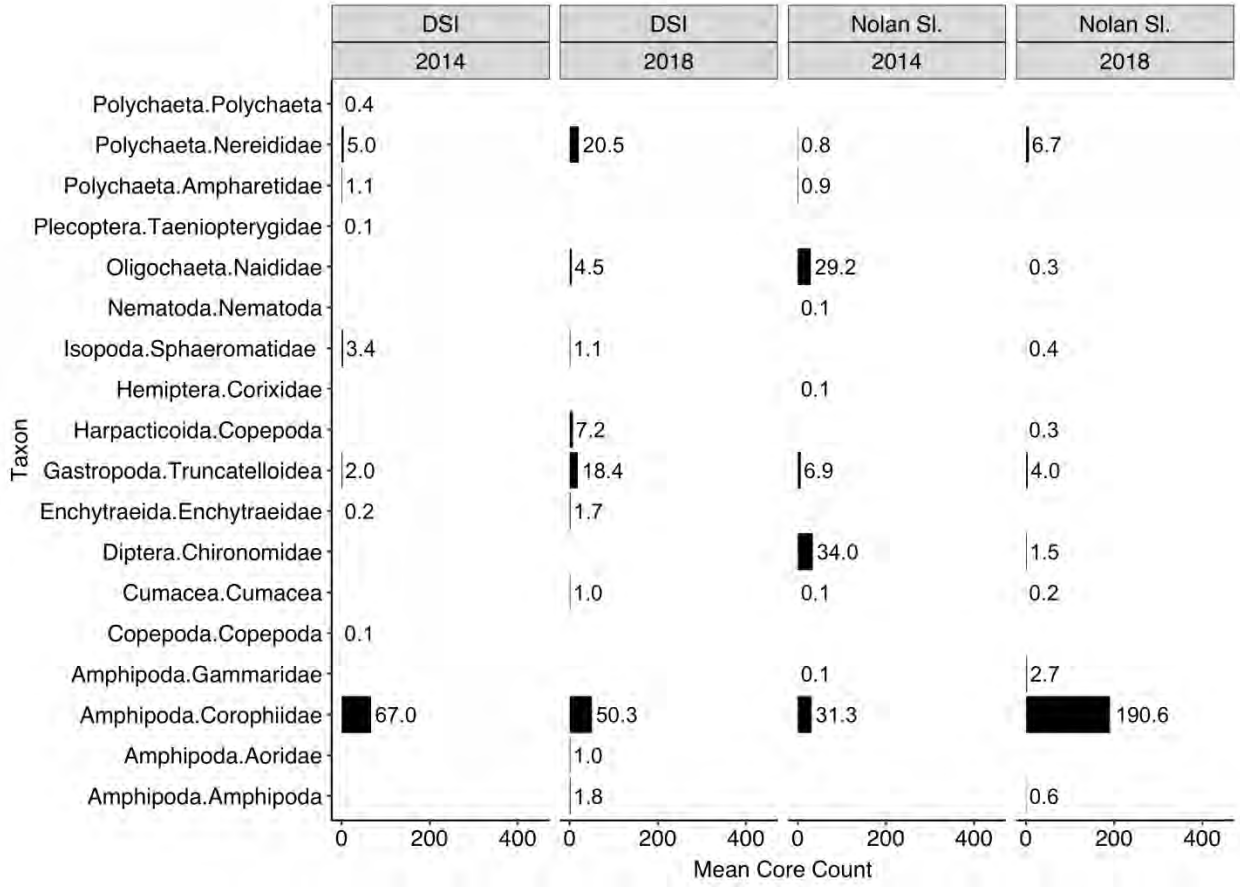

Figure A7.1. Mean abundance (counts/core) by channel reach for the ten most abundant benthic macroinvertebrate taxa in Nolan Slough and the natural high marsh reference site (Dry Stocking Island, DSI) for the pre- and post-restoration sampling periods.

Table A7.1. ANOVA test results for diversity metrics measured for benthic macroinvertebrates at the SFC and reference channel reaches. df = 1 for all tests.

			SFC channel reaches					
			Nolan Sl.		Blind Slough		Trib 1	
Reference channel reaches		Metric	F	P-value	F	P-value	F	P-value
	Trask R. Reference	Simple taxonomic richness	0.15	0.70	5.46	**<0.05**	8.97	**<0.01**
		Shannon index	38.28	**<0.001**	8.41	**<0.01**	14.80	**<0.001**
		Exp. Shannon	43.18	**<0.001**	7.66	**<0.01**	10.60	**<0.01**
		Exp. Simpson	155.82	**<0.001**	4.52	**<0.05**	6.66	**<0.01**
	Wilson R. Reference	Simple taxonomic richness	1.52	0.23	3.06	0.09	8.97	**<0.05**
		Shannon index	215.34	**<0.001**	2.66	0.11	14.804	0.97
		Exp. Shannon	174.27	**<0.001**	3.40	0.07	10.602	0.94
		Exp. Simpson	300.88	**<0.001**	12.18	**<0.01**	6.66	0.59
	DSI Reference	Simple taxonomic richness	10.58	**<0.01**	0.22	0.64	0.75	0.39
		Shannon index	41.11	**<0.001**	1.31	0.26	0.02	0.88
		Exp. Shannon	39.41	**<0.001**	1.79	0.19	0.04	0.85
		Exp. Simpson	37.49	**<0.001**	1.92	0.17	0.02	0.88

Table A8.1. Number of adult mosquitos captured at sampling stations during 2015.

Sample date	Number of adults captured	Species	Capture location
12-Mar	2	*Culex tarsalis*	Mouth of Blind Slough
23-Apr	1	*Culex tarsalis*	Cow pond
23-Apr	1	*Culex stigmatosoma*	Trib 2
7-May	1	*Culex tarsalis*	Mouth of Blind Slough
7-May	5	*Culex tarsalis*	Nolan
7-May	1	*Culex tarsalis*	Trib 2
21-May	4	*Culex tarsalis*	BS Lower
21-May	4	*Culex tarsalis*	Mouth of Blind Slough
21-May	5	*Culex tarsalis*	Cow pond
21-May	3	*Culex tarsalis*	Nolan
21-May	1	*Culex tarsalis*	Trib 2
4-Jun	2	*Culex tarsalis*	BS Lower
4-Jun	1	*Culex pipiens*	Cow pond
4-Jun	1	*Culex pipiens*	Forest
4-Jun	2	*Culex tarsalis*	Nolan
18-Jun	15	*Culex tarsalis* (13), *Culiseta particeps* (1), *Culiseta inornata* (1)	BS Lower
18-Jun	3	*Culex tarsalis*	Mouth of Blind Slough
18-Jun	8	*Culex tarsalis* (7 - 1 male), *Culex pipiens* (1)	Cow pond
18-Jun	1	*Culex pipiens*	Forest
18-Jun	7	*Culex tarsalis* (5), *Culex pipiens* (2)	Nolan
18-Jun	10	*Culex tarsalis*	Trib 2
1-Jul	15	*Culex tarsalis*	BS Lower
1-Jul	8	*Culex tarsalis* (7), *Culex pipiens* (1)	Mouth of Blind Slough
1-Jul	11	*Culex tarsalis*	Cow pond
1-Jul	8	*Culex tarsalis* (7), *Aedes aboriginis* (1)	Forest
1-Jul	8	*Culex tarsalis* (5), *Culex pipiens* (3)	Nolan
1-Jul	17	*Culex tarsalis* (15), *Culex pipiens* (1), *Culiseta particeps* (1)	Trib 2
17-Jul	9	*Culex tarsalis* (5), *Culex pipiens* (4)	BS Lower
17-Jul	6	*Culex tarsalis* (2), *Culex pipiens* (2), *Culex* sp. (1), *Culiseta inornata* (1)	Mouth of Blind Slough
17-Jul	3	*Culex tarsalis* (1), *Culex pipiens* (1), *Culiseta particeps* (1)	Forest
17-Jul	3	*Culex tarsalis*	Trib 2
11-Nov	3	*Culiseta inornata*	BS Lower
25-Nov	2	*Culiseta inornata*	Cow pond

Table A8.2. Number of adult mosquitos captured at sampling stations during 2017.

Sample date	Number of adults captured	Species	Capture location
10-May	1	*Culiseta inornata*	Trib 2
24-May	1	*Culiseta inornata*	Forest
7-Jun	1	*Culex pipiens*	BS Lower
7-Jun	3	*Culex pipiens* (2), *Culex tarsalis* (1)	BS Mouth
7-Jun	3	*Aedes* sp. (probably *A. sierrensis*)-*all males*	Forest
29-Jun	20	*Culiseta inornata*	BS Lower
29-Jun	4	*Culiseta inornata* (3), *Culex pipiens* (1)	BS Mouth
29-Jun	7	*Culex pipiens* (4), *Culiseta inornata* (3)	Cow pond
29-Jun	1	*Culiseta inornata*	Forest
29-Jun	13	*Culiseta inornata* (11), *Culex pipiens* (2)	Nolan
29-Jun	22	*Culiseta inornata*	Trib 2
13-Jul	6	*Culex pipiens* (4), *Culiseta inornata* (2)	BS Lower
13-Jul	16	*Culex pipiens* (11), *Culiseta inornata* (5)	BS Mouth
13-Jul	2	*Culex pipiens* (1), *Culex stigmatosoma* (1)	Cow pond
13-Jul	16	*Culex pipiens* (10), *Culiseta inornata* (4), *Culex tarsalis* (2)	Forest
13-Jul	21	*Culex pipiens* (13), *Culiseta inornata* (5), *Culex tarsalis* (3)	Nolan
13-Jul	21	*Culex pipiens* (13), *Culiseta inornata* (5), *Culex stigmatosoma* (3)	Trib 2
28-Jul	6	*Culex pipiens*	BS Lower
28-Jul	23	*Culex pipiens* (21), *Culiseta inornata* (2)	BS Mouth
28-Jul	4	*Culex pipiens* (3), *Culex tarsalis* (1)	Cow pond
28-Jul	15	*Culex pipiens* (9), *Culex tarsalis* (3), *Culiseta particeps* (3)	Forest
28-Jul	2	*Culex tarsalis*	Nolan
28-Jul	47	*Culex pipiens* (43), *Culex tarsalis* (3), *Culiseta inornata* (1)	Trib 2
11-Aug	6	*Culex pipiens*	BS Lower
11-Aug	1	*Culex pipiens*	BS Mouth
11-Aug	1	*Culex pipiens*	Cow pond
11-Aug	8	*Culex pipiens* (6), *Culiseta inornata* (2)	Forest
11-Aug	28	*Culex pipiens*	Nolan
11-Aug	31	*Culex pipiens*	Trib 2
8-Sep	21	*Culex pipiens*	BS Lower
8-Sep	37	*Culex pipiens*	BS Mouth
8-Sep	28	*Culex pipiens*	Cow pond
8-Sep	19	*Culex pipiens*	Forest
8-Sep	13	*Culex pipiens*	Nolan
8-Sep	26	*Culex pipiens*	Trib 2
5-Oct	1	*Culiseta inornata*	BS Mouth
5-Oct	1	*Aedes campestris*	Trib 2

Table A8.3. Number of adult mosquitos captured at sampling stations during 2018.

Sample date	Number of adults captured	Species	Capture location
5-May	2	*Culex pipiens*	Dog park
5-May	1	*Culex pipiens*	Hospital trail
15-May	1	*Culex pipiens*	Dog park
15-May	1	*Culex pipiens*	Forest 1
15-May	4	*Culex pipiens*	Hospital trail
15-May	2	*Culex pipiens*	New dike - North
1-Jun	8	*Culex pipiens* (7), *Culex tarsalis* (1)	Dog park
1-Jun	8	*Culex pipiens*	Forest 1
1-Jun	10	*Culex pipiens* (8), *Culex tarsalis* (2)	Hospital trail
1-Jun	4	*Culex pipiens*	New dike - North
1-Jun	3	*Culex pipiens*	New dike - South
14-Jun	21	*Culex pipiens* (15), *Culex tarsalis* (5), *Culiseta particeps* (1)	Dog park
14-Jun	4	*Culex pipiens*	Forest 1
14-Jun	1	*Culex pipiens*	Forest 2
14-Jun	8	*Culex pipiens* (7), *Culiseta particeps* (1)	Hospital trail
14-Jun	3	*Culex pipiens* (2), *Culex tarsalis* (1)	New dike - North
28-Jun	3	*Culex pipiens*	Dog park
28-Jun	2	*Culex pipiens* (1), *Aedes sticticus* (1)	Forest 2
28-Jun	34	*Culex pipiens* (32), *Culex tarsalis* (2)	Hospital trail
28-Jun	1	*Culex pipiens*	New dike - North
28-Jun	3	*Culex pipiens*	New dike - South
13-Jul	4	*Culex pipiens*	Dog park
13-Jul	4	*Culex pipiens* (2), *Culex tarsalis* (1), *Aedes sticticus* (1)	Forest 1
13-Jul	45	*Culex pipiens* (41), *Culex tarsalis* (3), *Culiseta inornata* (1)	Hospital trail
26-Jul	47	*Culex pipiens* (41), *Culex tarsalis* (3), *Culiseta inornata* (3)	Dog park
26-Jul	2	*Culex pipiens*	Forest 1
26-Jul	2	*Culex pipiens*	Forest 2
26-Jul	17	*Culex pipiens* (15), *Culiseta incidens* (1), *Culiseta inornata* (1)	Hospital trail
26-Jul	3	*Culex pipiens* (2), *Culex tarsalis* (1)	New dike - North
26-Jul	1	*Culex pipiens*	New dike - South
9-Aug	48	*Culex pipiens*	Dog park
9-Aug	14	*Culex pipiens*	Forest 1
9-Aug	6	*Culex pipiens*	Forest 2
9-Aug	23	*Culex pipiens* (21 - 1 male), *Culex tarsalis* (1), *Culiseta incidens* (1)	Hospital trail
9-Aug	7	*Culex pipiens* (6), *Culiseta incidens* (1)	New dike - North
30-Aug	51	*Culex pipiens* (50), *Culex tarsalis* (1)	Dog park
30-Aug	2	*Culex pipiens*	Forest 1
30-Aug	3	*Culex pipiens*	Forest 2
30-Aug	20	*Culex pipiens* (19), *Aedes* sp. (1)	Hospital trail
30-Aug	11	*Culex pipiens* (10), *Culex stigmatosoma* (1)	New dike - North
30-Aug	3	*Culex pipiens*	New dike - South
18-Oct	1	*Culiseta inornata*	Forest 2

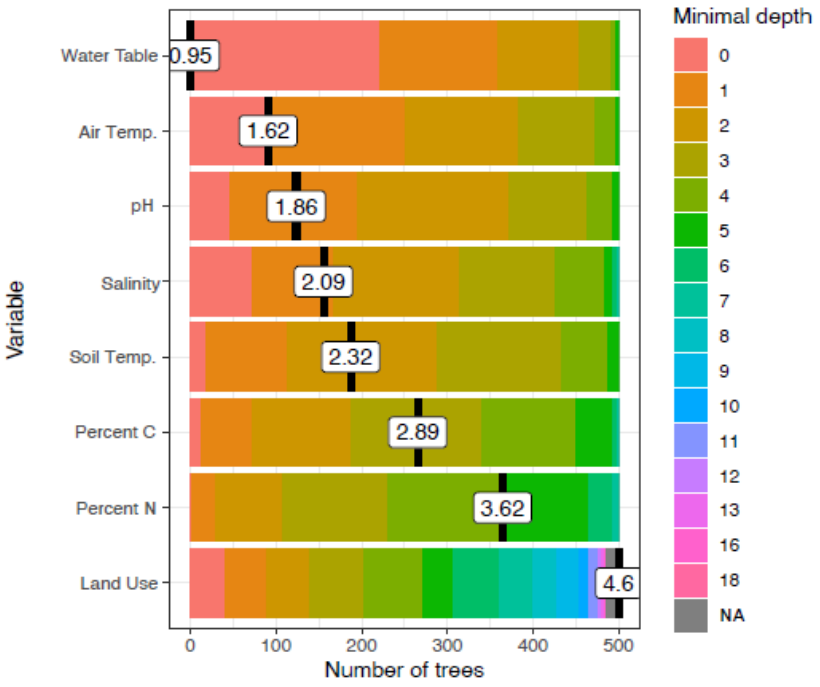

Figure A9.1. Distribution (colored bars) and mean (numbers in boxes) of the minimum depth of the nodes in all trees generated in the methane random forest model. A lower minimum depth indicates that a particular environmental variable is a more important predictor of methane flux.

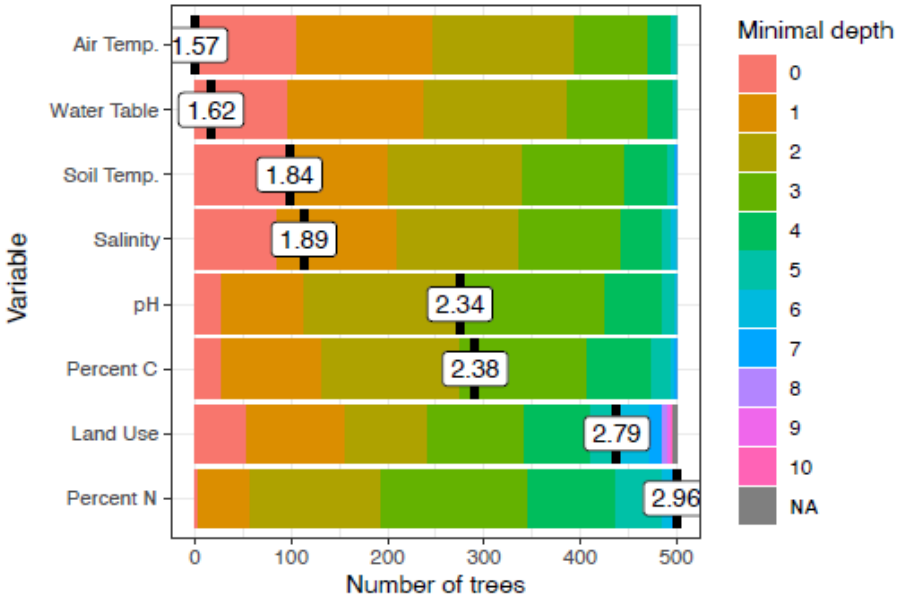

Figure A9.2. Distribution (colored bars) and mean (numbers in boxes) of the minimum depth of the nodes in the trees in the CO_2 flux random forest model. A consistently lower minimum depth indicates that a variable is a more important predictor of CO_2 flux.